Characterization of Gas and Aerosol Emissions from Mount Erebus Volcano, Antarctica

Grazyna A. Zreda-Gostynska

Dissertation

submitted in partial fulfillment of the requirements

for the degree of

Doctor of Philosophy in Geochemistry

New Mexico Institute of Mining and Technology

1995

ACKNOWLEDGEMENTS

I wish to thank Drs. Philip Kyle, Andrew Campbell, David Finnegan and Fred Phillips, for supervising this study. My special thanks to Philip Kyle for his patient assistance and critical comments during the later part of the work. I also greatly appreciate his help with the technical aspects of analytical work. Many other people have contributed to this study. Special thanks to Bob Andres, Dave Caldwell, Nelia Dunbar, Bill McIntosh, Kurt Panter, Franco Pratti, Ken Sims, and Lauri Sybeldon for their companionship and invaluable assistance in the field work, and to all other friends with whom I shared my time and experiences at the New Mexico Tech. I thank Lynn Brandvoldt, Jenny Verploegh, Sandy Schwartz and Chris McKee from New Mexico Bureau of Mines, and Mike Glascock and Jeff Denison from University of Missouri Research Reactor for the help with the analytical work. I am grateful to the Geoscience Department at New Mexico Tech for the financial support. I also wish to thank the Division of Polar Programs, NSF for providing the funding, and the U.S. Navy VXE-6 squadron for the logistic support.

My greatest thanks go to my family, Marek and Magda, for their patience, support and encouragement. This work is dedicated to them.

ABSTRACT

Mt. Erebus, at present the most active volcano in Antarctica, provides an opportunity to study gases and particles emitted from the unusual, highly alkaline magma. The purpose of this study was to characterize the composition of emissions from Mt. Erebus and assess the possible environmental impact of the volcano on the Antarctic environment. Study of the emissions from Mt. Erebus add to the knowledge on atmospheric gas and aerosol species emitted from natural sources.

During the period between December 1986 and January 1991, 60 samples of gas and particulates emitted from Mt. Erebus were collected. The volcanic plume contains large quantities of halogen and sulfur species. Between 1986 and 1991, the average concentrations of gases in the plume decreased from 907 $\mu g.m^{-3}$ to 149 $\mu g.m^{-3}$ Cl, 482 $\mu g.m^{-3}$ to 60 $\mu g.m^{-3}$ F, and 521 $\mu g.m^{-3}$ to 164 $\mu g.m^{-3}$ S. Throughout the study period the average yearly emissions of HF increased from 4.0 $Gg.yr^{-1}$ in 1986 to 6.0 $Gg.yr^{-1}$ in 1991, and HCl from 6.9 $Gg.yr^{-1}$ in 1986 to 13.3 $Gg.yr^{-1}$ in 1991. The currently observed outputs are much smaller from those observed in 1983 (30.5 $Gg.yr^{-1}$ HF and 60.9 $Gg.yr^{-1}$ HCl). The Erebus plume contains large concentrations of various trace elements. It is highly enriched in Co, Cd, Zn, As, Se, Sb, Au, Br, In and Hg. An increase in the emissions of trace elements was observed between 1986 and 1991, and together with the observed small increase in the ash content of the plume, may indicate a change in the degassing behavior of Mount Erebus.

There is no evidence of change in the composition of Erebus magma during the study period; however, a distinctive temporal variation in sulfur and halogen content of the gas was observed. This variation is attributed to heterogeneities within the magma chamber caused by the variable volatile content of the melt. The observed short-term, semi-cyclic variation in both SO_2 and halogen emissions are interpreted as being related to magma movement in the conduit. This hypothesis is partially supported by the results of modeling of the degassing process.

The salts occurring on the Erebus summit consist of mixed sulfates, chlorides, and possibly fluorides. All salts contain high concentrations of various trace elements (F, Cl S, As, Zn, Cd, Co, Hg, and In) corresponding to the composition of the Erebus plume. These low temperature deposits are clearly of volcanic origin, and form by an interaction between plume gasses and rocks exposed on the surface. The salts may contain the time-integrated record of the plume composition and provide an insight into the localized but intense environmental impact of Mt. Erebus activity.

The Erebus plume dispersed over the Antarctic continent could result in the deposition of 24-118 $ng.g^{-1}$ SO_4^{2-}, 11-55 $ng.g^{-1}$ Cl, and 5-27 $ng.g^{-1}$ F in Antarctic snow. This suggests that the contribution of Erebus to the Antarctic budgets of sulfur, halogens and trace metals can be substantial. The similarity between the trace element content of atmospheric aerosols sampled over the South Pole and in the Erebus volcanic plume point to Erebus as their potential source.

TABLE OF CONTENTS

APENDICES

LIST OF TABLES

APPENDICES

LIST OF FIGURES

1. INTRODUCTION

Because man, hanging on the thin basalt coat of a sphere whose nucleus is energy,
does not like to meet anything as irrational as he,
volcanoes have fascinated him from the beginning,
and he has willingly used his fragility
to unravel the mineral susceptibilities of this splendid evil.
Once gestures of magic were entwined around the crater,
today when they becoming scientific the fascination remains.
Nowhere else does reason so collide with the living image of the night of time.
What the possessed mountain spits
is the unconsummated, the virgin, the accomplice of origins,
the substance that already was when everything began.
How to observe objectively this initial crucible of creations?

(Max Gérard)

Human fascination with volcanoes reaches back to the times when volcanoes were associated with some unknown powerful godlike forces. Because volcanic activity could not be predicted, it was viewed as a fierce form of punishment, and was feared by all. In many parts of the world, like Tonga, New Zealand, Tahiti and Hawaii, where volcanic activity is common, native people used to worship volcanoes. In Hawaii, the cult of Pele - goddess of volcanoes - continues today. Similar associations of active volcanoes with actions of a god or gods are common to other civilizations from Mexico, Nicaragua, Java, Bali, Japan, and even in Christian tradition (Krafft and Krafft, 1980). Such reverence toward volcanoes no doubt lies in the fact that violent volcanic eruptions

like those of Vesuvius in Italy (~79 AD), Merapi in Indonesia (1006), Laki in Iceland (1783), Tambora and Krakatoa in Indonesia (1815 and 1883, respectively), Pelée in Martinique (1902), El Chichon in Mexico (1982) and Pinatubo in Philippines (1991), had pronounced damaging effects on large populations. Occasionally, volcanic eruptions can destroy entire civilizations. For example, the eruption of Santorini (Greece) in 1500 B.C. caused the decline of the Minoan world and might have been the source of the legend of Atlantis (Krafft and Krafft, 1980).

In recent years research has come closer to understanding the forces controlling volcanic eruptions and the role of volcanism in generating the very crust of our planet and in initiating the primordial atmosphere. Volcanic activity plays an important part in planetary evolution by renewing/recycling water, CO_2, and the earth's crust, and may even be linked to the origin of life (Decker and Decker, 1991). Volcanic activity can be destructive by burying vast parts of land by ash and mudflows, and poisoning air and water, and beneficial by providing fertile soils, warm springs, and in the long-term leading to the formation of ore-deposits (McDonald, 1972; Krafft and Krafft, 1980; Decker and Decker, 1991). Nutrient rich soils promote agriculture on volcanic slopes in Indonesia and Italy, which in turn leads to dense populations in the areas (McDonald, 1972; Williams and McBirney, 1979). In the United States, New Zealand, Japan, Mexico and Iceland, geothermal energy has a potential to become an alternative energy source.

People are still afraid of volcanoes, but we are coming closer to being able to predict their actions, and are better equipped to study them. We use our knowledge to address questions regarding the effects of volcanic eruptions on the global climate, global outputs of various volcanic components into the atmosphere, and other effects of volcanic activity on the natural environment. We now realize that a single large eruption leads to changes on a global scale; similarly, hundreds of small, passively degassing volcanic centers can contribute significant amounts of various volatiles to the global atmospheric budget. Large amounts of solid material and gases emitted during eruptions often exceed pollution from industrial processes (Williams and McBirney, 1979) reducing incident solar radiation (Lamb, 1970; Sear *et al.*, 1987) and even leading to decreases in surface temperatures and to cooling of the climate, such as happened following the eruptions of Laki and Asama in 1783, or Tambora in 1815 (year without a summer) (Williams and McBirney, 1979; Self *et al.*, 1981; Devine *et al.*, 1984; Self and Rampino, 1988; Stothers *et al.*, 1989; Rampino *et al.*, 1988; Rampino and Self; 1992). Aerosols present in the eruption cloud, especially H_2SO_4 droplets, can contribute to increased cloud cover, leading to increased absorption of solar and terrestrial radiation (Volz, 1975; Pollack *et al.*, 1976; Baldwin *et al.*, 1976; Lazrus *et al.*, 1979; Turco *et al.*, 1982). Due to their long residence time in the stratosphere, the effect of sulfate aerosols produced by a volcanic eruption can be devastating, although it is possible that other processes taking place in the plume may counteract formation of large quantities of sulfates (Pinto *et al.*, 1989). Another plume component, chlorine, can participate in the heterogeneous reaction leading to ozone destruction in the stratosphere (Johnston, 1980; Cicerone, 1981;

Hofmann and Solomon, 1989). It is thought, however, that most of the chlorine present in volcanic plumes is removed prior to its stratospheric injection (Tabazadeh and Turco, 1993).

Recent efforts to establish a global inventory of atmospheric emissions of trace elements from both natural and industrial sources show the need for an improved evaluation of volcanic emissions. Because of the diversity of composition of volcanic sources, and the episodic nature of emissions, it is difficult to estimate exact outputs. Nriagu (1989) estimated that volcanic emanations can contribute about 40-50% of Cd and Hg, and 20-40% of As, Cr, Cu, Ni, Pb and Sb emitted annually from natural sources, showing that volcanoes can potentially dominate the natural atmospheric outputs of some trace metals. Because Nriagu's calculations were based on few data, it is likely that the above values may be underestimated. Thus, if the natural background for estimating the extent of industrial pollution is to be known, there is a need for more accurate studies of volcanic emissions.

1.1. Volcanic gases - an overview of major gas components

Magmas contain various amounts of dissolved volatiles at high pressures that form separate fluid phases during magma ascent and give rise to volcanic gas plumes. Volcanic gases thus provide an opportunity to estimate the volatile content of magmas. However, during the upward travel of magma, the volatile content and speciation can

change when the magma comes in contact with cooler and more oxidized rocks containing meteoric water, sublimates, and organic matter. Furthermore, after degassing from the melt and mixing with atmospheric air, volatiles undergo rapid changes in temperature, pressure, and oxidation (Williams and McBirney, 1979). All of these processes can drastically affect the original composition of volatiles and thus the interpretation of the bulk composition of volcanic gases should be viewed cautiously.

Volcanic gases emitted from the melt cool rapidly and precipitate various solids (sublimates) (Symonds *et al.* 1987; Symonds and Reed, 1993). Some sublimates remain in the gas stream as solid aerosols whereas others are deposited on the walls of the vent forming colorful deposits called incrustations. Incrustations are mixtures of sublimates and other solids formed by processes such as high-temperature alteration of wall-rock (Symonds and Reed, 1993). Two types of incrustations can be distinguished: high- and low- temperature deposits. The chief difference between them is that low temperature incrustations form after the gas undergoes sufficient cooling and oxidation to permit condensation of H_2SO_4 and, subsequently, water, while the high temperature ones are deposited prior to the condensation of H_2SO_4 (Stoiber and Rose, 1974; Symonds et al , 1987; Symonds and Reed, 1993).

Volcanic gases are composed of H_2O, CO_2, SO_2, H_2S, HCl, HF, H_2, NH_3, CH_4, and other less common species. Water and CO_2 are the most abundant constituents and together typically exceed over 90% of total volume emitted (White and Waring, 1963;

Krauskopf, 1979). Apart from the major species, the gases or aerosols emitted by volcanoes also carry variable amounts of trace elements, mostly in the form of chlorides, fluorides, sulfides or sulfates and oxide compounds. Due to the large volume of H_2O and CO_2, these volatiles deserve the most interest, however, they are difficult to routinely measure in volcanic plumes.

Traditionally, other volatile species, such as SO_2 and halogens are considered more useful in characterizing the volcanic activity due to their distinct relation to the composition of a magma source and their fast response to changes in the degassing behavior. These species are also relatively easy to measure. Halogen species can be collected from the plume using filters or condensate bottles, whereas SO_2 can be measured remotely using correlation spectrometer (COSPEC).

1.2. Trace element content of volcanic emissions - general considerations

Trace elements transported in volcanic gases are an important source of information about the magmatic system because their assemblage directly reflects the magma composition and its source. Variations in the amounts of trace elements exsolved from a magma are indicative of the changes occurring in the magmatic body and thus, can possibly be used to predict the eruptive activity. Many of the trace elements emitted from volcanoes are either unique in the natural environment, or their outputs (when compared to that from other natural sources) are significantly higher. Because of these

characteristics, trace elements can be used as tracers for volcanic plumes. An understanding of the process of trace element exsolution and their fate in the plume is essential for predicting the effects of volcanic emissions on the environment. These studies also contribute to the database on the natural sources and chemistry of many atmospheric pollutants, and improves our estimates of global budgets. The correct assessment of natural background for many of these substances is important in order to compare the magnitude of natural emissions with those originating from anthropogenic sources.

A few trace elements such as Au, Cd, Hg, Mo, and W can be volatilized in their elemental states (Symonds *et al.,* 1987; Symonds and Reed, 1993) but generally vapor pressures of trace metals are too low to permit direct volatilization. Instead, the majority of trace elements become mobile by forming volatile compounds with halogens, sulfur and oxygen. Metal halides are characterized by the highest volatility, which accounts for their preponderance in volcanic gases. Less important, but also significant as volatile carriers for metals, are oxides and sulfates (Krauskopf, 1957; 1979; Naughton *et al.,* 1976) whereas volatilities of most sulfides are too low to be important in metal transport from magma.

When volcanic gases cool, most of the volatile metal-carrying compounds undergo a transition to a particulate phase and then possibly further conversion into more complex compounds due to interactions with gas or other particulate material present in the plume,

mixing with atmospheric gases, or due to reaction with wall rock. This complicates the later analysis of collected samples and renders difficult any attempt to reconstruct the original composition of the gas.

Thermodynamic calculations have been helpful in establishing which compounds are most stable in volcanic gases and therefore most likely to occur (Krauskopf, 1964; Symonds *et al.,* 1987; Symonds, 1990; Symonds and Reed, 1993). Such calculations, however, have numerous limitations due to simplifying assumptions used in modeling the magmatic conditions, and need to be used cautiously. Most calculations assume homogeneous equilibrium between the melt and exsolving gas phase, ideal behavior of gas species, and ideal mixing conditions. Another limitation is the reliability of available thermodynamic data. Some of the most extensive modeling examples were presented by Symonds *et al.* (1987), Symonds (1990), and Symonds and Reed (1993) who calculated the stability of over 40 species likely to occur in volcanic gas in the temperature range 100-900°C, at 1 bar pressure, in equilibrium with a dacitic-andesitic melt. Although their predictions may not be extendable to melts of significantly different composition, some observations agree well with data obtained from gas, aerosol, and incrustation samples collected at many volcanic systems.

1.3. Overview of techniques used to sample volcanic gases

The composition of volcanic gas emissions can be estimated using a variety of

methods. Ideally, samples should be collected as close to a gas source as possible to prevent changes in gas chemistry and dilution. The best samples are those collected from high temperature vents, or from low temperature sources visibly related to magmatic sources (Williams and McBirney, 1979). Finally, some residual amounts of gases can also be extracted from fresh lava (Williams and McBirney, 1979). Due to the danger and difficulty in approaching large, high temperature magmatic sources, most samples are collected from smaller vents or from volcanic plumes. In addition to selecting a sampling site, the choices of sampling methods also vary. Scientists are often interested in collecting as many gas species as possible, preferably the total gas samples. Many techniques have been developed to suit the needs of researchers and work best under specific field conditions.

The best samples of major volcanic gas are those collected into evacuated glass tubes inserted into vents or held close to lava during eruption. This technique was pioneered by Jaggar, Day and Shepherd during 1912-1924 at Kilauea (Shepherd, 1925; Jaggar, 1940; White and Waring, 1963), and was later used by Naughton *et al.* (1963). This technique assures low contamination with atmospheric air and provides the most meaningful data on gas composition; however, sampling size is severely limited.

The most popular sampling device for collecting volcanic gases and their condensates is an evacuated glass bottle filled with alkaline solution (Giggenbach, 1975). The bottle is connected through a metal (commonly Ti) tube to the fumarole vent, and

the gas is allowed to bubble through the solution. Gases contained in the head space of the bottle are analyzed by gas chromatography whereas the resulting solution is analyzed by ion chromatography or other wet chemical methods.

Another way of sampling the emitted material directly at the vent of a fumarole, or at close proximity to the crater is by using filter packs (Zoller *et al.*, 1983; Olmez *et al.*, 1986; Crowe *et al.*, 1987; Finnegan *et al.*, 1989; Kitto *et al.*, 1988). A filter pack is a stack of several filters consisting of at least 1 teflon (PTFA) or polycarbonate filter designed to sample particulates, followed by treated filters, which are cellulose filters impregnated with a mixture of base and glycerol and designed to capture acidic gases. A number of different bases can be used to prepare treated filters, ^{7}LiOH being most common. The filter pack is connected to a portable pump with flowmeter, and the sampling time and flow rates are monitored to establish the amount of air flowing through the filter pack. The advantage of this method is its versatility; the filter pack can be used either in the stationary mode or it can be mounted on an aircraft and sample aerosols while traversing the plume. Filters collected in such a way are then analyzed by instrumental neutron activation analysis (INAA), X-ray fluorescence (XRF), or ion chromatography; additionally, particulate filters can be inspected using scanning electron microscope (SEM) with energy dispersive X-ray probe (EDXRA) for the presence of solid particles.

The particles present in a volcanic plume can also be sampled using a variety of cascade impactors (Vie le Sage, 1983). A quartz crystal microbalance (QCM) (Chuan *et al.,* 1975; Rose *et al.,* 1980) is an example of such a device. The QCM allows one to study the size distribution of particles present in the plume and can also serve as a collector of aerosols for a qualitative analysis of shape and composition.

Among other methods used to study volcanic plume composition is the analysis of fresh volcanic ash leachates (Rose, 1977; Nehring and Johnston, 1981; Smith *et al.* 1983). Fresh volcanic ash contains abundant soluble salts, whose accumulation is probably caused by scavenging by ash particles of metal-chlorine and metal-sulfur compounds from the gas plume during fallout. Samples of fresh ash are leached, and the resulting solution is analyzed. In addition to the main species (Na, Ca, SO_4 and Cl), other elements (K, F, Mg, Mn, Zn, Cu, Ba, Se) are often detected in leachates. They occur mostly as trace substitutions in the halide and sulfate minerals, or as trace minerals. Based on their relative enrichments in the leachates compared to their concentrations in the ash itself, some elements such as Zn, Cu, Na, and K may be derived (at least partly) from the eruptive gas rather than the ash (Rose, 1977).

Finally, the chemistry and zoning of incrustation deposits can be used to interpret the distribution of trace elements in the volcanic gas and their cooling sequence (Stoiber and Rose, 1974; Symonds, 1992; and others). However the results can be misleading because of difficulties in distinguishing between sublimate and alteration deposits in

incrustations (Symonds and Reed, 1993). To overcome this, sublimates can be sampled directly from the vent in silica tubes (Le Guern and Bernard, 1982; Bernard and Le Guern, 1986).

In order to estimate the speciation of metal compounds in samples of volcanic gases and aerosols many workers use the statistical methods, for example calculating correlation coefficients for various ion pairs (Stoiber and Rose, 1970; Rose, 1977; Buat-Menard and Arnold, 1978; Smith *et al.,* 1983). This method helps to establish what phases are likely to occur in the volcanic plume by looking at the cation-anion pairs with strong correlation coefficients. Many of the compounds inferred this way have been described in volcanic plumes, which speaks favorably of the method. Many of the cations, however, tend to have high correlations with a group of ions rather than forming discrete pairs. These complicated arrangements probably indicate the formation of complex salts in the volcanic plumes.

1.4. Objectives of this work

The objectives for this study of Mount Erebus was two-fold. Firstly, because of its location, Mount Erebus provides a unique opportunity to monitor a natural volcanic source which discharges gases and aerosols into the Antarctic environment, one which is virtually devoid of anthropogenic pollutants. There is a need to evaluate such local sources to establish the background for monitoring global pollution. Secondly, study of

Mount Erebus provides data on the composition and concentrations of volatile emissions from an unusual, highly evolved, alkaline magma which emits gases containing high concentrations of halogens and various trace metals. Alkalic volcanism has been widespread in the geologic past, as manifested by the profusion of alkaline volcanic rocks in Eastern Africa and Antarctica, but presently active alkaline volcanoes are rare, making the thorough study of Erebus all the more important.

Previous studies of the halogen content of the Mount Erebus plume conducted during the 1986 field season indicated very high Cl content, which, when combined with the available SO_2 output data from COSPEC gave emission rates comparable to lower limits of global halogen emissions from volcanoes (Meeker, 1988; Kyle *et al.*, 1990). These findings brought serious doubts about the validity of such global evaluations, suggesting possible underestimation of volcanic Cl emissions. More importantly, they also brought questions about the environmental impact of Mount Erebus on the Antarctic atmosphere, in particular, the possible importance of Mount Erebus emissions as a source of Cl for ozone destruction. Another issue was a possibility of wide dispersal of the plume from Mt. Erebus over Antarctica leading to the deposition of volcanic Cl in snow and ice in the Antarctic Plateau. Samples for the study were collected in December 1988, November and December 1989, and January 1991.

The goal of this study was to provide a detailed record of the volcanic emissions of Mt. Erebus by summarizing the observations collected from Mt. Erebus over the last

few years (gas data collected between 1986-1991, measurements of SO_2 extend from 1983 to 1991). It was hoped that the extensive long-term monitoring of gases (combined SO_2 record and other gas data) would give a better understanding of changes in the eruptive behavior of Mount Erebus and insight into possible fluctuations in the composition of magma, and thus lead to the development of a model describing the degassing process at Mt. Erebus.

In particular, the project goals were to:

(1) assess changes in the gas composition as expressed by the discharged amounts of its major (S,F, and Cl) and trace (Na, K, Ca, Al, Fe, Cr, Zn, Cu, As, Se, Sb, Br, Co, Cd, Mo, W, Rb, Cs, In, Au, and REE) components;

(2) discuss possible processes governing transport of trace elements from the magma and their conversion in the plume by examining the relationship between concentrations of trace elements and halogen and sulfur content of the plume;

(3) evaluate Erebus activity on a global scale by comparing the total estimated emission rates of halogens, sulfur, and trace elements to these of other volcanoes;

(4) evaluate the potential impact of Erebus emissions on the Antarctic environment; and

(5) improve sampling techniques and establish simple analytical procedures for filter analysis for future work.

A second aspect of this study was directed to the study of salts occurring in the summit area of Mt. Erebus. These salts are thought to originate from the interaction of

the volcanic plume and rocks present in the area. The objective of this study was to determine a possible link between the formation of salts and the composition of the Mt. Erebus plume. Such correlations can be useful in the studies of extinct volcanoes, and would allow the partial reconstruction of gas composition from the composition of volcanic salt deposits. The successive steps in this study were (1) mineralogical description of the salts; (2) description of salts occurrence in the summit area, and possible zoning with increasing distance from the crater; (3) comparison of the chemical composition of salts with the composition of the volcanic plume; and (4) development of a simple model describing the formation of the salts.

2. MT. EREBUS

2.1. Location and geology

Mt. Erebus, the only presently active volcano in Antarctica, is a stratovolcano situated on Ross Island (Figure 2.1). The rocks building Mt. Erebus and other adjacent volcanic centers (Moore and Kyle, 1990) belong to the McMurdo Volcanic Group which incorporates the Late Cenozoic and Recent intraplate alkaline volcanics occurring along the western margins of the Ross Sea and Ross Ice Shelf (Kyle, 1990). The McMurdo Volcanic Group is made up of several smaller subdivisions: Hallett, Melbourne and Erebus volcanic provinces (Kyle, 1990; Kyle and Cole, 1974). The Erebus volcanic province occupies the south-western part of the Ross Sea and adjacent parts of the Transantarctic Mountains. Mt. Erebus and the satellite volcanic centers (Mt. Terror, Mt. Bird, Hut Point Peninsula) are all located on Ross Island. In addition to the volcanoes mentioned above, the Erebus volcanic province also includes White Island, Black Island, Brown Peninsula, Mt. Discovery, Mt. Morning, Minna Bluff and Beaufort Island.

The volcanic centers found on Ross Island are radially distributed around Mt. Erebus at 120° angles. This geometry suggests radial fractures associated with the crustal doming caused by a raising mantle plume or a hot spot (Kyle *et al.*, 1992). Similar radial geometry is also displayed around Mt. Discovery.

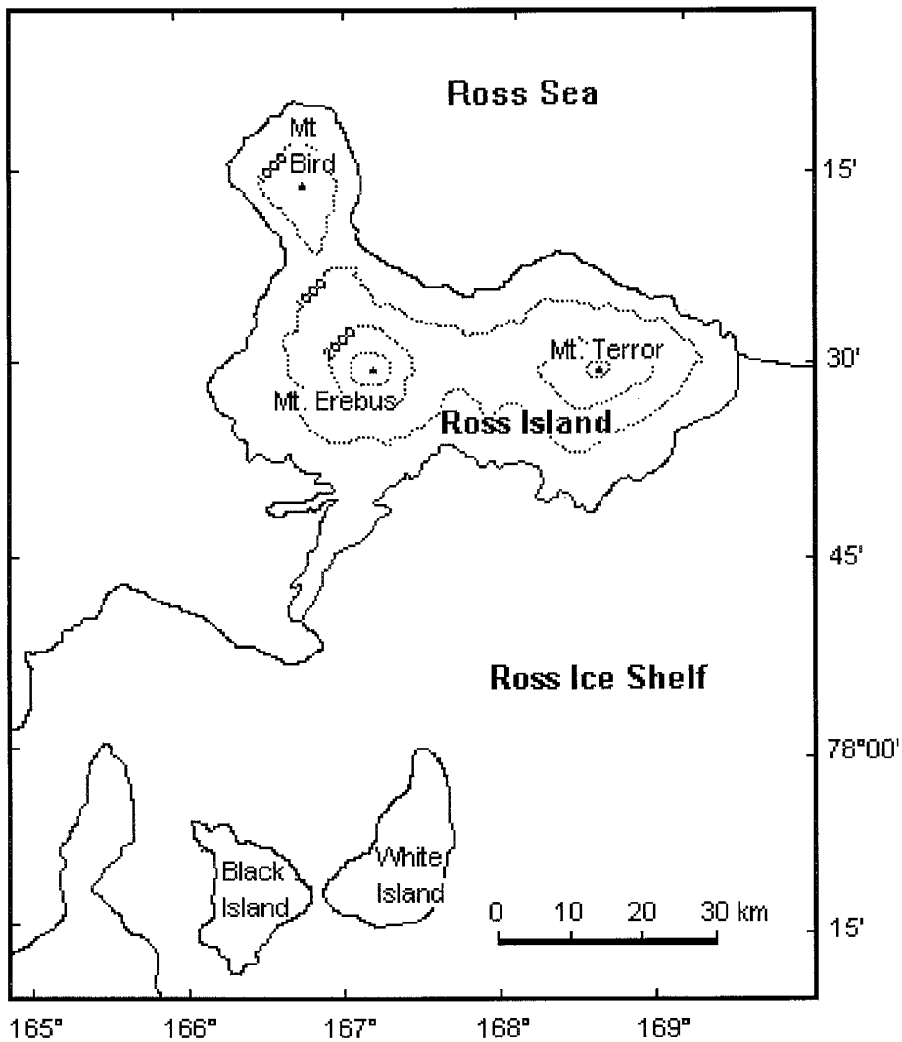

Fig. 2.1. Map of Ross Island showing location of Mt. Erebus.

The oldest surface samples in the Erebus volcanic province are dated by the K-Ar method at 19 Ma (Kyle, 1990). Ross Island volcanism commenced about 4 Ma when Mt. Bird was formed (4-3 Ma). Activity associated with the development of Mt. Terror lasted between 2 and 0.6 Ma, and that of Hut Point Peninsula between 1.8 and 0.4 Ma. Mt. Erebus, which is the youngest of all the volcanic centers on the island, is less than 1 Ma old. The ages of lavas building Mt. Erebus' slopes and plateau range from 0.94-

0.15 Ma, while the summit is probably 0.15 Ma or younger (Moore and Kyle, 1990).

Rocks building Mt. Erebus form a strongly undersaturated sodic differentiation trend (also called the Erebus Lineage, EL) consisting of basanite, ne-hawaiite, ne-mugearite, ne-benmoreite, and anorthoclase phonolite (Kyle *et al.*, 1992). The dominant rock type on Mt. Erebus is a porphyritic anorthoclase phonolite containing phenocrysts of anorthoclase, olivine, opaque oxides, clinopyroxene, apatite and nepheline. The geochemistry of Erebus lavas indicates that they evolved from a parental magma of basanite composition by fractional crystallization of observed phenocryst phases. Strontium isotope evidence ($^{87}Sr/^{86}Sr = 0.7032$) indicates negligible crustal contamination during the evolution of Erebus Lineage rocks (Kyle *et al.*, 1992 and references therein).

Other volcanic centers on Ross Island (mainly basanite in composition) define the Dry Valley Drilling Project (DVDP) lineage. Geochemistry of these rocks indicates that they evolved from a parental magma at lower temperature than EL rocks (Kyle, 1981). There is a minor amount of less undersaturated, iron rich rocks (benmoreites, phonolites and trachytes) forming the enriched iron series (EFS). The higher Sr isotope ratio of these lavas ($^{87}Sr/^{86}Sr = 0.7049$) indicates some crustal contamination effect (Kyle *et al.*, 1992).

Mt. Erebus is located in the western part of Ross Island (77°32' S, 167°10'E) and is the highest volcano (3794 m a.s.l.) in the McMurdo volcanic group. Below 2000 m

elevation Mt. Erebus forms a gentle sloping cone surrounded by a few parasitic vents. Above 2000 m elevation, the slopes are steeper (30-40°) and covered by anorthoclase phonolite flows. The summit region is a plateau surrounded by a high rim which probably represents an old infilled caldera. On the south side of the summit plateau lies the active summit cone covered by bombs and deposits of anorthoclase crystals. Within the cone there are two adjacent elliptical craters: the currently active "Main Crater" (600 m by 500 m) and a smaller inactive "Side Crater" on the south side. "Main Crater" is about 110 m deep with a flat floor. In the northern part of "Main Crater" lies a large depression ~ 250 m in diameter and ~ 100 m deep called "Inner Crater" which contains the active vent and phonolite lava lake (Kyle, 1990).

2.2. Eruptive history

Since the discovery of Mt. Erebus in 1841 by Sir James Ross who described violent eruptive activity of the volcano, little has been recorded about its eruptive behavior until 1971 when the direct surveillance of Mt Erebus began. A small lava lake inside its crater was discovered in 1972 (Giggenbach *et al.*, 1973). Following this discovery, a small increase in the lava lake area was observed from year to year until 1978 when the lake reached about 60 m in diameter (Kyle *et al.*, 1982; Kyle *et al.*, 1994). The lake then remained uniform in size until 1984. From 1972 to 1984 slow convective motion of the lava in the lake was observed together with explosive eruptive activity occurring at a frequency of about 4 to 6 eruptions per day. Small ash eruptions

with columns up to 0.5 to 1 km above the crater were rare. During stronger explosions, bombs were thrown over 500 m high and occasionally landed on the crater rim. Weak explosions or bursts within the lava lake were also observed, and non-explosive eruptions during which dark ash was emitted from the vents surrounding the lake (Dibble *et al.,* 1984; 1988; Kyle *et al.,* 1994). On September 13, 1984 Mt. Erebus entered a 4 month period with more frequent and larger eruptions. Bombs up to 10 m in diameter were ejected over 2 km from the vent and vertical ash columns reached 3 km above the crater. The Inner Crater was filled with the ejected material, and the lava lake was buried underneath it. By January 1985, a small pool of lava was exhumed from under the ejecta blanket. Since then there has been a slow increase in the size of the two small lava lakes. The frequency and size of strombolian eruptions declined in January 1985 with 1 to 2 small strombolian eruptions per day which very rarely ejected bombs onto the Crater rim and occasionally on the Main Crater floor. Less violent, burst-like events are still frequently observed. They are accompanied by emissions of water vapor and other gases from the lava lake and small vents located on the lake perimeter. The size and overall geometry of the lava lake are changing constantly in response to Erebus activity (Kyle *et al.*, 1994; Meeker, 1988). The level of activity increased slightly in January 1991, approaching pre-1984 levels and has continued (Kyle, pers. comm.).

2.3. Previous work

The monitoring of activity of Mt. Erebus includes studies of seismic activity, observations of eruptions and lava lake geometry, monitoring of SO_2 emissions and sampling of gases. Due to the remoteness of Mt. Erebus, most of those observations are not continuous, and are made during short field seasons, usually from December to January.

The first estimates of gaseous outputs from Erebus were made in 1978 by Polian and Lambert (1979) who estimated a SO_2 flux of 3 $Mg.day^{-1}$ (1 $Mg = 10^6 g$). Radke (1982) reported SO_2 flux ranging from 35 to 155 $Mg.day^{-1}$ (data collected in 1980). Regular observations of SO_2 output from Erebus using a Barringer correlation spectrometer (COSPEC V) started in 1983 (Rose *et al.*, 1985) and since then care has been taken to collect at least a few measurements during every field season. Most of the observations span a period of several hours per day. COSPEC measurements are considered to be more reliable than estimates obtained using other techniques (Kyle *et al.*, 1994) chiefly because they are based on a large number of measurements. The recent studies by Sybeldon (1991) and Kyle *et al.* (1994) summarize the results of COSPEC measurements collected at Erebus between 1983-1991. Chapter 3 gives a short description of the method. Chapter 4 presents short overview of previous studies, and a discussion of the temporal trends in the SO_2 record, concentrating on the results of a time-series analysis of data.

Meeker (1988) studied gas and aerosols emitted from Erebus and provided some insights into their composition. These preliminary data indicated that the Erebus plume is rich in halogens and is characterized by high Cl/S (9-62.5) and F/S (0.34-1.4) ratios. Meeker (1988) and Kyle *et al.* (1990) also noted that elements such as In, As, Hg, Zn, Au, Se, Co, W, Cs, Mo, Rb, Cu, Na, and K were enriched in the Erebus gas with respect to the magma. Most of the metals were postulated to be removed from the melt as chloride compounds but some of them may later react with other components of the plume. Especially interesting is the occurrence of elemental gold in aerosol samples, probably formed by reducing Au-Cl complexes by sulfur (Meeker *et al.*, 1991). Other studies of particulate aerosols were done by Chuan *et al.* (1986), Chuan (1994), Rose *et al.* (1985). Sheppard *et al.* (1994) presented estimates of composition of the Erebus plume and an evaluation of the outputs of various gases.

Zoller *et al.* (1974) and Maenhaut *et al.* (1979) described trace element composition of atmospheric aerosols near the South Pole indicating a possible volcanic input. Palais *et al.* (1989; 1994) detected high amounts of Cl and trace elements in snow samples from the Ross Island area suggesting that Erebus was a potential source for some of these elements.

Salts present in the summit area of Mount Erebus were studied by Keys (1980) and Keys and Williams (1981). They are composed of Al, Na, Mg, Fe, K, Ca, Cl, S, F, and Si (Keys, 1980). Among minerals identified were halite (NaCl), gypsum

($CaSO_4 \cdot 2H_2O$), alunite ($KAl_3(SO_4)_2(OH)_6$), thenardite (Na_2SO_4), sylvite (KCl), mirabilite ($Na_2SO_4 \cdot 10H_2O$) and calcite ($CaCO_3$). Many other substances were also tentatively identified: chloraluminate ($AlCl_3 \cdot 6H_2O$), alunogen ($Al_2(SO_4)_3 \cdot 18H_2O$), jarosite ($(K,Na)(Fe,Al)(SO_4)_2(OH)_6$), malladrite ($Na_2SiF_6$), sulphohalite ($Na_6ClF(SO_4)_2$), aluminum trifluoride ($AlF_3 \cdot 3H_2O$), sodium aluminum oxychloride ($NaAl_4O_4Cl_5$), hydromolysite ($FeCl_3 \cdot 6H_2O$) and ralstonite ($NaMgAl(Fe,OH) \cdot H_2O$) (Keys, 1980; Keys and Williams, 1981). Many of the salts found on Erebus are mixtures of mineral phases, and their identification by XRD is often complicated by peak overlap and ionic substitutions.

The chemistry of Erebus salts is unusual when compared to volcanic salts from other localities. As noted by Keys (1980), what makes the Erebus salts unique is the absence of elemental sulfur, the general predominance of chlorides, and the presence of unusual components such as $NaAl_4O_4Cl_5$. Components such as $AlF_3 \cdot 3H_2O$, not known previously to occur in nature, have also been described from Mt. Erebus (Rosenberg, 1988).

The origin of salts at Mt. Erebus is not fully understood. Keys (1980) attempted to determine the processes leading to the formation of different salts by comparing their trace and rare earth element composition, as well as their elemental and ionic ratios with those of Erebus rocks and with data available from other volcanoes. This comparison verified the volcanogenic origin for some types of salts. Although gas-rock interaction was proposed as the process leading to the formation of salts, Keys (1980) did not report

any consistent similarity between the phonolitic rock and salt composition. Keys (1980) also suggested that some salts could be deposited directly from the plume, and their distribution may be a function of the wind pattern. Direct deposition from the plume was also suggested as a possible origin of $AlF_3 \cdot 3H_2O$ in Erebus salts by Rosenberg (1988).

There is a possibility that some salts may be of marine origin or they may be formed by interaction of snow and ice "saturated" with acids from the plume with the rocks. In such a case the origin of salts can not be easily fingerprinted. Due to the complex mineralogy of salts the use of stable isotopes of oxygen or hydrogen is very restricted. Jones *et al.* (1983) successfully employed isotopes of strontium to distinguish between volcanic and marine sources for selected salts from Mt. Erebus. The strontium isotope signature of yellow salts from the Erebus summit (average $^{87}Sr/^{86}Sr=0.70345$) indicates their volcanogenic origin, but it is impossible to determine whether the salts were deposited directly from the plume or formed by weathering of the phonolite rocks. Some white salts (collected from the ice cave on Erebus) appear to have a high strontium isotope ratio ($^{87}Sr/^{86}Sr=0.7046$), indicating mixing between the two sources of Sr (volcanic and marine). The marine component in the salt is thought to be introduced by melting of the snow in the cave (Jones *et al.* 1983). Due to the limited number of samples analyzed in the study of Jones *et al.* (1983) it is difficult to extend this interpretation to the entire area of Erebus summit.

3. DATA COLLECTION AND ANALYTICAL TECHNIQUES

3.1. Sampling of gases

During December 1988, December 1989, and January 1991, 60 samples of gas and particulates were collected using the filter pack method (Finnegan *et al.* 1989; Kitto *et al.* 1988). In addition, I present new data on 9 samples collected in December 1986 and previously analyzed by Meeker (1988). Throughout the sampling period, 2 kinds of filter packs were used: Nuclepore 47 mm filter packs, and custom-made filter packs, accepting 110 mm filters. Each filter pack consisted of 1 particulate filter followed by 2 or more base treated filters. Teflon (PTFE) Fluoropore and Zefluor 1.0 μm pore size filters were used as particulate filters; in 1988 we also used Nuclepore 0.4 μm filters; and in 1991 Sartorius PTFE filters. Base impregnated (treated) filters were prepared by saturating Whatman 41 (110 mm) and Whatman 541 (47 mm) filter papers with 3 M ^{7}LiOH solution prepared using purified ^{7}Li metal, 80% deionized water and 20% glycerol (Finnegan *et al.,* 1989). In 1986 we used 1 M ^{7}LiOH solution, which proved to be insufficient especially for longer sampling periods. The stronger base improved filter performance, and the treated filters did not become saturated with acids as quickly. All samples were collected from the same sampling site, located on the north and northeast rim of the Main Crater. During sampling the volcanic plume trailed over the sampling site; filter packs were suspended over the rim. Filter packs were connected to a small pump with attached flowmeter. Sampling times varied between 30 minutes and a few

hours. The average flow rate was 0.05 m^3 min^{-1}. After collection, filter packs were unloaded, filters folded in four to protect the outer surface, and stored in separate sterile plastic bags. All filters were kept frozen until the time of analysis. Table 3.1 gives the sample parameters (date of sampling, filter size and volume of the air).

Because of the remoteness of the sampling site and other logistic difficulties, sample collection at Erebus is restricted to the short period during Antarctic summer months (usually between November and January). To our knowledge (partially supported by monitoring of the seismic activity, and by the visual observations of the Erebus lava lake conducted for several months each year from New Zealand science camp), the activity of Erebus (as expressed by the frequency and magnitude of eruptions, and movement of lava in the lake) does not appear to change drastically from month to month. Therefore, we believe that data collected within the sampling periods are representative of the whole year.

Table 3.1. Date, filter size and volume of samples collected on Erebus.

Sample	date	size	vol m^3
86-1	Dec. 19	110	1.38
86-2	Dec. 19	110	4.96
86-3	Dec. 20	110	3.15
86-4	Dec. 20	110	2.10
86-5	Dec. 21	110	3.80
86-6	Dec. 22	110	4.32
86-7	Dec. 23	110	1.80
86-8	Dec. 24	110	1.11
86-9	Dec. 24	110	5.07
88-1	Dec. 13	110	7.00
88-4	Dec. 16	47	1.10
88-5	Dec. 16	47	1.20
88-6	Dec. 16	47	1.20
88-7	Dec. 16	47	1.00
88-8	Dec. 16	47	1.01
88-9	Dec. 16	47	1.01
88-2	Dec. 16	110	6.22
88-3	Dec. 17	110	9.38
88-11	Dec. 20	110	3.73
88-13	Dec. 20	110	11.19
88-15	Dec. 21	110	6.75
89-1	Nov. 24	110	1.50
89-2	Dec. 02	110	2.92
89-3	Dec. 03	110	3.46
89-4	Dec. 04	110	4.02
89-5	Dec. 06	110	8.54
89-6	Dec. 07	110	13.12
89-15	Dec. 11	47	2.07
89-16	Dec. 11	47	2.80
89-17	Dec. 11	110	4.82
89-20	Dec. 14	110	10.78
89-21	Dec. 14	110	9.35
89-23	Dec. 16	110	12.27
89-24	Dec. 17	110	15.50
89-25	Dec. 18	110	5.05
89-26	Dec. 20	47	2.47
91-1	Jan. 13	110	3.65
91-2	Jan. 14	110	9.79
91-3	Jan. 14	110	9.79
91-5	Jan. 15	110	6.93
91-6	Jan. 16	110	3.86
91-7	Jan. 16	110	6.43
91-8	Jan. 17	110	5.99
91-9	Jan. 17	110	4.59
91-11	Jan. 18	110	1.61
91-21	Jan. 22	110	10.36
91-23	Jan. 23	110	11.68

3.2. COSPEC measurements

Sulfur dioxide emissions were measured using a Barringer COSPEC V correlation spectrometer (Stoiber *et al.*, 1983). The COSPEC is equipped with a telescope which is directed toward the plume and scans the incident solar radiation. COSPEC measures the amount of solar radiation energy absorbed by SO_2 and compares it to the amount of radiation energy produced by SO_2. The ratio of the two energies is proportional to the amount of SO_2 present. The changes in the intensity of solar ultraviolet radiation during the day are corrected by an automatic gain control in the COSPEC which adjusts the sensitivity of the instrument. Moreover, the instrument is frequently calibrated by inserting a cell with a known amount of SO_2 into its field of view. Meeker (1988), Sybeldon (1991) and Kyle *et al.* (1994) give detailed descriptions of the method and discuss the process of data reduction and associated errors.

The first COSPEC measurements of SO_2 at Erebus in 1983 were made by flying an aircraft equipped with a COSPEC (Rose *et al.*, 1985). The instrument looked up vertically through the plume. Since 1984, measurements have been made in the stationary mode, with the instrument in a fixed position on the ground. Data collected between 1984 and 1987 were obtained by manually scanning the COSPEC across the plume, while the output was recorded on a strip chart recorder. Since 1988, the COSPEC has been mounted on an automatic scanning head which improves the scan angles and allows an increase in the duration of data collection. In the automated

technique, data are collected and stored using a lap-top computer (Kyle and McIntosh, 1989).

Data reduction requires the information on the distance from the plume (approximately 2 km), scan angle (measured by Brunton compass mounted on COSPEC) and information on plume rise velocity. Plume velocities were obtained using video recordings of the plume which accompany most of COSPEC measurements.

3.3. INAA

The majority of analyses performed on both filter samples and salts were performed using INAA which allows for acquisition of data on many major and trace elements in small quantities of sample.

In the analysis of filter samples, portions of a filter (a quarter of 110 mm filter or a half of 47 mm filter) were loaded in small polyethylene vials. Whenever possible, the same part of a filter was used throughout the analysis. The first part of the procedure (analysis of elements with short half-lives) took place directly in the reactor facility. Samples collected in 1986, 1988 and 1989 were analyzed using the automated pneumatic tube system in Omega West Reactor, at Los Alamos National Laboratory (LANL), Los Alamos, New Mexico. Samples collected in 1991 were analyzed using a similar procedure at the University of Missouri Research Reactor (MURR) in Columbia,

Missouri. In the second part of the procedure (analysis of elements with longer half-lives), the sample vials were loaded in aluminum cans and irradiated for 14 hrs at the Texas A&M reactor, and then shipped back to NMIMT for counting.

A slightly different procedure was used to analyze salt samples. The analysis of short-lived elements took place at LANL. Small aliquots of sample (50 mg) were sealed into polyethylene bags, irradiated in the pneumatic tube system at the Omega West Reactor at LANL and analyzed in the counting facility. The second part of the procedure follows the standard technique used for rock samples as described by Hallett and Kyle (1993). A 50-100 mg aliquot of sample was tamped and sealed in ultra-pure silica vials. Samples, aligned side by side, were wrapped in a sheet of aluminum foil for irradiation at MURR. The package containing the samples was aligned around the wall of 3.35 inch diameter irradiation container and rotated during irradiation. Samples were left to cool in the reactor pool for 50-100 hours before shipment to NMIMT where they were counted. The details of the procedure, together with the discussion of possible sources of errors, and the assessment of precision and accuracy of the measurements are given in the appendix A1.

3.4. Ion chromatography

Sulfur (as sulfate ion) on all filters, as well as F on particulate filters were analyzed using ion chromatography (Finnegan *et al.*, 1989). A portion of each filter was

leached in 10 g of deionized water containing ~1 g H_2O_2. Plastic disposable centrifuge tubes containing the samples in leaching solution were left in an ultrasonic bath for 24 hrs, then placed on a shaker for 12 hrs. Such treatment usually resulted in disintegration of treated filters. The solution was then filtered through 0.22 μm filters and analyzed. All analyses were performed at the New Mexico Bureau of Mines and Mineral Resources laboratory using a Dionex 4000i model ion chromatograph. To assure the similarity of matrix in samples and standards, a large number of treated filters were leached using the same proportion of filter-to-leaching solution. The leachate was then filtered and used as the matrix in standard preparation. All standards were prepared gravimetrically by dissolving a known amount of K_2SO_4 and KF reagent grade salts in the matrix, and then by proportional dilution. In the analysis of particulate filters, deionized water + H_2O_2 was used as the matrix for standard preparation. Quality assurance standards were prepared by pipetting a known amount of K_2SO_4 and KF water-based solutions onto treated filters. For the details of standard and unknown preparation see appendix A2.

The precision of measurements was assessed by measuring selected samples and standards in duplicates; the reproducibility of the results was better than 5%. The accuracy of measurements was assessed by comparing the obtained values with the known concentrations of the quality assurance standards; the measured concentrations were usually within 2 sigma from the expected values. Because the obtained values were consistently lower than the standard concentrations, it was suspected that the leaching of filters was not complete. After extending the leaching time for filter samples, the

accuracy of the measurements improved to 1-1.5 sigma.

3.5. XRD

To obtain information on salt mineralogy, salt samples were analyzed using X-ray diffraction (XRD) technique. Samples were powdered in an agate mortar, and pressed into small pellets. X-ray diffraction spectra were obtained using a step scan of 0.05° over 2θ angles between 3 and 60°. The background and Cu-K_α peaks in each X-ray powder diffraction pattern were determined using the RIGAKU peak finding program. The initial comparison and matching of patterns based on d-spacings, 2θ values and intensities was performed using the RIGAKU search program. The final identification was done by comparison of patterns with JCPDS file cards.

4. SO_2 EMISSIONS

Sulfur dioxide is one of the routinely measured volatiles at volcanoes. Although it is less abundant in volcanic gases than water and CO_2 and constitutes usually only 2-30 mole% (Anderson, 1975), it is often considered to be the most sensitive volatile in predicting eruptive behavior. It can be measured with great precision due to low background in the atmosphere and its concentrations are not likely to be affected by contamination with groundwater, meteoric water or ambient air (Gerlach, 1980). Other S-bearing gaseous components (H_2S, COS, etc.) are usually less important in volcanic emissions, because of their rapid oxidation in the atmosphere; such conditions are usually dominant at most volcanoes (Symonds *et al.* 1990).

SO_2 measurements at Erebus were performed using a Barringer COSPEC V correlation spectrometer (Chapter 3). Sybeldon (1991) and Kyle *et al.* (1994) presented reviews of the method and detailed descriptions of collected data. The amount of SO_2 emitted from Erebus fluctuated during the study period (1983-1991) and shows a weak correlation with the size of the exposed lava lake in the crater. Kyle *et al.* (1994) postulated that a decrease in lava lake size significantly diminishes the volume of magma from which exsolution of SO_2 occurs; this leads to the conclusion that S exsolution from the melt occurs at very shallow depths. This finding is in agreement with the studies by Gerlach (1986) at Kilauea volcano. Another particular characteristic of SO_2 output from Erebus is that it occurs in discrete burst or puffs. Puffing is a characteristic of many

volcanoes, but its cause is not well understood; it could be related to the dynamics of magma vesiculation (Andres *et al.* 1991; Sybeldon, 1991; Sparks 1977; Wilson and Head, 1981). Observations of the magnitude of SO_2 outputs following small eruptions at Erebus show no increase or sometimes a small decrease in SO_2 emissions. This indicates that volatiles exsolving at greater depths do not contain S, which supports the above idea of S exsolution from the magma (Kyle *et al.,* 1994). The observed fluctuations in SO_2 output combined with observations of variable proportions of other volatiles found in gas samples (Chapter 5) point to the conclusion that the exsolution of volatiles is not a steady-state process. It could be that the process of exsolution of volatiles from melt has rates similar to the bubble travel time through the magma column; thus gas composition would be expected to vary over short intervals. It can be hypothesized that magma entering the Erebus conduit is already partially vesiculated (probably due to CO_2 exsolution). The critical state of vesiculation when magma can no longer hold the volatiles, can thus be reached at depths below the saturation depth of S (or other volatiles), leading to differences in gas composition. This hypothesis is further expanded in Chapters 5 and 6.

Some of the observed fluctuations in SO_2 output are of large magnitude (exceeding the precision of measurement) and appear to be semi-cyclic. This cyclicity may be associated with convection rates within the magma column (Kyle *et al.,* 1994). This hypothesis is supported by qualitative observations of lava movement on the exposed lake surface. To test this hypothesis Sybeldon (1991) attempted to use time-series analysis

of COSPEC measurements to isolate consistent periodic behavior in the data. The study led to the identification of signals occurring with a periodicities of 10-15 minutes, 20 minutes, 30-40 minutes, and 80-100 minutes. Data sets vary between years in the type of signals but generally short-term periodicity (about 10 minutes) was observed in most sets (Sybeldon, 1991). Most data sets also have one or two strongly defined cycles with long periods, 30-50 minutes and 60-80 minutes. There are many limitations to this analytical approach (see for example Shumway, 1988; Sybeldon, 1991) such as the limit to periods shorter in length than one-half of the total length of the data series, or restriction to periods that are represented by regular sinusoidal cycles. Furthermore, the actual data sets differ in the number of observations and in spacing between observations, and many data sets contain long gaps. All these features may severely distort the picture of the actual process.

In this study I have analyzed selected data sets in order to further isolate the periodic signals in SO_2 output, using the method of spectral analysis described by Shumway (1988) and program routine developed by Shumway (1988). The program calculates the smoothed spectrum for each input series. Because program requires that the input series is stationary (the mean value is constant over time), all input series are detrended by applying a transformation which improves the stationarity. In this case, a linear filter was used to adjust for the possible linear trend present in some series. If necessary, series are also extended (by adding zeros) to the length T'. The new length is the nearest power of 2 greater than the existing length of series (T). The DFT

(Discrete Fourier transform) of the random variable X(k) is calculated from :

$$X(k) = T^{-1/2} \sum_{t=0}^{T'-1} x_t \exp(-2\pi i \nu_k t) \quad (1)$$

for values of k ranging from 0 to T'-1, with the frequency interval υ_k=k/T' (measured in cycles per point). The program computes the smoothed spectrum, which is then subsampled at frequencies of the form ω_k=k/M, where M<T'. The DFT can also be represented in terms of sine and cosine transforms:

$$X_S(k) = T^{-1/2} \sum_{t=o}^{T'-1} x_t \sin(2\pi \nu_k t) \quad (2)$$

$$X_C(k) = T^{-1/2} \sum_{t=o}^{T'-1} x_t \cos(2\pi \nu_k t) \quad (3)$$

Because the time lags of different frequencies may produce negative values of either sine of cosine components of the transform, they are combined into a periodogram function P_x(k) which gives the measure of the sample variance as a function of frequency υ_k:

$$P_x(\nu_k) = [X_C^2(k) + X_S^2(k)] \quad (4)$$

To minimize signal distortion I limited the input series to the portion of data set portion containing the longest uninterrupted measurements with no gaps longer than twice the duration of the sampling interval (commonly 2-3 minutes). Figures 4.1-4.4 show the periodograms obtained in the calculations. The period of each signal (manifested by a peak on the periodogram) is simply a reciprocal of the frequency. In general, the results of these calculations are similar to those of Sybeldon (1991) but more similarity was

observed when individual data sets were compared. Also, by selecting long sequences of uninterrupted data, better resolution of the frequency peaks was obtained. The observed signals have periodicities varying from 10 to 100 minutes (Figures 4.1-4.4). In particular, signals with periodicities of 4-6, 7-8, 10-15 minutes, ~20 minutes, ~30 and 50-60 minutes, 80-100 minutes, and > 100 minutes were isolated. Period lengths shorter than 4 minutes were rejected because their length approaches that of the sampling interval. It seems reasonable to assume that the observed semi-cyclicity in SO_2 emissions is related to magma movement and the consistency in the obtained results supports this. The longer periods could be related to upwelling movements of magma in the conduit which supplies fresh undegassed melt. The short-term periodicity is possibly a manifestation of magma movement in the lake.

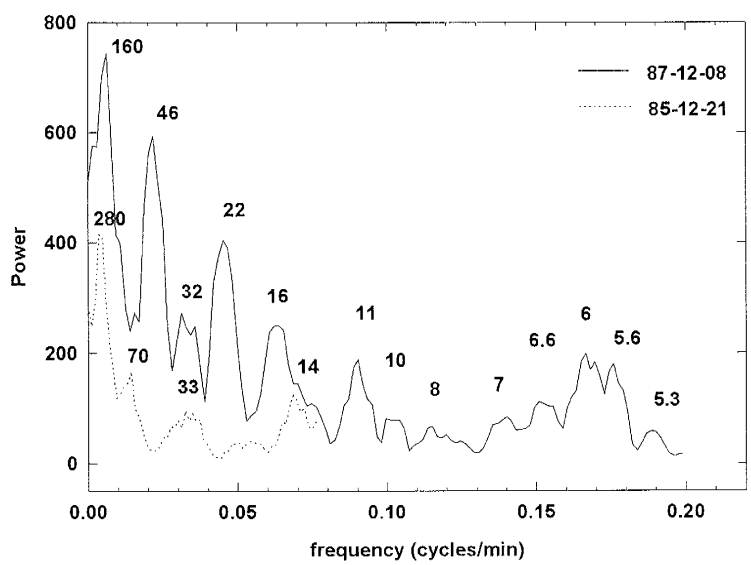

Fig. 4.1 Periodogram for selected 1985 and 1987 COSPEC data. Numbers above peaks indicate periodicity in minutes. Strong signals with periods of 5-6, 10-11, 16, 22, 32-33, 40, 70 and >100 minutes can be observed.

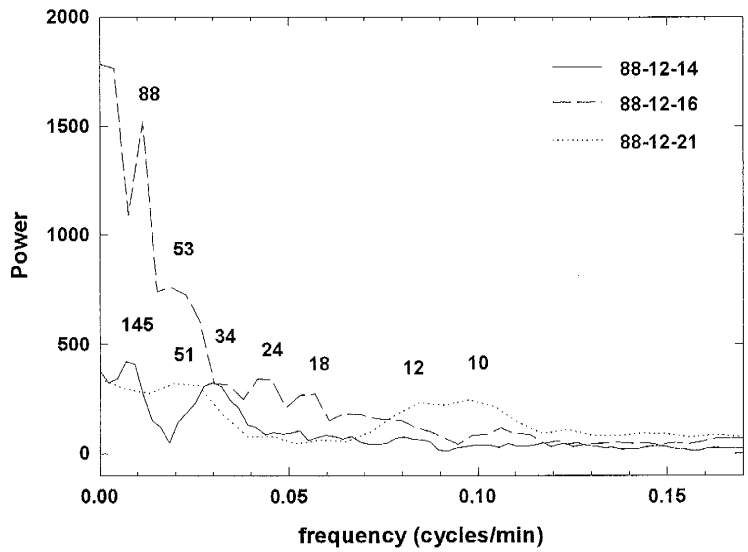

Fig. 4.2. Periodogram for selected 1988 COSPEC data. Signals with periods of 10-12, 18-24, 34, 51-53, 88 and 145 minutes can be observed.

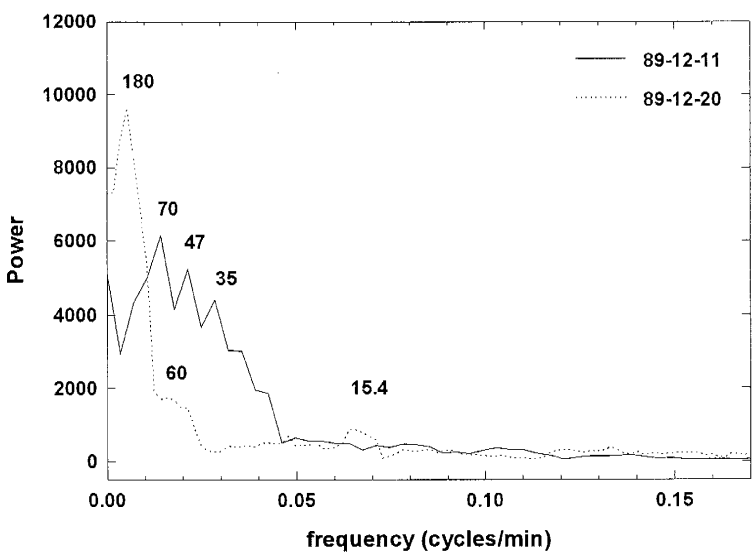

Fig. 4.3. Periodogram for selected 1989 COSPEC data. Signals with periods of 15, 35, 47, 60, 70, and 180 minutes can be observed.

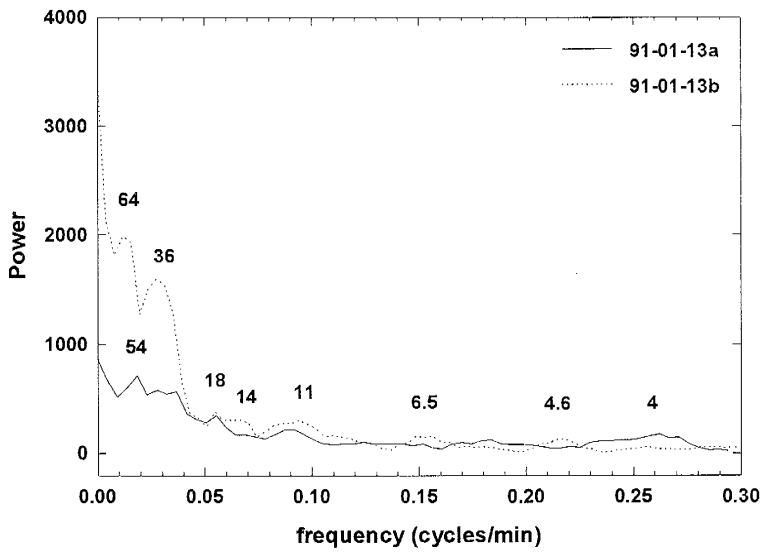

Fig. 4.4. Periodogram for selected 1991 COSPEC data. Signals with periods of 4-5, 6-7, 11, 14, 18, 36, 54, and 64 minutes can be observed.

5. AEROSOL AND GAS EMISSIONS

5.1. Results

Analyses of the particulate and treated filters were combined to give a total element concentration for each sample collected. Analyses of filters collected in 1986, 1988, 1989 and 1991 are reported as μg of element per m^3 of air in Tables 5.1 to 5.4, respectively, and corresponding mean values for each year and % of total concentration of each element are shown in Table 5.5. The corresponding raw data for all filters are given in appendix B. The elemental concentrations for samples collected in 1986 are from Meeker (1988) with the exception of the S analyses.

The total concentrations of elements on filter samples generally decrease in time (Table 5.5). In 1986 the total concentrations ranged from 851 to 3395 $\mu g.m^{-3}$, whereas in 1991 they ranged from 117 to 915 $\mu g.m^{-3}$. Individually, elements on filters also showed a similar decreasing trend, especially the three main plume components: F, S, and Cl. The average Cl concentrations decreased from 907 $\mu g.m^{-3}$ in 1986 to 149 $\mu g.m^{-3}$ in 1991. Similarly, during the same period between 1986 and 1991 the average F concentrations decreased from 482 to 60 $\mu g.m^{-3}$, and the S concentrations decreased from 521 to 164 $\mu g.m^{-3}$. This trend is also shown by Br, As, Se, and Sb. The majority of the trace elements detected on the filters (Na, Al, K, V, Cr, Mn, Fe, Co, Cu, Zn, Au, and REE) showed the highest concentrations in 1986 followed by a sharp decrease in

Table 5.1. Concentrations of elements in Erebus plume samples collected in December 1986. All values in $\mu g.m^{-3}$

	86-1	86-2	86-3	86-4	86-5	86-6	86-7	86-8	86-9
F	183	166	806	649	658	228	936	455	258
Na	27.6	32.1	126	128	132	30.9	52.9	63.7	64.3
Al	3.5	7.2	5.1	19.2	7.05	5	20.1	16.8	70.5
S	187.3	342.2	479.3	492.1	n.d.	516.1	469.8	595.7	1087.9
Cl	399	334	1830	1588	1784	664	670	444	448
K	26.1	25.9	113	79.1	134	26.1	39	43.8	29.2
Ca	n.d.	n.d.	14	23	n.d.	7.3	18.6	35.5	20.9
Sc	0.001	0.001	0.001	0.003	n.d.	0.001	0.002	0.003	0.008
Ti	n.d.	n.d.	n.d.	n.d.	n.d.	n.d.	n.d.	n.d.	n.d.
V	0.02	n.d.	0.02	0.005	n.d.	n.d.	0.03	0.08	n.d.
Cr	1.2	0.09	0.05	0.1	0.16	0.01	0.18	0.11	0.4
Mn	0.08	0.4	0.55	0.86	0.34	0.13	0.45	0.52	1.6
Fe	19.9	14	7.4	18.9	9.1	6.8	20.6	26.2	42.2
Co	0.18	n.d.	n.d.	n.d.	n.d.	0.004	0.01	0.57	0.001
Ni	n.d.	n.d.	n.d.	n.d.	n.d.	n.d.	n.d.	n.d.	n.d.
Cu	0.02	n.d.	3.8	4.9	n.d.	0.84	n.d.	0.008	n.d.
Zn	1.1	1.2	4	2.1	3	2.5	4.8	3.5	2.6
As	0.06	0.5	2	2	1.5	0.36	0.54	0.51	0.48
Se	0.08	0.01	0.05	0.03	0.04	0.05	n.d.	n.d.	0.03
Br	1.8	1	2.8	3.1	4.8	1.6	2.2	1.3	0.9
Rb	n.d.	0.23	0.72	0.68	0.81	0.16	n.d.	0.32	n.d
Mo	n.d.	n.d.	n.d.	n.d.	0.02	0.07	0.9	5.4	0.04
Cd	n.d.	n.d.	n.d.	n.d.	n.d.	n.d.	n.d.	n.d.	n.d.
In	0.06	0.05	0.19	0.17	0.2	0.04	0.04	0.04	0.03
Sb	0.005	0.01	0.06	0.08	0.03	0.007	0.026	0.04	0.04
Cs	0.005	0.01	0.02	0.02	0.04	0.007	0.015	0.01	n.d.
La	0.004	0.05	0.02	0.04	0.02	0.011	0.046	0.06	0.14
Ce	n.d.	0.09	0.03	0.07	0.03	0.046	0.154	n.d.	0.27
Sm	n.d.	0.01	n.d.	n.d.	0.004	0.001	0.005	0.006	0.02
Eu	n.d.	0.002	0.015	0.01	n.d.	0.001	n.d.	n.d.	0.002
Yb	0.02	0.006	0.008	0.01	0.01	0.023	0.098	0.2	0.08
Hf	0.02	0.003	n.d.	0.006	0.008	0.055	0.008	0.01	0.02
Ta	0.03	0.006	0.002	0.04	0.01	n.d.	n.d.	n.d.	0.009
W	0.015	0.01	0.08	0.006	n.d.	0.01	n.d.	0.004	n.d.
Au	n.d.	0.00052	n.d.	0.00062	n.d.	0.00131	0.000122	0.00058	0.00075
total	851.10	925.08	3395.22	3011.53	2735.17	1490.13	2236.50	1693.39	2027.67

All data from Meeker (1988) except S concentrations; n.d. = not detected

Table 5.2. Concentrations of elements in Erebus plume samples collected in December 1988. All values in $\mu g.m^{-3}$

	88-1	88-2	88-3	88-4	88-5	88-6	88-7	88-8	88-9	88-11	88-13	88-15
F	67.1	149.0	85.3	141.5	117.2	100.4	114.9	128.3	166.0	93.1	36.1	75.7
Na	13.7	18.9	15.6	13.1	7.4	7.2	12.1	11.9	12.9	12.8	4.8	6.5
Al	n.d.	12.2	1.3	5.4	17.9	n.d.	n.d.	n.d.	n.d.	n.d.	n.d.	n.d.
S	341.0	447.7	259.9	269.8	163.0	234.2	256.6	387.7	258.7	226.4	89.4	155.6
Cl	201.6	427.3	271.4	346.4	251.9	238.9	275.0	324.3	369.1	169.4	93.3	226.5
K	13.5	14.1	16.3	19.0	14.5	n.d.	13.4	17.6	15.4	15.6	5.4	11.9
Ca	1.7	n.d.	n.d.	5.4	6.7	21.7	18.0	n.d.	n.d.	n.d.	n.d.	n.d.
Sc	0.0003	0.0006	0.0002	0.0004	0.0042	0.0003	0.0004	0.0024	0.0004	0.0002	3.6e-05	0.0001
Ti	0.29	n.d.	n.d.	n.d.	n.d.	n.d.	1.00	0.99	0.99	n.d.	n.d.	n.d.
V	0.006	n.d.	0.043	n.d.	n.d.	n.d.	n.d.	n.d.	n.d.	0.021	n.d.	n.d.
Cr	0.015	0.045	n.d.	0.129	0.110	0.090	n.d.	n.d.	0.069	n.d.	0.001	n.d.
Mn	n.d.	0.109	n.d	0.027	0.042	0.033	0.020	n.d.	0.039	0.075	0.021	0.024
Fe	1.11	8.18	1.35	2.05	n.d.	n.d.	0.94	2.60	n.d.	2.57	0.75	1.85
Co	0.002	n.d.	n.d.	n.d.	n.d.	n.d.	0.009	3.9e-04	n.d.	4.3e-04	1.8e-04	1.2e-04
Ni	n.d.	n.d.	n.d.	n.d.	n.d.	n.d.	n.d	n.d.	n.d.	n.d	n.d	n.d
Cu	n.d.	n.d.	n.d.	n.d.	n.d.	n.d.	n.d	n.d.	n.d.	n.d	n.d	n.d
Zn	0.23	0.27	0.28	0.86	0.66	0.54	0.28	n.d.	1.27	0.31	0.15	0.21
As	0.2214	0.3002	0.2494	0.2470	0.3532	0.2386	0.2557	0.3658	0.4240	0.1978	0.0655	0.1084
Se	n.d.	n.d.	n.d.	n.d.	n.d.	n.d.	n.d.	n.d.	n.d.	0.0063	n.d.	n.d.
Br	0.58	1.43	0.66	0.34	0.47	0.44	0.52	0.77	0.82	0.39	0.19	0.37
Rb	0.079	0.085	0.098	n.d.	0.062	n.d.	0.068	0.115	0.103	0.078	0.031	0.033
Mo	0.012	0.013	n.d.	n.d.	n.d.	n.d.	n.d.	n.d.	n.d.	0.012	0.005	0.008
Cd	0.054	0.058	0.074	0.063	n.d.	n.d.	n.d.	n.d.	n.d.	0.103	0.036	0.096
In	0.021	0.019	0.023	0.025	0.016	0.018	0.028	0.036	0.028	0.025	0.010	0.014
Sb	0.009	0.014	0.005	0.028	0.003	0.003	0.009	0.005	0.013	0.004	0.002	0.021
Cs	0.003	0.003	0.004	n.d.	0.002	0.002	0.003	0.003	0.004	0.003	0.001	0.002
La	n.d.	0.004	0.001	n.d.	n.d.	n.d.	n.d.	n.d.	n.d.	3.2e-04	3.9e-04	4.7e-04
Ce	n.d.	0.012	n.d.	n.d.	n.d.	n.d.	n.d.	n.d.	n.d.	0.001	0.001	n.d.
Sm	n.d.	4.5e-04	2.6e-04	n.d.	n.d.	n.d.	n.d.	n.d.	n.d.	1.1e-04	3.6e-05	n.d.
Eu	n.d.	n.d.	n.d.	n.d.	n.d.	n.d.	n.d.	n.d.	n.d.	n.d.	n.d.	n.d.
Yb	n.d.	n.d.	n.d.	n.d.	n.d.	n.d.	n.d.	n.d.	n.d.	n.d.	n.d.	n.d.
Hf	n.d.	n.d.	n.d.	n.d.	n.d.	n.d.	n.d.	n.d.	n.d.	n.d.	n.d.	n.d.
Ta	n.d.	n.d.	n.d.	n.d.	n.d.	n.d.	n.d.	n.d.	n.d.	n.d.	n.d.	n.d.
W	n.d.	0.009	n.d.	n.d.	n.d.	n.d.	n.d.	n.d.	n.d.	n.d.	n.d.	n.d.
Au	n.d.	0.001	0.003	n.d.	n.d.	1.2e-03	4.0e-04	n.d.	0.008	n.d.	n.d.	n.d.
total	641.19	1079.74	652.59	804.38	580.23	603.69	693.06	874.63	825.90	521.21	230.16	478.84

n.d. = not detected

Table 5.3. Concentrations of elements in Erebus plume samples collected in December 1989. All values in $\mu g.m^{-3}$

	89-1	89-2	89-3	89-4	89-5	89-6	89-15	89-16	89-17	89-20	89-21	89-23	89-24	89-25	89-26
F	188.7	252.9	97.4	251.9	160.2	106.6	84.9	69.8	75.9	81.3	81.2	180.3	60.3	335.1	158.2
Na	44.1	20.1	7.2	22.8	14.0	12.4	7.0	7.9	4.1	12.7	4.1	19.0	5.3	34.9	16.1
Al	n.d.	n.d.	n.d.	2.2	n.d.	0.3	4.5	13.1	0.8	0.4	n.d.	2.0	n.d.	0.9	0.4
S	419.4	223.1	150.3	583.6	98.6	115.2	140.4	99.1	136.5	135.7	111.6	199.4	87.3	281.2	61.1
Cl	300.1	341.7	120.8	306.2	267.7	187.1	212.5	165.2	154.0	118.2	104.5	310.6	147.9	831.8	410.2
K	18.7	22.5	8.1	27.6	12.5	n.d.	9.4	12.8	1.1	14.1	n.d.	21.6	6.0	39.1	13.3
Ca	84.2	15.4	43.6	n.d.	18.7	n.d.	11.6	15.4	5.0	30.8	2.1	2.6	4.6	13.5	4.9
Sc	6.2e-04	6.8e-04	6.3e-04	1.4e-03	4.7e-05	2.1e-04	6.8e-04	3.0e-04	2.5e-04	1.9e-04	1.6e-03	7.4e-05	5.0e-05	2.4e-04	8.1e-05
Ti	15.9	n.d.	5.8	n.d.	2.8	n.d.	0.6	1.1	5.4	2.8	1.5	n.d.	1.0	0.5	0.2
V	n.d.	n.d.	n.d.	n.d.	n.d.	0.006	n.d.	n.d.	n.d.	0.004	n.d.	n.d.	n.d.	0.008	n.d.
Cr	0.040	0.680	0.091	n.d.	n.d.	0.026	0.029	n.d.	0.043	n.d.	0.008	0.012	0.406	0.546	0.066
Mn	0.133	0.055	0.023	0.057	0.033	n.d.	0.045	0.062	0.041	0.004	0.021	0.007	0.023	0.010	0.049
Fe	4.36	3.14	6.63	3.02	5.31	1.56	0.92	1.75	1.56	0.87	0.18	1.57	0.56	4.61	0.94
Co	4.3e-03	1.1e-03	1.7e-03	1.4e-04	1.8e-03	2.8e-04	1.3e-03	1.1e-03	4.3e-04	3.2e-04	2.6e-04	8.6e-04	5e-04	1.9e-03	1.3e-03
Ni	0.247	0.042	0.057	n.d.	n.d.	0.035	n.d.	n.d.	0.034	0.035	0.020	0.008	0.031	0.359	0.109
Cu	n.d.	n.d.	n.d.	n.d.	n.d.	n.d.	n.d.	n.d.	n.d.	n.d.	n.d.	0.0978	n.d.	n.d.	n.d.
Zn	3.58	1.13	5.66	1.13	1.39	1.26	5.22	0.44	2.56	1.42	0.29	0.52	0.14	1.64	1.07
As	0.3216	0.3217	0.1164	0.2505	0.3026	0.1790	0.2055	0.1375	0.1318	0.1629	0.1038	0.2942	0.1115	0.5208	0.2374
Se	0.0128	n.d.	0.0090	0.0113	0.0018	0.0021	n.d.	0.0071	n.d.	0.0063	0.0054	0.0009	0.0023	0.0094	0.0028
Br	1.05	0.55	0.38	0.62	0.38	0.21	0.40	0.30	0.19	0.37	0.07	0.23	0.10	0.32	0.50
Rb	0.122	0.123	0.040	0.159	0.006	0.077	0.048	0.053	n.d.	0.079	0.025	0.149	0.038	0.259	0.122
Mo	0.029	n.d.	n.d.	0.028	0.091	0.013	0.018	0.028	n.d.	0.016	0.008	0.025	0.007	0.045	0.034
Cd	n.d.	0.140	0.055	0.161	0.149	0.071	0.061	0.069	n.d.	0.019	0.033	0.117	0.034	0.197	0.077
In	0.037	0.004	0.014	0.054	0.034	0.025	0.014	0.015	0.008	0.033	0.010	0.036	0.016	0.071	0.042
Sb	0.059	0.011	0.050	0.010	0.007	0.008	0.002	0.002	0.025	0.004	0.002	0.007	0.003	0.015	0.003
Cs	0.005	0.005	0.002	0.007	0.004	0.004	0.002	0.002	0.002	0.003	0.001	0.006	0.002	0.011	0.005
La	0.007	0.001	3.8e-04	0.001	0.001	0.001	2.3e-04	0.003	0.009	0.001	0.002	0.002	0.001	0.007	0.001
Ce	0.010	0.008	0.002	0.004	0.002	0.002	n.d.	0.007	0.014	0.002	0.005	0.004	0.003	0.019	4.1e-04
Sm	9.6e-04	2.9e-04	n.d.	1.2e-04	1.0e-04	1.3e-04	n.d.	4.1e-04	2.4e-04	8.5e-05	n.d.	1.9e-04	1.8e-04	1.1e-03	n.d.
Eu	n.d.	2.2e-04	n.d.	1.4e-04	n.d.	n.d.	n.d.	n.d.	n.d.	n.d.	n.d.	n.d.	n.d.	n.d.	n.d.
Yb	n.d.	n.d.	n.d.	3.2e-04	n.d.	n.d.	n.d.	n.d.	n.d.	n.d.	n.d.	n.d.	n.d.	7.1e-04	n.d.
Hf	n.d.	n.d.	n.d.	n.d.	n.d.	n.d.	n.d.	n.d.	1.1e-03	n.d.	n.d.	n.d.	n.d.	n.d.	n.d.
Ta	n.d.	1.9e-04	n.d.	n.d.	1.5e-04	n.d.	n.d.	n.d.	n.d.	n.d.	n.d.	1.7e-04	n.d.	1.2e-03	n.d.
W	1.3e-02	3.3e-03	4.4e-03	1.2e-03	n.d.	3.8e-03	n.d.	3.2e-02	n.d.	2.7e-03	n.d.	1.4e-03	n.d.	n.d.	4.9e-03
Au	n.d.	n.d.	n.d.	n.d.	n.d.	n.d.	n.d.	n.d.	n.d.	n.d.	n.d.	n.d.	1.6e-03	n.d.	1.2e-04
total	1081.07	881.92	446.40	1199.88	582.31	425.19	477.83	387.26	387.49	398.93	305.79	738.45	313.93	1545.71	667.57

n.d. = not detected

Table 5.4. Concentrations of elements in Erebus plume samples collected in January 1991. All values in $\mu g.m^{-3}$

	91-1	91-2	91-3	91-5	91-6	91-7	91-8	91-9	91-11	91-21	91-23
F	67.7	62.5	32.0	112.7	18.5	84.6	36.7	36.4	32.6	110.4	68.0
Na	20.1	18.8	11.1	28.9	5.9	21.3	22.8	30.7	10.5	22.6	7.0
Al	5.7	1.7	3.5	7.0	4.3	8.5	24.7	74.2	12.7	3.4	3.7
S	131.6	168.1	97.2	354.9	47.1	263.7	166.0	157.7	45.6	307.2	66.1
Cl	198.7	159.7	89.5	376.7	25.1	217.5	57.0	60.8	64.0	246.8	146.3
K	13.3	9.8	9.3	25.2	3.4	12.8	17.3	24.9	n.d.	20.5	n.d.
Ca	2.3	0.5	0.3	n.d.	n.d.	n.d.	3.1	n.d.	n.d.	n.d.	2.0
Sc	3.4e-04	1.7e-04	1.5e-04	2.8e-04	3.2e-04	2.8e-04	8.9e-04	1.1e-03	3.2e-04	2.0e-04	2.5e-04
Ti	0.37	0.44	n.d.	n.d.	1.17	0.91	0.85	2.41	n.d.	n.d.	n.d.
V	0.157	0.004	0.026	0.002	0.003	0.090	0.016	0.055	0.167	0.061	0.035
Cr	0.483	0.013	n.d.	0.017	0.137	0.131	0.109	0.219	1.130	0.139	0.057
Mn	0.056	0.028	0.077	0.182	0.078	0.170	0.546	0.717	0.194	0.208	0.186
Fe	3.74	1.31	0.95	4.99	2.27	4.45	12.75	17.07	4.45	3.61	2.45
Co	1.5	1.7e-03	2.0e-04	n.d.	n.d.	n.d.	0.001	0.002	n.d.	n.d.	n.d.
Ni	n.d.	n.d.	n.d.	n.d.	n.d.	n.d.	0.133	n.d.	n.d.	n.d.	n.d.
Cu	n.d.	0.445	0.443	n.d.	n.d.	0.617	1.328	n.d.	2.665	0.236	0.357
Zn	0.20	0.21	0.09	0.51	8.55	3.74	0.39	0.32	0.00	5.18	4.77
As	0.1639	0.1383	0.0894	0.4436	0.0703	0.2635	0.2063	0.2263	0.1351	0.2178	0.0950
Se	0.0221	0.0163	n.d.	0.0075	0.0231	0.0129	n.d.	n.d.	0.1214	0.0080	0.0076
Br	0.79	0.31	0.14	0.67	0.04	0.23	0.33	0.43	0.15	0.73	0.40
Rb	n.d.	0.057	n.d.	n.d.	0.040	0.112	0.107	0.121	n.d.	0.112	0.027
Mo	n.d.	n.d.	n.d.	n.d.	n.d.	n.d.	n.d.	n.d.	n.d.	n.d.	n.d.
Cd	0.110	0.060	0.049	0.165	n.d.	0.112	n.d.	0.082	0.071	0.134	0.024
In	0.019	0.016	0.014	0.040	0.008	0.028	0.018	0.022	0.010	0.031	0.008
Sb	0.009	0.005	0.003	0.011	n.d.	0.004	0.007	0.015	n.d.	0.007	0.039
Cs	0.003	0.003	0.002	0.008	0.001	0.005	0.003	0.004	0.003	0.005	0.001
La	0.004	0.002	0.002	0.011	0.011	0.014	0.043	0.058	0.017	0.005	0.007
Ce	5.00e-04	n.d.	n.d.	0.027	0.029	0.032	0.097	0.132	0.045	0.011	0.018
Sm	n.d.	2.5e-04	3.3e-04	1.4e-03	1.4e-03	0.002	0.005	0.007	0.002	5.71e-04	7.3e-04
Eu	2.0e-04	n.d.	9.8e-05	3.2e-04	3.4e-04	4.8e-04	1.3e-03	1.9e-03	n.d.	n.d.	1.7e-04
Yb	n.d.	n.d.	n.d.	n.d.	n.d.	n.d.	n.d.	0.003	n.d.	1.5e-03	4.9e-04
Hf	n.d.	n.d.	n.d.	0.002	0.003	0.003	0.009	0.013	n.d.	8.5e-04	1.2e-03
Ta	6.74e-04	n.d.	n.d.	1.91e-03	n.d.	2.05e-03	5.57e-03	0.008	n.d.	5.7e-04	6.8e-04
W	n.d.	n.d.	6.13e-03	n.d.	n.d.	n.d.	n.d.	1.7e-04	0.494	0.007	0.002
Au	0.306	0.020	n.d.	3.013	0.002	0.009	0.032	0.003	0.060	0.067	0.333
total	447.35	424.33	244.76	915.44	116.70	619.26	344.57	406.62	175.15	721.73	301.87

n.d. = not detected

1988 and 1989 and then a slight increase in 1991.

Absolute concentrations of elements on the filters (expressed in $\mu g.m^{-3}$) can be affected by plume dilution, filter position in the plume and amount of LiOH used to impregnate the filters. Therefore, it is more convenient to express concentrations of elements as a percentage of total concentration (Table 5.5). Such normalization allows comparison between samples collected at different times. It is also more useful in describing the trends of a given group of elements. Figure 5.1 shows that Cl, F, and S together represent more than 85-90% of the total mass collected. The most abundant element is Cl, contributing on the average from 43% in 1986 to 34% in 1991. Fluorine contributes 23 and 14%, and sulfur 25 and 38% in 1986 and 1991, respectively. Due to their abundances and importance for metal transport, Cl, F, and S in the plume deserve the greatest attention and are treated separately below.

Na and K are the most abundant cations on the filters. Together they exceed the fraction of the remaining elements, contributing from 3.5 and 2.7% in 1986, to 4.2 and 3.5% in 1991, respectively. The typical ranges in contributions of the remaining elements as % of total mass are: alkaline earth elements 0.5-10%, Al $\sim$1%, Fe 0.5-5%, Cr 0.2%, Zn 0.1-0.7%; with the other elements usually constituting less than 0.1% of total mass. In 1991, Al was present in unusually high concentrations, $>$3% total. Because of this the respective percentages of other elements are biased towards lower values.

Table 5.5. Average concentrations of plume components in $\mu g.m^{-3}$ and as % of total concentration.

	December 1986			December 1988			December 1989			January 1991		
	mean	std	% total	mean	std	% total	mean	std	% total	mean	std	% total
F	482.1	290.4	22.9	106.2	37.4	15.6	145.6	82.8	22.0	60.2	32.3	13.9
Na	73.1	43.9	3.5	11.4	4.1	1.7	15.4	11.5	2.3	18.1	8.4	4.2
Al	17.2	21.0	0.8	9.2	7.3	1.3	2.7	4.1	0.4	13.6	21.1	3.1
S	521.3	260.6	24.7	257.5	99.7	37.8	189.5	142.0	28.6	164.1	104.7	37.8
Cl	906.8	633.6	43.0	266.2	91.7	39.1	265.2	182.5	40.0	149.3	105.4	34.4
K	57.4	41.4	2.7	14.2	3.6	2.1	15.9	10.1	2.4	15.2	7.4	3.5
Ca	19.9	9.5	0.9	10.7	8.6	1.6	19.4	22.8	2.9	1.6	1.2	0.4
Sc	0.002	0.002	1.1e-04	0.001	0.001	1.2e-04	0.0005	0.0005	7.1e-05	0.00039	0.0003	8.9e-05
Ti	n.d.			0.82	0.35	0.1	3.43	4.57	0.5	1.02	0.74	0.2
V	0.031	0.029	1.5e-03	0.023	0.018	3.4e-03	0.006	0.002	8.9e-04	0.056	0.059	1.3e-02
Cr	0.256	0.371	1.2e-02	0.066	0.048	9.7e-03	0.177	0.245	2.7e-02	0.244	0.339	5.6e-02
Mn	0.548	0.457	2.6e-02	0.043	0.030	6.4e-03	0.040	0.033	6.1e-03	0.222	0.215	5.1e-02
Fe	18.3	11.2	8.7e-01	2.4	2.3	0.3	2.5	1.95	0.4	5.3	5.1	1.2
Co	0.153	0.245	7.3e-03	0.002	0.003	2.8e-04	0.001	0.001	1.7e-04	0.303	0.675	7.0e-02
Ni	n.d.			n.d.			0.089	0.112	1.3e-02	0.133		3.1e-02
Cu	1.914	2.283	9.1e-02	n.d.			0.098		1.5e-02	0.870	0.868	2.0e-01
Zn	2.76	1.23	1.3e-01	0.46	0.35	6.8e-02	1.83	1.71	2.8e-01	2.18	2.919	5.0e-01
As	0.883	0.741	4.2e-02	0.252	0.102	3.7e-02	0.226	0.113	3.4e-02	0.186	0.106	4.3e-02
Se	0.041	0.022	2.0e-03	0.006		9.3e-04	0.006	0.004	8.9e-04	0.027	0.038	6.3e-03
Br	2.17	1.24	1.0e-01	0.58	0.32	8.6e-02	0.38	0.24	5.7e-02	0.38	0.25	8.8e-02
Rb	0.487	0.282	2.3e-02	0.075	0.028	1.1e-02	0.093	0.068	1.4e-02	0.082	0.040	1.9e-02
Mo	1.286	2.330	6.1e-02	0.010	0.004	1.5e-03	0.029	0.022	4.3e-03	n.d.		
Cd	n.d.			0.069	0.024	1.0e-02	0.091	0.056	1.4e-02	0.090	0.044	2.1e-02
In	0.091	0.072	4.3e-03	0.022	0.007	3.2e-03	0.027	0.019	4.1e-03	0.020	0.010	4.5e-03
Sb	0.0331	0.0252	1.6e-03	0.0098	0.0081	1.4e-03	0.0139	0.0178	2.1e-03	0.0113	0.0111	2.6e-03
Cs	0.0159	0.0112	7.5e-04	0.0027	0.0010	3.9e-04	0.0041	0.0027	6.2e-04	0.0035	0.0019	8.0e-04
La	0.0434	0.0409	2.1e-03	0.0012	0.0014	1.8e-04	0.0026	0.0029	3.9e-04	0.0157	0.0181	3.6e-03
Ce	0.0986	0.0871	4.7e-03	0.0049	0.0065	7.2e-04	0.0058	0.0053	8.8e-04	0.0436	0.0431	1.0e-02
Sm	0.0077	0.0067	3.6e-04	0.0002	0.00002	3.1e-05	0.0003	0.0004	5.3e-05	0.0021	0.0023	4.8e-04
Eu	0.006	0.006	2.8e-04	n.d.			0.00018	0.00006	2.7e-05	0.0006	0.0006	1.4e-04
Yb	0.051	0.065	2.4e-03	n.d.			0.00054	0.00028	7.8e-05	0.0016	0.0012	3.8e-04
Hf	0.016	0.017	7.7e-04	n.d.			0.0011		1.6e-04	0.0047	0.0046	1.1e-03
Ta	0.016	0.015	7.7e-04	n.d.			0.00042	0.00051	6.4e-05	0.0028	0.0030	6.5e-04
W	0.021	0.029	9.9e-04	0.009		1.4e-03	0.007	0.0099	1.1e-03	0.102	0.219	2.3e-02
Au	0.001	0.0003	3.1e-05	0.003	0.003	4.1e-04	0.001	0.0011	1.3e-04	0.384	0.932	8.9e-02
total	2106.9			680.3			662.9			433.8		

n.d. = not detected; std = standard deviation

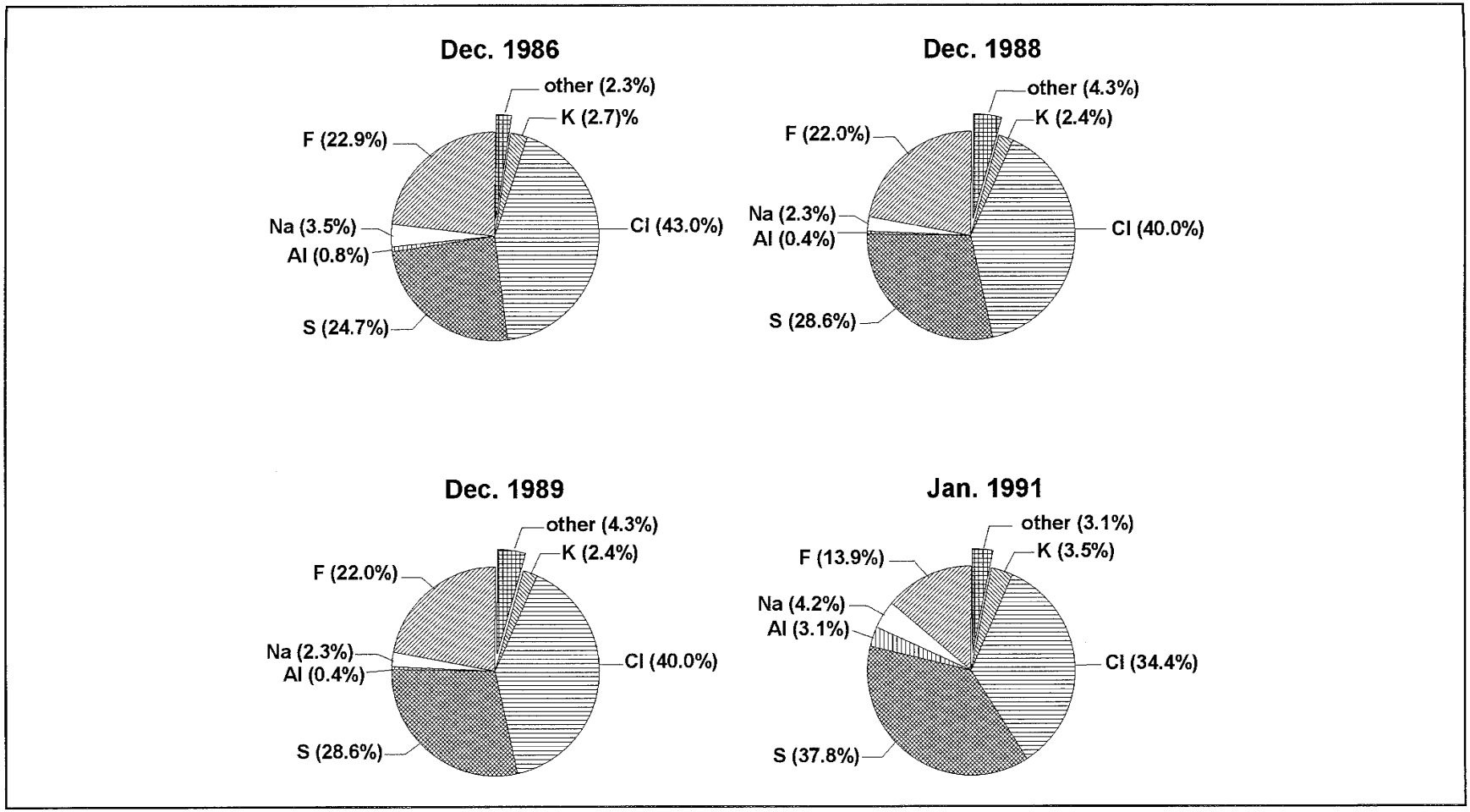

Fig. 5.1. Concentrations of elements on Mt. Erebus filters as a percent of total mass collected.

Figures 5.2 to 5.7 show the concentration distributions of the elements in samples of gas collected in 1986, 1988, 1989 and 1991. Data are given in % of the total concentration (calculated from Tables 5.1-5.4) and are represented as box plots. Each box shows the spread of distribution between the 25 and 75 percentiles (represented by the box height) and between the 10 and 90 percentiles (shown by the "whiskers"), whereas the points below and above "whiskers" represent data beyond the 10th and 90th percentile. The solid line in each box is a median, and the dotted line gives the average (arithmetic mean) for each data set. The distributions of elemental concentrations are log-normal, as shown by the deviation of the average from the median value. In almost all cases, both mean and median values delineate the same general trends.

Changes in the concentrations of fluorine and sulfur as a % of total concentration on the filters are negatively correlated: F is higher in 1986 and 1989, and lower in 1988 and 1991, whereas S exhibits an opposite trend (Fig. 5.2). Chlorine remains constant in 1986 through 1989 and then decreases slightly, however this decrease is only apparent due to the unusually high Al content of samples in 1991. If Al data are not taken into account in the normalization, Cl concentrations can be regarded as constant throughout the period 1986-1991. The variation of the remaining halogen Br, is much less significant. Bromine concentrations decrease slightly between 1986 and 1989, and then increase in 1991. The changes in the proportions of F, Cl, and S are described fully below.

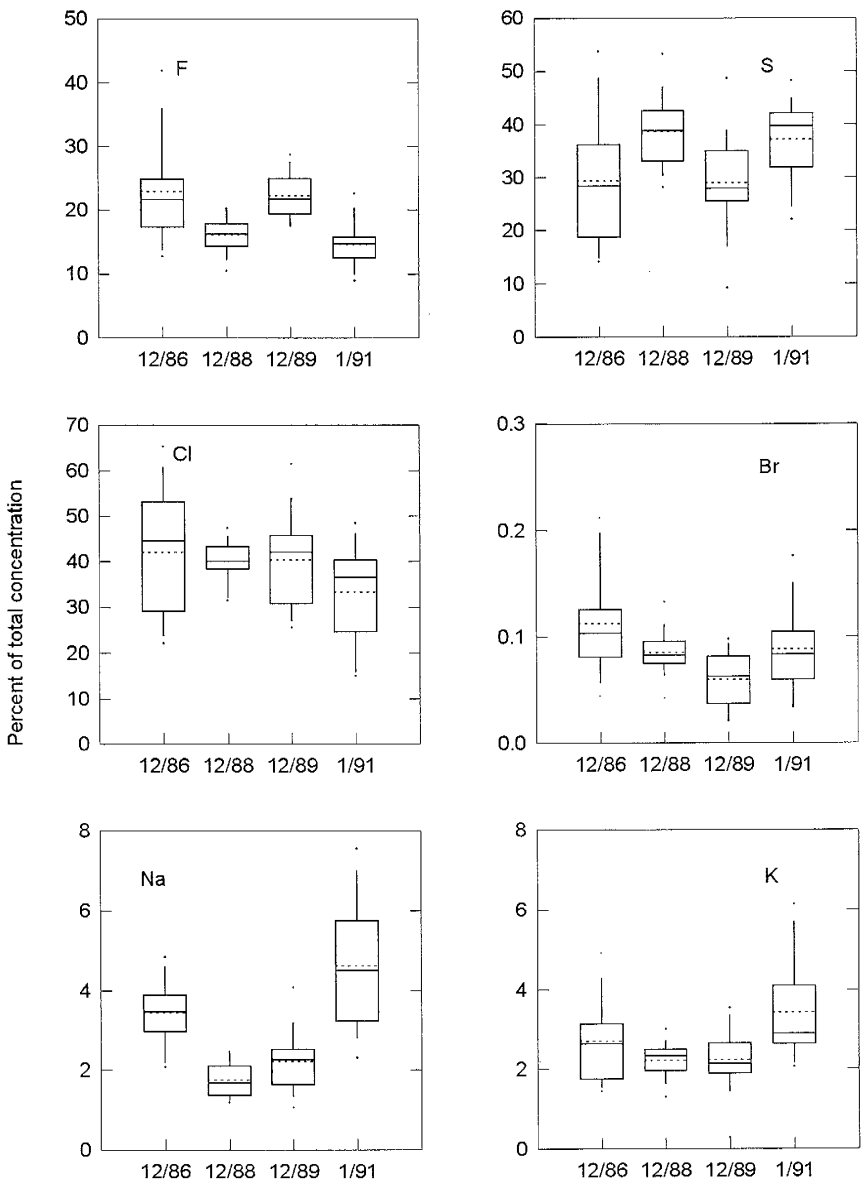

Fig. 5.2. Distribution plots for F, S, Cl, Br, Na, and K on Erebus filters.

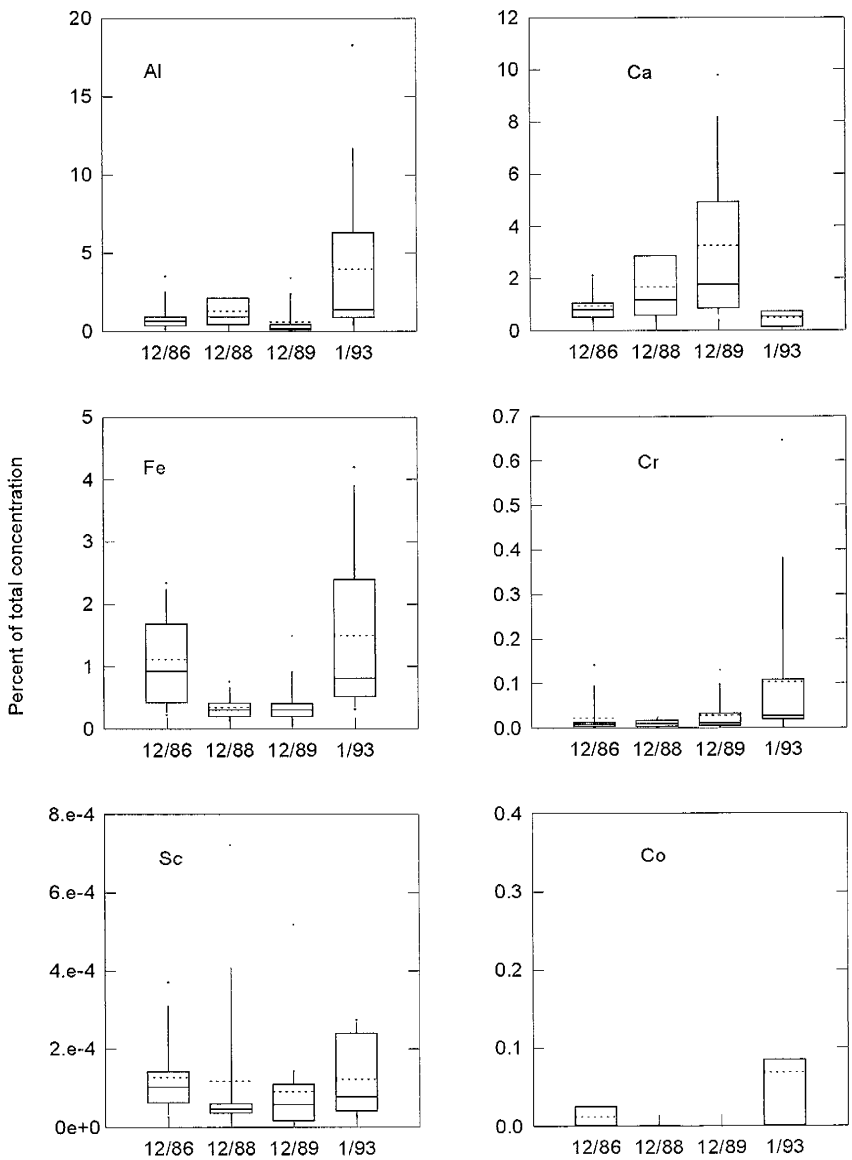

Fig. 5.3. Distribution plots for Al, Ca, Sc, Cr, Fe, and Co on Erebus filters.

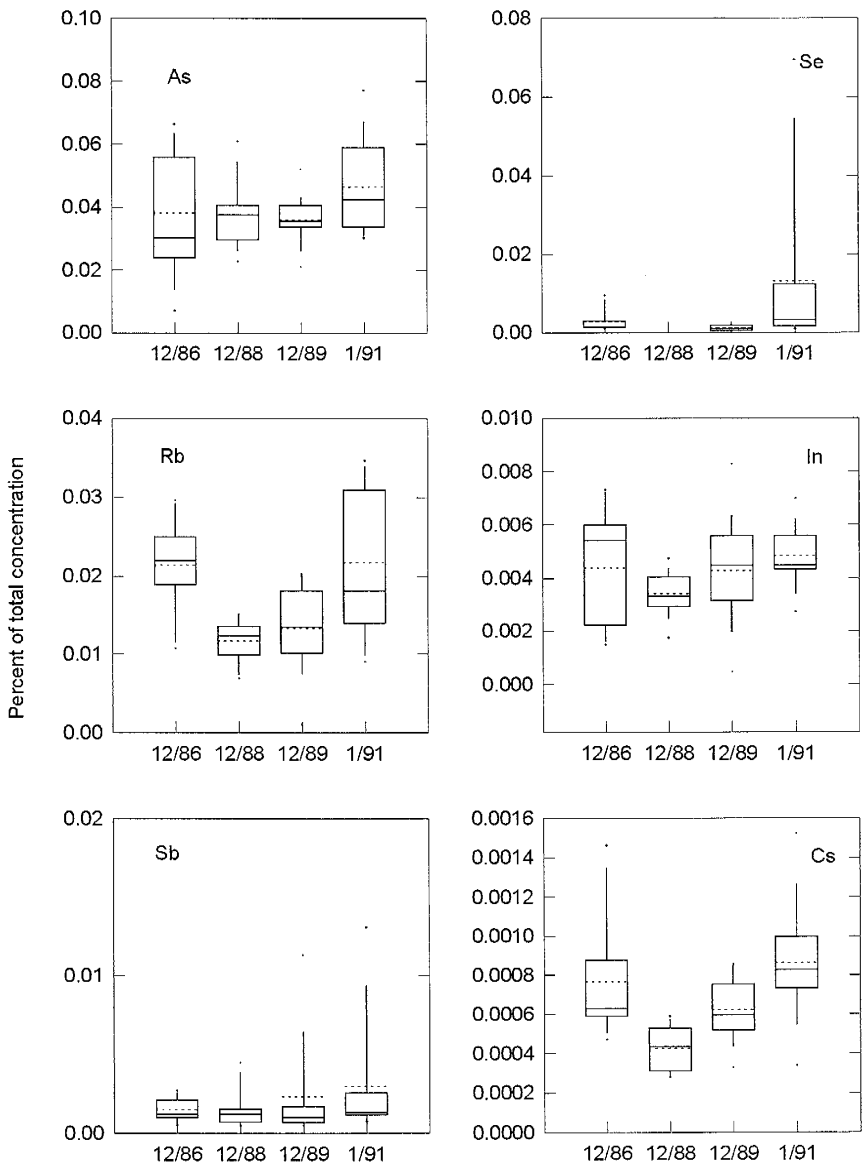

Fig. 5.4. Distribution plots for As, Se, Rb, In, Sb, and Cs on Erebus filters.

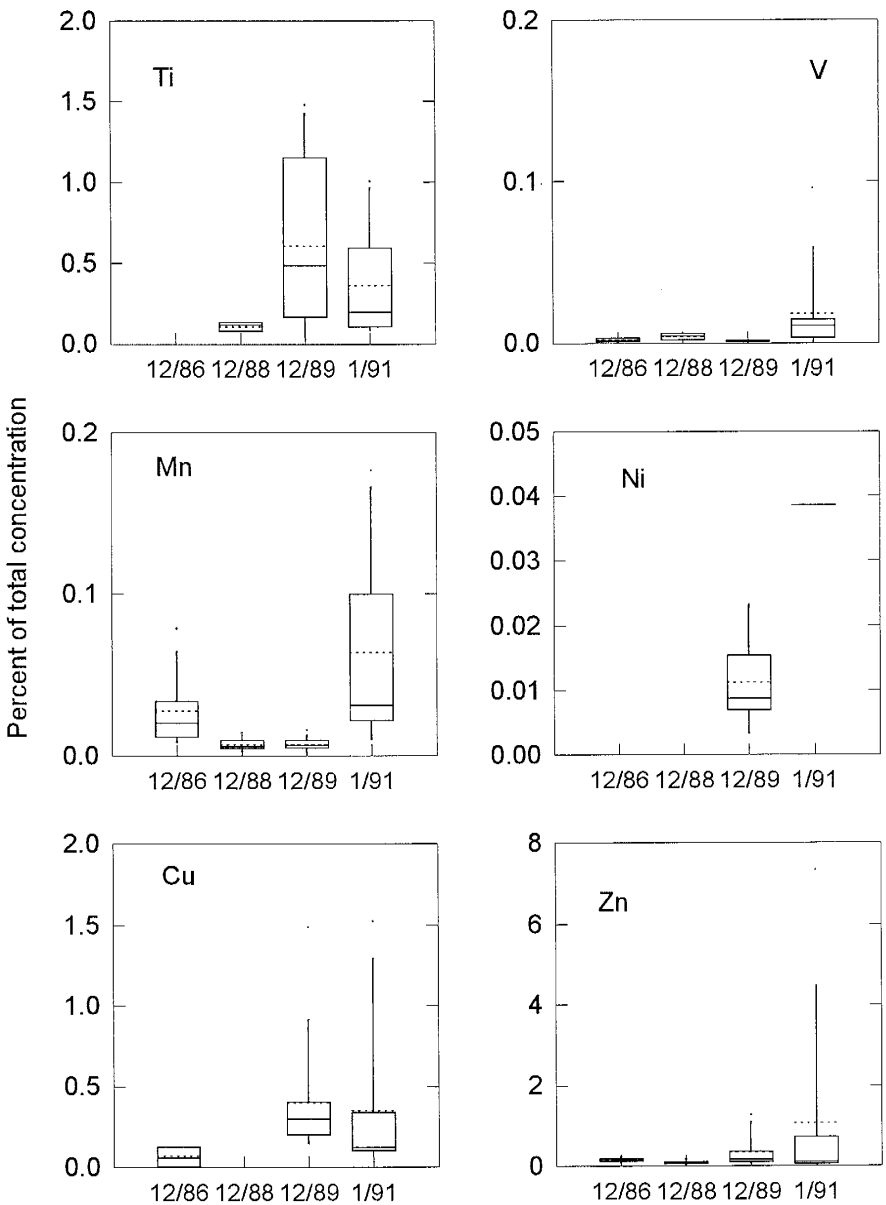

Fig. 5.5. Distribution plots for Ti, V, Mn, Ni, Cu, and Zn on Erebus filters.

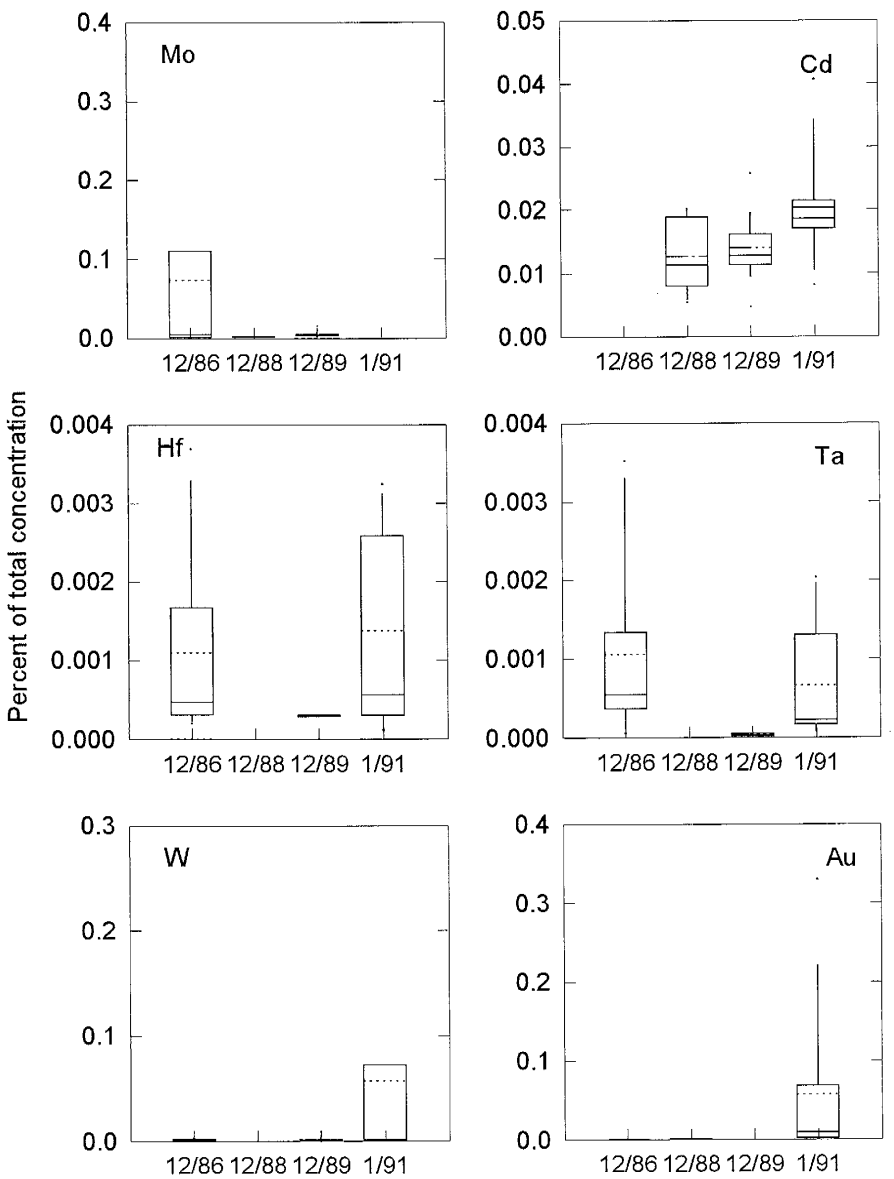

Fig. 5.6. Distribution plots for Mo, Cd, Hf, Ta, W, and Au on Erebus filters.

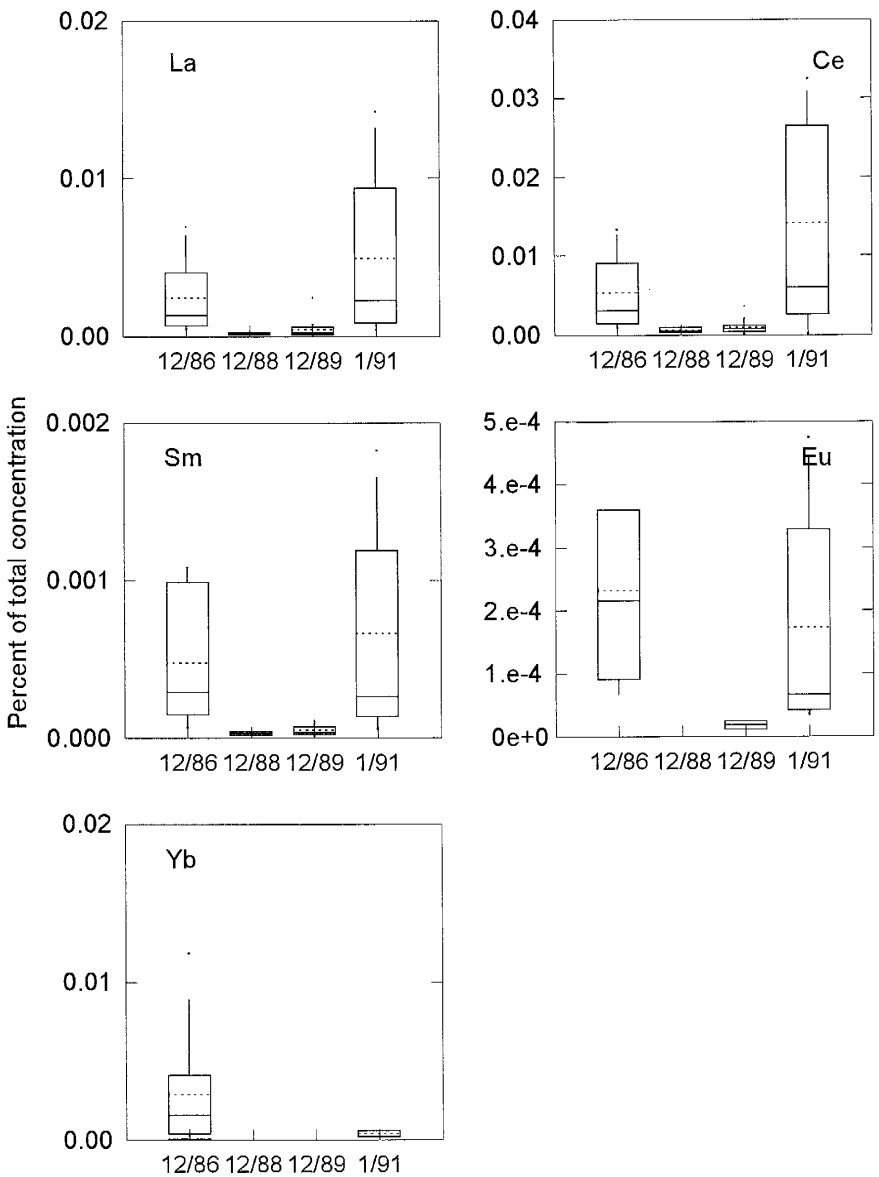

Fig. 5.7. Distribution plots for La, Ce, Sm, Eu, and Yb on Erebus filters.

Variations in the relative content of trace components were less pronounced than those for halogens and sulfur. The two most abundant trace elements, Na and K, were higher in 1986 and 1991 and lower in 1988 and 1989 (Fig. 5.3), the same is true for the other alkali metals Rb and Cs (Fig. 5.4). Calcium remained constant in all years except 1989 when it was slightly higher (Fig. 5.3). Most metals (V, Cr, Mn, Co, Cu, Zn, Cd, W, Au, and Al) were also constant in all years with an exception of Al in 1991 (Fig. 5.3, 5.5, 5.6). Iron, the most abundant transition metal on filter samples, In, and REEs La, Ce, Sm, Eu and Yb showed a trend similar to that of alkali metals, being high in 1986 and 1991 and low in 1988 and 1989 (Fig. 5.3, 5.4, 5.7). Arsenic and Se were constant in 1986 though 1989 and then increased slightly in 1991 (Fig. 5.4). Scandium and Sb remained constant in all years (Fig. 5.4).

5.1.1. Chlorine, fluorine and sulfur

To discuss the changes in the proportions of the three most abundant species: Cl, S, and F, I refer to the % of each component relative to the sum of all three. There is a large spread in the values for all filter samples within each sampling period (Figure 5.8), but on the average samples collected in 1986 and 1989 have higher F and lower S content compared to those collected in 1988 and 1991. This variation, which is referred to as long-term variability, becomes clearer when average concentrations for each year are compared.

The average Cl content of the gas remained almost constant (40-47%) in all four years whereas F and S exhibited more distinct changes. Samples collected in 1986 and 1989 had relatively high F (25% and 24%, respectively) and low S content (27% and 32%, respectively), whereas those collected in 1988 and 1991 were characterized by lower F (17% and 16%) and higher S (41% and 44%) content. The means for each year formed two separate clusters, the means calculated for 1986 and 1989 forming one, and the means for 1988 and 1991 another (Figure 5.8). T-test analysis (using either F or S normalized concentrations) indicates that the means of the two groups of data collected in 1986 and 1989, and in 1988 and 1991 are different at the 95% confidence level (appendix C).

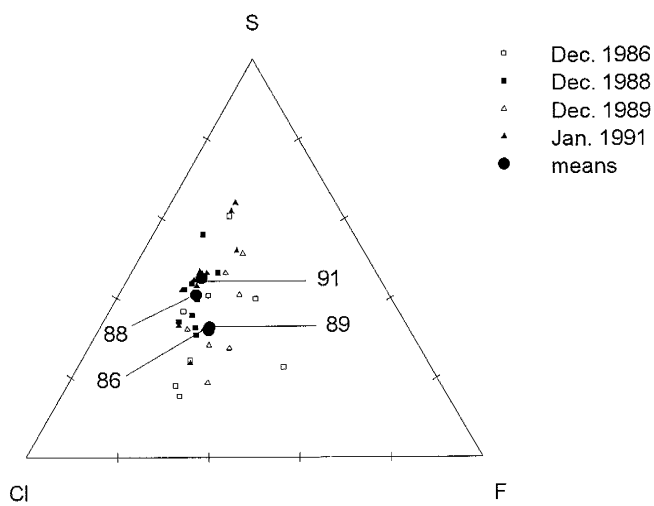

Fig. 5.8. Relative proportions of F, S, and Cl in the Erebus plume. Small symbols represent samples, large filled circles are means, all data from Table 5.5.

Apart from the long-term variability in the F, Cl, and S content of the Erebus emissions that are manifested by changes in the yearly averages, there were also large temporal variations in F/Cl and S/Cl ratios within each sampling period (Figure 5.9). These are referred to as short-term variability. The magnitude of these changes often exceeded the average value for each set by more than one standard deviation.

5.1.2. Emission rates

The average element-to-sulfur ratios combined with COSPEC estimates of S emission rates (Kyle *et al.*, 1994) permit the calculation of the emission rates of halogens (as HCl and HF) and other elements from Mt. Erebus. If we assume that no major change in the gas composition nor in the eruptive behavior occurred within the last decade (an assumption supported by our observations of the lava lake), then estimates can be extended in time to calculate the emission rates of halogens and other components in other years (for which only COSPEC estimates of SO_2 output are available). The average element-to-sulfur ratios for the 1986, 1988, 1989, and 1991, and the average of all years are given in Table 5.6. The average F/S ratios for 1986 and 1989 samples are higher (0.99 and 0.92) than for 1988 and 1991 (0.44 and 0.44). The average Cl/S ratios in 1986 and 1989 were 1.75 and 1.8, and in 1988 and 1991, 1.09 and 1.00, respectively. The grand-total average F/S and Cl/S ratios of 0.69 and 1.41, respectively, were used to calculate the outputs of halogens in years for which no filter data were available.

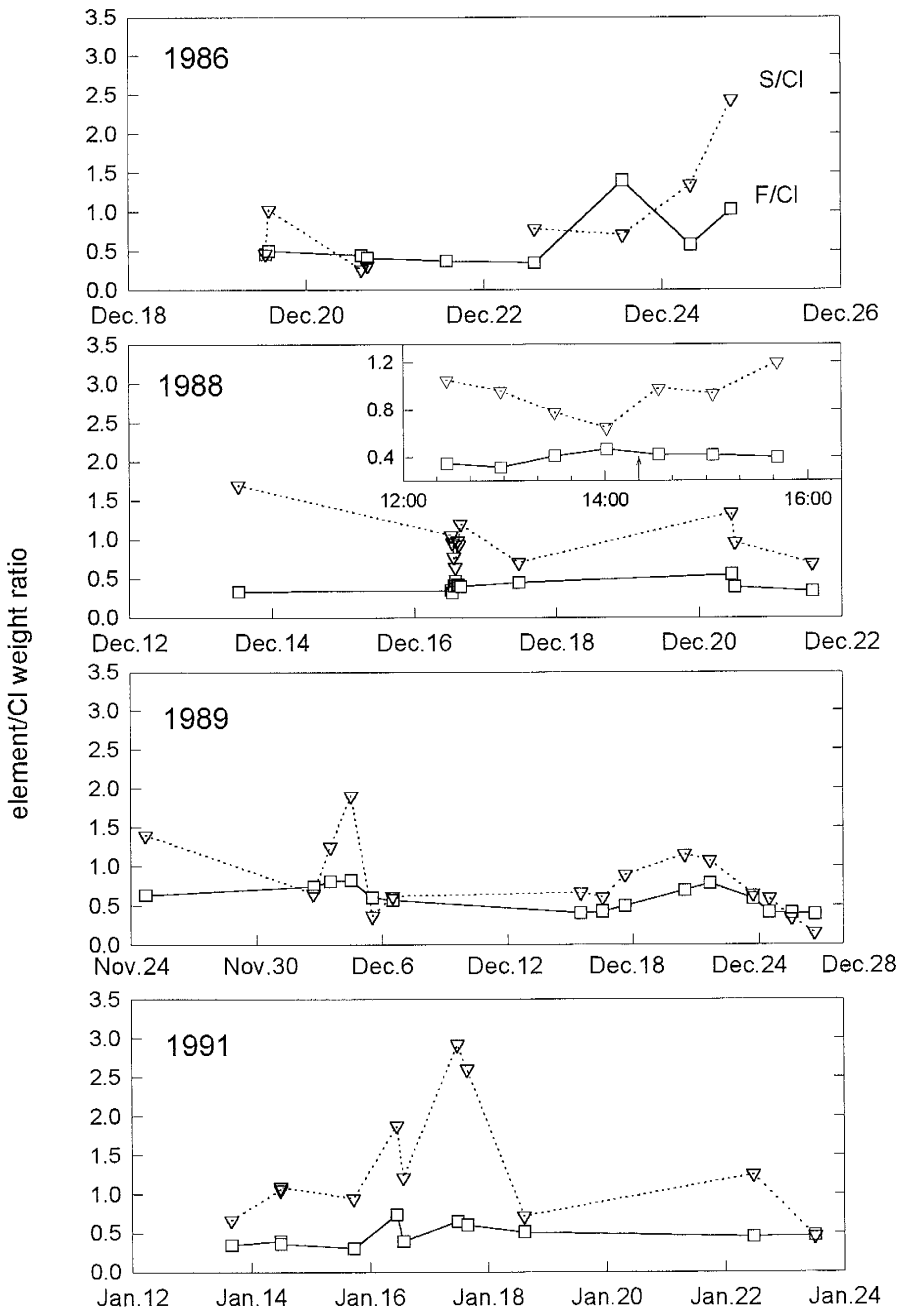

Fig. 5.9. Short-time variability in F, Cl, and S content of the Erebus plume as expressed by F/Cl (filled squares) and S/Cl (open triangles) weight ratios. Vertical arrow in the inset indicates an eruption observed on Dec. 16, at 14:20 local time.

Table 5.6. Average element-to-S weight ratios calculated for Erebus samples.

Ratios	Dec. 1986		Dec. 1988		Dec. 1989		Jan. 1991		All years	
	mean	std.	mean	std.	mean	std.	mean	std.	mean	std.
F/S	0.99	0.63	0.44	0.14	0.92	0.56	0.44	0.24	0.69	0.49
Na/S	0.14	0.08	0.05	0.01	0.09	0.06	0.13	0.05	0.10	0.06
Al/S	0.03	0.02	0.04	0.05	0.02	0.04	0.11	0.14	0.06	0.09
Cl/S	1.75	1.21	1.09	0.29	1.80	1.52	1.00	0.55	1.41	1.09
K/S	0.11	0.07	0.06	0.02	0.09	0.05	0.09	0.03	0.09	0.05
Ca/S	0.035	0.017	0.046	0.036	0.113	0.090	0.014	0.011	0.068	0.074
Sc/S	4.15e-06	2.10e-06	3.54e-06	7.12e-06	2.79e-06	3.42e-06	3.38e-06	2.62e-06	3.36e-06	4.30e-06
Ti/S	n.d.		0.0028	0.0014	0.0192	0.0147	0.0090	0.0091	0.0131	0.0133
V/S	7.14e-05	4.97e-05	9.19e-05	7.37e-05	3.62e-05	1.45e-05	6.11e-04	1.07e-03	3.39e-04	7.87e-04
Cr/S	9.92e-04	2.19e-03	2.81e-04	2.47e-04	1.12e-03	1.51e-03	3.53e-03	7.56e-03	1.60e-03	4.23e-03
Mn/S	1.01e-03	4.98e-04	1.89e-04	8.32e-05	2.68e-04	2.21e-04	1.80e-03	1.63e-03	7.92e-04	1.08e-03
Fe/S	0.043	0.029	0.008	0.005	0.015	0.015	0.042	0.037	0.026	0.027
Co/S	3.90e-04	5.20e-04	7.46e-06	1.29e-05	7.49e-06	5.90e-06	2.30e-03	5.13e-03	4.39e-04	2.06e-03
Ni/S	n.d.		n.d.		5.09e-04	5.34e-04	7.99e-04		5.33e-04	5.16e-04
Cu/S	3.93e-03	4.68e-03	n.d.		4.90e-04		1.17e-02	2.07e-02	7.86e-03	1.55e-02
Zn/S	0.0057	0.0026	0.0020	0.0014	0.0119	0.0117	0.0294	0.0578	0.0123	0.0291
As/S	0.0016	0.0016	0.0010	0.0004	0.0015	0.0009	0.0013	0.0006	0.0014	0.0009
Se/S	1.24e-04	1.52e-04	2.80e-05		3.52e-05	1.96e-05	4.53e-04	9.04e-04	1.79e-04	5.09e-04
Br/S	4.43e-03	2.79e-03	2.25e-03	6.11e-04	2.43e-03	1.83e-03	2.65e-03	1.81e-03	2.78e-03	1.92e-03
Rb/S	8.81e-04	5.30e-04	3.04e-04	7.59e-05	5.65e-04	4.74e-04	5.45e-04	2.10e-04	5.32e-04	3.97e-04
Mo/S	2.79e-03	4.27e-03	4.43e-05	1.06e-05	2.23e-04	2.60e-04	n.d.		6.69e-04	1.97e-03
Cd/S	n.d.		3.27e-04	1.76e-04	6.08e-04	3.91e-04	6.08e-04	3.84e-04	5.40e-04	3.59e-04
In/S	1.83e-04	1.47e-04	8.99e-05	2.08e-05	1.86e-04	1.64e-04	1.34e-04	3.66e-05	1.48e-04	1.17e-04
Sb/S	6.46e-05	5.27e-05	4.11e-05	3.92e-05	7.42e-05	8.62e-05	1.04e-04	1.86e-04	6.96e-05	1.01e-04
Cs/S	2.87e-05	1.08e-05	1.10e-05	3.21e-06	2.61e-05	1.82e-05	2.42e-05	1.19e-05	2.23e-05	1.43e-05
La/S	7.99e-05	4.76e-05	4.43e-06	2.48e-06	1.59e-05	1.72e-05	1.35e-04	1.42e-04	6.11e-05	9.33e-05
Ce/S	1.89e-04	1.06e-04	1.49e-05	1.15e-05	3.40e-05	2.86e-05	3.93e-04	3.72e-04	1.62e-04	2.51e-04
Sm/S	1.41e-05	1.03e-05	7.16e-07	3.24e-07	1.78e-06	1.30e-06	1.81e-05	1.82e-05	9.11e-06	1.34e-05
Eu/S	1.22e-05	1.31e-05	n.d.		6.10e-07	5.26e-07	4.35e-06	4.17e-06	6.48e-06	8.77e-06
Yb/S	1.03e-04	1.14e-04	n.d.		1.54e-06	1.41e-06	1.02e-05	7.06e-06	6.60e-05	1.00e-04
Hf/S	4.09e-05	4.50e-05	n.d.		7.90e-06		3.42e-05	3.13e-05	3.56e-05	3.69e-05
Ta/S	5.43e-05	6.69e-05	n.d.		1.86e-06	1.61e-06	1.66e-05	1.89e-05	2.47e-05	4.24e-05
W/S	5.24e-05	6.20e-05	2.08e-05		6.01e-05	1.02e-04	2.19e-03	4.83e-03	5.62e-04	2.35e-03
Au/S	1.21e-06	7.86e-07	1.05e-05	1.29e-05	1.02e-05	1.17e-05	1.78e-03	2.85e-03	7.77e-04	2.03e-03

n.d.- not detected

Similarly, the average element-to-sulfur ratios were used to calculated the emission rates of other elements present in the plume. Table 5.7 presents the calculated emission rates of combined gas and aerosols from Mount Erebus.

The outputs of SO_2 and other volatiles have increased since 1985 (Table 5.7) corresponding to the increase in the size of the lava lake (Chapter 4). The total amount of the three most abundant volatiles (SO_2+HF+HCl) has increased from 20 $Gg.yr^{-1}$ in 1986 to about 45 $Gg.yr^{-1}$ in 1991 (1 Gg=10^9 g). Between 1986 and 1991, the emissions of HF increased from 4.0 to 6.0 $Gg.yr^{-1}$ with the highest value of 9.2 $Gg.yr^{-1}$ in 1991. The HCl emissions increased from 6.9 to 13.3 $Gg.yr^{-1}$, and reached the highest value of 17.6 $Gg.yr^{-1}$ in 1989. During 1983, when Mount Erebus emissions of SO_2 reached 84 $Gg.yr^{-1}$, the HF and HCl output are estimated as 30.5 and 60.9 $Gg.yr^{-1}$, respectively. Emissions of other components also show an increase in time, for example Na emissions increased from 0.5 to 1.7 $Gg.yr^{-1}$ between 1986 and 1991; during the same period K emissions increased from 0.4 to 1.1 $Gg.yr^{-1}$. Aluminum showed a sudden increase from 0.1 in 1986 to 1.4 $Gg.yr^{-1}$ in 1991, which may signify an increase in the ash content of the plume. A similar large increases, often several orders of magnitude, were observed in 1991 for V, Cr, Mn, Fe, Co, Ni, Cu, Zn, REEs, Hf, Ta, W, and Au.

Table 5.7. Estimated emission rates of Erebus plume components for 1983-1991 period. All data in $Gg.yr^{-1}$.

	1983		1984		1985		1986	
	mean	std	mean	std	mean	std	mean	std
SO_2	84	33	9.1	3.5	5.5	2.6	7.7	4
HF	30.5	28.2	3.3	3.0	2.0	2.0	4.0	3.8
Na	4.0	3.7	0.4	0.4	0.3	0.3	0.5	0.5
Al	2.4	4.5	0.3	0.5	0.2	0.3	0.11	0.1
HCl	60.9	60.7	6.6	6.5	4.0	4.2	6.9	7.1
K	3.6	3.0	0.39	0.3	0.23	0.2	0.4	0.4
Ca	2.9	3.8	0.31	0.4	0.19	0.3	0.13	0.1
Sc	1.4e-04	2.1e-04	1.5e-05	2.3e-05	9.2e-06	1.5e-05	1.6e-05	1.4e-05
Ti	0.55	0.69	0.06	0.07	0.04	0.05		
V	0.014	0.036	1.5e-03	3.9e-03	9.3e-04	2.4e-03	2.7e-04	2.9e-04
Cr	0.07	0.19	7.3e-03	2.1e-02	4.4e-03	1.3e-02	3.8e-03	9.6e-03
Mn	0.033	0.053	3.6e-03	5.7e-03	2.2e-03	3.6e-03	3.9e-03	3.4e-03
Fe	1.08	1.41	0.12	0.15	0.07	0.10	0.16	0.17
Co	0.018	0.090	2.0e-03	9.8e-03	1.2e-03	6.0e-03	1.5e-03	2.5e-03
Ni	0.022	0.027	2.4e-03	2.9e-03	1.5e-03	1.9e-03		
Cu	0.33	0.73	0.04	0.08	0.02	0.05	0.02	0.02
Zn	0.52	1.34	0.06	0.14	0.03	0.09	0.02	0.02
As	0.057	0.053	6.2e-03	5.7e-03	3.7e-03	3.7e-03	6.3e-03	8.2e-03
Se	7.5e-03	2.3e-02	8.1e-04	2.5e-03	4.9e-04	1.5e-03	4.8e-04	7.4e-04
Br	0.117	0.111	0.013	0.012	0.008	0.008	0.017	0.017
Rb	0.022	0.022	2.4e-03	2.4e-03	1.5e-03	1.6e-03	3.4e-03	3.3e-03
Mo	0.028	0.089	3.0e-03	9.6e-03	1.8e-03	5.9e-03	1.1e-02	2.0e-02
Cd	0.023	0.021	2.5e-03	2.3e-03	1.5e-03	1.5e-03		
In	6.2e-03	6.5e-03	6.7e-04	7.0e-04	4.1e-04	4.5e-04	7.1e-04	8.1e-04
Sb	2.9e-03	4.9e-03	3.2e-04	5.3e-04	1.9e-04	3.3e-04	2.5e-04	2.9e-04
Cs	9.4e-04	8.5e-04	1.0e-04	9.1e-05	6.1e-05	5.9e-05	1.1e-04	8.6e-05
La	2.6e-03	4.5e-03	2.8e-04	4.9e-04	1.7e-04	3.0e-04	3.1e-04	3.0e-04
Ce	6.8e-03	1.2e-02	7.4e-04	1.3e-03	4.5e-04	8.2e-04	7.3e-04	6.8e-04
Sm	3.8e-04	6.5e-04	4.1e-05	7.0e-05	2.5e-05	4.4e-05	5.4e-05	5.9e-05
Eu	2.7e-04	4.3e-04	3.0e-05	4.7e-05	1.8e-05	2.9e-05	4.7e-05	6.6e-05
Yb	2.8e-03	4.8e-03	3.0e-04	5.2e-04	1.8e-04	3.3e-04	4.0e-04	5.7e-04
Hf	1.5e-03	1.9e-03	1.6e-04	2.1e-04	9.8e-05	1.3e-04	1.6e-04	2.3e-04
Ta	1.0e-03	2.0e-03	1.1e-04	2.2e-04	6.8e-05	1.4e-04	2.1e-04	3.3e-04
W	0.024	0.104	2.6e-03	1.1e-02	1.5e-03	6.9e-03	2.0e-04	3.0e-04
Au	0.033	0.092	3.5e-03	1.0e-02	2.1e-03	6.2e-03	4.6e-06	4.7e-06

SO_2 emission rates from Kyle *et al.*, (1994). Values calculated using element-to-S ratios from Table 5.6, as explained in text.

Table 5.7. (cont.)

	1987		1988		1989		1991	
	mean	std	mean	std	mean	std	mean	std
SO_2	16.1	9.9	9.8	3.3	19	7.7	25.9	7.3
HF	5.8	6.4	2.3	1.2	9.2	7.7	6.0	4.1
Na	0.8	0.8	0.2	0.1	0.9	0.8	1.7	1.0
Al	0.5	0.9	0.2	0.3	0.2	0.4	1.4	2.1
HCl	11.7	13.6	5.5	2.8	17.5	18.9	13.3	9.5
K	0.7	0.7	0.3	0.2	0.9	0.8	1.1	0.6
Ca	0.5	0.8	0.2	0.2	1.1	1.1	0.2	0.2
Sc	2.7e-05	4.5e-05	1.7e-05	3.8e-05	2.7e-05	3.9e-05	4.4e-05	4.1e-05
Ti	0.11	0.15	0.014	0.010	0.18	0.19	0.12	0.14
V	2.7e-03	7.3e-03	4.5e-04	4.6e-04	3.4e-04	2.4e-04	7.9e-03	1.5e-02
Cr	0.013	0.039	1.4e-03	1.5e-03	0.011	0.017	0.046	0.105
Mn	6.4e-03	1.1e-02	9.2e-04	6.2e-04	2.5e-03	2.8e-03	0.023	0.025
Fe	0.21	0.30	0.042	0.033	0.15	0.18	0.54	0.57
Co	3.5e-03	1.8e-02	3.7e-05	7.0e-05	7.1e-05	7.5e-05	0.030	0.071
Ni	4.3e-03	5.9e-03			4.8e-03	6.3e-03	0.010	0.003
Cu	0.06	0.15			4.7e-03	1.9e-03	0.15	0.29
Zn	0.10	0.27	9.9e-03	9.2e-03	0.11	0.14	0.38	0.81
As	0.011	0.012	5.0e-03	3.4e-03	0.014	0.012	0.017	0.011
Se	1.4e-03	4.6e-03	1.4e-04	4.6e-05	3.3e-04	2.8e-04	5.9e-03	1.3e-02
Br	0.022	0.025	0.011	0.006	0.023	0.024	0.034	0.029
Rb	4.3e-03	5.1e-03	1.5e-03	7.6e-04	5.4e-03	5.9e-03	7.1e-03	4.1e-03
Mo	5.4e-03	1.8e-02	2.2e-04	1.1e-04	2.1e-03	3.0e-03		
Cd	4.3e-03	4.8e-03	1.6e-03	1.2e-03	5.8e-03	5.3e-03	7.9e-03	6.4e-03
In	1.2e-03	1.5e-03	4.4e-04	2.2e-04	1.8e-03	2.0e-03	1.7e-03	8.3e-04
Sb	5.6e-04	1.0e-03	2.0e-04	2.3e-04	7.1e-04	9.9e-04	1.3e-03	2.6e-03
Cs	1.8e-04	2.0e-04	5.4e-05	2.9e-05	2.5e-04	2.4e-04	3.1e-04	2.1e-04
La	4.9e-04	9.4e-04	2.2e-05	1.7e-05	1.5e-04	2.0e-04	1.7e-03	2.1e-03
Ce	1.3e-03	2.5e-03	7.3e-05	7.2e-05	3.2e-04	3.6e-04	5.1e-03	5.7e-03
Sm	7.3e-05	1.4e-04	3.5e-06	2.4e-06	1.7e-05	1.7e-05	2.3e-04	2.7e-04
Eu	5.2e-05	9.1e-05			5.8e-06	6.5e-06	5.6e-05	6.3e-05
Yb	5.3e-04	1.0e-03			1.5e-05	1.7e-05	1.3e-04	1.1e-04
Hf	2.9e-04	4.1e-04			7.5e-05	3.0e-05	4.4e-04	4.8e-04
Ta	2.0e-04	4.2e-04			1.8e-05	2.0e-05	2.1e-04	2.8e-04
W	4.5e-03	2.0e-02	1.0e-04	3.4e-05	5.7e-04	1.1e-03	2.8e-02	6.7e-02
Au	6.3e-03	1.9e-02	5.2e-05	7.3e-05	9.7e-05	1.3e-04	2.3e-02	4.1e-02

SO_2 emission rates from Kyle *et al.*, (1994). Values calculated using element-to-S ratios from Table 5.6, as explained in text.

The error associated with the calculation of emission rates is a combination of (1) analytical errors associated with measurement of elemental concentrations, (2) uncertainty associated with calculations of SO_2 flux, (3) uncertainty associated with reproducibility in sample collection. The analytical errors are between 5 to 10%; their sources are mainly due to uncertainty associated with (a) reproducibility in sample-to-detector geometry, and (b) determination of photopeak areas (see appendix A1). Accuracy of INAA measurements was determined by comparison of concentrations obtained for quality assurance standards with recommended values and is generally found to be good (within 1-2 sigma). Precision of the method was determined independently by running duplicates or triplicates of samples and quality assurance standards, as was calculated as standard deviation from the mean value. Precision of the measurements was better than 10%. The errors associated with calculations of SO_2 flux are due to number of parameters including estimates of plume rise rate (wind speed), distance to the plume, scan rate, and errors associated with data reduction. The cumulative errors are between 7-30% depending on the methods used to evaluate each of the composite parameters (Kyle *et al.*, 1994; Sybeldon, 1991). The uncertainties associated with the reproducibility in sample collection are probably the largest source of error for the total estimate; however, these uncertainties are most difficult to evaluate.

The overall uncertainty associated with emission rate values for each element (σ_F) was calculated as:

$$\sigma_F = \sqrt{x_\Phi^2 \sigma_r^2 + x_r^2 \sigma_\Phi^2 + 2 x_\Phi x_r \sigma_\Phi \sigma_r} \qquad (1)$$

(Journel and Huijbregts, 1978) where x_Φ and σ_Φ are mean and standard deviation values of S flux (from Kyle *et al.*, 1994), and x_r and σ_r are mean and standard deviation values of element-to-sulfur ratio (from Table 5.6).

5.2. Discussion

5.2.1. Halogens

The total concentrations and relative abundances of F, Cl, and S are often of particular interest to volcanologists. Many workers have shown a dependence between the relative abundances of these elements in the plume and changes in volcanic activity or other processes associated with the exsolution of gas and its interaction with the wall-rock. Noguchi and Kamiya (1963), Murata *et al.* (1964), Stoiber and Rose (1970), Menyailov (1975), and Giggenbach (1976) have observed a decrease in the Cl/S ratio prior to an eruption, and suggested such a trend can be used to predict eruptions. Others have reported the opposite trend, with Cl/S ratio increasing prior to an eruption (Naughton *et al.*, 1975; Hirabayashi *et al.*, 1982; 1986). The F/Cl ratio also displays temporal variations which may be related to the preferential exsolution of Cl from the magma. Murata *et al.* (1964) suggested that the F/Cl ratio could be affected by the reaction of halogen gases with the lava or by the preferential release of Cl during cooling and crystallization of lava. Noble *et al.* (1967), showed that during crystallization magma retains more fluorine than chlorine because the latter is released faster due to its

larger size. For the 1985 eruptive episode of Pu'u O'o vent at Kilauea, Miller *et al.* (1990) reported higher F/Cl values in the emissions associated with the influx of fresh magma, and the progressive decrease of the F/Cl ratio between eruptive episodes. These observations were corroborated by Yoshida (1990). However, as pointed out by Naboko (1959), the variation in the F content of the magma, and thus the resulting F/Cl ratio, may be attributed to other processes such as groundwater or seawater contamination, or reaction of halogens (particularly of F) with the wall-rock.

Both sulfur and halogens scavenge other elements from the magma, and their relative abundances affect the trace element content of volcanic gases (Zoller *et al.*, 1983; Thomas *et al.*, 1982; Phelan *et al.*, 1982; Rose *et al.*, 1982; Varekamp *et al.*, 1986; Gemmell 1987; Miller *et al.*, 1990). Oskarsson (1981) and Yoshida (1990) noted that the relative proportions of F and Cl in the gas affect the trace element content of sublimates. The observed changes in the trace element composition of Erebus gases are discussed in part 5.2.2.

Data collected at Mt. Erebus show significant variations (both long- and short-term) in F/S and S/Cl ratios in the gas. Because the activity of Erebus remained constant during the study period (1986-1990) and no significant eruptions were observed, it seems reasonable to conclude that these changes can only be related to other processes occurring during volatile exsolution in the conduit. A possible explanation for the observed relations between F, Cl and S is discussed in the following sections. The Cl/S ratios

determined in this study range from 0.4 to 6.71, with an average of 1.41. Meeker (1988) previously reported Cl/S ratios ranging from 9 to 62.5 with an average of 27.5. Those values are now believed to be in error due to incorrect S analyses. The F/S ratios in the gas range from 0.2 to 2.59, with an average F/S weight ratio of 0.69. Mt Erebus emissions are rich in fluorine, and moderately high in chlorine when compared to other volcanoes (Table 5.8).

Table 5.8. Comparison of halogen emission rates from Mount Erebus with that from various global sources of halogens. Values in $Gg.yr^{-1}$ (1 $Gg = 10^9 g$).

Year	HF	HCl	Ref.
Dec. 1983*	30.5	60.9	
Dec. 1984*	3.3	6.6	
Dec. 1985*	2.0	4.0	
Dec. 1986	4.0	6.9	
Dec. 1987*	5.8	11.7	
Dec. 1988	2.3	5.5	
Dec. 1989	9.2	17.6	
Jan. 1991	6.0	13.3	
Global volcanism	$0.06\text{-}6\times10^3$	$0.4\text{-}11\times10^3$	a,b
Oceans (sea-salt)	$0.4\text{-}1\times10^3$	$5.2\text{-}15\times10^6$	c
Anthropogenic	0.5×10^3	3×10^3	c
Passively degassing volcanoes:			
White Island, 1983	4.7	153.3	b
Masaya, 1979-85	5.8	303	d
Poas, 1982	1.1	14.6	b
Merapi, 1984	0.73	11	b
Etna, 1976	nd	113.2	b
Augustine, 1986	nd	2920	b

* Halogen emissions are estimates based on average F/S and Cl/S ratios (see text).
nd- not determined.
a) Stoiber *et al.* (1987); b) Symonds *et al.* (1988); c) Friend (1989), d) Stoiber *et al.* (1986).

The relative proportions of halogens and sulfur in gas collected from Mt. Erebus are similar to those collected from volcanoes with high F content such as Mt. St. Helens (Vossler *et al.*, 1981; Phelan *et al.*, 1982) or Icelandic volcanoes (Oskarsson, 1980) (Figure 5.10). Data for Sakurajima volcano (Hirabayashi *et al.*, 1982; 1986) indicate even higher proportions of F accompanied by lower levels of Cl and S. Elevated Cl/S ratios were also observed at Mt. Etna (Buat-Menard and Arnold, 1978; Finnegan, 1984). Note that many volcanic systems shown in Figure 5.10 are characterized by extremely low F content. The high F and Cl content of Mt. Erebus emissions indicates the highly evolved character of the alkaline magma (Meeker, 1988; Kyle *et al.*, 1990).

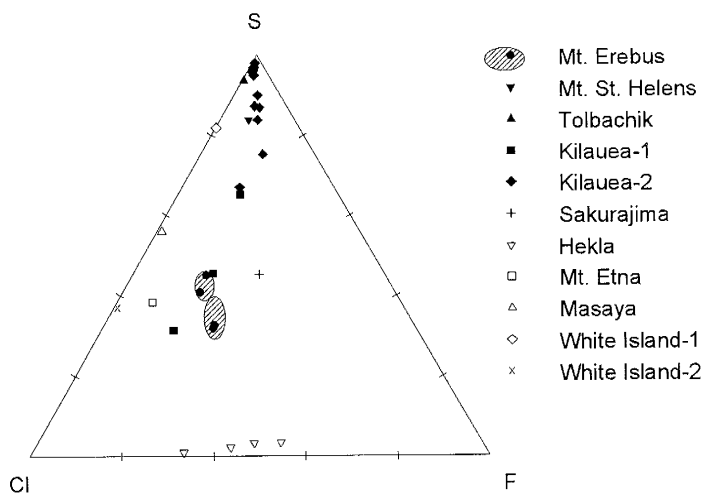

Fig. 5.10. Comparison of F, S, and Cl content of Erebus with that of other volcanoes. Sources: Mt. Erebus, this work; Mt. St. Helens, Phelan et al. (1982); Kilauea-1, Olmez et al. (1986); Kilauea-2, Crowe et al. (1987); Tolbachik, Menyailov and Nikitina (1980); Sakurajima, Hirabayashi et al. (1982, 1986); Hekla, Oskarsson (1980); Mt. Etna, Buat-Menard and Arnold (1978), Varekamp et al. (1986); Masaya, Stoiber et al. (1986); White Island-1, Giggenbach (1975); White Island-2, Rose et al. (1986).

5.2.1.1. Long-term variability in halogen and sulfur content

The quasi-cyclic temporal variations in the proportions of sulfur and halogen gases observed in Mt. Erebus emissions from years 1986-1991 can be interpreted as a indication of a heterogeneous distribution of volatiles in the Erebus magma. At least two possible explanations for the existence of such heterogeneities can be suggested. Heterogeneities may be present in the magma chamber as "packets" of melt having different composition slowly convecting upwards and discharging their volatiles, or as zones in the magma chamber. Although the term "heterogeneity" may imply distinct compositional differences in the melt, in the case of Erebus it may be only manifested by variations in the volatile content of the melt. This is consistent with the lack of evidence of significant compositional variability in major and trace element composition of glass and phenocrysts erupted between 1972-1986 (Caldwell and Kyle, 1994). The possibility of heterogeneities in Erebus magma is supported by Reagan *et al.* (1992) who reported differences in $(^{230}Th)/(^{232}Th)$ ratios in glasses from bombs erupted in 1984 and 1988. It is a significant finding because hitherto no geochemical data were available to support a hypothesis of the existence of heterogeneities in the Erebus magma. At least two models can be considered to explain the observed variation in gas composition: either (1) the magma chamber could contain discrete volatile-rich packets, or (2) the magma chamber could be zoned, that is contain layers with various volatile content.

Volatile-rich packets within magma chamber

In this model, the heterogeneity may be established by periodic injections of volatile-rich magma in the base of Erebus magma chamber from a deeper part of the Erebus magmatic system. Assuming fast convection rates, the volatile rich packet could move upward without significant loss of volatiles due to diffusion into the surrounding melt until reaching shallower depths where exsolution would occur. It can also be assumed that the depth at which the saturation of volatiles (and initiation of vesiculation of the melt) occurs would vary, depending on the amount of dissolved volatiles. The only two volatiles that are likely to be present in the melt in sufficiently high quantities to control the process of vesiculation are CO_2 and H_2O. Thus, their presence and relative proportions could be a factor determining the exsolution of other volatiles present in the melt.

As magma convects upward, most of the CO_2 and water partitioned into the CO_2 are lost, accompanied by the exsolution of Cl and F in the upper part of the conduit. Sulfur probably becomes saturated at shallow depths and its loss from the magma may be largely controlled by the size of the magma lake (Kyle *et al.*, 1990; Kyle *et al.*, 1994). Following the addition of volatile-rich magma, the depth at which both halogens would become supersaturated would increase, thus increasing the volume of the magma column from which halogens could be exsolved. This could be manifested in the composition of the gas by relatively higher halogen-to sulfur ratios. In periods when the magma chamber is not re-supplied by fresh magma the melt would become depleted in

volatile content due to the continuous loss of CO_2. With the loss of CO_2, vesiculation would be delayed in the magma and the saturation of halogens would occur at shallower depths; consequently, smaller amounts of halogens would be exsolved from the melt. During such periods, the composition of exsolved gas would be dominated by sulfur.

Zonation of the magma chamber

Another explanation for the existence of heterogeneities in the magma chamber is zonation. The bottom of the magma chamber would be constantly enriched in volatiles from the deeper part of the system, whereas the upper zone would be degassed. The occasional mixing between the two zones (or complete overturn) could enrich the upper part of the chamber in volatiles, and lead to changes in the proportions of emitted volatiles in the same way as was explained above. The experimental work of Turner and Campbell (1986) showed that the existence of compositional zonation in magma chamber can be preserved despite the presence of a strong convective movement. Thus it does not seem unrealistic to assume that this process could take place in the Erebus magma chamber.

Although the gas composition (as expressed in terms of its 3 major components) seems to oscillate between the two endpoints as exemplified by averages for 1986 plus 1989, and 1988 plus 1991, it does not imply, however, a 2-3 years cycle of compositional changes. In fact the process (whether it is upward movement of volatile-rich plumes or overturn of a zoned magma chamber) does not have to be necessarily

periodic and could be much faster. At present, our intermittent record does not allow us to make any predictions as to the timing of this process. Moreover, future data may reveal that the evolution of the volatile composition proceeds along different paths.

The model involving injection of new volatile rich magma is similar to that proposed by Caldwell *et al.* (1989) as a mechanism for the 1984 eruptive activity. Caldwell *et al.* (1989) noted the summit area inflated and numerous micro-earthquake swarms preceded the 1984 eruptions, in support of injection of the new material into the magma chamber. The frequency and size of the eruptions have decreased significantly since 1984. The seismic activity is low and earthquake swarms are infrequent (Kaminuma, 1994). It is therefore likely that magma emplacement events are uncommon. The model could be modified by assuming that the local enrichment of volatiles is accomplished by slow addition of volatile-rich fluids into the lower part of the chamber rather than by addition of new magma. In such a case the increase in total volume of the magma chamber would be smaller than if a batch of fresh magma was added.

5.2.1.2. Short-term variability in halogen and sulfur content and its implications to the degassing mechanism

The short-term variability observed in the data collected each year may be related to the mechanism of gas exsolution. The relative proportions of Cl, F, and S gases in

the emissions are related to the depth at which their exsolution occurs or, more directly, the variable amounts of magma convecting through the saturation depths for each of the three elements. Thus the S/Cl and F/Cl ratios in the gas are influenced by the movement of the magma in the conduit. Sulfur is exsolved from the magma at lower pressures (shallower depths) than halogens whose behavior is probably more similar to that of water (Burnham, 1979; Holloway, 1981), therefore, the upper part (< 150 m below the surface) of the magma column is depleted in volatile S (Gerlach, 1986). Halogens, on the other hand, tend to exsolve from the melt at higher pressures (greater depths), though the knowledge on their solubility in a melt, let alone in a phonolitic melt, is limited. From the data on the partitioning of F and Cl between the melt and the fluid phase (Webster, 1990; Webster and Holloway, 1988) we can predict that chlorine is more incompatible than fluorine. The exsolution of Cl should occur before F. Thus, if a packet of magma starts to ascend in the conduit, its presence will manifest itself by higher Cl output resulting in low S/Cl and F/Cl ratios. As the magma ascent continues, the amount of Cl present in the gas diminishes, so that both S/Cl and F/Cl ratios will increase. The increase in the F/Cl accompanying magma ascent was reported from Kilauea (Miller *et al.*, 1990) and from Sakurajima by Hirabayashi *et al.* (1986) who noted correlation between the S/Cl and F/Cl throughout the eruptive cycle similar to that described in this work.

Let us assume that a packet of fresh magma is being injected into a column in which upper part is already degassed (Figure 5.11). As the packet passes the Cl

saturation depth, the evolved gas will be characterized by a high Cl content (low S/Cl and F/Cl ratios). As the packet moves upward it passes through the F saturation depth and so the F/Cl ratio of the emissions will increase. After the packet passes the S saturation depth, the S/Cl will increase until the volatile content falls below the saturation level. The magma traveling along the outermost streamline loses most of its volatile content, whereas the inner part of the convecting cell is still rich in S and F. Moreover, the total overturn time for the central part of the convection cell is shorter, so it can resupply its Cl content before the outermost part does.

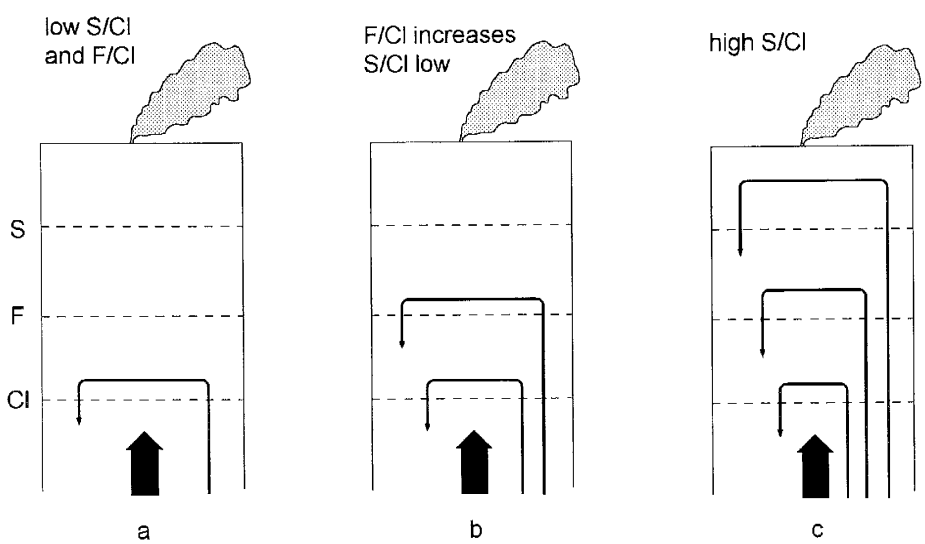

Fig. 5.11. Schematic representation of the upper part of Erebus conduit showing a packet of fresh magma moving upward. Dashed lines show saturation depths of S, F, and Cl, and curved lines mark magma movement (for clarity only a half of each convection cell is shown). As magma ascends, it passes though the Cl saturation depth first, and the exsolved gas is high in Cl, but low in S and F (a). If the packet moves through F saturation depth, the amount of exsolved F increases, so F/Cl of the gas increases (b). As magma reaches the top of the conduit, S is exsolved (c). The S/Cl of the gas increases because most of Cl is already exsolved from the melt in the uppermost portion of the column

The inset on the Figure 5.9 shows the F/Cl and S/Cl ratios on filters collected on Dec. 16, 1988 within a very short period of time between 12:26 and 15:04. On that day, a small strombolian eruption was observed at 14:20 local time, which is indicated by the vertical arrow in the inset. The S/Cl ratio showed a decrease prior to this eruption as the magma packet travelled upward past the Cl saturation depth. Then a sudden increase in this ratio was observed which was synchronous with the eruption, probably due to the rapid exsolution of sulfur at low pressures. This was then followed by a period during which the S/Cl decreased again, perhaps due to the fact that during the eruption the magma had lost most of the sulfur. The F/Cl ratio was low during this period, and increased only slightly after the eruption.

COSPEC measurements show short-time variability within the daily record of SO_2 emissions (Kyle *et al.*, 1994). These changes are often cyclic with about a 1 hour period, and seem to be related to the amount of SO_2 being supplied to the lava lake by the convection in the conduit beneath it. We believe the observed short-time variability in the Cl, F, and S content of the gas is governed by the same process as the daily variations in SO_2 output. Although the rapidity of COSPEC observations results in time resolution of the convection process superior to that which can be obtained from the gas samples, both methods lead to very similar conclusions. By increasing the frequency of gas sampling we could attain better understanding of magma movement in the conduit and the mechanism of gas exsolution.

5.2.2. *Trace components of the Erebus plume*

5.2.2.1. Data representation procedures

When comparing aerosol and gas data from different volcanoes or even between samples collected at the same volcano we are interested in learning which elements are most abundant in the plume and how their abundance compares with the magma from which they were volatilized. Therefore, rather than comparing the absolute concentrations ($\mu g.m^{-3}$), data are usually normalized. The conventional way of normalizing volcanic gas data is by calculation of the enrichment factor (Zoller *et al.*, 1983), which is defined as:

$$EF_{sample} = \frac{(X/R)_{sample}}{(X/R)_{magma}} \qquad (2)$$

where EF_{sample} is the enrichment factor of element X in the sample, $(X/R)_{sample}$ is the ratio of element X to the reference element R in the sample, and $(X/R)_{magma}$ is the ratio of element X to the reference element in the magma. Because the composition of the actual magma is difficult to assess, many authors prefer to use the composition of fresh lava or volcanic ash as the reference material. Using the composition of volcanic ash or lava from a selected volcanic system as the reference material in calculations of the enrichment factor permits one to show which elements in the gas are being preferentially volatilized and consequently enriched in the gas. However, such data cannot be used to compare between volcanic systems of differing magma composition. Such comparisons are possible if EFs are calculated with respect to the mean crustal composition. For

gases exsolving from basaltic melts, the enrichment factors calculated relative to the crust are generally lower, notably for elements such as Th and La (Vie le Sage, 1983) due to the fact that the mean crustal composition is biased toward granites and sedimentary rocks.

The reference element used in the calculation of EF should be characterized by well established concentrations in the source and by the low reactivity of its compounds in the atmosphere. Usually, aluminum, scandium, iron and magnesium are used as the reference elements for normalizing atmospheric and volcanic plume data (Vie le Sage, 1983). These elements are important constituents of both ash and crustal material, and have low chemical reactivity. However, these elements are not suitable for normalizing data collected in plumes that have high or variable ash content because the values obtained by the normalization depend on the amount of ash collected on filter. Crowe *et al.* (1987) found that the enrichment factors normalized to ash constituents are minimum values and proposed the use of a volatile phase (S, As, Se, Cl, F, or Br) as a reference element instead. They decided against the use of sulfur, arsenic or selenium because filter collection systems may not be sufficiently quantitative for these elements. Moreover, the release rate of sulfur changes through the eruption cycle. Crowe *et al.* (1987) have found that Cl, F and Br provide constant calculations of enrichment factors. The use of Br as the reference element is preferred because of the importance of chlorine and fluorine in the transport of trace metals. However, some metal-bromide compounds are characterized by high vapor pressures under magmatic conditions, often higher than

those of metal-fluorides and thus Br may play a significant role in metal transport (Gemmell, 1987). In such situations, bromine will not be suitable as a reference element. Bromine-normalized values must be multiplied by a 10^5 factor which represents the approximate enrichment of Br in the gas phase and adjusts the enrichment factors for non-enriched ash elements to unity. This allows a comparison between Br-normalized and conventional EFs values (Crowe *et al.,* 1987).

Because the Erebus plume is ash-poor (Meeker, 1988) use of either Al, Sc or Br produces similar results in calculating EFs. In this work I used Sc as the reference element for several reasons: (1) Sc is easily analyzed by INAA even at very low concentrations whereas in some cases high precision determination of Br was a problem due to high blank concentrations; (2) using Sc allows Br enrichment in the plume to be determined; this is important because Br may be important in volatilization of some metals; (3) using Sc to calculate EF for gas samples permits direct comparison with EF calculated for salts samples (see chapter 7). Neither Al nor Br could be used as reference elements for EF for salts, Al being a significant component in salt composition, and Br being usually present in concentrations below the detection limit.

5.2.2.2. Enrichment factors in Erebus plume

Table 5.9 gives the enrichment factors calculated for the annual average gas compositions. The EF patterns calculated using either Sc or Br as the reference element are comparable indicating that the plume has a low ash content (Figure 5.12a,b), even for 1991 samples which have the highest proportion of Al (compare the distribution plot of Al, Figure 5.3).

Gas in the Erebus plume is very strongly enriched (relative to the magma) in halogens (F, Cl, Br), S, In, Au, As, Se, Sb, W, Cu, Zn, Mo, Co, Cr. Elements less enriched include Na, K, Rb, Cs, Ca, and REE Ce, Eu, and Yb. Elements Al, Fe, Mn, and also La and Sm are usually depleted suggesting that they are not readily volatilized or that they are removed easily from the plume due to precipitation in close proximity to the lava lake. Samples collected in 1991 are exception, and show a slight enrichment of Al and Fe. That, together with the high concentrations of these elements on filters in 1991 could indicate more efficient volatilization of those elements during that year but it is more likely that the enrichment is due to higher ash content.

Differences in enrichment factors between the four years are small (Figure 5.13), with the exception of Au which is high in 1991, and low in 1986. Ca is depleted in 1991 but enriched in the remaining years. Samples from 1988 and 1989 are more depleted in REEs. Enrichment factors calculated using analyses of filters collected in 1978 by

Germani (1980) are generally in agreement with data presented here. Although several elements (alkali metals, In, Cd, and REE, especially Ce) show higher enrichments, the general pattern is preserved.

Table 5.9. Average values of log (EF) for samples collected in 1986, 1988, 1989, and 1991. EF calculated relative to Sc using estimates of the Mt. Erebus magma as reference material.

	Dec. 1986	Dec. 1988	Dec. 1989	Jan. 1991	Reference material (ppm)	source
F	2.53	2.34	2.71	2.41	2140	Bg
Na	0.24	-0.10	0.26	0.42	63275	Bwr
Al	-0.62	-0.41	-0.72	0.07	106000	Bwr
S	3.48	3.64	3.74	3.76	260	Bwr
Cl	2.98	2.93	3.15	2.99	1400	Bg
K	0.35	0.22	0.50	0.56	37935	Bwr
Ca	0.19	0.40	0.88	-0.10	19011	Bwr
Sc	0	0	0	0	3.52	Bg
Ti		-0.16	0.68	0.25	5300	TMc
V	0.27	0.62	0.25	1.31	25	Mwr
Cr	1.43	1.32	1.98	2.20	14	Mwr
Mn	-1.09	-1.72	-1.52	-0.70	10068	Bwr
Fe	-0.03	-0.44	-0.20	0.22	29099	Bwr
Co	1.98	0.56	0.56	3.07	2.36	Mg
Ni			0.80	1.06	105	TMc
Cu	2.34		1.75	2.79	13	Mwr
Zn	1.55	1.25	2.08	2.24	115	Mwr
As	2.56	2.49	2.67	2.67	3.6	Mg
Se	1.64	1.30	1.50	2.25	1.4	TMc
Br	2.96	2.86	2.90	2.99	3.57	Mg
Rb	0.82	0.49	0.80	0.84	109	Bwr
Mo	2.07	0.44	1.12		16.2	Kg
Cd		3.50	3.84	3.92	0.098	TMc
In	3.13	2.99	3.31	3.25	0.1	Tc
Sb	1.99	1.94	2.32	2.31	0.5	Bg
Cs	1.07	0.78	1.19	1.20	2	Mg
La	-0.51	-1.58	-1.03	-0.16	207.6	Mg
Ce	0.41	-0.42	-0.12	0.84	57.3	Mg
Sm	-0.36	-1.44	-1.00	-0.13	26	Mg
Eu	0.57		-0.25	0.36	2.4	Mg
Yb	1.16		-0.13	0.45	5.25	Mg
Hf	-0.05		-0.53	0.20	27.4	Mg
Ta	0.12		-0.76	0.15	18.1	Mg
W	1.32	1.44	1.57	2.79	1.5	Tc
Au	1.62	2.74	2.45	5.18	0.023	Mg

Source: Bg - Erebus glass (Bigelow, 1984); Mg - Erebus glass (Meeker, 1988); Kg -Erebus glass (Kyle and Moore, 1992); Bwr - Erebus whole rock and lava (Bigelow, 1984); Mwr - Meeker whole rock and lava (Meeker, 1988); Tc - crustal average (Taylor, 1964); TMc - crustal average (Taylor and McLennan, 1985.)

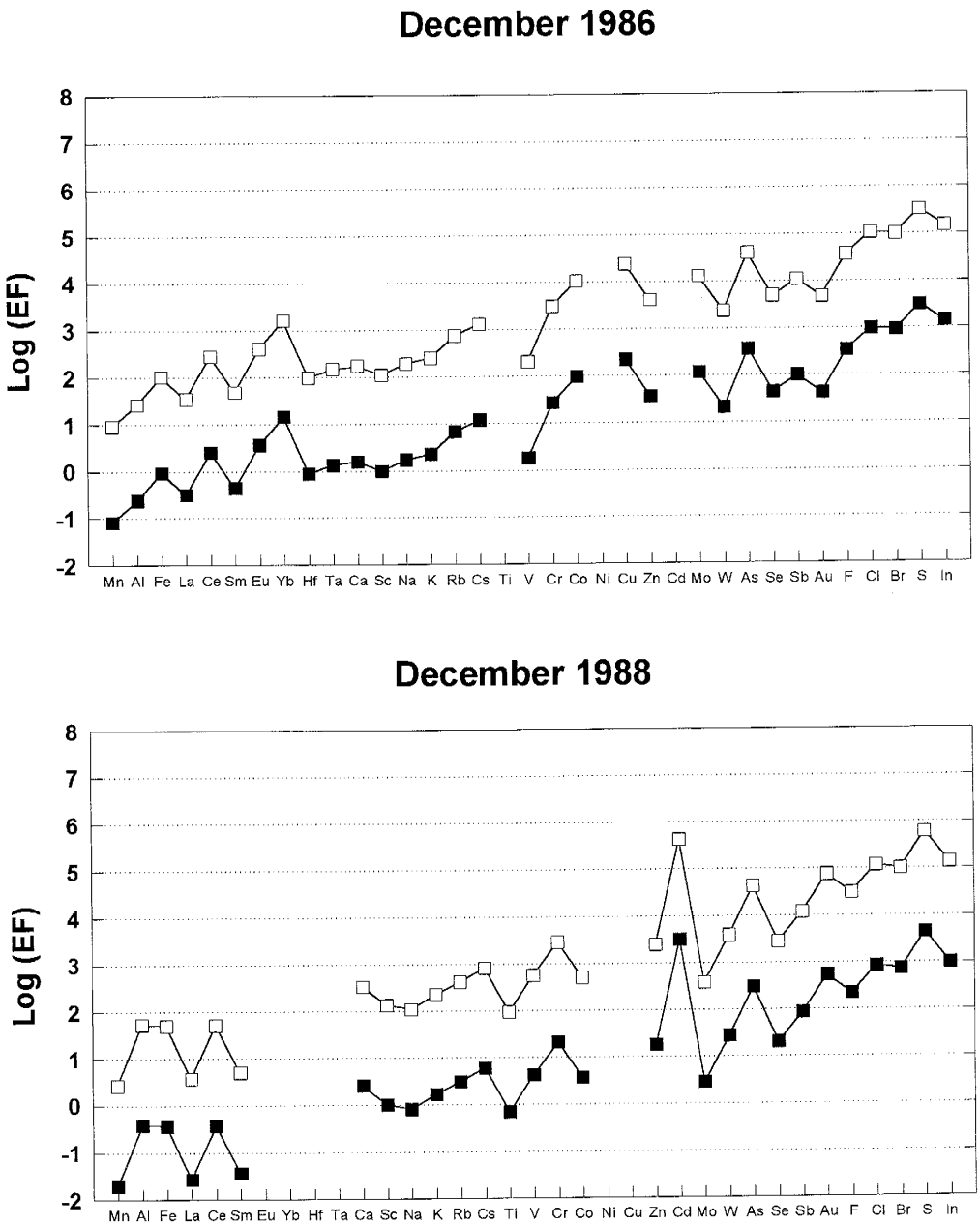

Fig. 5.12a. Comparison of enrichment factors calculated using Br (open squares) and Sc (solid squares) as reference element. Br-normalized EFs are multiplied by 10^5 (see text).

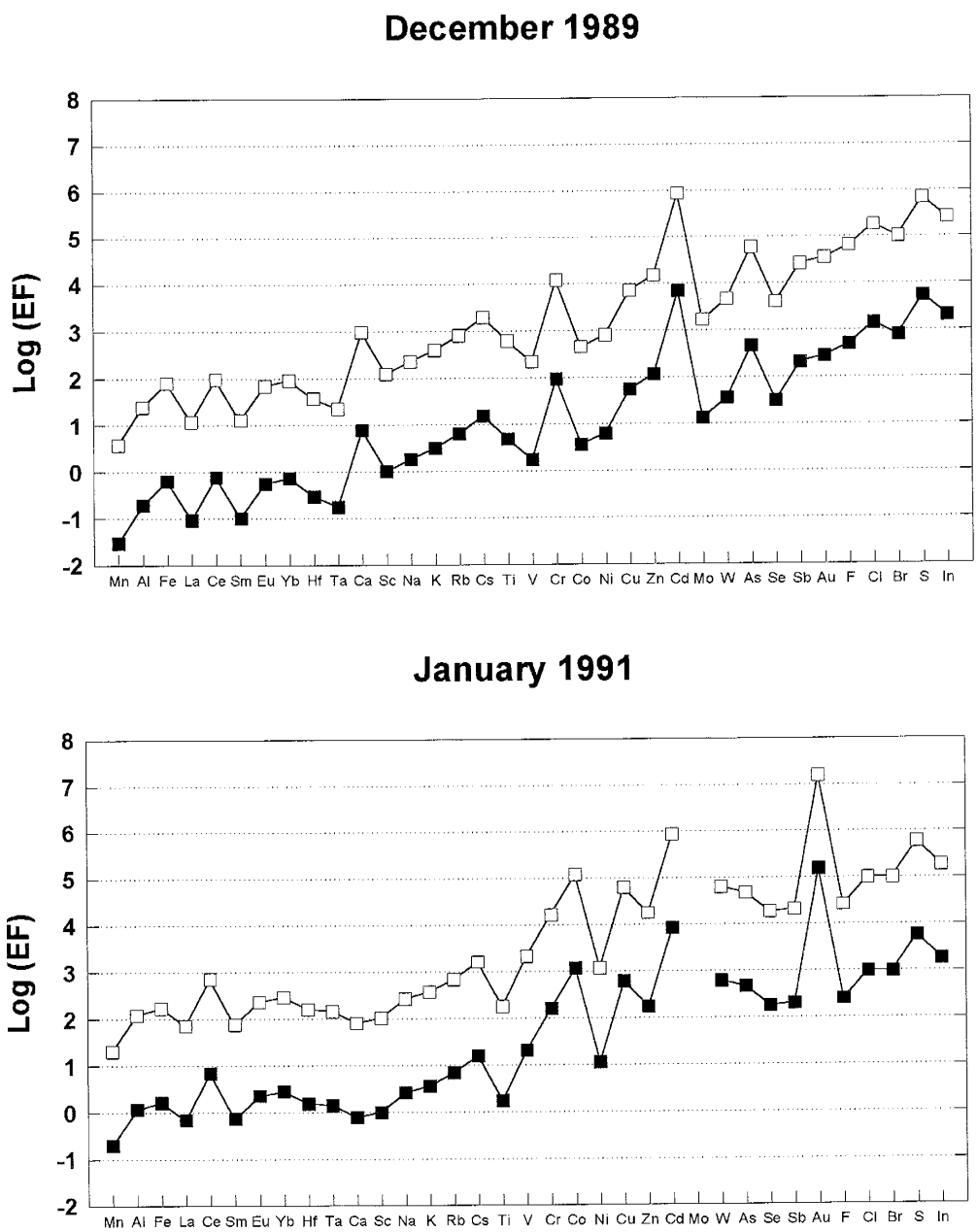

Fig. 5.12b. Comparison of enrichment factors calculated using Br (open squares) and Sc (solid squares) as reference element. Br-normalized EFs are multiplied by 10^5 (see text).

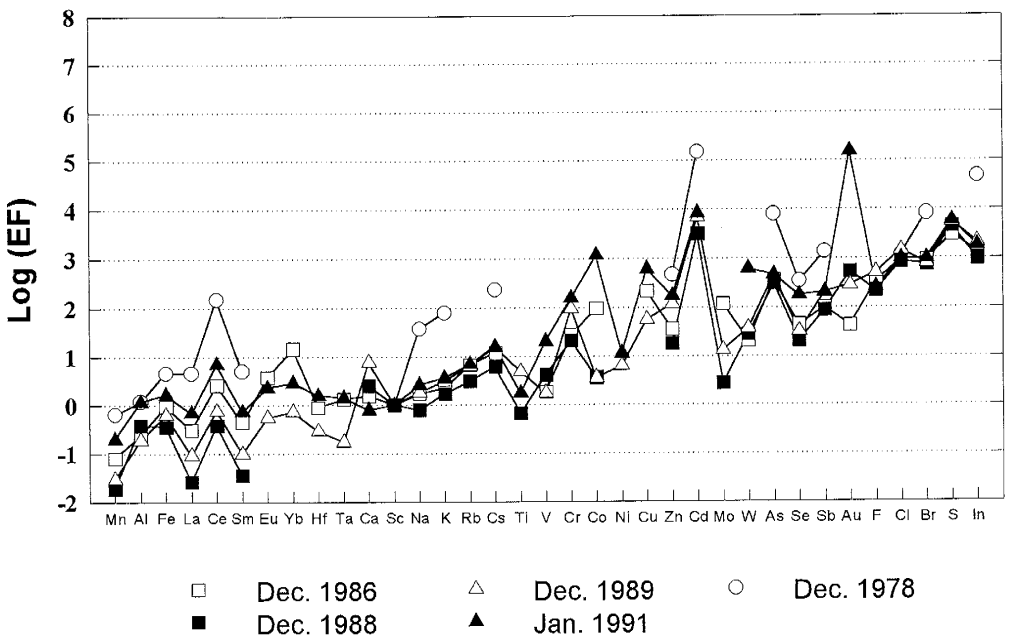

Fig. 5.13. Comparison of average Sc-normalized enrichment factors for 1986-1991 Mt. Erebus filters data with data from 1978 (Germani, 1980).

The general pattern of enrichment factors observed in Erebus samples is comparable to what is observed at other volcanoes (Buat-Menard and Arnold, 1978; Olmez *et al.*, 1978; Symonds *et al.*, 1987; Lepel *et al.*, 1978; and others) even though there may be large differences in actual values of EFs. Elements such as S, F, Cl, Br, Se, Hg, Cd, Ag, Au, and In are among the most enriched (EF often $>>100$) followed by Zn, Cu, Pb, As, W, Ir, and Sb. Alkali metals form the next group in order of decreasing enrichment. Other elements (Mn, Al, Ti, Sc, Fe, Mn, Ni, V, Cr, Co, and REE) are usually not enriched in the plume. The enrichment of elements decreases with the temperature of the gas. Cooling of the gas produces only a slight decrease in EF for

volatiles (S, F, Cl, Br, As and Se) but influences greatly the volatility of metals for which the drop in EFs may be several orders of magnitude (see for example Buat-Menard and Arnold, 1978; Crowe *et al.*, 1987).

The type of bond is helpful in predicting the behavior of volatile elements during cooling. The compounds with stronger covalent bonds are more stable in a vapor phase and less likely to precipitate from the plume. Conversely, the compounds with ionic bonds are less volatile, and usually appear as a particulate fraction in volcanic emissions (Vie le Sage, 1983). The order in which these precipitates are formed can be inferred from the general sequence of sublimation, and it appears in good agreement with the theoretical prediction of Vie le Sage (1983). From high to low temperatures those are: Si, Fe, Al-oxides, Mo-sulfides, Na,K-chlorides, Cd, Fe-sulfides, Pb, As-sulfides (Le Guern and Bernard, 1982; Bernard and Le Guern, 1986). The major drawback of Vie le Sage's reasoning is that it cannot predict the chemical composition of volatile species. For that purpose, careful thermodynamic calculations are necessary, that take into account the composition of a melt, and other physical conditions affecting the process of volatilization and cooling of evolved gas.

In the following section I discuss the occurrence of trace components on filters. For each group of elements I outline the current knowledge about the chemical composition of substances volatilized and the consecutive paths of their transformation from the vapor to a solid phase. I then compare the theoretical composition of those

substances to those described from either Erebus or other volcanic plumes, and try to evaluate the possible chemical form in which trace elements could be present on filters. Elemental concentrations on filters were used to calculate correlation coefficients (Table 5.10) for all possible pairs of elements. The values of the correlation coefficient *r* (which lies between -1 and 1) show whether the concentrations of two elements in the plume are correlated with each other. However, it is impossible to tell whether one correlation is statistically stronger than another. I will consider values of $r > 0.8$ as indicative of a good correlation between elements.

5.2.2.2.1. Alkali metals

The alkali metals detected on the filters include Na, K, Rb, and Cs. All show strong correlation with halogens (Table 5.10) ($r > 0.8$). The close association of alkali metals with halogens is not surprising. Thermodynamic calculations of Symonds *et al.* (1987), Symonds (1990), and Symonds and Reed (1993) indicate that alkali metals are volatilized mainly as monomeric chlorides (NaCl, KCl, RbCl, CsCl), and, to a lesser degree as hydroxides, fluorides, dimeric chlorides, bromides and elemental species. Upon cooling, they also form mixed species such as $NaAlF_4$ (Symonds, 1990). These species precipitate from the vapor as halite (NaCl), sylvite (KCl), $RbCl_{(s)}$, $CsCl_{(s)}$. Most of these species are preserved in this form, although the presence of the H_2SO_4 aerosol in the plume probably causes at least partial conversion of metal-halogen compounds to sulfates. This may explain the correlation between the alkali metals and sulfur observed on filters. These theoretical considerations are supported by the presence of halite and

sylvite in particulate material sampled at Erebus (Chuan *et al.,* 1986; Chuan, 1994). Thenardite (Na_2SO_4) was also detected, and was inferred to represent a reaction product of H_2SO_4 droplets, which were detected in samples of particulates mantling ash particles, with halite (Chuan, 1994). The presence of sodium sulfate explains the good correlation of Na with S on some filters, especially those from 1989 and 1991. Data collected in 1988 also correlate well but they are characterized by much lower Na concentrations that change the slope of the regression line. Both halite and sylvite have been reported in numerous studies of both aerosol particles and sublimates collected at active vents (e.g. Stoiber and Rose, 1970; Le Guern and Bernard, 1982; Menyailow *et al.,* 1986; Bernard and Le Guern, 1986; Symonds *et al.*, 1987; Quisefit *et al.*, 1989; Toutain *et al.*, 1980). It should also be noted that some alkali metals bearing compounds detected in QCM samples were identified as fragments of silicate material, perhaps volcanic glass (Chuan, 1994). In some samples the presence of K_2S was also reported (Chuan, 1994), although the K-sulfate seems more likely.

Table 5.10. Correlation coefficients (r) for elements analyzed on Erebus filters.

	F	Na	Al	S	Cl	K	Ca	Sc	Ti	V	Cr	Mn	Fe	Co	Ni	Cu	Zn	As	Se	Br	Rb	Mo	Cd	In	Sb	Cs	La	Ce	Sm	Eu	Yb	Hf	Ta	W	Au
F	1	0.84	0.06	0.50	0.85	0.80	0.18	0.34	0.05	-0.14	-0.03	0.42	0.46	0.02	0.14	0.43	0.30	0.80	0.17	0.81	0.76	0.27	0.20	0.77	0.58	0.81	0.32	0.29	0.21	0.58	0.23	0.04	0.25	-0.06	-0.07
Na		1	0.20	0.53	0.92	0.92	0.22	0.38	0.10	-0.10	-0.03	0.61	0.52	0.08	0.16	0.54	0.23	0.93	0.25	0.89	0.94	0.20	0.15	0.92	0.69	0.90	0.44	0.32	0.33	0.65	0.06	0.04	0.39	-0.04	-0.02
Al			1	0.42	-0.03	0.05	0.12	0.63	0.03	0.09	0.09	0.76	0.69	-0.06	0.01	0.12	-0.07	0.07	0.08	0.04	0.00	0.08	-0.04	-0.05	0.21	-0.00	0.79	0.79	0.75	0.02	0.19	0.14	0.13	0.01	-0.11
S				1	0.41	0.35	0.28	0.71	0.13	-0.08	-0.08	0.70	0.70	0.00	0.17	0.15	0.12	0.42	0.08	0.42	0.35	0.26	0.25	0.33	0.44	0.34	0.70	0.61	0.62	0.22	0.34	0.29	0.16	-0.16	0.01
Cl					1	0.93	0.08	0.22	-0.01	-0.18	-0.05	0.37	0.29	0.00	0.19	0.57	0.18	0.95	0.24	0.89	0.93	0.04	0.20	0.96	0.58	0.90	0.19	0.13	0.12	0.70	-0.10	0.10	0.34	-0.05	-0.00
K						1	0.08	0.22	-0.01	-0.08	0.00	0.42	0.33	0.03	0.11	0.48	0.18	0.89	0.29	0.88	0.94	0.13	0.13	0.94	0.54	0.93	0.25	0.15	0.19	0.62	-0.06	0.01	0.26	0.05	0.01
Ca							1	0.13	0.82	0.00	-0.02	0.12	0.22	-0.06	0.33	0.10	0.33	0.12	-0.02	0.17	0.08	0.21	0.05	0.11	0.51	0.10	0.12	0.01	0.09	0.11	0.23	-0.02	0.13	-0.05	-0.01
Sc								1	0.01	-0.01	0.07	0.75	0.78	0.02	-0.01	0.17	0.12	0.29	0.13	0.26	0.20	0.24	0.01	0.16	0.35	0.17	0.79	0.72	0.75	0.14	0.39	0.17	0.30	-0.05	-0.11
Ti									1	-0.02	-0.10	-0.00	0.04	-0.12	0.24	0.02	0.22	0.01	-0.02	0.08	0.01	-0.01	-0.03	0.01	0.49	0.02	-0.03	-0.07	-0.05	0.04	0.02	-0.01	0.04	-0.05	0.03
V										1	0.41	-0.02	0.03	0.60	-0.07	-0.02	-0.01	-0.16	0.42	-0.09	-0.05	0.22	0.04	-0.18	-0.06	-0.11	0.05	-0.04	0.09	-0.19	0.17	0.01	-0.22	0.58	-0.16
Cr											1	0.03	0.22	0.20	0.13	0.02	-0.11	-0.13	0.66	0.01	0.00	-0.02	0.19	-0.03	-0.10	-0.03	0.05	0.10	0.09	-0.11	-0.04	0.12	0.23	0.53	-0.09
Mn												1	0.86	-0.00	0.04	0.34	0.16	0.47	0.18	0.39	0.42	0.20	0.00	0.35	0.51	0.36	0.92	0.85	0.83	0.32	0.25	0.08	0.30	0.01	-0.08
Fe													1	0.11	0.08	0.09	0.16	0.33	0.26	0.41	0.32	0.41	0.08	0.26	0.43	0.32	0.89	0.82	0.83	0.16	0.46	0.19	0.38	-0.05	-0.11
Co														1	0.00	-0.06	-0.04	0.00	0.09	0.10	0.11	0.34	0.10	0.00	0.03	0.02	0.03	-0.10	0.06	-0.09	0.25	-0.03	-0.07	0.01	0.05
Ni															1	0.05	0.08	0.11	0.03	0.07	0.13	-0.01	0.43	0.17	0.19	0.15	0.06	0.07	0.05	0.01	-0.12	0.03	-0.04	0.03	0.00
Cu																1	0.03	0.71	0.30	0.39	0.56	-0.20	-0.01	0.56	0.54	0.36	0.14	0.12	0.04	0.75	-0.24	-0.08	0.42	0.33	-0.02
Zn																	1	0.17	0.07	0.20	0.15	0.19	0.01	0.15	0.44	0.19	0.12	0.07	0.08	0.10	0.12	-0.14	-0.05	-0.00	-0.11
As																		1	0.19	0.82	0.93	0.08	0.15	0.93	0.65	0.83	0.28	0.18	0.17	0.79	-0.08	-0.03	0.37	-0.01	0.01
Se																			1	0.32	0.30	0.05	-0.08	0.23	0.15	0.19	0.15	0.21	0.13	0.22	-0.01	0.32	0.35	0.74	-0.12
Br																				1	0.86	0.12	0.05	0.87	0.52	0.91	0.25	0.20	0.19	0.50	0.01	0.14	0.44	-0.08	-0.04
Rb																					1	0.17	0.16	0.95	0.59	0.91	0.26	0.13	0.17	0.65	-0.06	-0.02	0.36	0.04	-0.01
Mo																						1	0.01	0.01	0.23	0.11	0.31	0.07	0.19	0.01	0.83	-0.06	0.01	-0.03	-0.05
Cd																							1	0.18	-0.04	0.21	0.01	-0.04	-0.04	-0.08	-0.11	-0.06	-0.21	-0.05	0.33
In																								1	0.55	0.91	0.16	0.07	0.10	0.70	-0.19	0.01	0.39	-0.04	0.01
Sb																									1	0.47	0.37	0.25	0.26	0.57	0.12	-0.10	0.36	-0.00	-0.04
Cs																										1	0.24	0.17	0.19	0.44	-0.03	-0.02	0.25	-0.04	0.03
La																											1	0.92	0.94	0.12	0.41	0.10	0.18	0.02	-0.11
Ce																												1	0.88	0.05	0.25	0.17	0.20	0.05	-0.12
Sm																													1	0.03	0.31	0.11	0.11	0.00	-0.11
Eu																														1	-0.10	-0.04	0.35	0.09	-0.14
Yb																															1	0.05	-0.04	-0.00	-0.06
Hf																																1	0.13	-0.02	-0.18
Ta																																	1	-0.04	-0.16
W																																		1	-0.01
Au																																			1

5.2.2.2.2. Alkaline earth elements

The aerosol samples contain very little Ca and Mg (detected only in samples from 1991, see appendix B). Although Ca-bearing aerosols (mostly $CaSO_4$) were described from other volcanoes, either present as crystals or as overgrowths on silicates (Varekamp *et al.*, 1986), they have not been found in particulates collected on Mt. Erebus. The distribution plots (Figures 5.2-5.7) show that the Ca concentration changes in a different pattern from the alkali metals, and is highest in 1989. With the exception of the 1991 samples, Ca is sufficiently enriched in filter samples (EF are comparable to that of Rb and Cs) to suggest it is volatilized. Calcium correlates poorly with F in filter samples, and there is no significant correlation with Cl or S. This suggess that Ca may be volatilized partially as CaF_2 (Table 5.10). The association of Ca and F is consistent with experimental work of Webster (1990) who suggested that the two elements are together partitioned from the melt into a fluid phase. However, the results of thermodynamic modeling led Symonds and Reed (1993) to reject a hypothesis of substantial volatilization of Ca. Despite including numerous Ca-bearing species in the model, the modeled concentrations consistently underestimated the observed values. Thus Symonds and Reed (1993) concluded that the majority of Ca (and other refractory elements) detected in volcanic gas comes from wall-rock erosion. This is the also the most likely explanation for the Ca present in the Erebus aerosols, and is supported by correlation of Ca with Al and Sc in some samples.

5.2.2.2.3. Transition metals

The following transition metals were detected in filter samples: Sc, Ti, V, Cr, Mn, Fe, Co, Ni, Cu, Zn, Mo, Cd, W, Au and Hg. Most transition metals form volatile compounds with Cl (AgCl, $CoCl_2$, CuCl, $FeCl_2$, $MnCl_2$, and $ZnCl_2$ are the most commonly found chloride species), sometimes with Br (AgBr, CuBr, $MnBr_2$, $ZnBr_2$), and less often with F (Symonds, 1990; Symonds and Reed, 1993). Other, less common species are hydroxides. For example, at high temperatures $Fe(OH)_2$ may be an important Fe-bearing compound. Some metals (Co, Cu, Fe, Mn, and Zn) can also be volatilized in their elemental state but their abundance in volcanic gas is usually low with the exception of Zn which exceeds $ZnCl_2$ at high temperatures (Symonds, 1990; Symonds and Reed, 1993). Other transition metals (Au, Cd, Hg, Mo, and W) do not form volatile chlorides, and are transported mainly as AuS or Au, Cd and CdS, Hg, oxyacids H_2MoO_4 and H_2WO_4 (at higher temperature) and MoO_2Cl_2 and WO_2Cl_2 (at lower temperatures) (Symonds, 1990). Cr may be transported either as oxychloride species CrO_2Cl_2 at higher temperatures, or as $CrCl_2$ at lower temperatures (Symonds *et al.*, 1987).

Volatilities of all these species vary greatly depending on the properties of each component. Transition metals forming compounds with stronger covalent character are more enriched in the plume (for example Cr, Co, Cu, Zn, Mo, W, and Au) whereas elements that form components with bonds having more ionic character (Mn, Fe and V) precipitate earlier in the cooling sequence and thus are usually less enriched or depleted.

Iron and manganese are usually depleted transition metals detected on filters. Iron, because of the low volatility of its compounds, should easily precipitate from the gas as magnetite or pyrite by the following reactions (in order of decreasing temperatures):

$$3Fe(OH)_{2(g)} = \underset{magnetite}{Fe_3O_{4(s)}} + 2H_2O_{(g)} + H_{2(g)} \qquad T<910°C \qquad (3)$$

$$3FeCl_{2(g)} + 4H_2O_{(g)} = \underset{magnetite}{Fe_3O_{4(s)}} + 6HCl_{(g)} + H_{2(g)} \qquad T<760°C \qquad (4)$$

$$FeCl_{2(g)} + 2H_2S_{(g)} = \underset{pyrite}{FeS_{2(s)}} + 2HCl_{(g)} + H_{2(g)} \qquad T<300°C \qquad (5)$$

(Symonds, 1990; Symonds and Reed, 1993). Those temperatures are probably below the possible temperature of the lake surface in the Erebus crater (the temperature of the melt is thought to be about 1000°C, see chaper 6), where the gas is cooled rapidly upon leaving the magma. It can be hypothesized that most Fe-bearing sublimates are deposited on the lava lake surface or its proximity, and it is unlikely that they are carried in the plume. Iron-bearing phases (magnetite, hercynite ($FeAl_2O_4$), and pyrite) have been described from sublimate samples (e.g. Le Guern and Bernard, 1982; Symonds *et al.*, 1987) as the first precipitates forming in the sampling tubes, thus clearly indicating the low volatility of these compounds. Pyrite, has also been found in sublimate samples, at slightly lower temperatures than magnetite (Symonds *et al.*, 1987). Iron oxides were described in QCM samples on Mt. Erebus (Chuan *et al.*, 1986; Chuan, 1994) and by Varekamp *et al.* (1986) in particulates sampled at Mount St. Helens; but it is more likely that they represent rock fragments rather than true sublimates. In samples collected during this study, iron is an important component and it can constitute up to 4% of the

total concentration, but the values of EFs suggest strong depletion in most samples (with the exception of 1991 samples). That, together with the evidence of correlation between Fe and other non-volatile elements: Al, Sc, Mn, Ni, La, Ce and Sm (Table 5.10), suggests association of Fe with some non-volatile phase, most likely silicate.

Manganese is among the least enriched elements not only in the Erebus plume but also at other volcanoes. One of its most volatile compounds, $MnCl_2$, forms ionic bonds (Vie le Sage, 1983) and precipitates easily as $MnWO_4$, MnS, $MnCl_2$, and MnF_2 (Symonds, 1990; Symonds and Reed, 1993). In sublimate samples Mn is often associated with the pyrite and sphalerite zone formed between 400 and 260°C (Symonds *et al.*, 1987; Symonds and Reed, 1993) indicating the instability of Mn compounds even at high temperatures. On Erebus, Mn is the most depleted element (Figure 5.12) and its presence in filter samples, as for Fe, probably suggests the presence of ash or rock fragments.

A group of five other transition metals, Ti, V, Cr, Co, and Ni, is characterized by variable EFs patterns ranging from depleted or slightly enriched to moderately enriched in the Erebus plume. Buat-Menard and Arnold (1978) show some evidence of volatilization of Ni, V, Cr and Co, but the enrichment of these elements in the Mt. Etna plume is strongly influenced by temperature changes. Little is known about volatilization of those elements, but it is likely that they behave similarly to Cr. Chromium EFs are relatively high (Figures 5.12, 5.13) which shows that due to its tendency to form more

covalent bonds. Cr-bearing compounds are more volatile and less susceptible to precipitation. Chromium does not correlate with either Cl, F or S, which suggests that it is precipitated possibly as an oxide. Chromium oxides were found in QCM samples from Mount Erebus (Chuan *et al.*, 1986; Chuan, 1994). Cr correlates poorly ($r = \sim 0.4$) with V suggesting that the two elements may occur together in some mixed compound.

The presence of Ti and V in samples may be attributed to contamination with the ash, although there is no correlation between these and ash-related elements. Cobalt can be transported in the vapor phase as chloride. It precipitates as $CoFe_2O_{4(s)}$ between 590 and 510°C or as $CoS_{(s)}$ below 510°C (Symonds, 1990; Symonds and Reed, 1993). In the Erebus plume Co is among the moderately enriched elements, but its EFs show the largest variation between years, with the highest enrichment noted in 1986 and 1991.

Several transition metals including Cu, Mo, Cd, and Zn are transported in the gas as various compounds, and may precipitate as sulfides (bornite, molybdenite, greenockite, and sphalerite, respectively) according to the following reactions:

$$5CuCl_{(g)} + FeCl_{2(g)} + 4H_2S_{(g)} = \underset{bornite}{Cu_5FeS_{4(s)}} + 7HCl_{(g)} + \frac{1}{2}H_{2(g)} \qquad T<770°C \quad \textbf{(6)}$$

$$H_2MoO_{4_{(g)}} + H_2S_{(g)} + H_{2_{(g)}} = \underset{molybdenite}{MoS_{2(s)}} + 3H_2O_{(g)} \qquad T<620°C \quad \textbf{(7)}$$

$$Cd_{(g)} + H_2S_{(g)} = \underset{greenockite}{CdS_{(s)}} + H_{2(g)} \qquad 140°C<T<470°C \quad \textbf{(8)}$$

$$ZnCl_{2_{(g)}} + H_2S_{(g)} = \underset{sphalerite}{ZnS_{(s)}} + HCl_{(g)} \qquad T<460°C \quad \textbf{(9)}$$

(Symonds, 1990; Symonds and Reed, 1993). These compounds have been described in sublimate samples (Symonds *et al.*, 1987; Le Guern and Bernard, 1982; Bernard and Le Guern, 1986), and their occurrence is restricted to high temperature, low oxygen fugacities f_{02}. It is therefore not surprising that in the presence of ambient air these are unstable and undergo conversion to mixed chlorides, fluorides and sulfates as visible in sublimate samples collected by Naughton *et al.* (1974) from lava fountains at Kilauea. Similar conversion processes were observed in many sublimate samples (collected at lower temperatures), and therefore may also pertain to particulate material sampled in volcanic plumes. As a result Zn, and Cu (and sometimes also Fe) are often associated as traces with Na, K chlorides and Na, Ca, Mg, K sulfates (cf. Symonds *et al.*, 1987; Varekamp *et al.*, 1986), or they are present as sulfates or other mixed compounds ($CuSO_4$, $Zn(SO_4)(Cl,OH)_4$, $K_2Zn(SO_4)(Cl)_3$). Formation of these compounds reflects increasingly oxidizing conditions due to mixing of volcanic gases with the atmosphere, and is a result of reaction of sublimates with sulfuric acid, water vapor and other gases present in the plume and in ambient air. In addition to the formation of sulfates, conversion reactions may also produce oxides (Symonds, 1990; Symonds and Reed, 1993). A notable example is the formation of zincite (ZnO) as described by Thomas *et al.* (1982) in the Mt. St. Helens plume. This conversion takes place in reactions:

$$ZnCl_{2(g)} + \frac{1}{2}O_{2(g)} = \underset{zincite}{ZnO_{(s)}} + Cl_{2(g)} \qquad \textbf{(10)}$$

$$ZnCl_{2_{(g)}} + H_2O_{(g)} = \underset{zincite}{ZnO_{(s)}} + 2HCl_{(g)} \qquad \textbf{(11)}$$

Zincite is often converted to $ZnCO_{3(s)}$ by reaction with CO_2 (Thomas *et al.*, 1982). Zn,

Cu, and Cd are among the most enriched transition metals in the Erebus plume. Meeker (1988) reported Zn-S compounds in Erebus QCM samples, but no Cu- or Cd-bearing compounds. There is no correlation between Zn and S in filter samples, nor between Zn and Cl. Therefore, if Zn-chlorides or Zn-sulfides are initially present in the Erebus plume, they are probably quickly converted into other stable compounds.

The same reasoning applies to Cd. Cadmium is correlated with both F (r=0.4) and Cl (r=0.6) and could be present in the plume in either or both forms. Cadmium could also precipitate between 130° and 110°C from the plume as $CdCl_{2(s)}$, (Symonds and Reed, 1993). A relatively good correlation between Cd and Au in Erebus gas may suggest that the two metals follow the same pathways for volatilization and cooling.

Gold forms highly volatile sulfides which at low temperature lead to precipitation of native Au by the reaction:

$$AuS_{(g)} + H_{2_{(g)}} = Au_{(s)} + H_2S_{(g)} \qquad T<410°C \qquad \textbf{(12)}$$

(Symonds, 1990; Symonds and Reed, 1993). Particles of elemental Au were detected in the Erebus plume (Meeker, 1988; Meeker *et al.*, 1991; Chuan, 1994), although it has been hypothesized that Au-Cl rather than Au-S compounds are responsible for gold removal from the melt. However, lack of thermodynamic data for Au-Cl compounds does not allow predictions of their role in volcanic gas. In some samples collected by QCM, particles containing both Au and Cl were recognized. It is unclear, however, whether those represent original precipitates or are products of a reaction between Au

(or AuS) and HCl present in the plume. Gold on filter samples collected at Erebus does not show a good correlation with halogens or sulfur. Gold is a highly enriched element in Erebus filter samples and shows its highest enrichment in 1991. In some samples, the concentration of Au is unreasonably high, and contamination cannot be ruled out.

Scandium does not partition into the vapor phase, and its presence on filter samples is solely due to the presence of silicate (ash) fragments. Sc concentrations on filters do not vary with time, and show good correlation with Al and some metals (Fe, Mn) (Table 5.10). It also correlates well with S, which is hard to explain and perhaps reflects the presence of H_2SO_4 droplets enveloping the small ash particles. Because Sc was used as reference element in calculations of EFs, its enrichment in samples cannot be evaluated. When Br is used as reference element, scandium EFs are close to that of Al and Mn, thus it is a non-enriched element in the plume.

5.2.2.2.4. Other trace elements

Only As, Se, S, and Sb of groups VA and VIA were determined in Erebus filters. Discussion is restricted to the volatile components of As, Se, and Sb because S is treated separately. Arsenic and antimony form sulfides at temperatures $>800°C$ (AsS above 640°C, As_4S_4 below 180°C, and SbS above 540°C). Arsenic can also be present as As_4 between 640° and 180°C, and in smaller amounts as As_2, As, As_3, AsH_3, As_4O_6, and $AsCl_3$. Other species of antimony include $SbCl_3$ at temperatures $<540°C$, Sb, Sb_2, Sb_2S_3, and Sb_4O_6 (Symonds and Reed, 1993). The precipitation of As is mostly in the

form of an elemental solid (between 200° and 170°C) or as realgar (AsS) below 110°C, whereas the form of Sb removal from the vapor is unclear (Symonds, 1990; Symonds and Reed, 1993). The behavior of Se has been studied by Greenland and Aruscavage (1986). Because of its chemical similarity to sulfur, selenium could form either hydrides, oxides or be volatilized in its elemental state. Selenium is likely to be most stable as H_2Se or Se_2 (Symonds, 1990; Symonds and Reed, 1993), and it could react with other elements forming components such as PbSe which according to the calculations of Symonds (1990) is an important secondary volatile form of Pb. All three elements (As, Sb, and Se) are characterized by high EFs in Erebus gas, and display relatively small variation between years. Arsenic concentrations show a good correlation with Cl and with S ($r > 0.9$) (Table 5.10), which supports the above reasoning about conversion of AsS to chlorides. Antimony shows a moderate correlation both with Cl and As ($r > 0.6$). The data for Se on filters are too few to judge about its association with other elements, but its correlation with As and S is poor. Because of the strong covalent character of bonds in most of these compounds, they are likely to remain volatile in the gas, which is consistent with As, Se and Sb occurring mainly on treated filters rather than the particle filters. Alternatively, those compounds may be re-mobilized by acidic gases from the particulate phase into gas phase and subsequently be collected on the treated filters.

Only Al and In from group IIIA were detected on filters. Although Al and In are often classified together because of similar chemical properties, the behavior of these two

elements in volcanic plumes is strikingly different. Aluminum is a refractory element and its species are characterized by a low volatility (Vie le Sage, 1983). It shows a strong affinity to F, forming numerous components: high temperature oxyfluoride AlF_2O, low temperature $NaAlF_4$, and minor species AlF_3, $AlClF_2$, $AlCl_2F$ (Symonds *et al.*, 1987; Symonds, 1990; Symonds and Reed, 1993). Aluminum precipitates from the plume at high temperatures as hercynite $FeAl_2O_4$ and is associated with magnetite and cristobalite in sublimate samples (Symonds *et al.*, 1987). Symonds (1990), and Symonds and Reed (1993) suggested that formation of $AlF_{3(s)}$ may also occur in the plume. Oskarsson (1992) reported the presence of $AlF_{3(s)}$, based on strong correlation between Al and F in ash leachates from Hekla. Rosenberg (1988) described $AlF_{3(s)}$ from incrustations found at the Erebus summit area and hypothesized that it gives evidence of volatilization of Al as AlF_3. The presence of $AlF_{3(s)}$ in the Erebus QCM samples has not, however, been proven (Chuan *et al.*, 1986). In the plume, $AlF_{3(s)}$ may undergo conversion to sulfate (Varekamp *et al.*, 1986) according to the following reaction :

$$2AlF_{3(s)} + 3H_2SO_4 = Al_2(SO_4)_{3(s)} + 6HF_{(g)} \qquad \textbf{(13)}$$

This reaction may also occur in the Erebus plume as indicated by the presence of Al-sulfate in aerosols samples (Chuan *et al.*, 1986). Generally, Al does not show good correlation with F, Cl or S in Erebus filter samples which contradicts the Al volatilization hypothesis of Rosenberg (1988). Instead, Al correlates with Fe which may be an indication of the presence of mixed Al-Fe-oxides. On the other hand, Al correlates well with Sc, La, Ce, Sm and thus, it is most likely that it is mainly associated with small rock fragments on filters.

In contrast to aluminum, indium is one of the most enriched elements in the Erebus plume. The high EF values may, however, be overestimated because In concentrations in Erebus rocks are difficult to measure and so the crustal concentration are instead used to calculate EFs. High volatility of In compounds could be due to its high polarizing power. Symonds *et al.* (1987) found that In correlated well with both Zn and Cd, and was likely to form a volatile compound with Cl. During precipitation from the plume In could substitute for either Zn in sphalerite, or for Bi in galena (Symonds *et al.*, 1987). Alternatively, like Cd, In could precipitate as chloride $InCl_{3(s)}$ and this hypothesis is supported by the strong correlation between the two elements ($r > 0.9$).

There is very little data on the volatility of the REE or Ta and Hf. Varekamp *et al.* (1986) described high Ce and Eu content in gypsum particulates collected at Mt. Etna. Possibly those elements were substituting for Ca in this phase, and were volatilized together with Ca as fluorides. It is unclear however, why REEs do not accompany Al in particulates sampled at the same volcano. In Erebus filter samples La, Ce, and Sm show a good correlation with Al suggesting their origin from the rock fragments or ash in the plume. Europium does not correlate well with Al, instead it correlates moderately well with F and Cl (Table 5.10), and may represent a volatile component. The data on filters for other elements (Yb, Ta, Hf) are too few to allow for testing their correlation with either Al or Ca. The enrichment factors of REEs show some variability between years, in general 1991 samples have the highest EFs and 1988

lowest. The three REEs: Ce, Eu and Yb, consistently have greater values of EFs than other REE but only in samples collected in 1986 and 1991 are they enriched in the plume. Cerium is the most enriched REE in samples of Erebus aerosols, as pointed by Germani (1980) who noted unusually high concentrations of Ce in the plume. Ce and La correlated well with each other, and with S (r=0.6).

5.2.3. Comparison of the trace element emissions from Erebus with global volcanic outputs

The obtained mean annual emission rates of trace elements can be compared with the available data on global volcanic outputs. Unfortunately, while there is a increasing number of studies done for individual volcanoes, the estimates of the global volcanic outputs are rather limited. The most comprehensive study was presented by Nriagu (1989) who attempted to combine all data on the selected trace element emissions from natural sources. The study by Nriagu (1989) concentrated mostly on the toxic metals, and neglected many other elements common in volcanic emissions (such as Na, K, Ca, Br, In, Ir, Au, etc.). Table 5.11 presents the comparison of the mean annual outputs of trace elements from Erebus (calculated from data in Table 5.7) with the data from Nriagu (1989).

Table 5.11. Comparison of mean annual emission rates from Mt. Erebus with the estimates of global volcanic outputs for selected trace elements.

Element	Mt. Erebus ($Gg.yr^{-1}$)		global volcanic outputs($Gg.yr^{-1}$)	
	mean	std	mean	range
V	0.004	0.005	5.6	0.21-11
Cr	0.019	0.024	15	0.81-29
Mn	0.010	0.012	42	4.2-80
Co	0.007	0.011	0.96	0.02-1.9
Ni	0.006	0.008	14	0.93-28
Cu	0.078	0.113	9.4	0.9-18
Zn	0.15	0.19	9.6	0.31-19
As	0.015	0.018	3.8	0.15-7.5
Se	2.1e-03	2.9e-03	0.95	0.1-1.8
Mo	0.006	0.009	0.4	0.04-0.75
Cd	0.006	0.007	0.82	0.14-1.5
Sb	8.1e-04	9.4e-04	0.71	0.01-1.4

Values for Mt. Erebus calculated from Table 5.7, global volcanic estimates from Nriagu (1989).

The outputs of trace elements from Mt. Erebus are very small when compared with the available global estimates. The only exception is Zn for which the average emission rates from Mt. Erebus are approaching 50% of the lower limits of the global output. This may indicate that the global values are underestimated and in need of improvement. The lack of data does not allow comparison of outputs of other trace elements emitted from Erebus, especially In, Au, and alkali metals. It is likely, however, that the Erebus contribution to the global budgets is rather insignificant, considering the low activity observed at Erebus. On the other hand, Erebus' contribution to the trace elements budget on the regional scale may be quite important. According to Nriagu (1989) volcanic emissions are dominant natural source of the As, Cd, Cr, Cu, Ni, and Sb, other important sources are crustal weathering or sea spray aerosols.

Because of its location in Antarctica, Erebus is (at present) the closest active volcano, and its emissions may be strongly influencing the trace element content of the Antarctic atmosphere. The possible impact of Erebus activity in Antarctica is further examined in Chapter 8.

5.3. Conclusions

The volcanic plume emitted from Mount Erebus contains high concentrations of halogens and sulfur. The long-term observation of the relative proportions of these gas components lead to the conclusion that the overall composition of the gas changed with time. These changes occur on a very small-scale and probably do not indicate changes in the composition of the magmatic source. However, they may imply the existence of heterogeneities within the magma chamber/column, caused by the variable content of volatiles dissolved in the melt. The observed small-scale, cyclic temporal variation in the F/Cl and S/Cl ratio of the emitted gas seem to be related to gas exsolution processes occurring in the volcanic conduit. This supports the hypothesis of a cyclic degassing pattern obtained from the COSPEC record.

The estimated emission rates of halogens and trace elements show a small increase between 1986 and 1991, paralleling the increase in SO_2 emissions. In 1986, the estimated emissions were about 7.7 $Gg.yr^{-1}$ SO_2, 4 $Gg.yr^{-1}$ HF, and 6.9 $Gg.yr^{-1}$ HCl. The emissions increased to 25.9 $Gg.yr^{-1}$ SO_2, 6 $Gg.yr^{-1}$ HF, and 13.3 $Gg.yr^{-1}$ HCl in 1991.

The 1991 samples also contain a higher content of ash and minute rock fragments as shown by the increased concentrations of Al and Fe. All this may be indicative of a change in the eruptive behavior of Erebus. The present emission rates are however much lower than for 1983, when the outputs of gases were estimated as 84 $Gg.yr^{-1}$ SO_2, 30.5 $Gg.yr^{-1}$ HF, and 60.9 $Gg.yr^{-1}$ HCl.

The plume is enriched in many trace elements such as Na, K, Rb, Cs, Co, Zn, Cd, As, Se, Sb, Au, Hg, and In. Other elements detected in the plume (Al, Fe, Mn, REEs) probably represent small rock fragments. A good correlation between the concentrations of trace elements and halogens shows that most of the trace elements appear to be volatilized as metal-halogen compounds. The lack of data on the composition of high-temperature sublimates deposited near the lava lake does not allow for verification of this conclusion. There is also some evidence that the composition of many compounds is altered by reactions in the plume, for example by oxidation and by reactions with sulfuric acid.

The strongly enriched trace elements and high halogen/sulfur ratios of the gas form a unique characteristic of Erebus. Many elements present in the plume (for example F, In, Au) could serve as potential tracers of gas emitted from this volcano.

6. MODEL OF MAGMATIC DEGASSING AT MT. EREBUS

6.1. Solubility considerations

Volcanic gases originate by exsolution of a fluid from a magma. Magmas of different chemical compositions contain variable amounts and proportions of volatiles. Water (35 to 90 mol. %), carbon dioxide (5 to 50 mol. %), and sulfur dioxide (2 to 30 mol. %) are the most abundant volatile species in most magmas; other components (H_2, CO, COS, S_2, H_2S, S_2, O_2, HCl, N_2, HF, HBr, metal halogens, and noble gases) constitute usually less than 2 mol. % of all volatile species (Fisher and Schmincke, 1984; Anderson 1975; Gerlach 1981). The solubility of water in silicate melts increases with pressure, and decreases very slightly with temperature. According to the theory of Burnham (1975, 1979), water in melts acts as a network modifier (breaking Si-O-Si bonds) and is incorporated into a melt as OH^- groups. Other models (Stolper 1982, Silver and Stolper 1989) suggest that in melts containing more that 2 wt. % water, molecular H_2O is also present, in addition to OH^- molecules.

The solubility of carbon dioxide depends strongly on pressure but also on the composition of the melt, and is generally higher in mafic melts. In mafic alkalic magmas, CO_2 is the predominant volatile (Wyllie, 1979; Fischer and Schmincke, 1984). Carbon dioxide can be present in the melt in the form of a carbonate ion (CO_3^{2-}) and lead to the polymerization of the melt, or it can form metal-carbonate complexes and cause

the de-polymerization of the melt (Holloway, 1981; Fisher and Schmincke, 1984). Because the solubility of CO_2 is much lower than other volatile species, its exsolution begins at greater pressures and initiates vesiculation in a melt. In systems high in CO_2 this process can lead to substantial changes in the melt viscosity and density, and may affect the dissolution of other volatile species.

The solubility of sulfur in magmas depends on the S_2, O_2, and H_2O fugacities (Holloway, 1981). In an anhydrous melt at high oxygen fugacity ($\log f_{o2} > QFM+1$, where QFM is quartz-fayalite-magnetite buffer), sulfur dissolves in the melt as SO_4^{2-}, whereas at low oxygen fugacity ($<QFM$) it is present as S^{2-} or as FeS_{melt}. In the presence of water in a melt, at low f_{O2} ($<QFM+1$) the most dominant species in the fluid phase is H_2S. Burnham (1979) suggested that, similar to water, H_2S dissolves in the melt as HS^-, or reacts with FeO present in the melt forming FeS_{melt}. At high oxygen fugacity and low pressures (low water fugacity), H_2S undergoes hydrolysis and forms SO_2. SO_2 solubility in a melt is low, and the mechanism of its exsolution is similar to that of CO_2. In Erebus magma, the calculated oxygen fugacity is $10^{-12.2}$ at 1000°C (Kyle, 1977), and lies below QFM buffer (Figure 6.1). The calculated sulfur fugacity (from the composition of pyrrhotite) is $10^{-2.7}$ at the same temperature (Kyle, 1977), and is very close to volcanic gases from Kilauea volcano. The temperature of Erebus magma was obtained from fluid inclusion analysis (Clocchiatti *et al.*, 1976) and supported by mineral chemistry (Kyle, 1977).

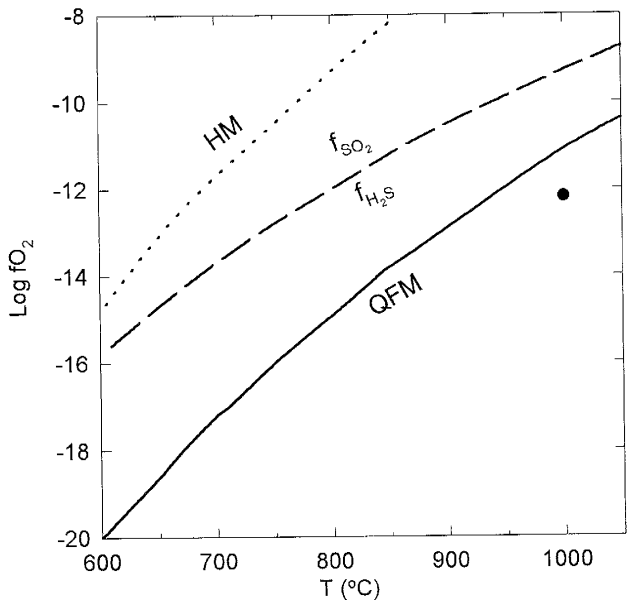

Fig. 6.1. Calculated oxygen fugacity for Mt. Erebus melt (solid dot) from Kyle (1977). Solid line represents quartz-fayalite-magnetite (QFM) buffer, dotted line is hematite-magnetite buffer (HM), dashed line is fSO_2/fH_2S equilibrium boundary.

Other common volatiles present in a melt are chlorine and fluorine. They dissolve in the melt similarly to water (Burnham, 1979) forming Cl^-_{melt} and F^-_{melt}. Fluorine is thought to be slightly more soluble than water in a melt, whereas chlorine is much less soluble than both water and fluorine (Burnham, 1979; Webster and Holloway, 1988; Webster, 1990) possibly due to the larger size of Cl^-. Burnham (1979) calculates that the saturation mole fraction of HF (X_{HF}melt) is approximately 1.25 times the value of X_{H2O}melt; a similar value is given by Webster (1990). The solubility of Cl in water saturated melt is much smaller. Unfortunately, there is very little experimental data on the solubility of halogens in melts of different compositions. Experimental work of Webster and Holloway (1988) shows that Cl is stabilized in a melt by forming complexes with Na, K and Fe, hence its solubility increases with the melt peralkalinity.

The partitioning of Cl between a melt and fluid depends strongly on the proportion of H_2O and CO_2 in the fluid. As the $X_{H2O}/(X_{H2O}+X_{CO2})$ in fluid increases (for example when magma rises toward the surface), Cl partitions more strongly toward the fluid. In the fluid phase, Cl will again tend to form species with Na, K and Fe. Other elements (Al and Ca) tend to form complexes with F if it is present in the fluid. If the amount of Cl in the fluid is larger than the concentration of metals, some Cl can also be present in the fluid as HCl^0 (Webster and Holloway, 1988). Experimental work of Webster (1990) shows that F in a fluid is associated with metal cations rather than being present as HF. Except for very F-rich melt compositions, fluorine usually partitions into the melt. The fluid-melt partition coefficient for F is also slightly influenced by increasing $X_{H2O}/(X_{H2O}+X_{CO2})$ of the fluid, although less strongly than in the case of Cl.

6.2. Solubility of volatiles in phonolitic melts - available data

Using the method described in Burnham (1979 a,b) and the data in Table 6.1, I have calculated the solubility of water in a melt of phonolitic composition (Figure 6.2) at 1000°C. The experimental solubility (Dunbar *et al.* 1994) is lower than that predicted from the theoretically calculated curve, possibly due to the presence of other volatiles which lower the solubility of water in the melt used for the experiment.

Table 6.1. Data for calculations of water solubility in Erebus magma (see text) using method of Burnham (1979), and analyses of Erebus matrix glass (Dunbar *et al.*, 1994).

	MW	wt.%	mole % metal	mole % oxygen
SiO_2	60.1	55.0	0.915381	1.830761
Al_2O_3	102.0	20.2	0.396229	0.594343
TiO_2	79.9	1.0	0.012519	0.025038
FeO	71.8	5.6	0.077944	0.077944
MgO	40.3	0.9	0.02233	0.02233
CaO	56.1	1.9	0.033882	0.033882
Na_2O	62.0	9.5	0.306556	0.153278
K_2O	94.2	5.5	0.116778	0.058389
Total		99.6	1.881618	2.795965

The actual pre-eruptive concentrations of volatiles in the Erebus magma are unknown. Analysis of matrix glass and glass inclusions in phenocrysts (Dunbar and Kyle, 1990; Dunbar *et al.* 1994) reveals almost no difference in volatile content, which suggests that the growing crystals trapped an already partially degassed melt. Both matrix glass and glass inclusions contain about 0.2 wt.% H_2O, 0.3 wt.% F, 0.18 wt.% Cl, and 0.065 wt. % S (Dunbar *et al.*, 1990); the CO_2 content is unknown.

The only available estimate of Cl solubility limits in rocks of phonolitic composition (Metrich and Rutherford, 1992) gives 6270 ppm at 1 kb pressure. Because F is more soluble than Cl and water, one can infer that the initial F concentrations could be higher than the Cl and water content ($\sim$8000 ppm).

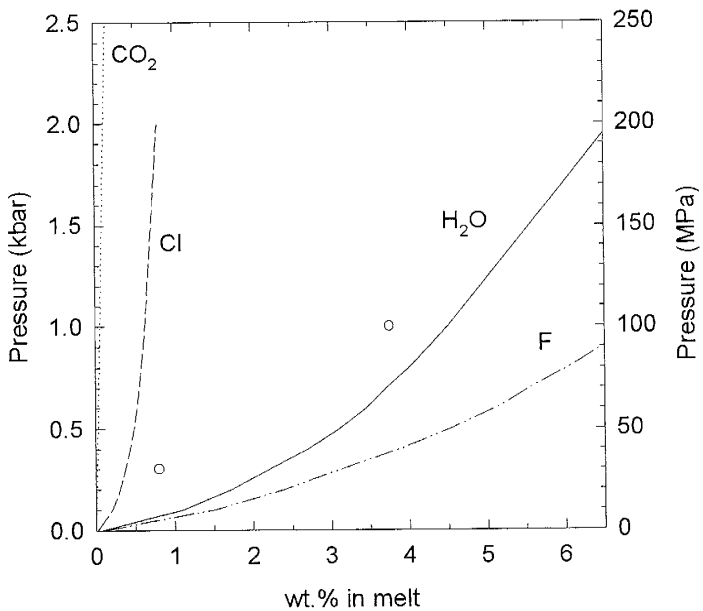

Fig. 6.2. Estimate of solubility of volatiles (wt.%) in melt of phonolite composition as a function of pressure. Theoretical solubility of water (solid line) calculated using method described by Burnham (1979) as explained in text, and experimental data (open circles) from Dunbar et al. (1994). Chlorine and fluorine solubility estimated from data in Mettrich (1992). CO_2 solubility (dotted line) assumed to be similar to that in basaltic magmas and calculated from data in Harris (1981).

There are no data to constrain the solubility limits of either S or CO_2 in phonolitic melt. In my considerations, I used the equation given by Harris (1981) for calculating the CO_2 solubility in basaltic magmas. I have assumed that for pressures lower than 50MPa (5 kb) the effect of melt composition on CO_2 solubility can be neglected.

6.3. Degassing model for Erebus

The above values for solubility limits of various volatiles are likely to be overestimated because they do not consider the effect of simultaneous presence of other volatiles (especially CO_2). Gerlach (1986) attempted to overcome this problem by developing a model of H_2O, CO_2, and S exsolution from Kilauea. I used this model to perform similar calculations for Erebus, modifying it to better describe the Erebus

system. The major difference between the two models is that Cl and F are important constituents of melt and gas at Erebus and cannot be neglected in the model calculations in the same manner as in Gerlach's Kilauea model. The details of the calculations for the model are given in Gerlach (1986). The model uses the composition of gas to describe the proportions between exsolved gas components, and back-calculates the composition of volatiles in the melt using available experimental and theoretical data. Assumptions and simplifications for the model are similar to those of Gerlach (1986) with a few exceptions. The volatiles exsolved from the Erebus melt are mainly composed of H_2O, CO_2, S, HCl and HF. Although H_2S is the main S species in the melt, upon volatilization it is no longer stable and must be converted into SO_2. I assume a temperature of 1000°C for the magma reservoir, and neglect temperature gradients towards the surface. Similarly to the conditions of the Kilauea model (Gerlach, 1986), I assume progressive exsolution of volatiles and the same level of saturation. Ideal behavior of gases is assumed.

The model requires some initial conditions to describe the relations between H_2O, CO_2, S and halogens. I assumed that the H_2O and CO_2 together constitute 90% of all gas by volume, whereas the remaining 10% are S and halogens in varying proportions. I used the highest observed values of Cl/S=6.05 and F/S=4.36 ratios (from data collected on filter samples, recalculated to molar proportions) to estimate the initial proportions of the three volatiles.

From:

$$X_S + X_{Cl} + X_F = 0.1 \quad (1)$$

where X_i is mol fraction of element i, and using the molar element-to-sulfur ratios given above, the calculated initial conditions are $X_{Cl}=0.053$, $X_F=0.038$, and $X_S=0.0088$. An additional condition was also imposed, based on the lowest observed values of Cl/S and F/S molar ratios (0.31 and 0.33, respectively). The lower limits were calculated as $X_{Cl}=0.037$, $X_F=0.042$, and $X_S=0.1205$. The model assumes that the mol fraction of Cl, F, and S change during the magma ascent. (This is consistent with the observed changes in Cl/S and F/S ratios and represents the major difference between this model and that of Gerlach (1986)). For each component present in the melt and in the gas the mass balance has to be considered

$$W_{i,e} + W_{i,m} = W_{i,*} \quad (2)$$

where $W_{i,e}$, and $W_{i,m}$ are weight percent of an exsolved and dissolved component, and $W_{i,*}$ is a total wt. % of that component. To model exsolution of water I used Burnham's (1979) model (see section 6.2). Assuming ideal gas behavior, the mole fraction of water in the melt $X_{H2O,m}$ can be calculated from

$$(X_{H_2O,m})2 = \frac{P_{H_2O}}{kP} \quad (3)$$

where P_{H2O} is partial pressure of water, P is total pressure and k is an analog of the Henry's law constant. After transforming equation 3 to wt. % , the equation changes to

$$W_{H_2O,m} = \frac{MW_{melt}\times 100}{MW_{melt}[kP/P_{H_2O}]^{0.5} - MW_{melt} + MW_{H_2O}} \quad (4)$$

For pressures lower than 50 MPa, ln k and ln P_{H2O} are linearly dependent. By fitting a

line though data in Burnham and Davis (1974) I found the relation to be

$$\ln k = b \ln P_{H_2O} + a = -1.0175 \ln P_{H_2O} + 6.03971 \quad (5)$$

Using molecular weights of water (MW_{H2O}=18.02) and anhydrous rock component (MW_{melt}=251.4), and substituting (5) in exponential form into (4) I obtained

$$W_{H_2O,m} = \frac{MW_{H_2O} \times 100}{MW_{melt} \exp(a) \left[P_{H_2O}^{(b-1)} P\right]^{0.5} - MW_{melt} + MW_{H_2O}} \quad (6)$$

where a,b are constants from equation (5). For CO_2 solubility as explained in section 6.2, I used the equation of Harris (1981) which has the form

$$W_{CO_2,m} = 0.0005 + (5.9 \times 10^{-4})\ P \quad (7)$$

The amounts of other volatiles (S, Cl, F) are constrained by

$$X_S = 0.12781 \exp(-0.29455\ P) \quad at\ P<P_{sat}\ (1.5\ MPa) \quad (8)$$

$$X_{Cl} = 0.00414 \ln(40099.28278\ P) \quad at\ P<P_{sat}\ (9.1\ MPa) \quad (9)$$

$$X_F = 0.04062 \exp(-0.00777\ P) \quad at\ P<P_{sat}\ (6.5\ MPa) \quad (10)$$

Equations (8-10) were obtained by fitting curves to observed high- and low-limits of element/S mole ratios in ranges between saturation pressure and P=0.2 MPa. The limits were calculated from experimental element/S ratios (molar) using the highest observed values for upper limit (Cl/S=6.05, F/S=4.36) and lowest observed ratios (Cl/S=0.31, F/S=0.33), assuming that the sum of mole fractions of all components increases uniformly from 0.1 to 0.2 between P=9.1 and 0.2 MPa. The choice of exponential/log rather than linear relationships between variables was made because of the exponential nature of the curves describing the exsolution of water. At each step, the following relationship will also hold (in terms of mol fractions X_i, number of moles N_i and

pressures P_i):

$$\frac{X_S + X_{Cl} + X_F}{X_{H_2O} + X_{CO_2}} = \frac{N_S + N_{Cl} + N_F}{N_{H_2O} + N_{CO_2}} = \frac{P_S + P_{Cl} + P_F}{P_{H_2O} + P_{CO_2}} = R \quad (11)$$

The numerical value of R can be estimated once equations 8-10 are solved.

For each component of the gas phase we have

$$P_i = X_i P \quad (12)$$

For water vapor we have :

$$X_{H_2O} = \frac{N_{H_2O}}{N_S+N_{Cl}+N_F+N_{CO_2}+N_{H_2O}} = \frac{N_{H_2O}}{(R+1)(N_{H_2O}+N_{CO_2})} \quad (13)$$

Combining eq.12 and 13 leads to the expression for water vapor pressure:

$$P_{H_2O} = \frac{P\, MW_{CO_2}\, W_{H_2O,e}}{(1+R)(W_{H_2O,e} MW_{CO_2} + W_{CO_2,e} MW_{H_2O})} \quad (14)$$

Rearranging eq.14 gives :

$$W_{H_2O,e} = \frac{(1+R) MW_{H_2O} P_{H_2O} W_{CO_2,e}}{MW_{CO_2}[P-(1+R)P_{H_2O}]} \quad (15)$$

I assumed a starting composition of 0.25 wt.% H_2O, 0.05 wt.% CO_2, 0.2 wt.% Cl, 0.3 wt.% F, and 0.065 wt.% S. From these data the model calculates the apparent vapor saturation pressure (here 84 MPa) (Gerlach, 1986). Next, P is decreased by some incremental value and at each pressure the equations are iteratively solved for $W_{CO2,m}$, $W_{CO2,e}$, $W_{H2O,e}$, $W_{S,e}$, $W_{Cl,e}$, $W_{F,e}$,and P_{H2O}. Next, the model calculates X_{H2O}, X_{CO2}, P_{CO2}, P_S, P_{Cl}, P_F. The total wt.% of exsolved volatiles is

$$W_e = W_{H_2O,e} + W_{CO_2,e} + W_{S,e} + W_{Cl,e} + W_{F,e} \quad (16)$$

At each pressure, the magma fragmentation potential (Sparks, 1978) is evaluated

as the ratio of V_g/V_m (volume of vapor to volume of melt). For 100g of melt of density 2400 $kg.m^{-3}$, $V_m=41.7\times10^{-6}$ m^3. Assuming ideal gas behavior, the volume of the gas is:

$$V_g = \frac{RTN_e}{P} \tag{17}$$

where $R=8.31451$ $J.mol^{-1}.K^{-1}$, $T=1000°C$ ($=1273.15$ K), N_e is total number of moles of exsolved gas given by:

$$N_e = \sum \frac{W_{i,e}}{M_{i,e}} \tag{18}$$

where $W_{i,e}$ is wt.% of exsolved i-th gas component, and M_i is the corresponding molecular weight. After substituting numerical values, the volume ratio V_g/V_m is calculated from:

$$\frac{V_g}{V_m} = 254.05 \frac{N_e}{P} \tag{19}$$

where P is pressure in MPa.

The results of the calculations are shown in Table 6.2, and Figures 6.3 and 6.4a,b. The model predicts that mol fractions of exsolved H_2O and CO_2 are almost 1:1 when the pressure decreases to 2-3 MPa. A similar ratio between the two components was measured in Nyiragongo (Gerlach, 1982).

Table 6.2. Calculated exsolution of volatiles from phonolitic melt initially containing 0.25 wt.% H_2O, 0.05 wt.% CO_2, 0.065 wt.% S, 0.30 wt.% F, and 0.20 wt.% Cl.

P (MPa)	Depth* (m)	$W_{H2O,m}$	$W_{CO2,m}$	$W_{S,m}$	$W_{Cl,m}$	$W_{F,m}$	W_e	X_{H2O}	X_{CO2}	X_S	X_{Cl}	X_F	V_g/V_m	Cl/S	F/S
20.00	834	0.2465	0.0123	0.0647	0.1978	0.2992	0.0446	0.166	0.7342	0.0088	0.053	0.038	0.01	6.02	4.32
15.00	626	0.2455	0.0093	0.0646	0.1976	0.2991	0.0489	0.1907	0.7095	0.0088	0.053	0.038	0.02	6.02	4.32
10.00	417	0.2438	0.0064	0.0646	0.1972	0.2989	0.0541	0.2317	0.6686	0.0088	0.053	0.038	0.04	6.02	4.32
9.50	396	0.2436	0.0061	0.0646	0.1972	0.2989	0.0547	0.2374	0.6628	0.0088	0.053	0.038	0.04	6.02	4.32
9.00	375	0.2433	0.0058	0.0646	0.1971	0.2989	0.0553	0.2436	0.6565	0.009	0.053	0.0379	0.04	5.89	4.21
8.00	334	0.2426	0.0052	0.0644	0.197	0.2988	0.0569	0.2576	0.6397	0.0121	0.0525	0.0382	0.05	4.34	3.16
6.00	250	0.2407	0.004	0.0638	0.1968	0.2987	0.061	0.2947	0.5934	0.0218	0.0513	0.0388	0.07	2.35	1.78
5.00	209	0.2391	0.0034	0.0632	0.1966	0.2986	0.064	0.3206	0.5605	0.0293	0.0505	0.0391	0.10	1.72	1.33
4.00	167	0.2368	0.0029	0.0624	0.1964	0.2984	0.0682	0.3547	0.5169	0.0393	0.0496	0.0394	0.13	1.26	1.00
3.50	146	0.2351	0.0026	0.0618	0.1962	0.2983	0.0711	0.3764	0.4894	0.0456	0.0491	0.0395	0.16	1.08	0.87
3.00	125	0.2328	0.0023	0.061	0.1959	0.2982	0.0748	0.4025	0.4566	0.0528	0.0484	0.0397	0.20	0.92	0.75
2.50	104	0.2295	0.002	0.0599	0.1956	0.298	0.0801	0.4345	0.4168	0.0612	0.0477	0.0398	0.27	0.78	0.65
2.00	83	0.2244	0.0017	0.0582	0.195	0.2977	0.0879	0.4749	0.3674	0.0709	0.0467	0.04	0.38	0.66	0.56
1.75	73	0.2207	0.0015	0.057	0.1947	0.2975	0.0935	0.4992	0.3382	0.0763	0.0462	0.0401	0.47	0.61	0.53
1.25	52	0.2085	0.0012	0.0533	0.1934	0.2968	0.1117	0.558	0.2685	0.0884	0.0448	0.0402	0.84	0.51	0.45
0.75	31	0.1819	0.0009	0.0453	0.1909	0.2954	0.1506	0.6289	0.1856	0.1025	0.0427	0.0404	2.03	0.42	0.39
0.50	21	0.1569	0.0008	0.0375	0.1887	0.294	0.1872	0.6645	0.1437	0.1103	0.041	0.0405	3.95	0.37	0.37
0.40	17	0.1431	0.0007	0.0331	0.1876	0.2933	0.2072	0.6779	0.1279	0.1136	0.0401	0.0405	5.56	0.35	0.36
0.30	13	0.1262	0.0007	0.0277	0.1863	0.2923	0.2317	0.6908	0.1127	0.117	0.0389	0.0405	8.42	0.33	0.35
0.20	8	0.105	0.0006	0.0208	0.1849	0.2912	0.2625	0.7036	0.0981	0.1205	0.0372	0.0406	14.53	0.31	0.34

All symbols are explained in text. W_i in wt.%, X_i in mol fractions.
* Depth calculated assuming a magma density of 2400 $kg.m^{-3}$

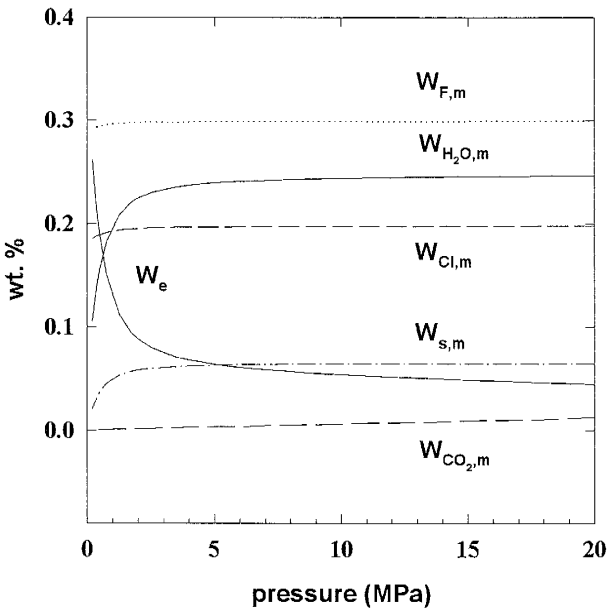

Fig. 6.3. Calculated exsolution from Erebus reservoir as a function of pressure during ascent of magma containing initially 0.25 wt.% H_2O, 0.05 wt.% CO_2, 0.065 wt.% S, 0.30 wt.% F, and 0.20 wt.% Cl. The curves show change in the volatile content of melt in wt.%, for water ($W_{H2O,m}$), CO_2 ($W_{CO2,m}$), S ($W_{S,m}$), F ($W_{F,m}$), and Cl ($W_{Cl,m}$). The curve marked W_e gives the wt.% of total exsolved volatiles. All data from Table 6.2.

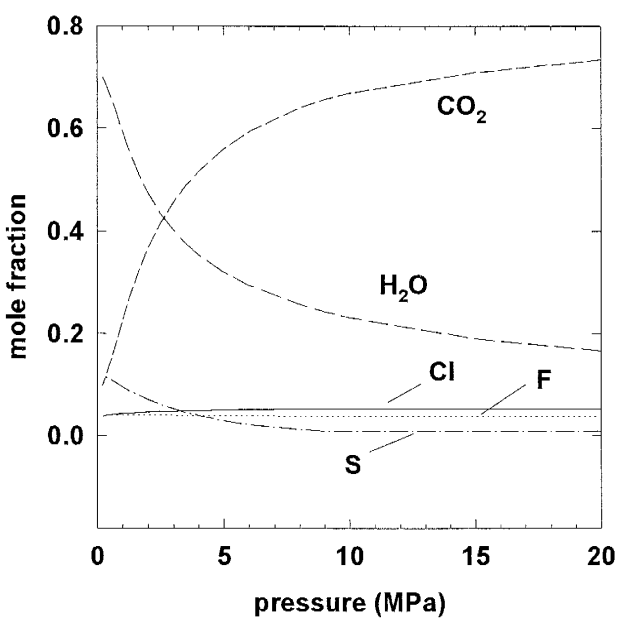

Fig. 6.4a. Calculated mole fraction compositions of cumulative exsolved gas as a function of pressure during ascent of magma saturated in volatiles at 84 MPa. Initial conditions as in Fig. 6.3 and in Table 6.2.

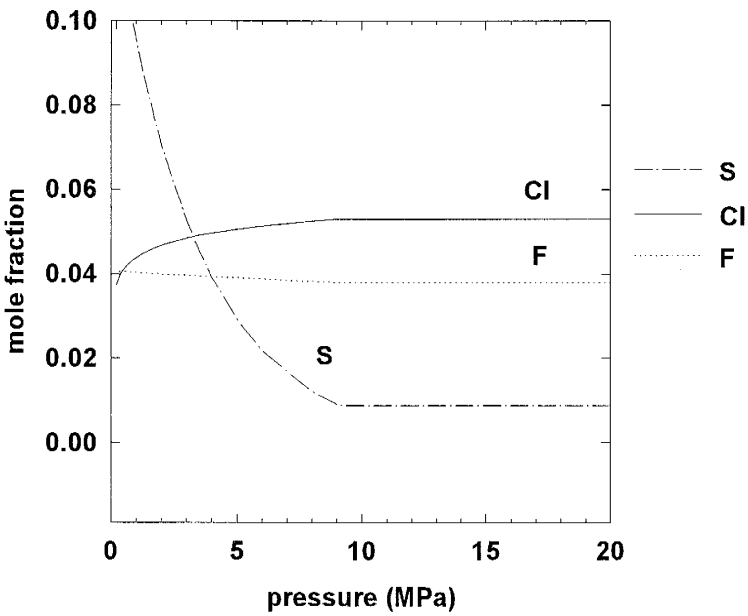

Fig. 6.4b. Enlarged portion of Fig. 6.4a showing curves for mol fraction of cumulative exsolved gas (S, Cl, and F).

The model successfully simulates the varying ratios of halogens and sulfur (Figure 6.5) with the ascent of magma in the conduit. This shows that the model suggested in chapter 5 which relates variable Cl/S and F/S ratios of the gas to the convection of magma in the conduit, may be justified. Interestingly, model calculations show that large amounts of Cl, F and water can be exsolved from the packet of melt without significant change in its volatile content. The similarity between the volatile content of melt inclusions present in phenocrysts (2700-2900$\pm$400ppm F, 1700-1800$\pm$140 ppm Cl) and the volatile content of the matrix glass (3000$\pm$200 ppm F, 1800$\pm$100 ppm Cl) was though to support the theory of the shallow depth of crystalization within Erebus conduit. Crystalization is thus thought to be triggered by the degassing of the melt (Dunbar *et. al,* 1994). However, according to the model calculations shown in Table 6.2, the decrease in Cl content of the

melt corresponding to the difference in depth of several hundred meters is less than 200 ppm, whereas that of F is less than 100 ppm. Both values are within the uncertainty limits of microprobe measurements, and so they cannot be resolved with confidence in melt inclusions. It is therefore possible that the melt trapped in phenocrysts from Erebus was not entirely degassed as suggested by Dunbar *et al.* (1994). In fact, crystals might have been formed in a quite broad range of depths trapping melts of composition differing slightly in volatile content.

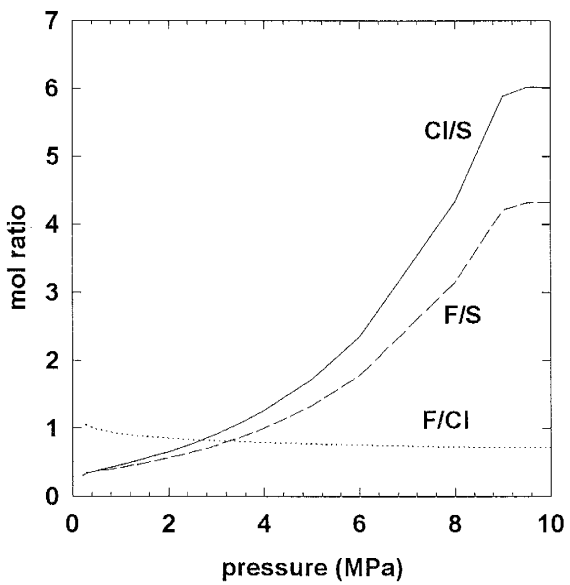

Fig. 6.5. Calculated Cl/S, F/S, and F/Cl mol ratios. Note that due to necessary simplification in assumptions, the model does not correctly predict element ratios above saturation pressure of Cl (here 9.1 MPa), F(6.5 MPa), and S(1.5 MPa), but instead uses predefined values.

Calculations of V_g/V_m show that magma is not vesiculated enough to explode during most of the ascent. The critical value of 3-5 (Sparks, 1978) is reached below 0.5 MPa (which roughly corresponds to depths shallower than 20-30m). Thus the bursts observed on the surface of lava lake would bring up melt coming from relatively shallow depths in the conduit.

7. VOLCANIC SALTS FROM THE SUMMIT AREA OF MOUNT EREBUS

7.1. Introduction

Salts (incrustations) are often found surrounding fumaroles and the summit area of volcanoes, and can be a valuable source of information about gas composition. There are two main processes by which incrustations can form: (1) by direct deposition from the plume (sublimates), and (2) by interaction of volcanic acids present in the plume with rocks (Oskarsson, 1981; Stoiber and Rose, 1974; Symonds and Reed, 1993). The major factors controlling the development of incrustations are temperature and oxygen fugacity (Stoiber and Rose, 1974) and changes in these result in the formation of zoning patterns. The zonation of salts is exemplified by specific mineral assemblages and by their trace element contents (Symonds *et al.*, 1987).

The composition of sublimates is also related to the amount of halogens and sulfur in the volcanic gas because they are the major transporting agents for metals. Thus, the composition of sublimates can provide information about the gas content. However, the original composition of sublimates is rarely preserved in the plume and in the resulting deposits which surround volcanic vents. Most sublimates undergo significant changes in composition at lower temperatures and vapor pressures, forming more stable species (oxides, sulfates, carbonates etc.). Furthermore, sublimates and their more stable

products react with other components in the plume (Naughton *et al.,* 1974, Symonds, 1990, also see Chapter 5). Those reactions, in combination with some dissolution and re-precipitation (which occurs unavoidably in the presence of water) result in compositional changes, and may be accompanied by extensive removal of some elements while concentrating other. Thus, the composition of incrustations surrounding volcanic vents can not be used uncritically to reconstruct plume compositions.

7.2. General description and occurrence

Although the area within the Erebus crater contains numerous occurrences of high temperature sublimate deposits, they have not been sampled. Salts found in the summit area of Mount Erebus are instead low temperature deposits, and bear little resemblance to the high temperature deposits described by other workers. Unlike the incrustations which are usually found close to some magmatic source, the salts are widely dispersed on the crater floor, on its walls, and over the entire summit plateau. Salts occur in a variety of forms. Five out of eight main types of deposits described by Keys (1980) are most common in the summit area: thick encrustations on the surface of rocks (mostly observed inside the crater), accumulations in joint cracks, accumulations in cavities in boulders, efflorescence or encrustations on the surface of regolith, and accumulations beneath boulders or smaller rock fragments. The general pattern in salt distribution is a decrease in the occurrences and the quantity of the deposits with distance from the crater (Keys, 1980). Moreover, the general appearance of the salts changes

depending on the location on the summit. Most of the deposits on the crater rim and inside the crater are characterized by a bright yellow color, and are found on the exposed surfaces. The salts found on the summit plateau surrounding the summit are white or yellowish-white, and are usually found beneath the boulders and smaller rock fragments, often under the weathered and exfoliating surfaces of boulders. The exception to this pattern are the salt deposits around Nausea Knob, about 100 m below and 500 m NW from the crater rim. These salts are similar in abundance to salts from the crater rim, and are also characterized by a bright yellow color. They occur in small cavities, and cracks in the rocks or beneath small rock fragments. Table 7.1 lists the salt samples, and gives their location, color and tentative identification. In many cases, the samples were mixtures of many different salts (as can be inferred from the chemical analyses, Table 7.2) and could not be identified.

7.3. Mineralogy

Among the salts identified positively during this study are thenardite Na_2SO_4, ralstonite $Na_xMg_xAl_{2-x}(F,OH)_6)\cdot H_2O$, halite NaCl, and khademite $Al(SO_4)(OH)\cdot 5H_2O$. Other tentatively identified phases include tamarugite $NaAl(SO_4)_2\cdot 6H_2O$, $AlF_3\cdot 3H_2O$, $NaAl_4O_4Cl_5$, NaF, natroalunite $NaAl_3(SO_4)_2(OH)_6$, natrojarosite $NaFe_3(SO_4)_2(OH)_6$, alunite $KAl_3(SO_4)_2(OH)_6$, malladrite Na_2SiF_6, hieratite K_2SiF_6, iron chloride $FeCl_2$, Fe-sulfates, gibbsite, illite, montmorillonite, nontronite, elpasolite K_2NaAlF_6, and different carbonates; also present are unidentified Ca, Fe, Zn, Ni- bearing phases. In many salts

various hydrated phosphates of Ca, Al, Fe, and Mn were also detected, such as xanthoxenite $Ca_2(Fe,Mn)(PO_4)_2(OH)\cdot H_2O$, kingite $Al_3(PO_4)_2(OH,F)_3\cdot 9H_2O$, sigloite $FeAl_2(PO_4)_2(OH)\cdot 8H_2O$ and other unidentified phosphates (Table 7.1). Because P was not analyzed in samples, it is impossible to verify this identification. However, the presence of phosphates is not unlikely because phonolite from Mount Erebus contains phenocrysts of apatite, and has a P_2O_5 content of 0.32 wt.% (Kyle, pers. comm.). In ES89-21 weilerite $BaAl_3(AsO_4)(SO_4)(OH)_6$ could be present. In some samples (ES81-407) meta-autunite $Ca(UO_2)(PO_4)_2\cdot 6H_2O$ was tentatively identified, although it is probably a minor phase. Problems with the salts identification, noted by other workers (Keys, 1980; Keys and Williams, 1981) are probably due to possible substitution of various ions in the crystalline structure, and the mixtures of many phases.

The presence of $NaAl_4O_4Cl_5$ in Erebus salts was first suggested by Rose (1987). In the course of this study it was impossible to positively verify this identification. This substance has never been described in the natural state and is known only as a man-made inorganic product. Its natural color is white, whereas the corresponding Erebus salt is brightly yellow. Rose (pers. comm. to P.R. Kyle) suggested that the coloring is due to the presence of mineral hydromolysite $FeCl_3\cdot 6H_2O$. The later mineral was not identified during this study in any of the samples tentatively identified as $NaAl_4O_4Cl_5$. Samples also appear to contain only one dominant mineral phase as determined from the results of the SEM/EDXRA analysis. The chemical analyses indicate that the salts are composed mostly of Na, Al, Fe, F, and Cl, with F content often higher than that of Cl. I postulate

that the chemical formula of this substance may be $Na(Al,Fe)_4O_4(F,Cl)_5$, with Fe substituting for Al, and F (and possibly also OH) for Cl. The substitution of Fe and F could possibly change the salt color from white to yellow. Another substance identified from the Erebus summit is $AlF_3 \cdot 3H_2O$ (Rosenberg, 1988). An XRD pattern similar to that given by Rosenberg (1988) for $AlF_3 \cdot 3H_2O$ was distinguished in few samples; however all of these samples appear to contain another mineral phase(s) making positive identification impossible.

Table 7.1. Description and tentative identification of salt samples from Erebus summit.

name	color	location	tentative identification
ES81-006	y	Nausea Knob	$NaAl_4O_4(F,Cl)_5$, Fe-Cl,
ES81-007	y	Nausea Knob	$NaAl_4O_4(F,Cl)_5$, Fe-Cl,
ES81-008	wh	Ice cave	Na_2SO_4
ES81-010	t	Ice cave (surface)	$NaMgAl(F,OH) \cdot H_2O$
ES81-407	y	Nausea Knob	$NaAl_4O_4(F,Cl)_5$, $NaAl(SO_4)_2 \cdot 6H_2O$, $MgCO_3$, Fe-Ti-oxides, Ca,Fe,Mn,Al -phosphates, $Al_3(PO_4)_2(OH,F)_3 \cdot 9H_2O$, $Ca(UO_2)(PO_4)_2 \cdot 6H_2O$
ES83-213	y	Nausea Knob	$NaAl_4O_4(F,Cl)_5$, Fe-Cl,
ES83-218	y/o	Nausea Knob	$NaAl_4O_4(F,Cl)_5$, Fe-Cl,
ES86-001	wh/y	E. of fumarole field	
ES86-002	wh/y	E. of fumarole field	
ES86-003	y/o	NE. rim	
ES86-004	wh	Lower Hut, flow	$Al(SO_4)(OH) \cdot 5H_2O$, NaCl, $MgCO_3$, MgF_2
ES86-005	wh		$Al(SO_4)(OH) \cdot 5H_2O$, Na-Al-SO_4,Ca-phosphate, $Ca(UO_2)(PO_4)_2 \cdot 6H_2O$
ES89-006	wh	Lower Hut, flow	$Al(SO_4)(OH) \cdot 5H_2O$, NaCl,
ES86-007	wh	Nausea Knob flow	NaCl, $Al(SO_4)(OH) \cdot 5H_2O$, NaF, $NaAl(SO_4)_2 \cdot 6H_2O$, $MgCO_3$, HgS, $NiCO_3$, phosphates
ES86-008	wh	E. beyond old caldera	
ES86-009	wh		NaCl, $AlSO_4(OH) \cdot 5H_2O$, HgS
ES86-010	y	Lower Hut, lava flow	

ES86-012	y	Nausea Knob	
ES89-001	wh	SE, lava flow	K-Ca-Mg-CO_3, $FeSO_4 \cdot 5H_2O$, montmorillonite, Na,K,Ca,Al-phosphates
ES89-007	y	W. flow, Tramway Ridge	
ES89-010	wh	NW. flow	$AlSO_4(OH) \cdot 5H_2O$, NaCl, montmorillonite, hectorite, Ca,Al, Fe-phosphates,
ES89-013	wh/p	E, old caldera	$NaAl_3(SO_4)_2(OH)_6$, Al,Fe-phosphates
ES89-017	br/wh	E, old caldera	$NaHCO_3$, $K_2Mg(SO_4)_2 \cdot 4H_2O$, $CaCO_3$, $NaAl(SO_4) \cdot 6H_2O$, montmorillonite, Ca,Al,Mn,Fe-phosphates
ES89-021	y	rim/camera site	$NaMgAlF \cdot 6H_2O$, K_2NaAlF_6, $FeAl_2O_4$, Na_2SiF_6, K_2SiF_6, $KAl_3(OH)_6(SO_4)_2$, ZnS, $BaAl_3(AsO_4)(SO_4)(OH)_6$, Fe,Al-phosphates
ES89-025	y	rim/Shackleton Cairn	$NaMgAlF \cdot 6H_2O$, $Al_2(SO_4)_3$, K_2SiF_6, Al-phosphates,
ES89-042	y	Nausea Knob	$NaFe_3(SO4)_2(OH)_6$, $NaAl_4O_4Cl_5$, Fe-Cl
ES89-047	y	Nausea Knob	$NaAl_4O_4(F,Cl)_5$, Fe-Cl, Al,Fe,Mg-phosphates
ES89-051	y	Nausea Knob	$NaAl_4O_4(F,Cl)_5$, Fe-Cl
ES89-055	y	Nausea Knob	$NaAl_4O_4(F,Cl)_5$, Fe-Cl, Mn-oxides, AlF_3
ES89-059	wh	Lower Hut, lava flow	As, HgS, montmorillonite, Ca,Fe,Al-phosphates, illite
ES89-061	y	Inside crater	Na_2SiF_6, $NaAl_4O_4(F,Cl)_5$, $FeCl_2$, $Fe_2(SO_4)_3 \cdot 10H_2O$, $(Zn,Fe)SO_4 \cdot 6H_2O$, gibbsite, Al,Fe-phosphates
ES89-065	wh/y	Lower Hut, lava flow	$Na_2Cu(SO_4)_2 \cdot 2H_2O$, Na_2SiF_6, ZnS, montmorillonite, Fe,Al-phosphates, carbonates
ES89-084	wh	E. lava flow	
ES89-090	y/wh	N. lava flow	$NaAl(SO_4)_2 \cdot 6H_2O$, $Al(SO_4)(OH) \cdot 5H_2O$, HgS, Ca,Al-phosphates
ES89-097	r/br	S. rim	
ES89-099	wh	N. lava flow	$Al(SO_4)(OH) \cdot 5H_2O$, NaCl, $MnCO_3$, HgS, Fe-oxides, phosphates
ES89-100	wh	N. lava flow	$Al(SO_4)(OH) \cdot 5H_2O$, NaCl, NaBr-Cl-O
ES89-103	wh	N. lava flow	$Al(SO_4)(OH) \cdot 5H_2O$
ES89-104	wh	N. lava flow	$Al(SO_4)(OH) \cdot 5H_2O$, NaCl, $CaCO_3$, $ZnFe_2O_4$
ES89-105	wh	N. lava flow	$Al(SO_4)(OH) \cdot 5H_2O$
ES89-106	wh	N. lava flow	$Al(SO_4)(OH) \cdot 5H_2O$, NaCl, FeS, $K_3Na(SO_3)_2$, phosphates

wh - white, y - yellow, o - orange, r -reddish, br - brown, t - tan, p - pink

7.4. Major and trace element content

The major and trace element content of salts was analyzed to examine possible relationships between the salt and gas compositions. Also, by comparing ratios of different elements one can look for similarities between salts from different locations. Table 7.2 lists the major and trace element concentrations in salts. Most of the salts appear to be composed of Na, Al, Cl, F, and Fe, and in some salts Ca was also detected. Among the most abundant trace elements often present in concentrations higher than 100 ppm are As, Zn, Rb, Sr, Zr, Ba, La, Ce, Nd. Some salts also contain In concentrations up to 28 ppm. To evaluate the enrichment (or depletion) of various elements relative to the composition of the phonolite rock samples from Mt. Erebus, I use enrichment factors (see Chapter 5) with Sc as the reference element. All salts, independent of their location, are enriched in Cl, F, As, and In, and depleted in Cr, Ba and Sr, and (with rare exceptions) Mn and W. The depletion of W may be due to not using the Erebus magma value for W. It is also common to all salts that Ce is the most enriched REE whereas Ta, Hf, and Sm are least enriched. All of the salts enriched in Co and Zn are characterized by enrichment of Br and REEs.

Table 7.2. Composition of salts from the summit area of Mt. Erebus, all data from INAA analyses in ppm.

	ES81-7	ES81-10	ES81-407	ES83-213	ES83-218	ES86-1	ES86-4	ES86-5
F	238000	162000	200000	150000	200000	94000	95000	150000
Na	94513	46069	94884	83385	89616	62205	59052	72109
Al	102000	118000	103000	94000	97000	97000	98000	92000
Cl	133000	3600	155000	127000	170000	79000	93000	119000
K		13282	2823			12452		24074
Ca				2859	3288	10006		4288
Sc	4.8	2.353	3.4	1.318	6.605	1.192	0.714	1.373
Cr	0.4	3.5	0.4		2.2	8.7	1.73	
Mn	1000	900	1300	3600	1200	2800	1400	1900
Fe	15049	54878	16145	13688	16666	15441	6700	22488
Co	1.77	2.35	2.322	5.66	2.0355	4.46	2.34	2.619
Ni						10		
Zn	113.8	326	130.3	495	148.1	163.1	89.3	189.7
As	114.8	91.8	109.5	18.4	76.9	80.4	12.7	59.8
Se	0.24	0.8	0.43		0.34	0.55	0.21	0.37
Br	1.13	3.8	6.6	41	3.25	1.05	1.29	2.12
Rb	43.2	140	22.6	87	17.6	76.25	72.9	197
Sr	82	338	66	85	45	110.5	36	88
Zr	171	727	324	329	234.5	446	122	448
Mo	3.8	31.1	2.6		2.9	3.8	2.1	2.8
Cd	14	23	26	60	17.55	31.5	19	37
In	3.90	7.00	10.00					
Sb	0.65	0.97	0.204	0.109	0.258	0.234	0.261	0.369
Cs	1.474	2.5	0.528	0.736	0.414	0.664	0.952	1.81
Ba	55	222			26	128.5	11	104
La	54	77.7	21.21	44.2	13.7	52.65	27.4	48.8
Ce	129.1	193.2	53.2	107.9	30.5	113.35	58.1	102
Nd	40.7	71	19	56.7	12.9	46.3	23.8	39.6
Sm	8.12	12.75	3.65	11.78	2.617	8.64	4.83	7.26
Eu	1.074	2.756	0.745	2.586	0.541	1.745	0.938	1.436
Tb	0.942	1.964	0.498	1.392	0.488	0.976	0.67	0.918
Yb	3.27	8.32	2.01	2.66	2.24	2.58	1.173	2.2
Lu	0.472	1.185	0.275	0.368	0.344	0.365	0.154	0.298
Hf	3.29	12.76	5.56	4.03	3.175	8.065	1.62	6.98
Ta	0.92	5.6	1.03	1.38	0.91	3.72	0.85	3.71
W		1.4	0.6		3	0.8		
Ag					0.275			0.14
Au						0.0017		
Hg			0.19	0.17	0.12	0.19		0.13
Th	5.06	146.7	3.44	3.59	1.36	5.73	2.02	5.64
U	2.4	9.4	3.2	6.6	3.1	4.3	1.1	5.2

	ES86-6	ES86-7	ES86-8	ES86-9	ES86-10	ES86-12	ES89-1	ES89-7
F	85000	98000	83000	125000	230000	204000	205000	77000
Na	64245	37686	133683	52227	93474	83570	119291	53414
Al	89000	108000	71000	98000	98000	102000	103000	93000
Cl	49000	39000	74000	72000	119000	179000	57000	30000
K		2324	18263	7471	18263		3653	6226
Ca			9291	5718	3431	3645	8934	
Sc	0.691	2.431	1.143	1.227	7.23	3.635	4.095	0.34
Cr		6.3			0.9	3	4.17	0.73
Mn	1100	1100	1300	3400	1100	1200	1400	600
Fe	2332	8154	12600	14722	14994	13517	19946	4330
Co	3.94	4.13	2.77	6.46	1.76	1.96	2.33	1.12
Ni						21		
Zn	167.6	21.8	264	215	83.3	137.7	95.7	43.1
As	24	15.5	38.7	72.4	66.6	78	164.1	24
Se	0.71	0.64	1.41		0.61	0.865	0.8	0.97
Br	0.25	0.35	1.21	2.34	1.29	9.3	1.29	0.51
Rb	33.4	22.2	47.5	37.6	61.2	38.8	85.2	23.2
Sr		45	164	115	134	87.5	245	41
Zr	133	136	542	612	290	254	571	94
Mo		1.2	2.1		4.7	3.3	4.4	3.1
Cd	48		51	32		18	18	16
In						3.6		
Sb	0.051	0.096	0.144	0.179	0.295	0.398	0.54	0.51
Cs	0.171	0.243	0.484	0.378	0.644	1.00	1.73	0.494
Ba		47	122	94	151	122	228	40
La	8.65	21.24	55	52.7	84.4	33.31	96.7	11.63
Ce	15.16	52.4	104.2	116	170.1	79.6	241.2	21.9
Nd	5.8	22.1	36.1	50	55.7	28.8	117	8.2
Sm	1.135	5.08	7.16	9.36	10.61	6.18	20.38	1.56
Eu	0.226	0.921	1.497	2.117	1.827	1.292	3.88	0.357
Tb	0.189	0.485	1.117	1.306	0.953	0.6785	1.951	0.246
Yb	1.00	0.82	4.77	3.19	2.37	1.98	5.18	0.68
Lu	0.166	0.09	0.728	0.446	0.268	0.272	0.667	0.103
Hf	1.33	2.16	8.92	10.31	5.54	4.44	11.24	1.39
Ta	0.337	1.137	4.53	3.26	2.95	2.105	5.74	0.682
W		0.22		1.4		0.02	0.02	
Ag						0.08		
Au		0.0008			0.0017			
Hg	0.17		0.17	0.14	0.09	0.13	0.18	0.11
Th	0.80	2.31	6.51	5.09	8.87	4.62	12.27	1.1
U	3.1	0.8	14.8	7.4	2.2	2.4	4.5	1.2

	ES89-10	ES89-13	ES89-17	ES89-21	ES89-25	ES89-42	ES89-47	ES89-51
F	96000	71000	117000	187000	156000	196000	91000	21000
Na	39615	43399	33977	52820	51040	69067	62316	39393
Al	90000	85000	90000	71000	74000	98000	79000	85000
Cl	24000	9000	20000	31000	50000	163000	101000	13000
K	6226		11622	31546	13282			24904
Ca				17153	5074			7218
Sc	0.517	0.415	0.914	2.195	2.167	1.782	1.665	2.361
Cr	0.68	0.49	8.5	3.7		2.8	1.4	
Mn	800	2600	5000	1600	1600	2200	1900	1700
Fe	1522	2697	23397	32569	28761	10533	21104	35795
Co	2.10	9.77	13.1	2.03	1.83	2.75	2.51	3.09
Ni								
Zn	39.2	68.9	678	171.5	300	298	160.8	183.8
As	4.13	10.1	1020	295	192	82.6	54.1	5.8
Se	0.21		2.6		0.9	0.55	0.56	0.9
Br	0.4	0.15	0.47	5.6	4.9	8.8	27.8	0.53
Rb	48.2	10.8	61.8	112	97	26.2	54.8	114.5
Sr	14	19	82	356	237	43	201	131.5
Zr	57	152	543	912	884	202	510	1140.5
Mo	1.3		5.2	11.5	14.4	2.1	6.7	5.15
Cd	4.2	4.6	278	5.8	27	22	24	
In			28	3.5	9	11		
Sb	0.049	0.058	0.909	1.143	1.44	0.228	0.486	0.364
Cs	0.357	0.092	0.873	2.02	2.46	0.587	0.738	1.463
Ba			37	434	339		267	346
La	19.78	13.95	29.21	139.6	126.8	20.86	89.6	115.6
Ce	41	29.3	52.9	274.4	256.1	45	206.2	206.75
Nd	16.3	11.3	21.2	96.9	74.6	14.6	97	63.55
Sm	3.28	2.566	3.63	17.07	14.9	3.32	16.46	12.915
Eu	0.642	0.547	0.755	3.56	3.26	0.723	3.57	2.576
Tb	0.441	0.372	0.653	2.038	1.866	0.797	1.744	1.672
Yb	0.708	1.104	2.63	6.44	5.82	3.15	4.07	6.285
Lu	0.084	0.164	0.379	0.891	0.682	0.454	0.532	0.792
Hf	0.614	1.78	9.43	20.23	18.11	3.94	10.92	23.95
Ta	0.231	0.282	2.74	16.68	14.13	1.67	8.69	16.7
W			0.61	1.9	0.027	0.01	0.025	0.36
Ag			0.18	0.15				
Au								
Hg		0.11	1.39	0.1	0.25	0.34	0.36	0.27
Th	0.88	1.20	3.7	20.3	19.1	2.7	11.1	22.3
U	0.8	1.7	15.5	5.7	5.1	2.4	3.1	4.5

	ES89-55	ES89-59	ES89-61	ES89-65	ES89-84	ES89-90	ES89-97	ES89-100
F	196000	119000	238000	116000	105000	154000		132000
Na	78118		70996	35498	73518	64764		38057
Al	102000	85000	88000	99000	94000	93000	129000	98000
Cl	184000	73000	82000	45000	120000	132000	9000	61000
K				2906				
Ca					6647	2859		
Sc	4.28	3.19	1.377	0.511	1.871	0.811	4.26	0.5
Cr	3.09	2.17	3.1	0.35	4.15	0.82		0.64
Mn	1200	1700	900	3200	1600	2300	1800	1300
Fe	10183	17723	19557	4971	23475	9716	61174	2534
Co	1.57	2.85	1.18	8.28	3.36	3.61	3.04	2.03
Ni	11							
Zn	129.7	108.1	224	303.5	157	227	226	173.1
As	36.7	644	123.1	23.85	32.7	34.9	14.5	8.8
Se	0.3	1.79	1.31	0.42		0.71		0.21
Br	5.6	0.9	4.9	0.2	4	0.58	4	
Rb	18	28.2	96.9	36.9	58.3	54.2	55.3	20.7
Sr	48	134	104	35	171	71	281	36
Zr	118	917	443	152.5	518	142	2036	300
Mo	2.9	9.5	6.1		3.8	5	4.5	
Cd	18.5	12	7.2	64.5	15	22		23
In	5			14		9		
Sb	0.14	0.96	0.23	0.09	0.22	0.16	0.5	0.04
Cs	0.305	0.499	1.156	0.333	0.825	0.576	1.09	0.11
Ba		116	112		230	53	444	
La	13.03	133.5	128.4	8.88	92.4	54.7	219.5	13.17
Ce	32.8	329	194.3	18.93	221.1	138.8	437	28.6
Nd	16	117	80	7.35	102	68.2	138	11.5
Sm	3.33	18.53	12.82	1.331	16.31	14.38	25.27	2.441
Eu	0.688	2.418	2.199	0.343	3.24	2.876	5.26	0.566
Tb	0.541	1.181	1.226	0.313	1.613	1.81	3.07	0.403
Yb	1.982	1.905	2.86	1.687	4.11	3.71	11.85	1.121
Lu	0.286	0.232	0.359	0.238	0.529	0.49	1.458	0.161
Hf	1.78	23.86	9.17	1.482	10.21	2.4	42.7	2.69
Ta	0.598	5.51	3.25	0.367	7.01	1.36	30.4	0.268
W	0.01	0.073	0.034	0.004	0.04		2.5	
Ag				0.132				0.096
Au			0.0013					0.0007
Hg	0.17	0.18		0.115	0.61	0.33	0.16	
Th	1.35	12.35	10.89	0.92	11.06	2.79	38.1	0.99
U	2.1	3.2	4.4	4.2	4.0	3.4	8.5	5.0

	ES89-103	ES89-104	ES89-105	ES89-106	24880[a]	24885[a]	24886[a]	ES81-8A
F	80000	105000	94000	104000	10000	48000	11000	
Na	55565	27078	16299	36153	82000	39000	18000	301936
Al	99000	110000	106000	102000	104000	88000	122000	1000
Cl	5500	40000	3300	57000	176000	53000	12000	18000
K	1992	4649		2961	3000	25000	11000	
Ca			2787		2100	16000	9000	
Sc	0.201	0.612	0.389	0.553				0.062
Cr	1.97	0.9						0.26
Mn	200	2600	2600	6000	1700	1100	1700	
Fe	364	5597	2814	4532	19000	25000	2700	72
Co	0.255	4.5	9.5	12.82				0.06
Ni		13		15				
Zn	19.25	366	257	552	112	200		1.51
As	2.745	31.8	11.2	23.4				3.2
Se	0.35	0.55	1.12	0.78				0.11
Br	0.245	0.19	0.13	0.33				9.1
Rb	13.4	19.1	4.9	9.2	76	22		1.59
Sr		37		46	158	89		
Zr	63.5	523	1115	488	642	340		27
Mo	1.05							5.6
Cd	4.5	53	30	103				
In		9	7	12				
Sb	0.034	0.038	0.203	0.044				0.08
Cs	0.103	0.08	0.029	0.053				0.03
Ba					266	40		
La	4.94	19.52	21.85	17.76				0.5
Ce	9.7	44.4	48.6	34.1				51.5
Nd	4.95	19.2	20.4	12.6				
Sm	0.85	4.14	3.95	2.91	7.4	10.4	11.6	0.056
Eu	0.182	0.992	0.898	0.721				0.022
Tb	0.102	0.781	0.542	0.681				0.016
Yb	0.32	2.53	1.49	2.34	2.2	3	40	0.98
Lu	0.044	0.37	0.226	0.353	0.2	1.3	190	0.146
Hf	0.54	5.6	12.48	4.32				0.105
Ta	0.014	0.329	0.08	0.067				0.005
W								
Ag		0.22		0.23				
Au			0.0014	0.0011				
Hg	0.195							
Th	0.48	1.54	0.98	0.84	11	3		4.18
U	0.6	8.3	13.6	9.1				1.2

[a] from Keys (1980), also contain 8700, 2800, 100000 ppm S,respectively;
[b] Rb, Sr, Zr, Zn, Ba, Th in these samples analyzed by XRF (Keys,1980).

7.4.1. Rim samples

Samples collected from the rim of Erebus or within the crater are collectively referred to as "rim samples". Salts form thick, bright-yellow deposits on the walls of the Inside Crater, and on the surface of bombs on the crater floor. Outside the crater, salts cover the surface of the regolith, and fill the cracks in small boulders. Two samples collected on the crater rim (ES89-21 and ES89-25) and a sample collected from the crater floor (ES89-61) have similar composition, being composed mainly of F, Al, Na, Cl, Fe and Mn. In addition, the two rim samples contain Ca and K. The crater sample has higher concentrations of F, Al, Na and Cl, but much lower concentrations of Fe and Mn. Similarly, the concentrations of trace elements including REEs are generally lower for this sample. The crater sample probably contains malladrite, Fe-chlorides and sulfates, gibbsite and possibly $NaAl_4O_4(F,Cl)_5$. The two rim samples were identified as containing ralstonite, malladrite, hieratite, and various phosphates. ES89-21 may also contain alunite, elpasolite and Fe-Al oxides. Another rim sample (ES89-97) differs both in color (reddish brown), mineralogy (probably a complex mixture of clays), and composition from other rim samples, and it is composed mainly of Al, Fe and Cl.

All rim samples (Figure 7.1) have very similar enrichment factor pattern with the exception of ES89-97. They are strongly enriched in F, Cl, As, Cd, In and Ce. Sample ES89-97 has the lowest EFs for Cl, As, Zn, Sb and Cs, and is depleted in Br and Rb. On the other hand it has the highest EFs for Hf, Ta. The small difference in enrichment

factor pattern could be due to difference in the plume composition caused by wind direction and be related to the sample location.. Sample ES89-97 was collected on the S-SE rim whereas samples ES89-21 and ES89-25 were collected from the E part of the crater and from Shackleton Cairn, on the NW crater rim, respectively. Alternatively, the differences may be due to the different mineralogy of the salts.

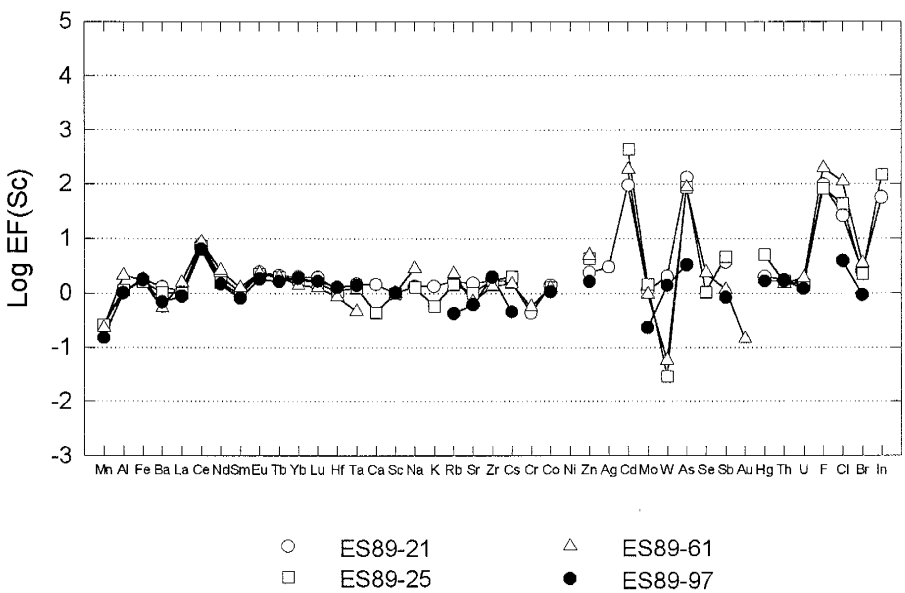

Fig. 7.1. Log (EF) for salt samples collected from the crater rim calculated relative to Erebus magma using Sc as reference element.

7.4.2. Nausea Knob salts

All salts collected at Nausea Knob (which lies about 500 m NW from the Inner Crater) are grouped together. Nausea Knob salts form very abundant, usually bright-yellow deposits. As noted by Keys (1980), the abundance of salts at Nausea Knob is unusual compared to other locations at this radius from the crater. Salts were tentatively identified as $NaAl_4O_4(F,Cl)_5$, Fe-chlorides, and carbonates. In addition, AlF_3 was identified in ES89-55, and natrojarosite in ES89-42. The chemical composition of salts from Nausea Knob closely resembles those from the crater rim. All salts contain high concentrations of Na, Fe, Al, F, Cl, and Mn, some also contain K and Ca. Although the absolute concentrations vary greatly, on the average the Na, Al, Cl and Br concentrations are higher than that of rim salts whereas the concentrations of F, Fe, Mn, most trace elements (with the exception of Cd and Co) and REEs are similar or lower.

Nausea Knob salts are strongly enriched in Cd, As, F, Cl, and In. Some are also enriched in Hg, Ni, Zn, U, Th, and Ce. Salts can be separated into two groups using their EFs pattern (Figure 7.2). One group is depleted in Br (ES81-7, ES83-218, ES86-7, ES89-51, ES89-55) (Figure 7.2a), the other is enriched in Br (ES81-407, ES83-213, ES86-12, ES89-42, ES89-47) (Figure 7.2b). All Nausea Knob salts are characterized by a wide range of EF for REE elements ranging from strongly enriched to strongly depleted. The reason for this may be dissolution of deposits by water from melting snow, and their re-precipitation.

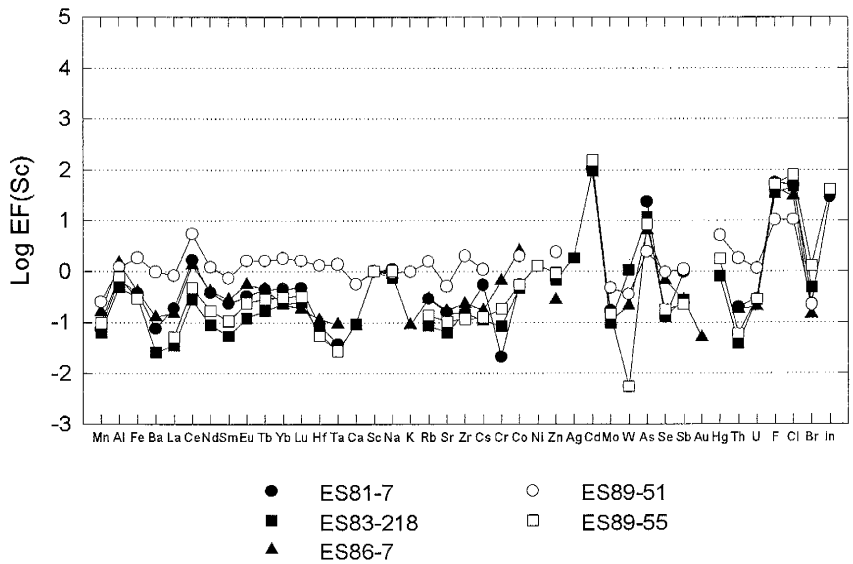

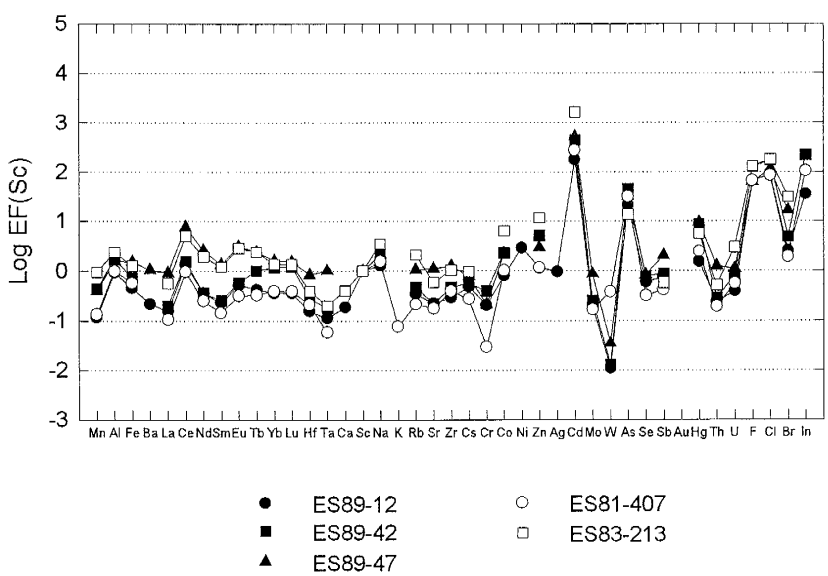

Fig. 7.2 (a,b). Log EF for salt samples collected from Nausea Knob calculated relative to Erebus magma using Sc as reference element

7.4.3. Lava flow salts

This group includes all salts sampled on the lava flows covering the summit area. Most of these salts are white or yellow-white in color, sometimes containing reddish-brown patches, which are probably an Fe-rich phase. They form abundant deposits on the lava flows covering the summit plateau, occurring on the rock surface, in cracks or underneath rocks and boulders. The mineralogy of lava flow salts is uniform, they are mostly composed of khademite and halite. Some salts contain clay minerals (montmorillonite, illite, hectorite), particularly common in sample ES89-59. Other minerals, such as NaF, tamarugite, Fe-oxides, carbonates and phosphates were also detected. The difference in mineralogy greatly affects the chemical composition of salts, and the clay-rich samples (ES89-59 and ES89-1) have much higher REE concentrations than other salts. The composition of salts from lava flows lava is variable; on average they have higher Al and Cl contents and lower F, Na, K, Fe, trace elements and REEs than rim samples. Like the samples from Nausea Knob, they have higher Co, Cd and In concentrations than samples from the crater rim.

Lava flow salts are strongly enriched in F, Cl, In, As, and Cd. Less enriched are Na, Ce, Co, Ni, Zn, Hg, Al, Rb, Zr and U (Figure 7.3a,b,c subdivided for clarity). Other elements, including REEs show a wide range of values. Generally, the EF patterns of all lava flow salts are similar. However samples containing clay minerals (ES89-1, ES89-10, ES89-65), and especially ES89-59 which is devoid of otherwise

common Al-sulfate and halite, have slightly lower enrichments than other salts. The pattern may indicate the mobility of elements and be related to dissolution and reprecipitation of salts.

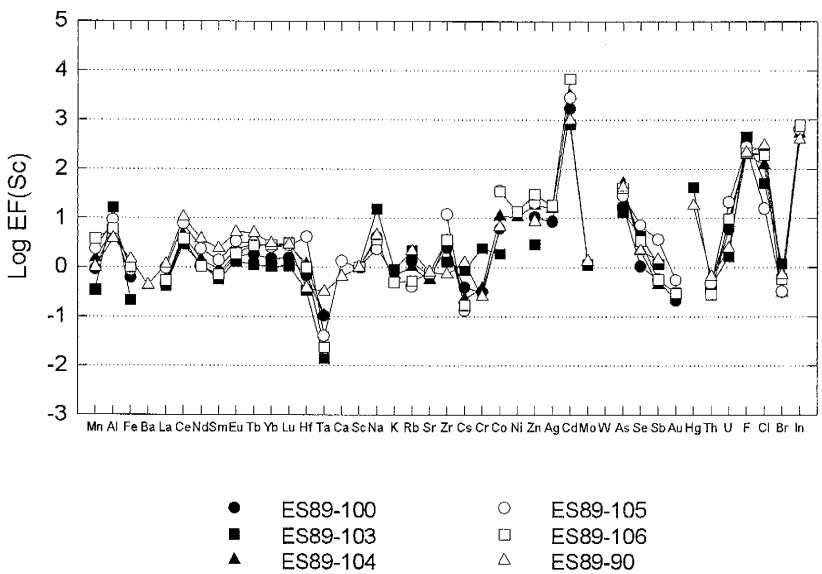

Fig. 7.3a. Log EF for salts collectd on lava flow calculated relative to Erebus magma using Sc as reference element .

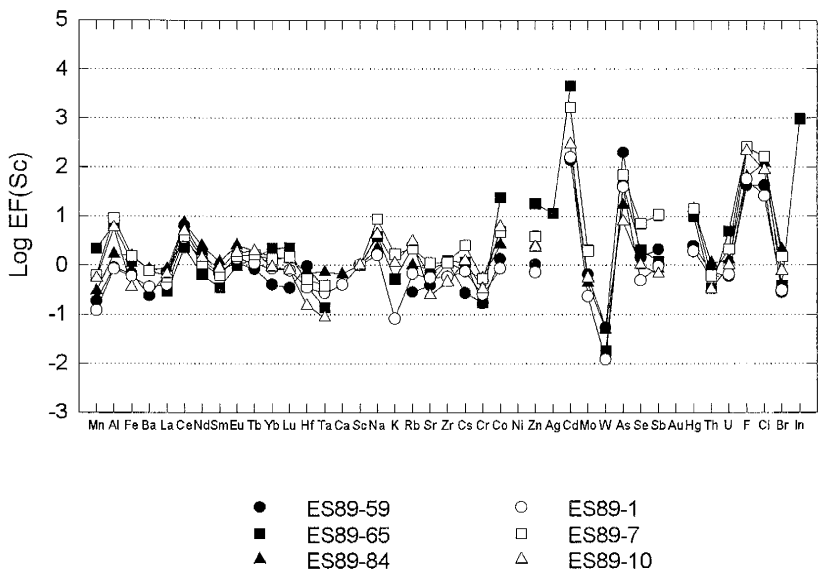

Fig. 7.3b.

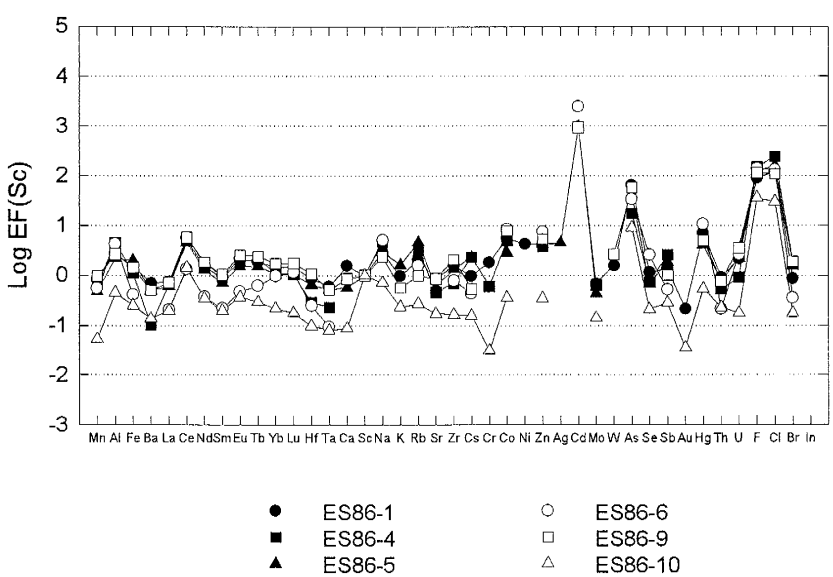

Fig. 7.3c.

7.4.4. Old caldera rim samples

This group includes samples collected from the rocks bordering the summit plateau, which are probably remnants of an old Erebus caldera (Chapter 2). Salt deposits in this region are very sparse, and are generally concentrated in sheltered areas, mostly in cracks. Salts are whitish-pink or brown. Sample ES89-13 contains natroalunite and phosphates. Sample ES89-17 contains mixture of tamarugite, K-Mg-sulfate, carbonates and bicarbonates, phosphates and montmorillonite. The chemical composition of salts from the old caldera rim resembles that of salts from lava flows. The salts are higher in Al, and lower in F, Na, Cl, K and Fe than the salts from the crater rim. Sample ES89-13 has similar concentrations of trace elements to flow samples, but sample ES89-17 has unusually high concentrations of Zn and As, exceeding concentrations observed in other samples from the Erebus summit area. Concentrations of other elements (Mn, Zr, Cd, In, and U) also are higher than observed in rim samples but comparable to levels in some flow samples.

Salts from the old caldera rim display EFs patterns very similar to salts from lava flows. Like these, they are enriched in F, Cl, In, Cd, As, Na, Ce, and Co (Figure 7.4). The major difference is in enrichment of REEs Eu, Tb, Yb, Lu in all samples from the old caldera rim. The same REEs are found enriched in some salts from lava flows, but generally Yb and Lu are less enriched from Eu and Tb.

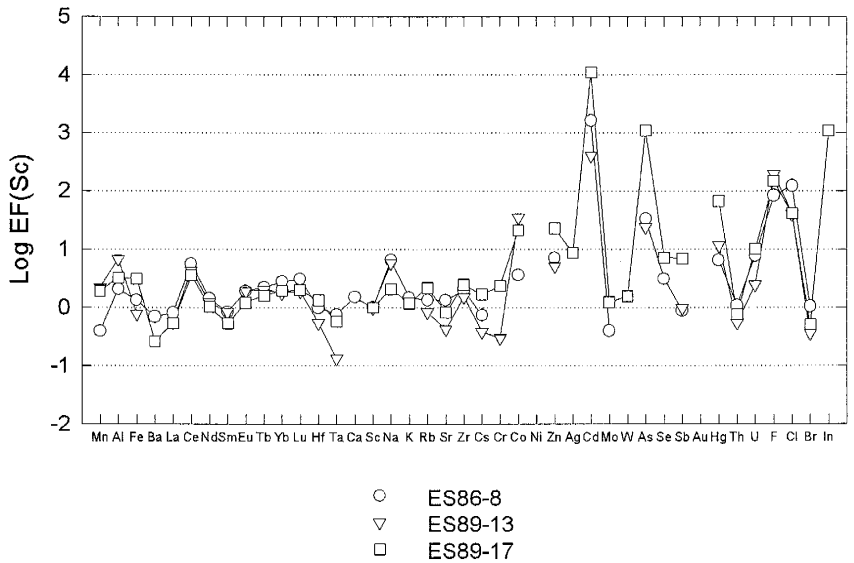

Fig. 7.4. Log EF for salt samples from the old caldera rim calculated relative to Erebus magma using Sc as reference element.

7.5. Discussion

The unusual mineralogy and chemical composition of salts with a high concentration of trace elements found also in the volcanic gas sampled at Erebus give clues to the volcanogenic origin of salts found on Erebus. They appear to be formed by a complex interaction of the volcanic plume with the rocks exposed in the crater and in the summit area. Keys (1980) also favors the volcanic origin of the salts, and implies the possiblility of acid-rock interactions as one of the mechanisms leading to their formation. All salts can be generally subdivided in two groups, depending on their mineralogy. Salts collected inside the crater or from the rim are mixed fluorides and

chlorides, whereas the lava flow salts are mostly sulfates. The correlation between the sample distance from the crater and its composition is however more complex. The enrichment factors of elements give a measure of the amount of change between the parental rock, volcanic gas and salts. Figure 7.5 shows the comparison of the EF of the Erebus gas with some salts. There is a good agreement between the enrichment patterns observed in the gas and in salts. Most elements highly enriched in the gas (F, Cl, As, In, Cd, Co, Zn) are also enriched in salts. Some elements present in the salts (Al, Fe, Mn, REEs) are not volatile and are not present in the gas in quantities large enough to form salt deposits; they must therefore have been leached from the phonolite.

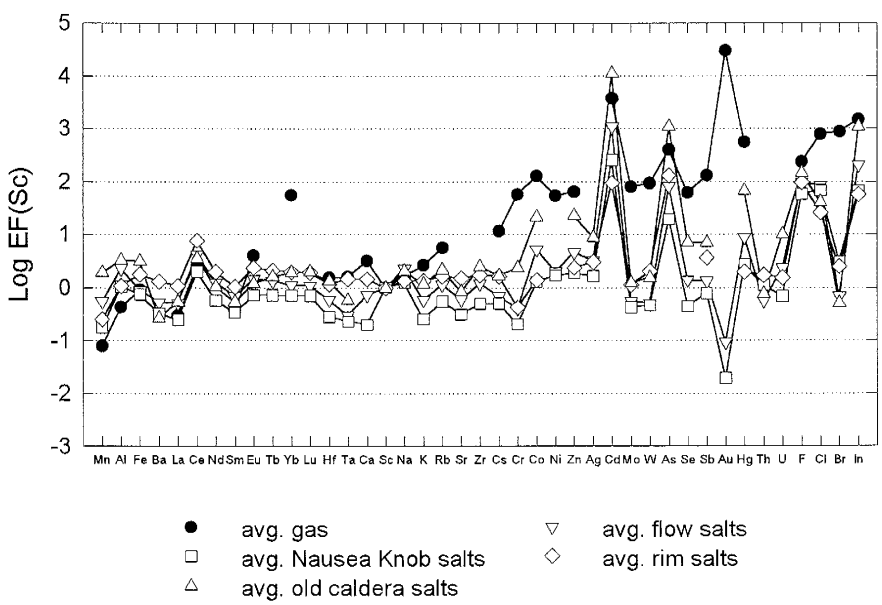

Fig. 7.5. Comparison of average composition of different groups of salts with the Erebus gas.

The elements from which the salts are composed can be separated into two groups depending on their source: the volcanogenic components (F, Cl, S, Br, As, Se, Sb, Zn, Co, Cd, In, Hg) and rock-derived components (Al, Fe, Mn, Na, K, Ca, P, REEs). Alkali metals (especially Na and K) are detected in the plume, and could be considered together with volcanogenic components. However, the ratio of these elements to F or Cl in salts greatly exceed the proportions found in the plume. Therefore, although a fraction of alkali metals detected in salts may represent volcanic sublimates, the majority are probably rock-derived.

7.5.1. Volcanogenic components of salts

The enrichment factors for the volcanogenic components show an increase with the distance from the crater (Figure 7.6) but a large spread in values is observed among salt even at the same location. Both F and As show a well defined increasing trend, whereas the increase in Cl enrichment is less pronounced. The increasing trend is not followed in case of samples collected within the crater and on the rim, which display much higher enrichment. The higher enrichments are probably caused by more intense interaction between the acidic plume and rocks. The plume is less diluted in proximity to the lava lake and the water vapor condensing within the crater also intensifies the leaching process. Volcanogenic trace elements (Hg, In, Cd, Zn) also show an increase in enrichment with distance from the crater (Figure 7.7).

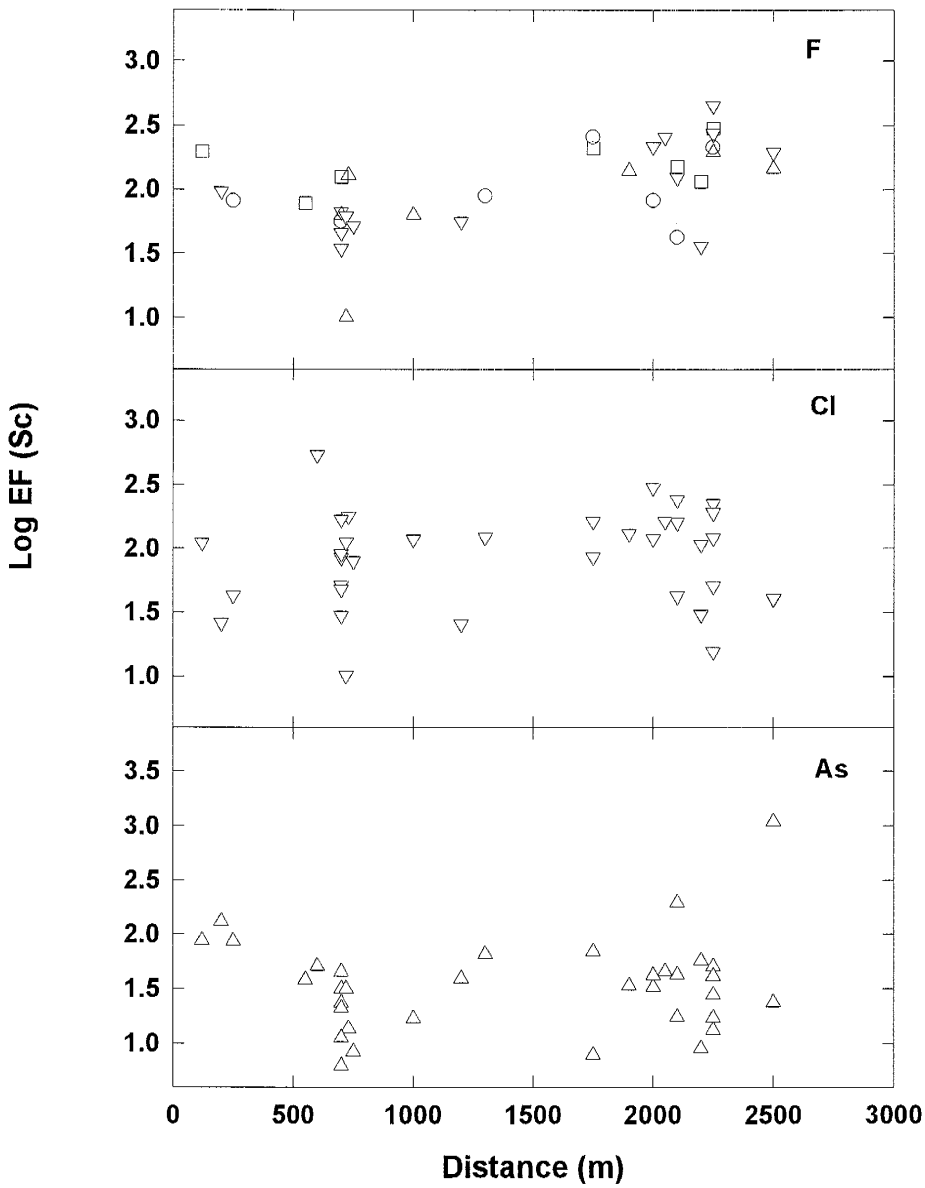

Fig. 7.6. Correlation between EF of F, Cl, and As in salt samples and estimated distance from lava lake.

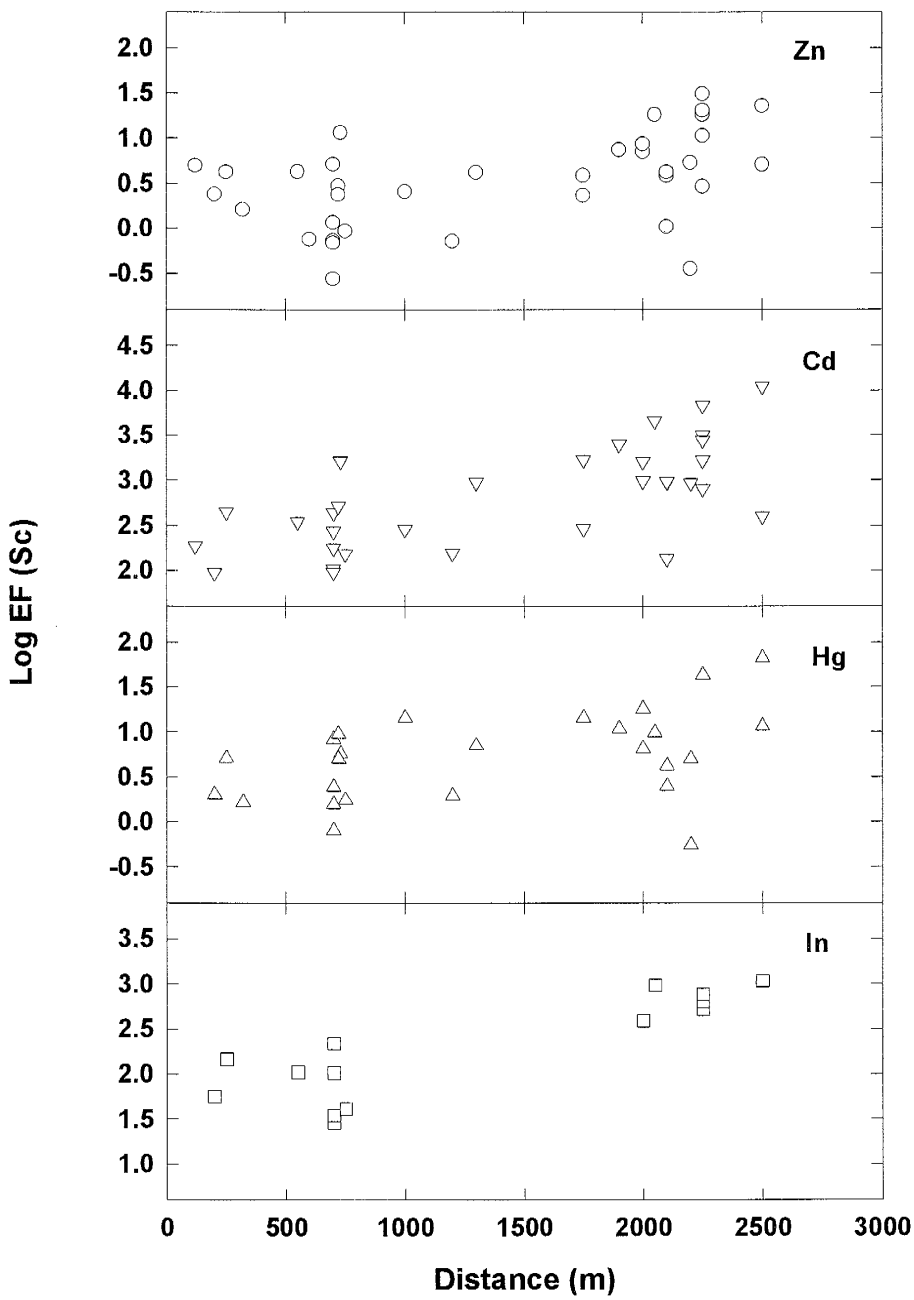

Fig.7.7. Correlation between EF of Cd, Hg, In, Zn in salt samples and estimated distance from lava lake.

7.5.2. Rock-derived components of salts

Many trace elements found in salts show either a very small enrichment relative to the parent rock of phonolite composition, or no enrichment at all. These elements are sometimes detected in the plume and there is evidence of their volatilization (for example Na, K). Other trace elements (Al, Fe, Mn, REEs) although also found in the plume are not of volatile origin but instead represent ash or small rock fragments. As discussed above, these elements could not have been concentrated in the salts from the summit at the observed levels, and are thus classified as rock-derived components. This represents the major difference between the origin of the low-temperature Erebus salts and high-temperature sublimates formed around active vents, where Fe, Al, Na, K-sublimates are deposited.

The rock-derived components show either an increase in enrichment with distance (Na, Al, Mn) (Figure 7.8), or a slight decreasing trend (Fe, Cr, REEs) (Figure 7.9). The amount of enrichment is related to the intensity of leaching, but perhaps it also indicates that Na and Al form more mobile compounds.

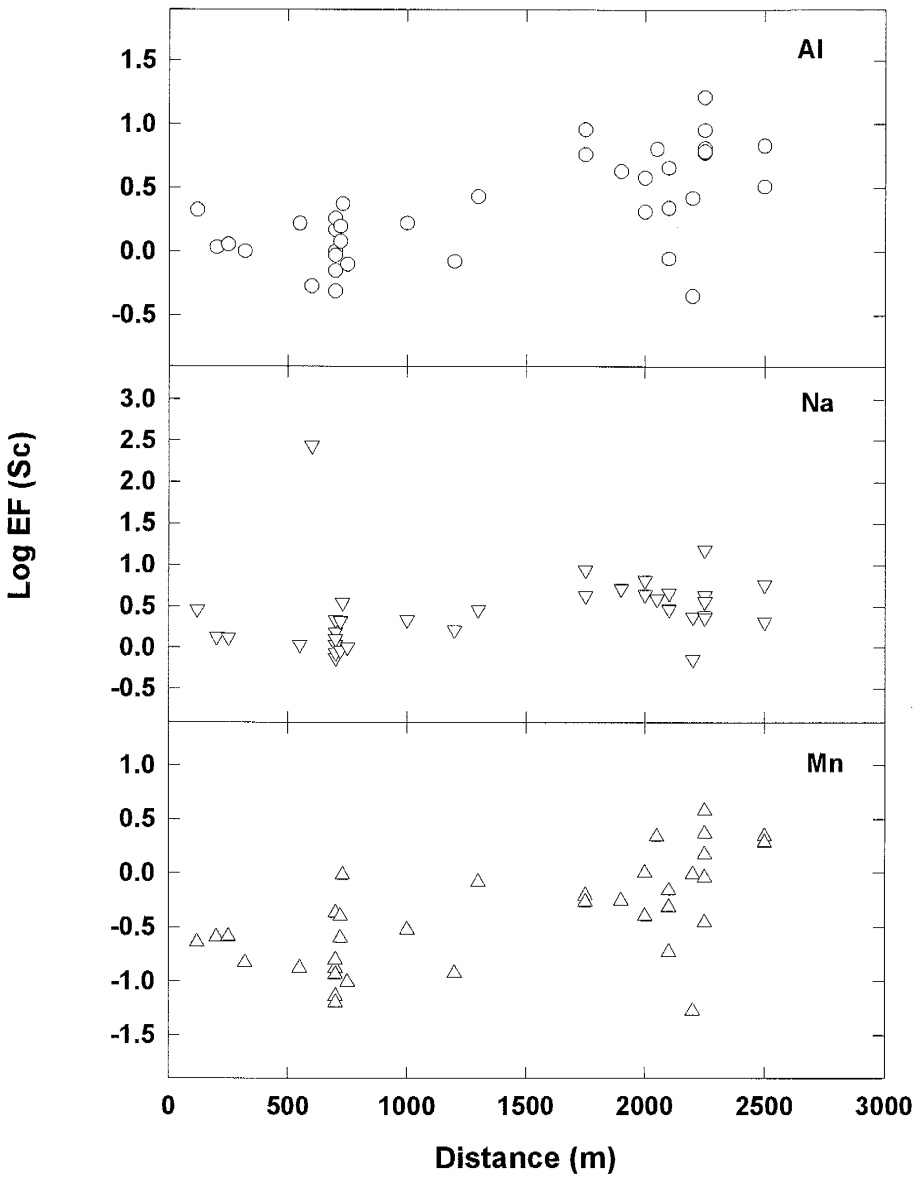

Fig. 7.8. Correlation between EF of Al, Na, and Mn in salt samples and estimated distance from lava lake.

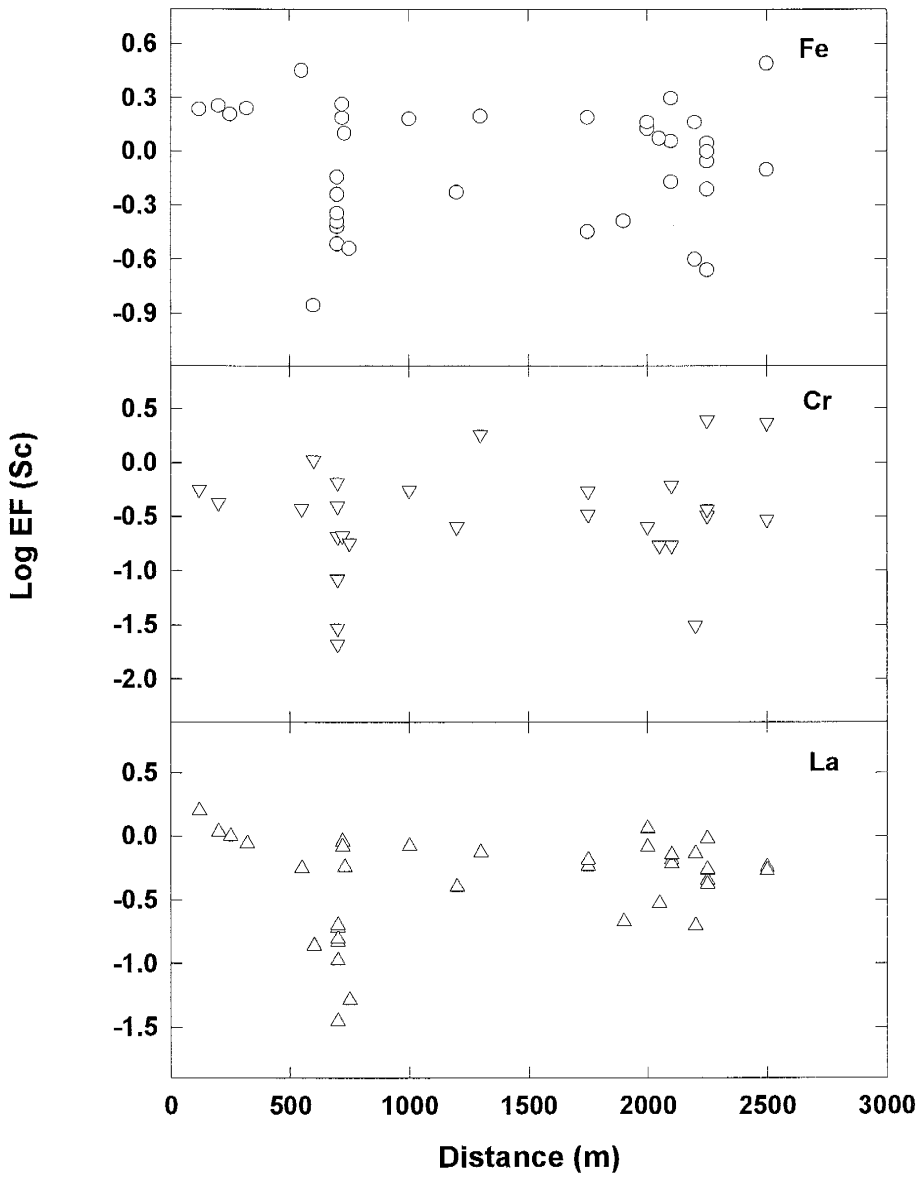

Fig. 7.9. Correlation between EF of Fe, Cr, and La in salt samples and estimated distance from lava lake.

In the case of the volcanogenic components of salts, the increasing enrichment may be caused (1) by a complex pattern of plume dispersal related in part by the topography of the summit area, (2) by different properties of elements present in the plume affecting the rate of their removal from the plume, and (3) by concentration of certain elements in salts due to their dissolution and reprecipitation. On the other hand, the change in the concentrations of rock-derived components is related to the intensity of leaching of a parent rock. Once the element is incorporated into the deposit, it may be remobilized, and form secondary deposits. The intensity of leaching of parent rock or resulting salts/clay mineral deposits is related to the pH of the solution. In this particular setting, the pH is controlled by the acidic gases adsorbed on snow. The field observations show that the pH of water from melted snow collected from lava flows near Lower Hut is about 4, but it varies depending on location. Thus, the factors affecting the distribution of acids in the plume also influence the distribution pattern of the rock-derived elements.

Due to the lack of data on the Erebus plume dispersal it is, at present, impossible to evaluate the dilution of plume at distance from the crater and the ground-level concentrations of plume components. It can only be hypothesized, that according to a simple gaussian model of plume dispersal (Pasquill, 1974; Pasquill and Smith, 1983), the ground-level concentrations reach a maximum at a specific distance from the plume source and continue to decrease from that point on. The position of maximum concentration is a function of many parameters including source strength, wind speed and

atmospheric stability. As shown in Chapter 5, the Erebus plume is constantly changing the magnitude of its output, and of variable meteorological conditions, it is therefore likely that the ground-level concentrations are also subjective to many changes. The present patterns of enrichment of volcanogenic component in salts may be a result of these changes.

Assuming an average pattern of plume dispersal over the summit plateau, one need further consider the difference in the properties of the plume components, which affect their removal from the plume. Presently, very little is known about the removal rates of different chemicals from atmospheric plumes, and the scarce experimental data may not be applicable to the conditions in Antarctica. This subject is considered in more detail in Chapter 8, and here it will be considered only qualitatively. The difference in removal rates, and in the manner the removal is occurring (for example coagulation and settling of particulates from the plume, rates of wet and dry deposition, adsorption on snow, ice and rock surfaces) is likely to produce compositional gradients of various elements along the plume axis. The gradients may be recorded in the salt composition.

Finally, the salt deposits are often fractionated due to dissolution and reprecipitation. Keys (1980) described many indications of this process, which leads to separation of different phases and results in concentrating some elements while removing others.

7.6. Origin of salts from the Erebus summit area

The formation of the salts may involve several steps. In the acidic environment, the dissolution of Erebus rock can be represented as:

$$\underset{albite}{NaAlSi_3O_8} + H^+ + 7H_2O = \underset{gibbsite}{Al(OH)_3} + Na^+ + 3H_4SiO_4 \quad (1)$$

during which gibbsite is formed, or :

$$\underset{albite}{2NaAlSi_3O_8} + 2H^+ + 9H_2O = \underset{kaolinite}{Al_2Si_2O_5(OH)_4} + 2Na^+ + 4H_4SiO_4 \quad (2)$$

where kaolinite is formed. An experiment in which a powdered sample of Erebus glass was suspended in acidic vapor produced various alteration products including gibbsite. Keys (1980) and Ugolini (1967) also predicted formation of gibbsite in soils from the Erebus summit area. In some salts (ES89-1, ES89-10, ES89-17, ES89-59, ES89-65) Na-montmorillonite was also detected, suggesting that the following reaction may also take place:

$$\underset{albite}{7NaAlSi_3O_8} + 6H^+ + 20H_2O = \underset{Na-montmorillonite}{3Na_{0.33}Al_{2.33}Si_{3.67}O_{10}(OH)_2} + 6Na^+ + 10H_4SiO_4 \quad (3)$$

Other clay minerals detected in salt samples included hectorite (Li-bearing smectite) in sample ES89-10, and illite in sample ES89-59.

Dissolution of glass, which is initiated by the acidic conditions sustained by dissolution of acidic volcanic gases in water, leads to mobilization of Na^+, K^+, Rb^+. These cations, as well as other trace elements, including soluble trivalent REEs, are removed from the weathering rock. Most of the Na^+ is then removed from solution by

reactions with the acidic components of the volcanic plume dissolved in water. The possible reactions are:

$$Na^+ + HCl_{(aq)} = NaCl_{(s)} + H^+ \quad (4)$$

$$2Na^+ + H_2SO_4 = Na_2SO_4 + 2H^+ \quad (5)$$

The dissolution of rock followed by the reaction of its products with volcanogenic acids provides an explanation for the formation of most salts observed in the summit area. For example:

$$NaAlSi_3O_8 + 2H_2SO_4 + 10H_2O = \underset{tamarugite}{NaAlSO_4 \cdot 6H_2O} + 3H_4SiO_4 \quad (6)$$

$$3NaAlSi_3O_8 + 3H_2SO_4 + 18H_2O = \underset{natroalunite}{NaAl_3(SO_4)_2(OH)_6} + 9H_4SiO_4 + Na_2SO_4 \quad (7)$$

A similar reaction leads to the formation of alunite ($KAl_3(SO_4)_2(OH)_6$. Gibbsite or kaolinite may be consumed by the reaction:

$$\underset{gibbsite}{Al(OH)_3} + H_2SO_4 + 3H_2O = \underset{khademite}{Al(SO_4)(OH) \cdot 5H_2O} \quad (8)$$

Khademite is one of the most wide-spread salts in the summit area, often accompanied by halite. Similar reactions of gibbsite with HF produce:

$$Al(OH)_3 + 3HF = AlF_3 \cdot 3H_2O \quad (9)$$

$AlF_3 \cdot 3H_2O$ was described from Erebus by Rosenberg (1988), who postulated it was a sublimate and formed in the plume. As discussed in Chapter 5, there is little evidence which supports the occurence of this process in the plume. Instead, the presence of $AlF_3 \cdot 3H_2O$ in salts may be caused by the reaction between acidic gas and rock, but this reaction does not appear to be very common. Anhydrous AlF_3 was detected only in one sample (ES89-55). The dehydration could have occurred during sample preparation and

storage. Other F-bearing salts include ralstonite, elpasolite, and malladrite. For example:

$$2NaAlSi_3O_8 + 12HF + 10H_2O = \underset{malladrite}{Na_2SiF_6} + 2AlF_3{\cdot}3H_2O + 5H_4SiO_4 \quad (10)$$

Dissolution of other rock components (such as olivine, which on Erebus has composition $Fo_{50}Fa_{50}$) produces Mg^{2+} and Fe^{2+}, which oxidizes to Fe^{3+}. For example:

$$\begin{aligned} Mg_2SiO_4 + 4H^+ &= 2Mg^{2+} + H_4SiO_4 \\ Fe_2SiO_4 + 4H^+ &= 2Fe^{2+} + H_4SiO_4 \end{aligned} \quad (11)$$

Iron compounds are often present in salts as manifested by their reddish-brown coloration. One of the Fe-compounds tentatively identified by Rose is hydromolysite (after Keys, 1980).

$$Fe^{3+} + 3HCl + 6H_2O = \underset{hydromolysite}{FeCl_3{\cdot}6H_2O} + 3H^+ \quad (12)$$

Formation of $NaAl_4O_4Cl_5$ which was identified tentatively by Rose (after Keys, 1980) as a component of the bright yellow salts (mostly from the rim and Nausea Knob localities) may proceed via the following reaction:

$$Al(OH)_3 + Na^+ + HCl = NaAl_4O_4Cl_5 + H^+ \quad (13)$$

Judging from the chemical composition of the yellow salts from Erebus, $NaAl_4O_4Cl_5$, if its identification is correct, is not likely to be an only phase present in the salt and could be accompanied by several other substances. The lack of clay minerals in the yellow salts suggest that they are also secondary deposits, formed by reprecipitation. However, this does not seem likely because the yellow salts are poorly soluble in water. Alternatively, they may be formed in situ, and their formation may completely remove

Al species from the weathering residue. As shown in Table 7.1, many salts may contain various mixed phosphates of Al, Fe, and less often of Ca, Na, and K. Formation of phosphates could provide an additional sink for Al from the weathering rock.

The formation of clays can lead to an increase in pH, and thus cause the precipitation of dissolved substances. Most cations precipitate by forming hydroxides, carbonates and other components. Clay minerals, hydroxides and salts that precipitate from the solution, provide surfaces for the adsorption of other components present in the plume. This process could account for the high enrichment of Co, Zn, Cd, As, Se, Sb, Hg, and In in salts. The resulting deposits composed of a mixture of clays, salts and adsorbed solids can undergo fractionation when water from the melted snow percolates through. Dissolved salts move from the primary deposit and precipitate again in small cracks, depressions on the surface of regolith and beneath rock fragments. Figure 7.10 shows the schematic pathways leading to the formation of salts in the summit area.

Keys (1980) noted many examples where salt deposits exhibited compositional fractionation clearly due to dissolution and reprecipitation. The abundant deposits of khademite and NaCl found on lava flows in the summit area (for example samples ES89-90, ES89-99, ES89-100, ES89-103, ES89-104, ES89-105, ES89-106) are most likely formed by this process. These deposits are devoid of clay minerals, which supports the idea that these deposits are formed be reprecipitation of salt-bearing solution.

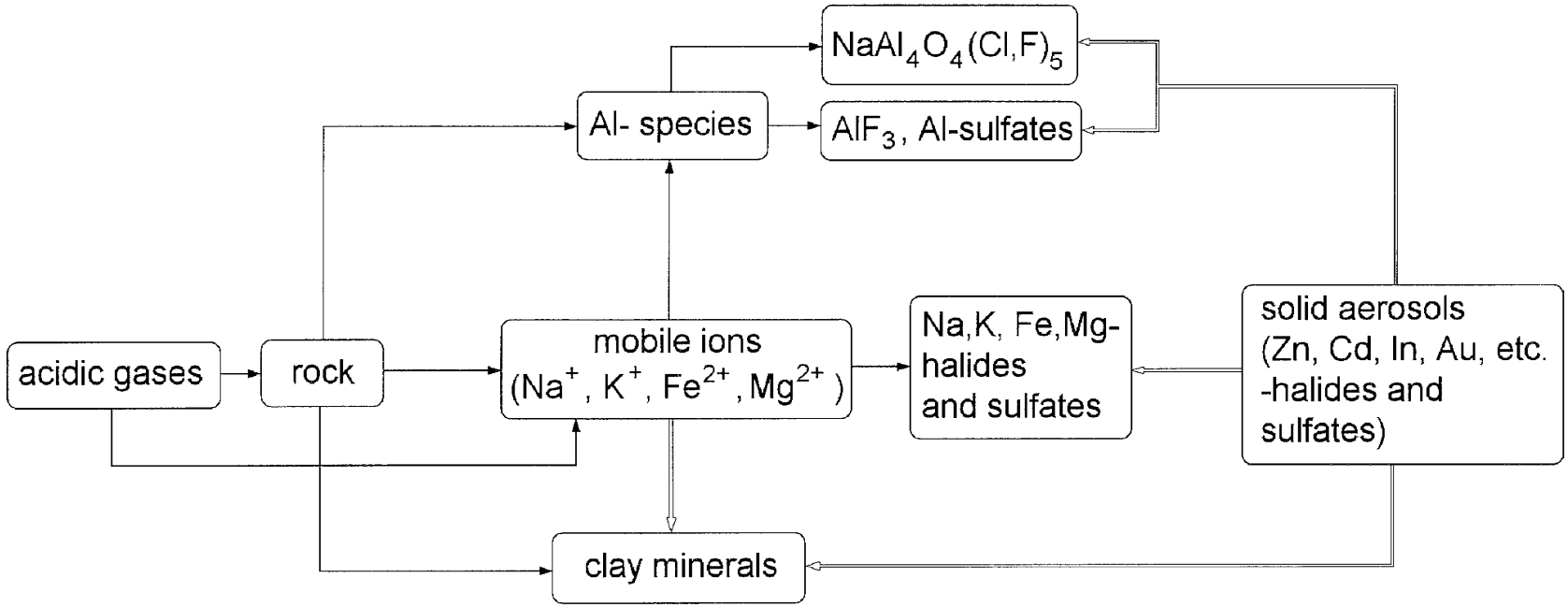

Fig. 7.10. Formation of volcanic salts at Mt. Erebus. Arrows show the major pathways for the reactions between gases and the rocks exposed on the surface, dissolution and precipitation reactions between components, and adsorption.

The above model of salt formation explains many of variations in the chemical composition of salts and their relationship to the Erebus rock and gas (Figure 7.5). Elements such as Al, Mn, and Fe, as well as some REEs represent the insoluble clay residue formed by weathering of the rock. The three most abundant gas species F, Cl and S are highly enriched in the salts and are clearly of volcanic origin (S was not analyzed in salts but its abundance is inferred from the preponderance of sulfates in the salts). The other moderately to highly enriched elements in salts (Co, Zn, Cd, As, Se, Sb, Hg, In) are also likely to be of volcanic origin. Their absolute concentrations in salts are often several orders of magnitude higher than in the parental rock. I postulate that these elements are incorporated into salts by adsorption either directly from the gas phase, or from liquid solution formed by melting of snow. As explained in Chapter 5, most metals detected in the volcanic plume form solids, but other elements (As, Se, Hg) are present as gases. Whereas solids may slowly precipitate from the plume and be deposited on the surface of rock and snow, gaseous substances are removed from the plume by more complex processes such as adsorption on snow. Water from the melted snow interacts with the parent rock and clays. Volcanogenic elements may either combine with ions leached from the rock, or get adsorbed on clays and hydroxides in the residue. The similar enrichment patterns in gas and salts from the summit area clearly support their volcanogenic origin. The effect of marine aerosols on the salt formation is probably not significant, as shown by (1) the unusual mineralogy of salt assemblages, as compared to salts found in other location in Antarctica (Keys, 1980; Keys and Williams, 1981), (2) enrichment of non-marine trace elements, and (3) generally non-

enriched Na content.

The results of this study support the conclusions of Keys (1980), Keys and Williams (1981) and Jones *et al.* (1983) who suggested the volcanogenic origin of salts from the Erebus summit, as well as possible interaction between acidic gases and rocks. Because many of the postulated reactions take place in the aqueous medium, a marine component (trace elements present in marine aerosols and deposited with snow on the summit) may also be introduced into salts. The exact contribution from these two sources (volcanogenic and marine) are at present still impossible to determine. The future studies of the isotopic composition of salts from Erebus may further resolve this problem.

8. ENVIRONMENTAL IMPLICATIONS OF MT. EREBUS EMISSIONS

8.1. Introduction

Four sources have been suggested for Antarctic aerosols : crustal, oceanic, volcanic and possibly anthropogenic (Zoller *et al.,* 1974; Duce *et al.*, 1975; Maenhaut *et al.*, 1979; Shaw, 1989; Dick, 1991 and others). Of these, the three natural sources contribute most of the total mass of aerosols in Antarctica. Crustal aerosol is a fine dust produced mainly by wind erosion of rock and soil, but also by glacial movement or running water. The particle size is typically large, with binomial distributions centered around 1-10 μm and 10-100 μm, but the larger particles do not participate in long-range transport (Shaw, 1989). Oceanic aerosols (also called sea salt aerosols) originate by disruption of surface film by wave motion, and by drops forming from bursting bubbles. The size of these particles can vary from 0.1 μm to >100 μm, but over 99% of the "giant" particles are scavenged and removed during their transport. Due to the turbulence of air masses along the coastline, sea salt aerosols can reach great heights, and the smaller particles can travel great distances. On the other hand, the concentration of near-surface (altitude <1 km) sea salt aerosols falls off exponentially with distance from the coast (Shaw, 1989). These aerosols can however reach the center of the continent during storms that bring moist marine air deeply inland (Shaw, 1989). Both crustal dust and sea-salt are primary (solid) aerosols (Delmas, 1992). Volcanic eruptions producing ash plumes are another source of primary aerosols. Primary volcanic aerosols are

composed of ash particles, most of which have a relatively large size or undergo a fast process of aggregation and growth and quickly falls out (Shaw, 1989). The remaining ash, less than a micron in size, (representing 10^{-3} -10^{-5} of the total injected mass) can be distributed worldwide. Secondary aerosols form another important group of volcanic aerosols. Those are liquids or solids produced by conversion from volcanic gases; of these droplets of H_2SO_4 are the most important. Large volcanic eruptions can be identified in Antarctic snow and ice cores by acidic bands (Delmas *et al.*, 1985).

Anthropogenic aerosols are mostly secondary aerosols produced during combustion processes by condensation from the gas phase. They are generally very small (submicron) in size; thus their residence time in the atmosphere can be long and they can be distributed worldwide (Shaw, 1989). Because of their long residence times, the presence of anthropogenic aerosols in the Antarctic atmosphere has been suggested by some authors (Dick, 1991) to account for certain elements (Pb, Zn, Cd, Cu). Other authors argue that the impact of global anthropogenic pollution on the Antarctic atmosphere is as yet negligible (based on the comparison of the contaminant levels in ancient and modern snow) whereas the observed contamination is localized, and due to the increased human activity on the continent (Boutron and Patterson, 1987).

The composition of the Antarctic atmosphere is affected by the combined interaction of aerosols (mostly H_2SO_4) and soluble gases (HNO_3, HCl, NH3, etc.). Most of the sulfate aerosols (70-80% of all polar aerosols by mass, (Shaw, 1989)) are

produced due to biogenic activity in the oceans (these are sometimes called non sea-salt sulfates, or nss-S) whereas sea-salt sulfate, volcanic activity and anthropogenic emissions are minor sources of SO_4^{2-}. Most of the non sea-salt sulfate compounds are formed by oxidation of DMS (dimethylsulfide $(CH_3)_2S$) produced by algae and phytoplankton in the oceans and bacteria in the marine boundary layer. The DMS in the atmosphere is oxidized via the following path:

$$(CH_3)_2S \rightarrow SO_2 \rightarrow CH_3SO_3H \rightarrow H_2SO_4 \qquad (1)$$

with MSA (methane sulfonic acid CH_3SO_3H) and H_2SO_4 being the main products (Shaw, 1989; Delmas, 1992).

The presence of nitrates in the atmosphere and in the snow/ice is due to the oxidation of various nitrogen gas species (NO_x) coming from various sources including biomass burning, lightning, pollution, oxidation of NH_3, etc. Nitrogen species play an important role in the processes of ozone destruction (Delmas, 1992).

Chlorine, present mostly as HCl, is generally thought to be of marine origin (for example Legrand and Delmas, 1988; Delmas, 1992), although volcanic Cl from major eruptions has been identified in ice cores (Herron, 1982). Chlorine in the Antarctic stratosphere plays an important role in the ozone destruction, yet the sources as well as the budgets for this element (influx and deposition rates) are uncertain. Fluorine has not been measured either in atmospheric samples or in Antarctic ice. Because volcanic emissions (in particular those of Mount Erebus) contain large concentrations of this

element, it is likely that if present, F would be associated with a volcanic source. Herron (1982) measured large concentrations of F in Greenland ice cores that correlate with peaks from volcanic eruptions showing that F like Cl and SO_4^{2-} is deposited in snow/ice and provides a record of volcanic activity. De Angelis and Legrand (1994) also measured F in Greenland snow and confirmed the volcanic source for high concentrations of F. They postulate that the source of background F concentrations present during nonvolcanic periods is probably associated with soil dust and biomass burning, and that some F in recent snow samples may be of anthropogenic origin. Because of the importance of Cl in the composition of the Antarctic atmosphere, the role of Erebus as a major contributor of this element is considered below (section 8.3).

Finally, the most diverse yet poorly known contributors to the Antarctic aerosols are trace elements. Their concentrations in the atmosphere are minute and range from a few ng (10^{-9}g) to fractions of pg (10^{-12}g) per cubic meter of air sampled. Most of the trace elements are present as particulates, although some may be also in gaseous form (for example As and Se compounds). Recently, there has been an increase of general interest in the trace element content of the atmosphere in remote areas, as many workers try to establish a composition of so called "background aerosols" in order to evaluate the extent of global industrial pollution. Many workers have sampled aerosols in remote Antarctica sites in search of "pristine" uncontaminated atmospheric conditions. Samples of snow and ice are also collected from trenches and cores to compare the composition of modern snow with that accumulated in the previous years. Zoller *et al.* (1974) noted

that several elements (Zn, Cu, Sb, Pb, Se and Br) detected in atmospheric samples from Antarctica were anomalously enriched when compared to the composition of the crust. Duce *et al.* (1975) have extended this list to include In, W, Ag, Au, As, Cl, Cd, S, I, Hg, and Pb in Antarctic samples after comparing the enrichment factors calculated relative to both crust and mean oceanic material. Similar measurements conducted by Maenhaut *et al.* (1979) in the polar region, closely approximated those results. The origin of trace elements in the Antarctic atmosphere is often uncertain, and although Erebus has been postulated by some authors as a source of these elements, so far there is no consensus on this subject.

The contribution of crustal and oceanic sources of trace elements in the Antarctic atmosphere can be evaluated by calculating the enrichment factors with reference to each material (i.e., average crustal composition or bulk sea-water). It is impractical, however, to use an "average volcanic gas" composition because of differences in gas composition between volcanoes in different geological settings. This causes a great uncertainty in assessing the global volcanic contribution to the atmosphere. Such estimates, however, can be made for a particular volcano if the composition of its emissions is well known. In Antarctica, there have been many attempts made to connect historic ice samples characterized by high concentrations of trace metals and other anions with particular eruptions such as Krakatoa (1883), Soufriere (1902), Agung (1963), Fuego (1974) etc. (see for example Boutron, 1980; Delmas, 1992; Delmas *et al.*, 1985).

Delmas (1982) has noted that, because of its location, Erebus could have a significant impact on the atmosphere over Antarctica. A Mt. Erebus "signature" was tentatively recognized in snow samples from the Ross Island area and vicinity (Palais *et al.*, 1994) based on Cl and trace element contents. An assessment of the Mt. Erebus contribution was made by Palais *et al.* (1994) based on a statistical approach utilizing the method of source apportionment. Due to the ambiguity of interpretation and general lack of knowledge of the behavior of many of trace elements in the atmosphere, this and many other approaches are still inconclusive.

It has been hypothesized that Mt. Erebus' plume may be the source of some highly enriched elements (for example Zn, Cd, Sb, Se, Br, Au, As, Cd and Hg) in aerosol samples collected over Antarctica (Chuan *et al.,* 1986; Chuan, 1994; Meeker *et al.*, 1991; Zoller *et al.*, 1974). The scarcity of measurements of Erebus emissions in the past made it impossible to evaluate the impact of this volcano fully, and many earlier calculations were based on either fragmentary or erroneous estimates of Erebus emissions (Delmas 1982). Thus, it is not surprising that the impact of Mt. Erebus was generally thought to be negligible and confined to the area in close proximity to the volcano.

After conducting the extensive sampling of Erebus emissions for several years, it is now possible to characterize their chemistry with greater confidence and establish more realistic flux values of major and trace components of the plume. With these in hand, it is possible to re-evaluate the results of other workers' calculations of plume

distribution. The results of these calculations suggest that the Erebus plume may significantly influence the chemistry of the Antarctic atmosphere and may lead to marked changes in snow and ice chemistry.

Of the elements present in the Antarctic atmosphere and snow/ice only a few bear relevance to this discussion: S, Cl, F, and few trace metals. Only the role of sulfur compounds in the Antarctic atmosphere is reasonably well known. Here I try to evaluate the available hypotheses on trace element distributions in Antarctica using Erebus as a possible source for some of the elements. The following questions are addressed: What are the observed levels of elements of interest (S, Cl, F, and trace metals)? Can the amounts of deposited elements be evaluated from the available data? What are the processes governing element distribution in the Antarctic atmosphere, and their deposition in snow/ice? How can these processes be quantified using simple models and the available experimental data?

8.2. Antarctic sulfur budget and Erebus contribution

The sulfate budget for Antarctica has been evaluated by Delmas (1982) using a simple box model in which the Antarctic atmosphere is represented as a rectangular box with a square base $A = 14 \times 10^6$ km^2 ($\sim 3742 \times 3742$ km) and height $h = 5$ km. Delmas (1982) reports typical concentrations of SO_2 in the Antarctic air of 0.1 μg.m^{-3} (equivalent to 0.15 μg.m^{-3} of SO_4^{2-}), and that of SO_4^{2-} of 0.3 μg.m^{-3}. Using the total average SO_4^{2-}

concentration in air C_{air}=0.5 $\mu g.m^{-3}$, and assuming an average wind speed v_{wind}=5 $m.s^{-1}$, and the area of vertical crossection A_c=3742 km×5 km, the estimated total input (T) of S (in form of SO_4^{2-}) can be calculated from

$$T = C_{air}\, v_{wind}\, A_c \qquad (2)$$

to be about 1500 $Gg.yr^{-1}$ of SO_4^{2-} (1 Gg=10^9 g). As shown in section 5.1.2 (Table 5.7), the average SO_2 emissions from Mt. Erebus are 22 $Gg.yr^{-1}$ (range from 6-84×10^9 $g.yr^{-1}$), equivalent to 33 $Gg.yr^{-1}$ (9-126×10^9 $g.yr^{-1}$) of SO_4^{2-}. It follows that Mt. Erebus can contribute about 2.2 (0.6 - 8.4) % of the total sulfur present in the Antarctic atmosphere.

Delmas (1982) also estimated the amount of S deposited in the snow D_d (by dry deposition), assuming homogeneous distribution over the continent using the equation

$$D_d = C_{air}\, v_d\, A \qquad (3)$$

where A is the area of deposition (area of Antarctica ~14 ×10^6 km^2), C_{air} is concentration of an element in air and v_d is the deposition velocity expressed in $cm.s^{-1}$. Using the following values for SO_2: v_d=0.08 $cm.s^{-1}$ and C_{air}=0.1 $\mu g.m^{-3}$, Delmas (1982) obtained 50 $Gg.yr^{-1}$ of SO_4^{2-}. The amount of deposited SO_4^{2-} was estimated from measurements in the Antarctic snow to be 130 $Gg.yr^{-1}$ of SO_4^{2-}. Thus the total amount of SO_4^{2-} deposited in Antarctica is ~180 $Gg.yr^{-1}$ (Delmas, 1982).

If the entire sulfur output of Mount Erebus was distributed homogeneously over Antarctica and deposited in the snow accumulating with the rate of 2-10 $g.cm^{-2}.yr^{-1}$, it could give from 24 to 120 ng SO_4^{2-} per g of snow, from 16-80% of the amount observed

($\sim 0.15\ \mu g.g^{-1}$ of SO_4^{2-}) (Delmas, 1982). This again emphasizes that the contributions of Erebus to the Antarctic atmosphere should not be neglected.

Delmas (1982) also estimates the residence time of sulfate in the Antarctic atmosphere to be about 50 days which is in agreement with the one month estimate of Shaw (1982). This being the case, it is entirely possible for the Erebus plume to be redistributed over much of Antarctica given a suitable pattern of air mass movement. This topic will be expanded in section 8.6.

8.3. Erebus as the source of excess Cl

Chlorine present in the Antarctic atmosphere and in the snow is usually associated with Na as in sea water. If the ratio of Cl/Na in snow is greater than 1.8, the additional Cl (in the form of HCl) is termed "excess". One explanation for the origin of excess Cl is that it is produced during the reaction between sea-salt and biogenic H_2SO_4

$$2NaCl + H_2SO_4 \rightarrow Na_2SO_4 + 2HCl \qquad (4)$$

(Legrand and Delmas, 1988). The excess Cl is usually found in snow accumulated during summer months (Figure 8.1, from Legrand and Delmas, 1988).

Because of the high halogen content of Mt. Erebus emissions, it has been suggested (Kyle *et al.*, 1990) that the volcanic activity of Mt. Erebus can be a source of excess Cl detected during summer months in snow samples from the Antarctic Plateau.

The results of previous calculations should, however, be disregarded due to the incorrect Cl emission rates for Erebus, and the calculations are repeated here with the new data. As in the calculations for S described above, a homogeneous distribution of Cl over Antarctica is assumed.

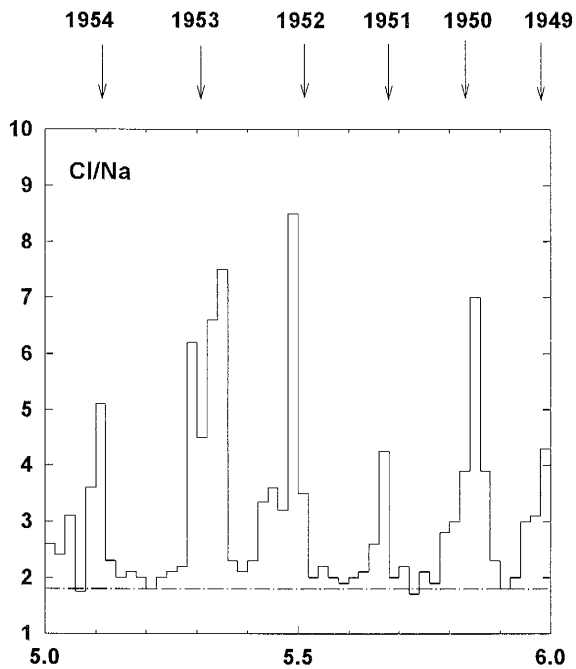

Fig. 8.1. Weight ratio of Cl/Na in snow samples from the South Pole showing correlation of high Cl concentration (events with "excess Cl") with austral summer. From Legrand and Delmas (1988).

The average input of Cl from Erebus to Antarctica can be calculated from the average Cl/S ratio of 1.41 ± 1.09 (0.39-6.71) and the average SO_2 output of 22 (5.5-84) $Gg.yr^{-1}$ which gives the amount of Cl emitted as 15.5 (1.1-282) $Gg.yr^{-1}$. This value distributed evenly over 14×10^6 km^2 gives the amount of chlorine deposited in snow to be about 1.1 (0.08-20) $kg.km^{-2}.yr^{-1}$, a value remarkably close to that measured by Legrand and Delmas (1988) in the snow (1-2 $kg.km^{-2}.yr^{-1}$). This supports the idea that excess Cl could originate from Mount Erebus. The average value of 1.1 $kg.km^{-2}.yr^{-1}$ can be expressed as the expected concentration of Cl in the snow by dividing it by the

average snow accumulation rate of 10 $g.cm^{-2}.yr^{-1}$. The resulting average concentration of Cl in snow is therefore ~11 (0.8-200) $ng.g^{-1}$ or 0.31 (0.02-5.6) $\mu eq.L^{-1}$.

If Erebus is the source of the excess Cl, then Cl should be accompanied by an enhanced F content in the snow, unless the two gases are fractionated in the atmosphere. Thus, analyzing the F content of snow could help to identify the source of the excess Cl. From the average F/S value of 0.69 ± 0.49 (0.20-2.59) and average SO_2 output, the range of F output is 7.6 (0.6-108.8) $Gg.yr^{-1}$. By similar reasoning to that presented above this gives about 0.54 (0.04-7.8) $kg.km^{-2}.yr^{-1}$ of F deposited in the snow. Assuming the snow accumulation rates of 10 $g.cm^{-2}.yr^{-1}$ (Delmas *et al.*, 1985) for the central Antarctica, we estimate the amount of F in the snow as about 5.4 (0.4-78) $ng.g^{-1}$. Unfortunately, we are not aware of any published analyses of F on the Central Antarctic snow samples. However, the published analyses do show a deficiency in anions of 0.8 $\mu eq.L^{-1}$ when the ionic mass balance is calculated (Delmas *et al.*, 1982). Our calculated value for F is 0.3 (0.02-4.1) $\mu eq.L^{-1}$ and is within the uncertainty of the published ionic mass balance.

8.4. Estimating deposition of Cl and F in Antarctica

The data available in the literature can be used to estimate several parameters regarding Cl and F distribution in the Antarctic atmosphere. Using the method described above I estimated the total input of Cl to the Antarctic atmosphere from equation 2. The Cl concentration in air $C_{air} = 10$ $ng.m^{-3}$ (Duce *et al.* 1973) was used. This concentration

is the best available estimate of total Cl in the Antarctic atmosphere and represents both particulate and gas phase. Thus, it is higher than the estimate of Maenhaut *et al.* (1979) who sampled only atmospheric particulates.

The amount of Cl dry-deposited in snow D_d can be calculated from the following expression:

$$D_d = C_{snow}\, k_{snow}\, A \qquad (5)$$

where C_{snow} is the concentration of an element in snow, k_{snow} is the snow accumulation rate (in $g.cm^{-2}.yr^{-1}$) and A is the area of the Antarctic continent (14×10^6 km^2). Using a concentration of Cl in snow equal to 42 $ng.g^{-1}$ (Delmas *et al.*, 1982) and the snow accumulation rate in the range 2-10 $g.cm^{-2}.yr^{-1}$, the calculated amount of Cl deposited is 12-59 $Gg.yr^{-1}$. The upper limit is much higher than the total input of Cl in Antarctica, yet not unrealistically high considering that it is proportional to the snow accumulation rate which in some areas of Antarctica can be higher than 10 $g.cm^{-2}.yr^{-1}$. I estimate a total input of Cl into the Antarctic atmosphere of $\sim$30 $Gg.yr^{-1}$. This probably underestimates the actual value because emissions of Cl from Erebus to the Antarctic atmosphere (15.5 $Gg.yr^{-1}$) is over half of the total amount, thus showing that contribution of Erebus to the total Cl budget is very significant.

The fraction of Cl present in the snow coming from sea-spray can be subtracted from the total Cl concentration in snow by assuming a Cl/Na ratio of 1.8 (that of seawater). From the Na concentration in snow of $\sim$ 12 $ng.g^{-1}$ (Delmas *et al.*, 1982), Cl_{sea} =

22 $ng.g^{-1}$, which leaves 20 $ng.g^{-1}$ of Cl deposited as HCl (47.6% of total Cl). It follows that the amount of "excess" Cl deposited is 5.7-28 $Gg.yr^{-1}$. The lower value is close to the average Cl emissions from Mt. Erebus (15.5 $Gg.yr^{-1}$), if the higher value is used then Erebus can account for ~25% of Cl deposited assuming no loss during transport.

I can now use equation 3 to estimate the deposition velocity of Cl on snow

$$v_d = \frac{D_d}{C_{air} A} \tag{6}$$

using Cl concentration in air C_{air}= 10 $ng.m^{-3}$ (Duce *et al.*, 1973). Calculated Cl deposition velocities range from 0.27 to 1.33 $cm.s^{-1}$. These are much lower than the experimental measurements of Dasch and Cadle (1986, after Davidson, 1989) who obtained values of 4.3±6.1 and 5.1±4.0 $cm.s^{-1}$ from measured Cl^- deposition velocities on surface snow and on a snow/water mixture, respectively. It is not unlikely that the low values calculated here are closer to reality in Antarctica.

Deposition velocities obtained above the can now be used to calculate the residence time T_R of Cl in the atmosphere:

$$T_R = \frac{C_{air} V_{atm}}{D_d} = \frac{C_{air} A\ h}{D_d} \tag{7}$$

where h can be assumed to be equal to 5 km (after Delmas, 1982). Eq. 7 simplifies to:

$$T_R = \frac{h}{v_d} \tag{8}$$

from which residence times of Cl in the Antarctic atmosphere are found to be 4.4 - 21

days. It is generally thought that volatile Cl injected into the troposphere by volcanoes has a short lifetime and is quickly removed by wet deposition (Tabazadeh and Turco, 1993) but to my best knowledge, no actual values for the residence time of Cl are quoted. Duce *et al.* (1973) stated that gaseous Br may have a residence time of 2-3 weeks. Because it is likely that gaseous Cl behaves similarly, the value calculated above seems reasonable. The long residence time of Cl supports the arguments made by Zreda-Gostynska *et al.* (1993) that the residence time of Cl in the Antarctic atmosphere is longer than that observed in the temperate climate zones.

Similar reasoning can be used to estimate the depositional velocities and residence time of F in Antarctica. If I assume that all F present in Antarctica is emitted from Erebus, then the dry deposition (D_d) is 7.6 $Gg.yr^{-1}$. Equation 6 uses the concentration of F in air which is unknown. The comparison of Erebus output and the total flux of Cl into the Antarctic atmosphere shows that Erebus could produce ~50% (4 - 100%) of Cl present in the atmosphere. In the best case 50-100% of all Cl measured in the air would be from Erebus, which gives 5-10 $ng.m^{-3}$ if the Cl content of air by Duce *et al.* (1973) is used. The average F/Cl ratio in Erebus gas is ~0.5, so if no fractionation occurs between the two halogens, F concentration in the air could measure between 2.5 and 5 $ng.m^{-3}$. Substituting these values into equation 6, I obtained deposition velocities between 0.34 and 0.69 $cm.s^{-1}$. Both values are similar to that obtained for Cl, which was expected. The calculated residence times of F (from equation 9) range between 17-34 days (Table 8.1). Finally, from estimated concentration of F in air and equation 2, the

total F input in the Antarctic atmosphere could range from 7 to 14 $Gg.yr^{-1}$, in agreement with previous assumptions that Erebus is probably the only source of this element in Antarctica.

In view of the above calculations, other aspects of the high halogen content of the Erebus plume should be considered. Could Erebus emissions play an important role in the process of ozone destruction over Antarctica? It seems that the average amount of HCl emitted by Erebus is too small to significantly affect the chemistry of the stratosphere, and the calculations presented above support the idea that most of the HCl emitted from Erebus remains in the troposphere. Unless a large part of the HCl is emitted directly into the stratosphere, its vertical transport is inhibited by the cold trap at the bottom of stratosphere, where it is scavenged by condensing water vapor (Tabazadeh and Turco, 1993; Pinto *et al.*, 1989). It is possible that during austral winter the Erebus plume is discharging directly into the stratosphere, however no evidence exists to support this surmise. If such a process exists, one should consider not only the reactions involving HCl present in Erebus plume but also F and S compounds, which have been hitherto neglected.

Table 8.1. Estimated deposition rates of sulfur, chlorine and fluorine in Antarctica.

	SO_4^{2-}	Cl	F
Total flux into Antarctica ($Gg.yr^{-1}$)	1500[a]	~30[b]	~7-14[b]
Estimated amount deposited ($Gg.yr^{-1}$)	180[a]	12-59	~7.6[b]
Average flux from Erebus ($Gg.yr^{-1}$)	33 (8.3-126)[b]	15.5 (1.1-282)[b]	7.6 (0.6-109)[b]
Observed concentration in snow ($ng.g^{-1}$)	~150[a] 70[c]	42[c]	n.d.
Estimated concentration in snow ($ng.g^{-1}$) from Erebus plume	24-118	11-55	5.4-27
Deposition velocity on snow ($cm\ s^{-1}$)	0.08 (as SO_2)[a] ~0.1(as SO_4^{2-})[a,c]	0.27-1.33[b]	0.34-0.69[b]
Residence time in atmosphere (days)	30-50[a,e]	4.4-21[b]	17-34[b]

n.d. - not determined
Sources: [a] Delmas (1982); [b] This work; [c] Delmas *et al.* (1982) at South Pole, [d] Davidson (1989). [e] Shaw (1982)

8.5. Trace element content of atmospheric aerosols and snow vs. Erebus output

Assuming homogeneous distribution of the plume (compare sections 8.2 and 8.3), I have calculated average concentrations of trace elements in the snow (Table 8.2). The average emissions of each element and S were used, calculated from data collected in 1986, 1988, 1989, and 1991. The average emissions for Au use only data from 1986, 1988, and 1989 because 1991 results are unreasonably high, possibly due to contamination. I have assumed the conservative value for the accumulation rate of snow of 10 $g.cm^{-2}.yr^{-1}$, probably representing the upper limit in the South Pole area where it can vary from 2-10 $g.cm^{-2}.yr^{-1}$ (Delmas *et al.*, 1985). The areas closer to the coasts and at lower elevations usually receive higher precipitation and the snow accumulation rates

could be 30-60 $g.cm^{-2}.yr^{-1}$ (Delmas *et al.*, 1985).

In Table 8.2, I compare estimated concentrations of several trace elements with the available data on the trace element content of the Antarctic snow and ice. It should be noted that of the major anions found in the snow only SO_4^{2-} and Cl are represented. The earlier work of Boutron and Lorius (1979), Boutron (1980), and Delmas (1982) contrasts with the new estimates of Wolff and Peel (1985) and Palais *et al.* (1994). Wolff and Peel (1985) questioned the earlier analyses of snow and ice collected in remote Antarctic sites, and attributed the high concentrations of many metals to the contamination during sampling. The new values, all markedly lower than earlier estimates, are currently considered to be the best values of trace element concentrations in the uncontaminated Antarctic snow. It should be noted that the concentrations of Cd, Cu, and Zn are for samples from the Antarctic Peninsula, while the other concentrations are for samples from West Antarctica; only S concentrations have actually been measured at the South Pole.

If my estimate is correct, the Erebus plume could easily account for the concentrations of such elements as Cu, Zn, Cd, V, As, and Au for which the predicted concentrations are close to those measured in snow samples. Thus, the values reported by Boutron and Lorius (1979) and Boutron (1980) do not necessarily have to be a result of contamination. Predicted concentrations of less volatile elements (Al, Ca, Fe, Mn and La) cannot account for the concentrations observed in the snow samples.

Table 8.2. Estimated concentrations of Erebus plume components in the Antarctic snow calculated using the model explained in text, and comparison with available measurements.

	Average emissions $Gg.yr^{-1}$	Estimated concentrations in snow for Erebus [1] (in $pg.g^{-1}$)		Measured South Pole concentrations (in $pg.g^{-1}$)			
		$10g.cm^{-2}$	$2g.cm^{-2}$	Palais *et al.* (1993)	Boutron and Lorius (1979)	Wolff and Peel (1985)	Delmas *et al.* (1982)
F	7.6	5420	27099				
Na	1.1	755	3775	4733	7700		12000
Al	0.6	440	2201	1310	1070	1000	
SO_4	33.0	23571	117857	40680		63333	70000
Cl	15.5	11092	55462	35500			42000
K	0.9	669	3343		370		
Ca	0.7	535	2675	1657	510		
Sc	3.7e-05	0.03	0.13				
Ti	1.4e-01	103	516				
V	3.7e-03	3	13	2.7			
Cr	1.8e-02	13	63				
Mn	8.7e-03	6	31	47	18		
Fe	2.8e-01	202	1009	4000	760		
Co	4.8e-03	3	17	1067			
Ni	5.9e-03	4	21				
Cu	8.6e-02	62	309		47	1.8	
Zn	1.4e-01	97	483		6.8	3.3	
As	0.015	11	53	11			
Se	2.0e-03	1	7	337			
Br	3.1e-02	22	109	663			
Rb	5.9e-03	4.2	21				
Mo	7.4e-03	5.3	26				
Cd	5.9e-03	4	21		3.8	0.26	
In	1.6e-03	1.2	5.8				
Sb	7.7e-04	0.5	2.7				
Cs	2.5e-04	0.2	0.9				
La	6.7e-04	0.5	2.4	3.3			
Ce	1.8e-03	1.3	6.4				
Sm	1.0e-04	0.07	0.36				
Eu	7.1e-05	0.05	0.25				
Yb	7.3e-04	0.52	2.6				
Hf	3.9e-04	0.3	1.4				
Ta	2.7e-04	0.2	1.0				
W	6.2e-03	4.4	22				
Au	8.1e-05	0.06	0.29				

[1] Estimated using rate of snow accumulation 2-10 $g.cm^{-2}$ (see text)

These elements are usually associated with crustal weathering, and are transported and deposited as dust.

Further studies of trace elements in snow and ice could be helpful in confirming the hypothesis that Erebus may be important in influencing the chemistry of the Antarctic atmosphere. Especially helpful would be more data on other trace elements, such as arsenic and indium, both of which are enriched in the Erebus plume. The continuing progress in analytical methods and improvement in sampling techniques allows for better determinations and lower detection limits, unavailable several years ago. By combining the trace element analysis with that of more abundant anions (Cl^-, SO_4^{2-}, F^-) it should be possible to trace the patterns of Erebus plume dispersal and resolve the question of the source of some contaminants often detected in snow samples.

The average composition of aerosols over South Pole can be compared with that of the Erebus plume by calculating enrichment factors using an average chemical composition of the crust as the reference material. As shown on Figure 8.2, the EF (Sc) calculated for the Erebus plume are higher from those calculated for aerosol samples for almost all elements except Br and Se, which probably are of marine origin. The enrichment factor patterns of the Erebus plume can be compared to aerosols sampled in other areas on the Antarctic continent (Figure 8.3).

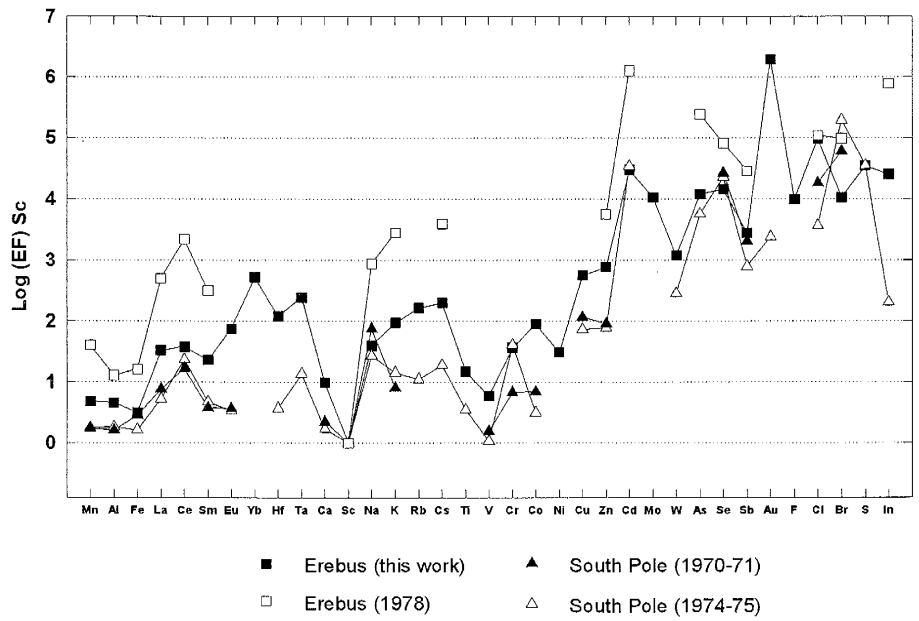

Fig. 8.2. Comparison of EF_{crust}(Sc) of Erebus aerosols with those sampled at South Pole. Solid squares are averages of Erebus gas collected in 1986-91 (this work), open squares are 1978 samples (Germani, 1980). South Pole 1974-75 data (open triangles) are from Maenhaut et al., 1979), and 1970-71 data (solid triangles) from Zoller et al., 1974, except for Cl which is from Duce et al., 1975.

Artaxo *et al.* (1992) measured trace elements in aerosols sampled on the Antarctic Peninsula. When the EFs_{crust}(Al) are compared to the Erebus plume and to aerosols from the South Pole they show more enrichment in Ca, Cr, Mn (regarded as an effect of crustal weathering) and in Na, Cl, Se, and Br associated with sea-spray. Unfortunately, there are no data on elements such as As, In, Au which could be used as markers of the Erebus plume. Therefore, it is not possible to recognize the Erebus influence on aerosol composition in this region. Guerzoni *et al.* (1992) sampled aerosols in the Terra Nova Bay (Ross Sea area).

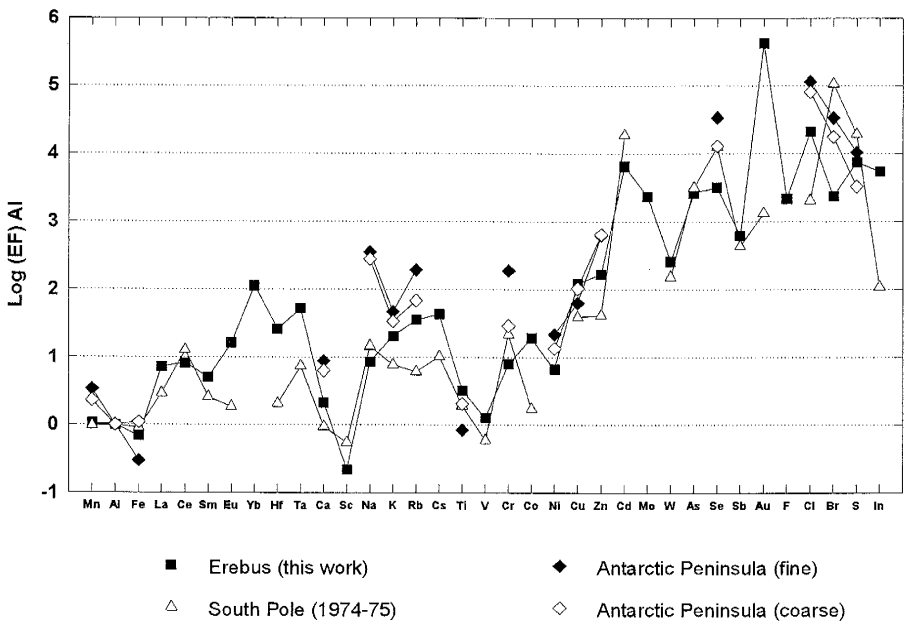

Fig. 8.3. Comparison of $EF_{crust}(Al)$ of average Erebus gas (solid squares) with the composition of aerosols sampled at South Pole (open triangles) (Maenhaut et al., 1979) and two sizes of aerosols collected at Antarctic Peninsula (solid and open diamonds) (Artaxo et al., 1992).

The calculated EF_{crust} show very few enriched elements (Na, Cd, Pb). The enrichment factors of Cd are too low to suggest Erebus as a source for this element. Because Erebus lies 350 km to the South from the Terra Nova Bay, the low EFs of Cd could be an indirect indication that the Erebus plume is transported toward higher latitudes rather than to the North. As in the previously described case, measurements for other elements are not available for this location making the problem unresolved.

8.6. Question of plume transport and removal of halogens

The dispersal directions of the Erebus plume are unknown. Although from the evidence presented above it seems that Cl and F could provide a good tracer of the Erebus plume, the general scarcity of Cl and F data in both the snow/ice and the atmospheric aerosols, makes it impossible to evaluate the extent of plume transport, and possible changes in its halogen content. From the preliminary estimates of the halogens residence times one can surmise that both Cl and F can remain in the atmosphere for days to weeks. One can also assume that dry deposition would be the most likely removal process of halogens in Antarctica, because their removal via wet deposition (which includes scavenging by forming snow/ice crystals) is precluded by the extreme aridity of air and absence of ice crystals (Tabazadeh and Turco, 1993). Therefore, given a favorable pattern of air-mass movement, the Erebus plume could be dispersed throughout the Antarctic atmosphere.

How could the Erebus plume reach the interior of the Antarctic continent? The circulation of air masses over Antarctica varies between summer and winter seasons. Analysis of monthly deviations from the mean annual pressure over the continent indicates that there is a net inflow of air into Antarctica during summer (October through January) and that during winter (from February through September) the air is moving away from the continent (Schwerdtfeger, 1970, after Mroz *et al.*, 1989). In winter this movement of air masses is due to the presence of the circumpolar vortex which

disappears in spring. Additionally, there is also evidence for the existence of meridional transport of air. In the lower atmosphere (corresponding to pressure > 600 mbar) air masses are moving outward from the continent; this movement is balanced by inflow from the oceans at higher altitudes (< 600 mbar). At the center of the continent the air masses sink delivering the aerosols from the upper troposphere and lower stratosphere. Partly due to the establishment of the polar vortex, the meridional pattern weakens during the winter and seems to be stronger during summer months, as reflected in the composition of summer aerosols which show enrichment in crustal dust, sea salt, volcanic emissions and radionuclides from the stratosphere (Mroz *et al.,* 1989). Strong winter storms can occasionally penetrate the circumpolar vortex and transport aerosols toward the inside of the continent, but such events are rare. The atmospheric tracer experiments (Mroz *et al.*, 1989) (Figure 8.4, from Mroz *et al.*, 1989) and the study of tropospheric flow patterns by Harris (1992) indicate the presence of rapid (lasting few days) poleward movement of air masses during the antarctic summer which strengthens the hypothesis that the Erebus plume can be transported inland. It also shows some evidence for vertical mixing of air masses on the edge of the continent, again a condition favorable for the plume because it allows for longe-range transport.

The problem of halogens removal from the plume is at yet impossible to resolve due to the scarcity of Cl and total lack of F measurements along the axes of plume dispersal. Data of Palais *et al.* (1994) may indicate that the removal is significant when Cl concentrations in the snow are compared in samples collected on Ross Island at

various distances from Erebus summit. These show a maximum at ~5 km at Fang Glacier, about 1.5 times higher then in sample collected at 2 km from the summit, and then decrease further with distance. This distribution of Cl concentrations in the snow may however be also a result of plume trailing over the slopes of Erebus. It can be roughly predicted from the solution of a dispersion equation, which predicts that that concentration of a contaminant in the aerial plume when measured at ground level do not show appreciable values until at certain distance from the source (Pasquill, 1974; Pasquill and Smith, 1983; Finlayson-Pitts and Pitts, 1986; Stern *et al.*, 1984).

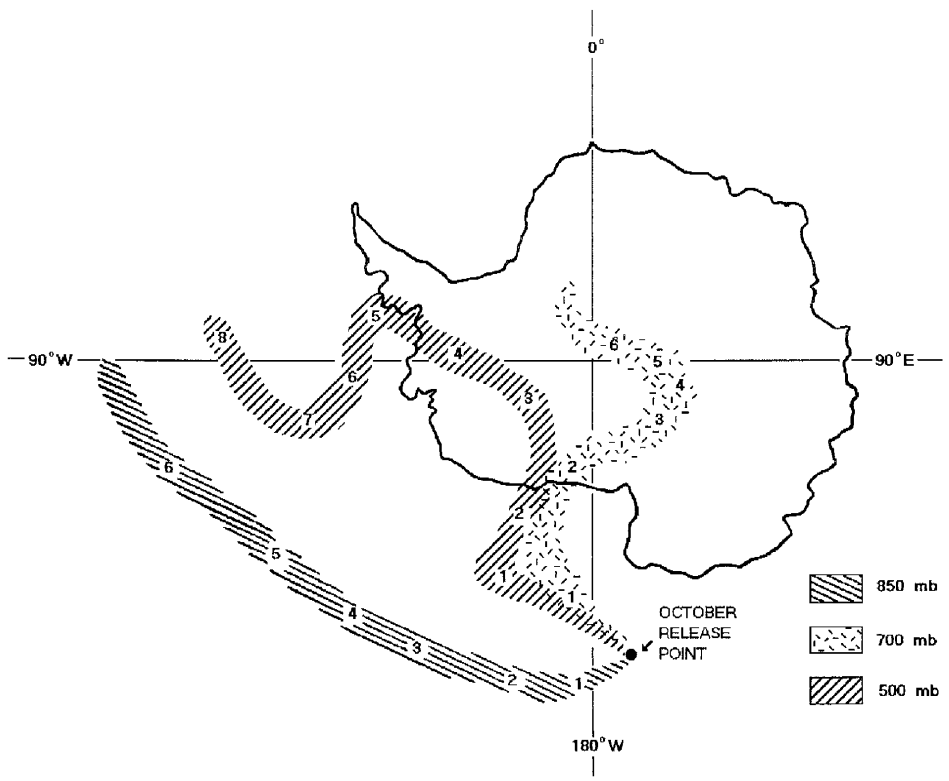

Fig. 8.4. Expected air mass trajectories following tracer release. Patterns marks the trajectory at different altitude; numbers indicate time (in days) elapsed since the release (from Mroz et al. , 1989).

The exact position of this maximum depends on the dispersivity parameters of the plume that are functions of wind speed, roughness of the surface etc., and can only be estimated for Erebus.

The above model could be further refined by taking the fact that the plume is not likely to be distributed evenly but its concentration will decrease exponentially away from the source. Thus, this process of Erebus requires further studies, perhaps including models utilizing advection-dispersion equation.

9. CONCLUSIONS

The composition of volcanic gases studied at Mt. Erebus is dominated by three volatile species: Cl, S, and F (the two major plume components, H_2O and CO_2, were not analyzed). During the study period between December 1986 and January 1991, the Cl content of the gas did not change on the average, however some fluctuations were observed in the relative proportions of S and F in the gas. These changes may be interpreted as an indication of temporal changes in the volatile content of Erebus magma or of the existence of heterogeneity in the magma chamber. Two models are proposed to account for this heterogeneity: (1) injection of fresh magma into the system, and (2) zonation of the magma chamber. The heterogeneity is thought to affect only the volatile content of the melt, and not its total composition, because no change in the major and trace element composition of Erebus magma has yet been observed. The freshly injected magma is likely to be rich in volatiles (CO_2 and H_2O), and it is hypothesized that their presence may affect the partitioning of halogens and sulfur into a vapor phase, resulting in varying amounts of these three species in the gas. Unfortunately, no experimental data are available to confirm this theory.

The periodicity observed in the COSPEC record of SO_2 emissions may be related to the movement of magma in the conduit and to the convection of the lake. Similarly, the changes in sulfur and halogens content of gas (as indicated by element-to-S ratio) observed on the short-time scale, are probably manifestation of the same process.

During magma upwelling in the conduit, the three volatiles (Cl, F and S) start exsolving at progressively shallower depths. The high Cl/S and F/S ratio of the gas signifies a fresh portion of magma approaching the surface, whereas the low Cl/S ratio indicates shallow convection during which mostly S is being exsolved from the melt. This interpretation of changes in element-to-S ratios is consistent with the results of a simple model of the Erebus degassing system.

The enrichment factors provide a good source of information on the Erebus plume composition. There is very little difference in the enrichment factor patterns between years, suggesting no major compositional change in the magmatic source of gas. The higher enrichment of Al, Fe, and REEs in 1991 can be explained by higher ash content of the plume. Due to the importance of Cl in the metal transport in the Erebus plume, the almost constant Cl content of the gas observed in 1986-1991 is probably responsible for keeping the average enrichment factors of metals fairly constant. This is especially apparent for elements volatilized predominantly as chlorides such as alkali metals, Cd and In. Several elements (Cr, Co, Zn, Cu, Mo, W and Au) display more variation between years. Because many of these elements are transported as other compounds (oxyacids, sulfides or in elemental state) their abundance in the plume is affected by factors other than Cl availability, which may be the reason for their variable enrichment in the plume.

The short-term variation in elemental concentrations in the gas during the sampling periods, similar to that displayed by halogens and sulfur, also manifests itself with trace elements. For some elements these changes parallel those of Cl, F, and S (alkali metals, In, As, Se, and Sb), but there are also elements (V, Cr, Co, Cu, Zn, Mo, W, and Au) which do not show such correlation. As in case of the short-term variability in F, Cl, and S content of the gas, it is likely that the changes in EF observed in samples are due to magma movement in the conduit, the high values being associated with upward fluxes of fresh magma which provided high-temperature gas rich in trace elements. The reason for the lack of correlation between the enrichment factors of V, Cr, Co, Cu, Zn, Mo, W, Au with S, halogens and other elements is unclear. The lack of correlation between elements depleted (or poorly enriched) in the plume and halogens or sulfur is probably due to the fact that these elements are associated with the ash present in the plume. For other elements, it could be due to changes in partitioning of these elements between melt and vapor phase caused by the loss of Cl or other substance.

Although not supported by field observations other than the enlarging of the lava lake, the increase in the metal concentration in the Erebus plume suggests an important change in the degassing behavior of Erebus, possibly due to increased convection rates in the magma chamber or inflow of a fresh melt from deeper part of the magmatic system. Also, the slightly higher ash content of samples collected in 1991 may signify a change in the eruptive style of Erebus.

The salt deposits found on the summit area of Mount Erebus appear to form by complex interaction between the acidic plume and rocks exposed in the crater and on the slopes of the volcano. Unlike incrustations often found surrounding the high temperature vent, they are not composed entirely of sublimates. However, there is good evidence that their major and trace element content reflect the composition of gas emitted from Erebus. Salts were identified as mostly fluorides, chlorides and sulfates, which is consistent with the high halogen content of the gas. The trace elements enriched in the salts (As, Zn, Cd, Hg, In) correspond very well to the trace elements abundant in the plume. It can be concluded that the low temperature salts from the volcanic areas contain a good record of the gas emitted. This information may be useful for the reconstruction of past gas compositions of inactive vents having well preserved salt deposits. The method, however, may be very limited in more humid environments because salt deposits are prone to dissolution and alteration.

The average emissions of halogens, SO_2 and trace elements from Erebus volcano show that it is an important component of the Antarctic environment. The results of a simple model presented above show that Erebus could account for observed concentrations of many elements found in snow and air samples in Antarctica, and it could significantly affect the chemistry of the Antarctic atmosphere if the distribution of the Erebus plume is indeed as wide as assumed. Because of the simplicity of the approach, which does not account for the exact direction of plume dispersal, its dilution, nor for different removal rates of elements, the results should be interpreted with caution

and reevaluated when more measurements become available. The need for more studies concerning this aspect of Erebus emissions is obvious. The fate of the plume and its components must be better known if the predictions made in this study are to be confirmed. Secondly, there is need for experimental work on the removal precesses of halogens and trace metals under conditions applicable to the Antarctic atmosphere.

Is Erebus really a significant contributor to the "excess" Cl found in the antarctic ice and snow? The Cl and S contents of the snow or ice samples alone are often insufficient to distinguish between the volcanic and oceanic source. Future studies of Antarctic aerosols and snow should include analyses of F, especially if the volcanic origin of the excess Cl is to be proven. To our knowledge, no such data presently exist. The distinctly high F emission rates by Erebus very likely constitute a unique source of this element in Antarctica, and its potential as a tracer should be examined. Also, many trace elements present in the Erebus plume (In, Au, As, Zn, Cd) may potentially serve as tracers of plume dispersal.

REFERENCES

Anderson, A. T., Some basaltic and andesitic gases, *Rev. Geophys. Space Physics*, *13*, 37-55, 1975.

Andres, R. J., Sulfur dioxide emission from the Episode 48A East Rift Zone eruption of Kilauea Volcano, Hawaii, *Bull. Volcanol.*, *52*, 113-117, 1989.

Artaxo, P., M. L. C. Rabello, W. Maenhaut, and R. Van Grieken, Trace elements and individual particle analysis of atmospheric aerosols from the Antarctic peninsula, *Tellus*, *44*, 318-334, 1992.

Baldwin, B., J. B. Pollack, A. Summers, O. B. Toon, C. Sagan, and W. Van Camp, Stratospheric aerosols and climatic change, *Nature*, *263*, 551-555, 1976.

Bernard, A., and F. Le Guern, Condensation of volatile elements in high-temperature gases of Mount St. Helens, *J. Volcanol. Geotherm. Res.*, *28*, 91-105, 1986.

Bigelow, E. A., *Techniques of volatile analysis in volcanic glass by quadrupole mass spectrometry and application to Mount Erebus, Antarctica*, M.S. Thesis, New Mexico Institute of Mining and Technology, Socorro, NM, 1985.

Boutron, C., Respective influence of global pollution and volcanic eruptions on the past variations of the trace metals content of Antarctic snows since 1880's, *J. Geophys. Res.*, *85*, 7426-7432, 1980.

Boutron, C., and C. Lorius, Trace metals in Antarctic snow since 1914, *Nature*, *277*, 551-554, 1979.

Boutron, C. F., and C. C. Patterson, The occurrence of lead in Antarctic recent snow, firn deposited over the last two centuries and prehistoric ice, *Geochim. Cosmochim. Acta*, *47*, 1355-1368, 1983.

Boutron, C. F., and C. C. Patterson, Relative levels of natural and anthropogenic lead in recent Antarctic snow, *J. Geophys. Res.*, *92*, 8454-8464, 1987.

Buat-Menard, P., and M. Arnold, The heavy metal chemistry of atmospheric particulate matter emitted by Mount Etna volcano, *Geophys. Res. Lett.*, *5*, 245-248, 1978.

Burnham, C. W., Water and magmas; a mixing model, *Geochim. Cosmochim. Acta*, *39*, 1077-1084, 1975.

Burnham, C. W., The importance of volatile constituents, in *The Evolution of Igneous Rocks, Fiftieth Anniversary Perspective*, edited by H. S. Yoder Jr., Princeton University Press, Princeton, 1979a.

Burnham, C. W., Magmas and Hydrothermal Fluids, in *Geochemistry of hydrothermal ore deposits*, 2nd ed., edited by H. L. Barnes, pp. 71-136, John Wiley & Sons, New York, 1979b.

Caldwell, D. A., and P. R. Kyle, Mineralogy and geochemistry of ejecta erupted from Mount Erebus, Antarctica between 1972 and 1986, in *Volcanological Studies of Mount Erebus. Antarctic Research Volume*, edited by P. R. Kyle, AGU, Washington, D.C., (in press), 1994.

Caldwell, D. A., P. R. Kyle, and W. C. McIntosh, Composition of 1972-1986 volcanic ejecta from Mt. Erebus, Antarctica: Implications for the 1984 eruptive activity, in *Continetal Magmatism Abstracts, 1989 Iavcei Meeting, Santa Fe, NM*, p. 36, NM Bureau of Mines & Mineral Resources, Bulletin 131, Socorro, NM, 1989.

Chuan, R. L., Rapid measurement of particulate size distribution in the atmosphere, in *Fine Particles: Aerosol Generation, Meassurement, Sampling and Analysis*, edited by B. Y. H. Liu, pp. 763-775, Academic Press, New York, 1975.

Chuan, R. L., Dispersal of volcanic-derived particles from Mount Erebus in the Antarctic atmosphere, in *Volcanological Studies of Mount Erebus. Antarctic Research Volume,* edited by P. R. Kyle, AGU, Washington, D.C., (in press), 1994.

Chuan, R. L., J. M. Palais, W. I. Rose, and P. R. Kyle, Fluxes, size, morphology and composition of particles in the Mt. Erebus volcanic plume, December 1983, *J. Atmos. Chem.*, *4*, 467-477, 1986.

Cicerone, R. J., Halogens in the atmosphere, *Rev. Geophys.*, *19*, 123-129, 1981.

Crowe, B. M., D. L. Finnegan, W. H. Zoller, and W. Boynton V, Trace element geochemistry of volcanic gases and particles from 1983-1984 eruptive episodes of Kilauea volcano, *J.Geophys. Res.*, *92*, 13708-13714, 1987.

Dasch, J. M., and S. H. Cadle, Dry deposition to snow in urban area, *Water Air Soil Poll.*, *29*, 297-308, 1986.

Davidson, C. I., Mechanism of wet and dry deposition of atmospheric contaminants to snow surfaces, in *The Environmetal Record in Glaciers and Ice Sheets*, edited by H. Oeschger, and C. C. Langway Jr., pp. 29-51, John Wiley & Sons, Chichester, 1989.

Decker, R. W., and B. B. Decker (eds.), *Mountains of Fire: the nature of volcanoes*, Cambridge University Press,, 1991.

Delmas, R. J., Antarctic sulphate budget, *Nature*, *299*, 677-678, 1982.

Delmas, R. J., Environmental information from ice cores, *Rev. Geophys.*, *30*, 1-21, 1992.

Delmas, R., R. Briat, and M. Legrand, Chemistry of South Polar snow, *J. Geophys. Res.*, *87*, 4314-4318, 1982.

Delmas, R. J., M. Legrand, A. J. Aristarain, and F. Zanolini, Volcanic deposits in Antarctic snow and ice, *J. Geophys. Res.*, *90*, 12901-12920, 1985.

Devine, J. D., H. Sigurdsson, A. N. Davis, and S. Self, Estimates of sulfur and chlorine yield to the atmosphere from volcanic eruptions and potential climatic effects, *J. Geophys. Res.*, *89*, 6309-6325, 1984.

Dibble, R. R., J. Kienle, P. R. Kyle, and K. Shibuya, Geophysical studies of Erebus volcano, Antarctica, from 1974 December to 1982 January, *N.Z. Jour. Geol. Geophys.*, *27*, 425-455, 1984.

Dibble, R. R., S. I. Barrett, K. Kaminuma, S. Miura, J. Kienle, C. A. Rowe, P. R. Kyle, and W. C. McIntosh, Time comparisons between video and seismic signals from explosions in the lava lake of Erebus Volcano, Antarctica, *Bull. Disas. Prev. Res. Inst. Kyoto Univ.*, *27*, 425-455, 1988.

Dick, A. L., Concentrations and sources of metals in the Antarctic Peninsula aerosol, *Geochim. Cosmochim. Acta*, *55*, 1827-1836, 1991.

Duce, R. A., W. H. Zoller, and J. L. Moyers, Particulate and gaseous halogens in the Antarctic atmosphere, *J. Geophys. Res.*, *78*, 7802-7811, 1973.

Duce, R. A., G. L. Hoffman, and W. H. Zoller, Atmospheric trace metal at remote northern and southern hemisphere sites: pollution or natural?, *Science, 187*, 59-61, 1975.

Finlayson-Pitts, B. J., and J. N. Pitts, Jr., *Atmospheric Chemistry: Fundamentals and Experimental Techniques*, J. Wiley & Sons, New York, 1986.

Finnegan, D. L., *The chemistry of trace elements and acidic species in fumarolic emissions, Ph.D. thesis*, Ph.D. Dissertation, University of Maryland, 1984.

Finnegan, D., J. P. Kotra, D. M. Herman, and W. H. Zoller, The use of ^{7}LiOH- impregnated filters for the collection of acidic gasees and analysis by instrumental neutron activation analysis, *Bull. Volcanol.*, *51*, 83-87, 1989.

Fisher, R. V., and H.-U. Schmincke (eds.), *Pyroclastic Rocks*, Springer-Verlag, Berlin, 1984.

Friend, J. P., Natural Chlorine and Fluorine in the Atmosphere, Water and Precipitation, in *Scientific Assessment of Stratospheric Ozone: 1989. World Meteorological Organization Global Ozone Research and Monitoring Project-Report No. 20*, vol. II, pp. 432-448,,, 1989.

Gemmell, J. B., Geochemistry of metallic trace elements in fumarolic condensates from Nicaraguan and Costa Rican volcanoes, *J. Volcanol. Geotherm. Res.*, *33*, 161-181, 1987.

Gerlach, T. M., Interpretation of Volcanic Gas Data from Tholeiitic and Alkaline Mafic Lavas, *Bull. Volcanol.*, *45*, 235-244, 1982.

Gerlach, T. M., Exsolution of H20, CO2, and S during eruptive episodes at Kilauea Volcano, Hawaii, *J. Geophys. Res.*, *91*, 12177-12185, 1986.

Germani, M. S., *Selected studies of four high-temperature air-pollution sources*, Ph.D. Dissertation, University of Maryland, 1980.

Giggenbach, W. F., A simple method for the collection and analysis of volcanic gas samples, *Bull. Volcanol.*, *39*, 132-145, 1975a.

Giggenbach, W. F., Variations in the carbon, sulfur and chlorine content of volcanic gas discharges from White Island, New Zealand, *Bull. Volcanol.*, *39*, 12-27, 1975b.

Giggenbach, W. F., and F. Le Guern, The chemistry of magmatic gases from Erta'Ale, Ethiopia, *Geochim. Cosmochim. Acta*, *40*, 25-30, 1976.

Giggenbach, W. F., P. R. Kyle, and G. Lyon, Present volcanic activity of Mt. Erebus, Ross Island, Antarctica, *Geology*, *1*, 135-136, 1973.

Gladney, E. S., B. T. O'Malley, I. Roelandts, and T. E. Gills (eds.), *Standard Reference Materials. Compilation of Elemental Concentration Data for NBS Clinical, Biological, Geological, and Environmental Standard Reference Materials. NBS Special Publication 260-111*, 1987.

Greenland, L. P., and P. Aruscavage, Volcanic emissions of Se, Te, and As from Kilauea volcano, Hawaii, *J. Volcanol. Geotherm. Res.*, *27*, 195-201, 1986.

Govindaraju, K., 1989 compilation of working values and sample description for 272 geostandards, *Geostandards Newsletter*, *13*, 1-113, 1989.

Guerzoni, S., R. Lenaz, G. Quarantotto, M. Taviani, G. Rampazzo, M. C. Facchini, and S. Fuzzi, Geochemistry of airborne particles from the lower troposphere of Terra Nova Bay, Antarctica, *Tellus*, *44B*, 304-310, 1992.

Hallett, R. B., and P. R. Kyle, XRF and INAA determinations of major and trace elements in Geological Survey of Japan igneous and sedimentary rock standards, *Geostandards Newsletter*, *17*, 127-133, 1993.

Harris, D. M., The concentration of CO_2 in submarine tholeiitic basalts, *J. Geol.*, *89*, 689-701, 1981.

Harris, J. M., An analysis of 5-day midtropospheric flow patterns for the South Pole:1985-1989, *Tellus*, *44*, 409-421, 1992.

Herron, M. M., Impurity sources of F^-, Cl^-, NO_3^-, and SO_4^{2-} in Greenland and Antarctic

precipitation, *J. Geophys. Res.*, *87*, 3052-3060, 1982.

Hirabayashi, J., J. Ossaka, and T. Ozawa, Relationship between volcanic activity and chemical composition of volcanic gase - A case study on the Sakurajima Volcano, *Geochem. J.*, *16*, 11-21, 1982.

Hirabayashi, J., J. Ossaka, and T. Ozawa, Geochemical study on volcanic gases at Sakurajima volcano, Japan, *J. Geophys. Res.*, *91*, 1986.

Hofmann, D. J., and S. Solomon, Ozone destruction through heterogeneous chemistry following the eruption of El Chichon, *J. Geophys. Res.*, *94*, 5029-5041, 1989.

Holloway, J. R., Volatile Interactions in Magmas, in *Advances in Physical Geochemistry*, edited by R. C. Newton, A. Navrotsky, and B. J. Wood, pp. 273-293, Springer Verlag, New York, 1981.

Jaggar, T. A., Magmatic gases, *Amer. Jour. Sci.*, *238*, 313-353, 1940.

Johnston, D. A., Volcanic contribution of chlorine to the stratosphere: More significant to ozone than previously estimated, *Science*, *209*, 491-493, 1980.

Jones, L. M., G. Faure, K. S. Taylor, and C. E. Corbato, The origin of salts on Mount Erebus and along the coast of Ross Island, Antarctica, *Isot. Geoscience*, *1*, 57-64, 1983.

Journel, A. G. and C. J. Huijbregts, *Mining Geostatistics*. Academic Press, London, 1978.

Kaminuma, K., The seismic activity of Mount Erebus in 1981-1990, in *Volcanological Studies of Mount Erebus. Antarctic Research Volume*, edited by P. R. Kyle, AGU, Washington, D.C., (in press), 1994

Keys, J. R., *Salts and their distribution in the McMurdo region, Antarctica*, Ph.D. Dissertation, Victoria University, Wellington, N.Z., 1980.

Keys, J. R., and K. Williams, Origin of crystalline, cold desert salts in the McMurdo region, Antarctica, *Geochim. Cosmochim. Acta*, *45*, 2299-2309, 1981.

Kitto, M. E., D. L. Anderson, and W. H. Zoller, Simultaneous collection of particles and gases followed by multielement analysis using nuclear techniques, *J. Atmos. Chem.*, *7*, 241-259, 1988.

Krafft, K., and M. Krafft (eds.), *Volcanoes: Earth's Awakening*, Hammomds Inc., Maplewood, N.J., 1980.

Krauskopf, K. B., The heavy metal content of magmatic vapor at 600°C, *Econ. Geol.*, *52*, 786-807, 1957.

Krauskopf, K. B. (ed.), *Introduction to Geochemistry*, 2nd ed., McGraw-Hill, New York, 1979.

Kyle, P. R., Mineralogy and glass chemistry of recent volcanic ejecta from Mt. Erebus, Ross Island, Antarctica, *N.Z. Jour. Geol. Geophys.*, *20*, 1123-1146, 1977.

Kyle, P. R., Erebus Volcanic Province, in *Volcanoes of the Antarctic Plate and Southern Oceans*, edited by W. E. LeMasurier, and J. W. Thompson, pp. 81-88, Amercian Geophysical Union, Washington, DC, 1990.

Kyle, P. R., R. R. Dibble, W. F. Giggenbach, and J. Keys, Volcanic activity associated with the anorthoclase phonolite lava lake, Mount Erebus, Antarctica, in *Antarctic Geoscience*, edited by C. Craddock, pp. 735-745, University of Wisconsin Press, Madison, 1982.

Kyle, P. R. and W. C. McIntosh, Automation of a correlation spectrometer for measuring volcanic SO_2 emissions. IAVCEI Continental Magmatism (abstr.) Santa Fe, June 25-July 1, *New Mexico Bureau of Mineral Resources Bulletin*, *131,* p. 158, 1989.

Kyle, P. R., K. Meeker, and D. Finnegan, Emission rates of sulfur dioxide, trace gases and metals from Mount Erebus, Antarctica, *Geophys. Res. Lett.*, *17*, 2125-2128, 1990.

Kyle, P. R., J. A. Moore, and M. F. Thirwall, Petrologic evolution of anorthoclase phonolite lavas at Mount Erebus, Ross Island, Antarctica, *J. Petrology*, *33*, 1-26, 1992.

Kyle, P. R., L. M. Sybeldon, W. C. McIntosh, K. Meeker, Symonds, R., Sulfur dioxide emission rates from Mount Erebus, Antarctica, in *Volcanological Studies of Mount Erebus. Antarctic Research Volume*, edited by P. R. Kyle, AGU, Washington, D.C., (in press), 1994.

Lamb, H. H., Volcanic dust in the atmosphere; with a chronology and assessment of its meteorological significance, *Phil. Trans. Roy. Soc. London*, *266A*, 425-533, 1970.

Lazrus, A. L., B. W. Gandrud, R. N. Woodard, and W. A. Sedlacek, Stratospheric halogen measurements, *Geophys. Res. Lett.*, *2*, 439-441, 1975.

Lazrus, A. L., R. D. Cadle, B. W. Gandrup, jp Greenberg, B. J. Huebert, and W. I. Rose Jr., Sulfur and halogen chemistry of the stratosphere and of the volcanic eruption plumes, *J.Geophys. Res.*, *84*, 7869-7875, 1979.

Legrand, M., and R. J. Delmas, A 220yr continuous record of volcanic H_2SO(-4 in the Antarctic ice sheet, *Nature*, *328*, 671-676, 1987.

Legrand, M. R., and R. J. Delmas, Formation of HCl in the Antarctic atmosphere, *J.Geophys. Res.*, *93*, 7153-7168, 1988.

Le Guern, F., and A. Bernard, A new method for sampling and analyzing volcanic sublimates-application to Merapi volcano, Java, *J. Volcanol. Geotherm. Res.*, *12*, 133-146, 1982.

MacDonald, G. A. (ed.), *Volcanoes*, Prentice Hall, Englewood Cliffs, N.J., 1972.

Maenhaut, W., W. Zoller, R. A. Duce, and G. L. Hoffman, Concentration and size distribution of particulate trace elements in the south polar atmosphere, *J. Geophys. Res., 84, 2421-2431*, 1979.

Meeker, K., *The emission of gases and aerosols from Mount Erebus volcano, Antarctica*, M.S. Thesis, New Mexico Institute of Mining and Technology, Socorro, NM, 1988.

Meeker, K. A., R. L. Chuan, P. R. Kyle, and J. M. Palais, Emission of elemental gold particles from Mount Erebus, Ross Island, Antarctica, *Geophys. Res. Lett., 18*, 1405-1408, 1991.

Menyailov, I. A., Prediction of eruptions using changes in composition of volcanic gases, *Bull. Volcanol., 39*, 112-125, 1975.

Menyailov, I. A., and L. P. Nikitina, Chemistry and metal content of magmatic gases: the new Tolbachik volcanoes gas (Kamchatka), *Bull. Volcanol., 43*, 197-207, 1980.

Menyailov, I. A., L. P. Nikitina, V. N. Shapar, and V. P. Pilipenko, Temperature increase and chemical change of fumarolic gases at Momotombo volcano, Nicaragua, in 1982-1985: Are these indicators of a possible eruption?, *J. Geophys. Res., 91*, 12199-12214, 1986.

Miller, I., and J. E. Freund, *Probability and Statistics for Engineers*, Prentice-Hall, Englewood Cliffs, 1987.

Miller, T. L., W. H. Zoller, B. M. Crowe, and D. L. Finnegan, Variations in trace metal and halogen ratios in magmatic gases through an eruptive cycle of the Pu'u O'o vent, Kilauea, Hawaii: July-August, 1985, *J. Geophys. Res., 95*, 12607-12615, 1990.

Minor, M. M., and S. R. Garcia, A computer-automated neutron activation analysis system, in *Use and developmente of low and medium flux research reactors*, edited by O. K. Harling, L. C. Clark Jr., and P. Von der Hardt, pp. 653-658, Karl Thiemig, Munchen, 1983.

Moore, J. A., and P. R. Kyle, Mount Erebus, in *Volcanoes of the Antarctic Plate and Southern Oceans*, edited by W. E. LeMasurier, and J. W. Thompson, pp. 103-108, American Geophysical Union, Washington, DC, 1990.

Mroz, E. J., M. Alei, J. H. Cappis, P. R. Guthals, A. S. Mason, and D. J. Rokop, Antarctic atmopheric tracer experiments, *J. Geophys. Res., 94*, 8577-8583, 1989.

Murata, K. J., W. U. Ault, and D. E. White, Halogen acids in fumarolic gases of Kilauea volcano, *Bull. Volcanol., 27*, 367-368, 1964.

Naboko, S. I., Volcanic exhalations and products of their reactions as exemplified by Kamchatka-Kuriles volcanoes, *Bull. Volcanol., 20*, 121-136, 1959.

Naughton, J. J., E. Heald, and I. L. Barnes Jr., The chemistry of volcanic gases. 1. Collection and analysis of equilibrium mixtures by gas chromatography, *J. Geophys. Res., 68*, 539-

557, 1963.

Naughton, J. J., V. A. Lewis, D. Hammond, and D. Nishimoto, The chemistry of sublimates collected directly from lava fountains at Kilauea Volcano, Hawaii, *Geochim. Cosmochim. Acta*, *38*, 1679-1690, 1974.

Naughton, J. J., V. Lewis, D. Thomas, and J. B. Finlayson, Fume composition found at various stages of activity at Kilauea Volcano, Hawaii, *J. Geophys. Res.*, *80*, 2963-2966, 1975.

Nehring, N. L., and D. A. Johnston, Use of ash leachates to monitor gas emissions, *U.S. Geol. Survey Prof. Paper*, *1250*, 251-254, 1981.

Noble, D. C., V. C. Smith, and L. C. Peck, Loss of halogens from crystallized and glassy silicic volcanic rocks, *Geochim. Cosmochim. Acta*, *31*, 215-223, 1967.

Noguchi, K., and H. Kamiya, Prediction of volcanic eruption by measuring the chemical composition and amount of gases, *Bull. Volcanol.*, *26*, 367-378, 1963.

Nriagu, J. O., A global assessment of natural sources of atmospheric trace metals, *Nature*, *338*, 47-49, 1989.

Olmez, I., D. L. Finnegan, and W. H. Zoller, Iridium emissions from Kilauea Volcano, *J. Geophys. Res.*, *91*, 653-663, 1986.

Oskarsson, N., The interaction between volcanic gases and tephra: Fluorine adhering to tephra of the 1970 Hekla eruption, *J. Volcanol. Geotherm. Res.*, *8*, 251-266, 1980.

Oskarsson, N., The chemistry of Icelandic lava incrustations and the latest stages of degassing, *J. Volcanol. Geotherm. Res.*, *10*, 93-111, 1981.

Oskarsson, N., Aluminium fluoride in a volcanic cloud: evidence from the 1991 Hekla eruption. Abstract: 20th Nordic Geological Winter Meeting, Reykjavik 1992, p. 129.

Palais, J. M., B. W. Mosher, and D. Lowenthal, Elemental tracers of volcanic emissions from Mt. Erebus in Antarctic snow samples, in *Volcanological Studies of Mount Erebus. Antarctic Research Volume*, edited by P. R. Kyle, AGU, Washington, D.C., (in press), 1994.

Pasquill, F., *Atmospheric Diffusion*, 2nd. ed., Halstead Press, New York, 1974.

Pasquill, F, and F. B. Smith, *Atmospheric Diffusion,* 3rd. ed. Halsted Press, New York, 1983.

Phelan, J. M., D. L. Finnegan, D. S. Ballantine, and W. H. Zoller, Airborne aerosol measurements in the quiescent plume of Mount St. Helens: September, 1980, *Geophys. Res. Lett.*, *9*, 1093-1096, 1982.

Pinto, J. P., R. P. Turco, and O. B. Toon, Self-limiting physical and chemical effects in volcanic eruption clouds, *J. Geophys. Res.*, *94*, 11165-11174, 1989.

Pollack, J. G., J. B. Toon, C. Sagan, A. Summers, B. Baldwin, and W. Van Camp, Volcanic explosions and climatic change: a theoretical assessment, *J. Geophys. Res.*, *81*, 1070-1085, 1976.

Quisefit, J. P., J. P. Toutain, G. Bergametti, M. Javoy, B. Cheynet, and A. Person, Evolution versus cooling of gaseous volcanic emissions from Momotombo Volcano, Nicaragua: Thermochemical model and observations, *Geochim. Cosmochim. Acta*, *53*, 2591-2608, 1989.

Radke, L. F., Sulfur and sulfate from Mt Erebus, *Nature*, *299*, 710-712, 1982.

Rampino, M. R., and S. Self, Volcanic winter and accelerated glaciations following the Toba super-eruption, *Nature*, *359*, 50-52, 1992.

Rampino, M. R., S. Self, and R. B. Stothers, Volcanic winters, *Ann. Rev. Earth Planet. Sci.*, *16*, 73-99, 1988.

Reagan, M. K., A. M. Volpe, and K. V. Cashman, ^{238}U- and ^{232}Th-series chronology of phonolite fractionation at Mount Erebus, Antarctica, *Geochim. Cosmochim. Acta*, *56*, 1401-1407, 1991.

Rose, W. I., R. R. Chuan, and D. C. Woods, Small particles in plumes of Mount St. Helens, *J. Geophys. Res.*, *87*, 4956-4962, 1982.

Rose, W. I., R. L. Chuan, and P. R. Kyle, Rate of sulphur dioxide emission from Erebus volcano, Antarctica, December 1983, *Nature*, *316*, 710-712, 1985.

Rose, W. I., R. L. Chuan, W. F. Giggenbach, P. R. Kyle, and R. B. Symonds, Rates of sulfur dioxide and particle emissions from White Island volcano, New Zealand, and an estimate of the total flux of major gaseous species, *Bull. Volcanol.*, *48*, 181-188, 1986.

Rose, W. I., G. Heiken, K. Wohletz, D. Eppler, S. Barr, T. Miller, R. Chuan, and R. B. Symonds, Direct rate measurements of eruption plumes at Augustine volcano: A problem of scaling and uncontrolled variables, *J. Geophys. Res.*, *93*, 4485-4499, 1988.

Rose, W. I., Jr., Scavenging of volcanic aerosol by ash: Atmospheric and volcanologic implications, *Geology*, *5*, 621-624, 1977.

Rose, W. I., Jr., Active Pyroclastic Processes Studied with Scanning Electron Microscopy, in *Clastic Particles. Scanning Electron Microscopy and Shape Analysis of Sedimentary and Volcanic Clasts*, edited by J. R. Marshall, pp. 136-158, Van Nostrand Reinhold Co., New York, 1987.

Rose, W. I., Jr., R. I. Chuan, R. D. Cadle, and D. C. Woods, Small particles in volcanic eruption clouds, *Amer. Jour. Sci.*, *280*, 671-696, 1980.

Rosenberg, P. E., Aluminum fluoride hydrates, volcanogenic salts from Mount Erebus, Antarctica, *Am. Mineral.*, *73*, 855-860, 1988.

Schwerdtfeger, W., The climate of the antarctic, in *World Survey of Climatology*, vol. 14. Climates of the Polar Region, edited by S. Orvig, pp. 253-322, Elsevier Science, New York, 1970.

Sear, C. B., P. M. Kelly, P. D. Jones, and C. M. Goodess, GLobal surface-temperature responses to major volcanic eruptions, *Nature*, *330*, 365-367, 1987.

Self, S., M. R. Rampino, and J. J. Barbera, The possible effects of large 19th and 20th century eruptions on zonal and hemispheric surface temperatures, *J. Volcanol. Geotherm. Res.*, *11*, 41-60, 1981.

Self, S., and M. R. Rampino, The relationship between volcanic eruptions and climate change: still a conundrum?, *EOS*, *69*, 74-75,85-86, 1988.

Shaw, G. E., On the residence time of the Antarctic ice sheet sulfate aerosol, *J. Geophys. Res.*, *87*, 4309-4313, 1982.

Shaw, G. E., Aerosol transport from sources to ice sheets, in *The Environmental Record in Glaciers and Ice Sheets*, edited by H. Oeschger, and C. C. Langway Jr., pp. 13-27, John Wiley & Sons, Chichester, 1989.

Shepherd, E. S., The analysis of gases obtained from volcanoes and from rocks, *J. Geol.*, *33*, 289-370, 1925.

Sheppard, D. S., F. Le Guern, and B. W. Christenson, Compositions and Mass Fluxes of the Mt. Erebus Volcanic Plume, in *Volcanological Studies of Mount Erebus, Antarctica*, edited by P. R. Kyle, AGU, Washington, D.C., 1993.

Silver, L., and E. Stolper, Water in albitic glasses, *J. Petrology*, *30*, 667-709, 1989.

Smith, D. B., R. A. Zielinski, H. E. Taylor, and M. B. Sawyer, Leaching characteristics of ash from the May 18, 1980 eruption of Mount St. Helens volcano, Washington, *Bull. Volcanol.*, *46*, 103-124, 1983.

Sparks, R. S. J., The dynamics of bubble formation and growth in magmas: A review and analysis, *J. Volcanol. Geotherm. Res.*, *3*, 1-37, 1978.

Stern, A. C., R. W. Boubel, D. B. Turner, and D. L. Fox, *Fundamentals of Air Pollution,* 2nd. ed., Academic Press, New York, 1984.

Stoiber, R. E., and W. I. Rose, The geochemistry of Central American volcanic gas condensates, *Geol. Soc. Am. Bull.*, *81*, 2891-2912, 1970.

Stoiber, R. E., and W. I. Rose Jr., Fumarole incrustations at active Central American volcanoes, *Geochim. Cosmochim. Acta*, *38*, 495-516, 1974.

Stoiber, R. E., L. L. Malinconico Jr., and S. N. Williams, Use of correlation spectrometer at volcanoes, in *Forecasting volcanic events*, edited by H. Tazieff, and J.-C. Sabroux, pp. 425-444, Elsevier, Amsterdam, 1983.

Stoiber, R. E., S. N. Williams, and B. J. Huebert, Sulfur and halogen gases at Masaya Caldera Complex, Nicaragua: Total flux and variations with time, *J.Geophys. Res.*, *91*, 12215-12231, 1986.

Stoiber, R. E., S. N. Williams, and B. Huebert, Annual contribution of sulfur dioxide to the atmosphere by volcanoes, *J. Volcanol. Geotherm. Res.*, *33*, 1-8, 1987.

Stolarski, R. S., and R. J. Cicerone, Stratospheric chlorine: a possble sink for ozone, *Can. J. Chem.*, *52*, 1610-1615, 1974.

Stolper, E., The speciation of water in silicate melts, *Geochim. Cosmochim. Acta*, *46*, 2609-2620, 1982.

Stothers, R. B., Volcanic winter? Climatic effects of the larges volcanic eruptions, in *IAVCEI Proceedings in Volcanology 1*, pp. 3-9, Springer-Verlag, Berlin, 1989.

Sybeldon, L. M., *Sulfur dioxide emissions from Pu'u O'o vent, Kilauea, Hawaii and Mount Erebus, Antarctica, M.S. thesis*, M.S Thesis, New Mexico Institute of Mining and Technology, Socorro, NM, 1991.

Symonds, R. B., *Applications of multicomponent chemical equilibria to volcanic gases at Augustine volcano, volcanic halogen emissions, and volcanological studies of gas-phase transport*, Ph.D. Dissertation, Michigan Technological University, 1990.

Symonds, R. B., and M. H. Reed, Calculation of multicompomemt chemical equilibria in gas-solid-liquid systems: calculation methods, thermochemical data, and applications to studies of high-temperature volcanic gases with examples from Mount St. Helens, *Amer. Jour. Sci.*, *293*, 758-864, 1993.

Symonds, R. B., P. R. Kyle, and W. I. Rose, SO_2 emission rates and the 1984 activity at Mount Erebus Volcano, Antarctica (abstract), *EOS*, *66*, 417, 1985.

Symonds, R. B., W. I. Rose, M. H. Reed, F. E. Lichte, and D. L. Finnegan, Volatilization, transport and sublimation of metallic and non-metallic elements in high temperature gases at Merapi volcano, Indonesia, *Geochim. Cosmochim. Acta*, *51*, 2083-2101, 1987.

Symonds, R. B., W. I. Rose, and M. H. Reed, Contribution of Cl- and F- bearing gases to the atmosphere by volcanoes, *Nature*, *334*, 415-418, 1988.

Symonds, R. B., W. I. Rose, T. M. Gerlach, P. H. Briggs, and R. S. Harmon, Evaluation of gases, condensates, and SO_2 emissions from Augustine volcano, Alaska: the degassing of a Cl-rich volcanic system, *Bull. Volcanol.*, *52*, 355-374, 1990.

Symonds, R. B., M. Reed, and W. I. Rose, Origin, speciation, and fluxes of trace-element gases at Augustine volcano, Alaska: Insights into magma degassing and fumarolic processes, *Geochim. Cosmochim. Acta*, *56*, 633-657, 1992.

Tabazadeh, A., and R. P. Turco, Stratospheric chlorine injection by volcanic eruptions: HCl scavenging and implications for ozone, *Science*, *260*, 1082-1086, 1993.

Taylor, S. R., The abundance of chemical elements in the continental crust - a new table, *Geochim. Cosmochim. Acta*, *28*, 1273-1285, 1964.

Taylor, S. R., and S. M. McLennan (eds.), *The Continental Crust: Its Composition and Evolution*, Blackwell Scientific Publ., Oxford, England, 1985.

Thomas, E., J. C. Varekamp, and P. R. Buseck, Zinc enrichment in the phreatic ashes of Mt. St. Helens, April 1980, *J. Volcanol. Geotherm. Res.*, *12*, 339-350, 1982.

Toutain, J. P., and G. Meyer, Iridium-bearing sublimates at a hot-spot volcano (Piton de la Fournaise, Indian Ocean), *Geophys. Res. Lett.*, *16*, 1391-1394, 1989.

Turco, R. P., R. C. Whitten, and O. B. Toon, Stratospheric aerosols: Observation and theory, *Rev. Geophys. Space Physics*, *20*, 233-279, 1982.

Turner, J. S., and I. H. Campbell, Convection and mixing in magma chambers, *Earth Sci. Rev.*, *23*, 255-352, 1986.

Varekamp, J. C., E. Thomas, M. Germani, and P. R. Buseck, Particle geochemistry of volcanic plumes of Etna and Mount St. Helens, *J. Geophys. Res.*, *91*, 12233-12248, 1986.

Vie le Sage, R., Chemistry of the volcanic aerosol, in *Forecasting volcanic events*, edited by H. Tazieff, and J.-C. Sabroux, pp. 445-474, Elsevier, Amsterdam, 1983.

Volz, F. E., Burden of volcanic dust and nuclear debris after injection into the strato-sphere at 40°-58°N, *J. Geophys. Res.*, *80*, 2649-2652, 1975.

Vossler, T., D. L. Anderson, N. K. Aras, J. M. Phelan, and W. H. Zoller, Trace element composition of the Mt. St. Helens plume: stratospheric samples from the May 18 eruption, *Science*, *211*, 827-830, 1981.

Webster, J. D., Partitioning of F between H_2O and CO_2 fluids and topaz rhyolite melt. Implications for mineralizing magmatic-hydrothermal fluids in F-rich granitic systems,

Contrib. Mineral. Petrol., *104*, 424-438, 1990.

Webster, J. D., and J. R. Holloway, Experimental constraints on the partitioning of Cl between topaz rhyolite melt and H_2O and H_2O+CO_2 fluids: New implications for granitic differentiation and ore deposition, *Geochim. Cosmochim. Acta*, *52*, 2091-2105, 1988.

White, O. E., and G. A. Waring, Volcanic emanations, in *Data on Geochemistry. U.S. Geol. Survey Prof. Pap. 440K*, pp. 1-29, 1963.

Williams, H., and A. R. McBirney (eds.), *Volcanology*, Freeman, Cooper & Co., San Francisco, CA, 1979.

Wolff, E. W., and D. A. Peel, The record of global pollution in polar snow and ice, *Nature*, *313*, 535-540, 1985.

Yoshida, M., Fractionation of fluorine and chlorine through the volcanic process, in *Geochemistry of gaseous elements and compounds*, edited by E. M. Durrance, E. M. Galimov, M. E. Hinkle, G. M. Reimer, R. Sugisaki, and S. S. Augustithis, pp. 163-184, Theophrastus Publications, S.A., Athens, 1990.

Zoller, W. H., E. S. Gladney, and R. A. Duce, Atmospheric concentrations and sources of trace elements at the South Pole, *Science*, *183*, 198-200, 1974.

Zoller, W. H., J. R. Parrington, and J. M. P. Kotra, Iridium enrichment in airborne particles from Kilauea volcano, *Science*, *222*, 1118-1121, 1983.

Zreda-Gostynska, G., P. R. Kyle, and D. L. Finnegan, Chlorine, fluorine, and sulfur emissions from Mount Erebus, Antarctica and estimated contributions to the Antarctic atmosphere, *Geophys. Res. Lett.*, *20*, 1959-1962, 1993.

APPENDICES

A1. INAA PROCEDURE

By using a combination of variable irradiation and decay times it was possible to analyze for over 30 elements. Table A1.1 lists the elements analyzed, irradiation, decay and counting times used, and the facility at which irradiation and counting was performed. In general, 3 separate irradiations were performed which I call here very short (VS) (5 s), short (S) (5-30 min), and long (L) (14 hrs for filters and 36 hrs for salts). The actual decay and counting times in VS and S experiments vary slightly at different facilities. At MURR, there were 2 separate counts performed on each samples during S experiment - first (lasting 10 minutes) after 5 minutes decay, and second immediately following that.

The long irradiation (L) on filter samples was performed at Texas A&M facility. Due to the danger of sample combustion and vials melting, the irradiation time was reduced to 14 hrs, either uninterrupted or broken into two intervals of 7 hrs. Upon samples return from the reactor (4-5 days after the irradiation) they were counted 3 times. The first count targeted the short lived elements and lasted 45 min-1 hr. Following that, another count was performed, lasting 2.5 to 3 hrs, on which both short lived and some of the long-lived elements were measured. Finally, after 30 days, the last count (lasting 3 hrs) was done to obtain long lived elements. This procedure was later modified to obtain better spectra resolution for the short-lived elements. The first count was extended to 3 hrs, then samples were allowed to decay another 3 days and counted again for 3 hrs. The last count remained unchanged.

The long irradiation procedure of salt samples varies from that done on filters. Samples were irradiated at University of Missouri Research Reactor with a neutron flux of $3x10^{13}$ $n.cm^{-2}.sec^{-1}$ for 36 hours. The counting procedure consists of 2 counts. The first count is done immediately upon samples return from the reactor (4-5 day after irradiation), the second count after 30-40 days of decay. During both

counts, unknowns are counted for 3 hours, whereas standards are counted for 6 hours.

Table A1.1. Elements analyzed on filter samples

Element(s)	Irradiation code/time		decay time	counting time	Irradiation facility	Counting facility
F	VS	5 s	10 s	30 s	LANL	LANL
	VS	5 s	15 s	20 s	MURR	MURR
Cl, Na, K, Ca, Al, Ti, V, Mn, Cu, Br, In, I	S	5 min	15 min	15 min	LANL	LANL
	S	30 min	5 min 15 min	10 min 15 min	MURR	MURR
Na, K, Ca, As, Sm, W, Br, La, U, Cd, Au	L	14 hrs	4-5 days (A-count)	3 hrs	Texas A&M	NMIMT
Sc, Cr, Fe, Co, Zn, Ni, Rb, Mo, Zr, Sb, Cs, Ce,			8 days (S-count)	3 hrs		
Nd, Eu, Tb, Yb, Lu, Hf, Ta, Th			30 days (L-count)	3 hrs		

Explanation of codes: VS-very short, S-short, L-long irradiation;
A, S, L-count refer to names of count schedules used in TEABAGS software.

Table A1.2. Elements analyzed for in salt samples

element(s)	irradiation time	decay time	counting time	Irradiation facility	Counting facility
F	5 s	10 s	30 s	LANL	LANL
Cl, Na, K, Ca, Al, Ti, V, Mn, Cu, Br, In, I	5 min	15 min	15 min	LANL	LANL
Na, K, Ca, As, Sm, W, Br, La, U, Cd, Au	36 hrs	6 days (S-count)	3 hrs	MURR	NMIMT
Sc, Cr, Fe, Co, Zn, Se, Ni, Rb, Mo, Zr, Sb, Cs, Ba, Ce, Nd, Eu, Tb, Yb, Lu, Hf, Ta, Th		30 days (L-count)	3 hrs		

Instrumentation

The neutron activation lab at NMIMT is equipped with the two EG&G Ortec Ge-detectors of coaxial type. The detectors efficiencies are 18 and 26% respectively, and have typical FWHM of 1.8 keV at 1332 keV and 0.6 keV at 122 keV. For each detector spectrum of 8192 channels is acquired in the ADC module (model ND 581) connected by Ethernet to Vax workstation 3100.

Data reduction procedures

Data collected at LANL was subsequently reduced using a program developed at LANL (Minor *et al.*, 1979). Data collected at MURR was reduced using Nuclear Data software on a VAX station 3100 microcomputer.

Data collected at NMIMT were processed using TEABAGS (Trace Element Analysis by Automated Gamma-ray Spectrometry) computer program which facilitates the reduction of data from instrumental neutron activation analysis (Lindstrom and Korotev, 1982). The latest VAX version of TEABAGS was used. TEABAGS is designed to analyze the spectra, find peaks, identify any nuclides present and calculate concentrations of elements. Initially, TEABAGS identifies the low and high energy boundary channels of each peak, whereas the remaining channels are used to estimate the background. Then the program calculates peak areas using the total peak area method. Poorly resolved peaks are corrected by comparing peak areas for a large peak (in the standard spectrum) with a small peak of the same energy (in the unknown spectrum). Assuming gaussian shape for all peaks TEABAGS increases the area of a small peak by calculated amount. Peaks are also corrected for interferences causing peaks overlap. Necessary information about possible interferences are contained in the 'control file' which lists the elements which need correction and their energy lines, as well as the energy lines causing the interference together with the energy line of a clean peak used for correction. TEABAGS calculates the

ratio of interfering peak to clean peak and subtracts the interference. Finally, TEABAGS produces the list of elements identified in the spectrum together with the calculated abundances. The program also allows for calculating the fission correction for Ba, Ce, La, Mo, Nd, and Zr. The isotopes analyzed for and photopeaks used in their analysis are listed in Table A1.3

Calibration standards

With few exceptions, NIST SRM 1633a (coal flyash) was used as a standard for most of the elements analyzed. The other commercial standard used was NIST SRM 1648 (urban particulate matter) as a standard for Br, Zn, Cd, and In. Standards for F and Cl for filter analysis were prepared by pipetting known amounts of standard solutions made from reagent grade KF and KCl powders (Baker Analyzed) on the Whatman 41 filter papers. Standards for F and Cl used in salts analysis were made by weighing about 50 mg of reagent grade KF and KCl powders. Standard for Au and In used in filter analysis was prepared from the commercial standard solution by pipetting the known amount of diluted solution on the Whatman 41 filter paper.

A number of commercial as well as "house" standards were used throughout the study as the quality assurance standards. Among the materials used were NIST SRM 1632-b, 1635, GRX-1, as well as F, Cl, In, and Au standards prepared as described above. In the analyses of salts apart of the materials mentioned above, such rock standards as BCR-1 and G-2 were also used as quality assurance (QA) standards. All standards used in the study, together with the recommended values of element concentrations are listed in Table A1.4.

Table A1.3. Isotopes and energy lines used for analysis.

Element	Isotope	Half life	Major energy line(s) (KeV)			
F	^{20}F	11s	1633.1			
Na	^{24}Na	15.02h	1368.53	1731.9		
Al	^{28}Al	2.3m	1779			
Ca	^{47}Ca	4.54d	1297			
Ca	^{49}Ca	8.72m	3084.15	4071		
Sc	^{46}Sc	83.8d	889.3	1120.5		
Ti	^{51}Ti	5.8m	320.1	608.55	928.63	
V	^{52}V	3.76m	1434			
Cr	^{51}Cr	27.7d	320.08			
Mn	^{56}Mn	2.58h	849.8	2113		
Fe	^{59}Fe	44.6d	1099.22	1297.1		
Co	^{60}Co	5.271y	1173.22	1332.5		
Ni	^{58}Co	70.8d	810.74			
Cu	^{64}Cu	12.71h	511	1345.8		
Zn	^{65}Zn	244.1d	1115.52			
As	^{76}As	26.32h	559.1			
Se	^{75}Se	119.78d	265.7			
Br	^{80}Br	4.4h	616.2	665.6		
Br	^{82}Br	35.34h	554.3	698.3	776.5	
Rb	^{86}Rb	148.65d	1076.63			
Sr	^{85}Sr	67.7d	514			
Zr	^{95}Zr	63.98d	756.7			
Zr	^{95}Nb	34.97d	765.8			
Mo	^{99}Mo	66.02h	140.57			
Cd	^{115}Cd	2.3d	527.7			
In	^{116m}In	54m	417	1097		
Sb	^{122}Sb	2.681d	564.1			
Sb	^{124}Sb	60.2d	1691			
I	^{128}I	25m	442.9			
Cs	^{134}Cs	2.062y	604.66	795.76		
La	^{140}La	40.27h	328.8	487	815.9	1596.6
Ce	^{141}Ce	32.55d	145.4			
Nd	^{147}Nd	10.98d	531			
Sm	^{153}Sm	46.8h	103.2			
Eu	^{152}Eu	13.2y	778.9	1408.1		
Tb	^{160}Tb	72.1d	298.6			
Yb	^{169}Yb	32.02d	177.2			
Yb	^{175}Yb	4.19d	282.5	396.5		
Lu	^{177m}Lu	6.71d	208.3			
Hf	^{181}Hf	42.45d	482			
Ta	^{182}Ta	115d	1198	1221.4	1231	
W	^{187}W	23.85h	479.5	685.8		
Au	^{198}Au	2.696d	411.8			
Th	^{233}Pa	26.95d	311.9			
U	^{293}Np	2.346d	228.1	277.6		

Table A1.4. Calibration standards used in the determination of major and trace elements.

Element	Standard	Concentration (ppm)*
Al	NIST SRM 1633a	144000.
As	NIST SRM 1633a	145.00
Au	Gold standard	10.
	GXR-1	3.3
Ba	NIST SRM 1633a	1320.00
Br	NIST SRM 1648	506.
Ca	NIST SRM 1633a	11100.00
Cd	NIST SRM 1648	75.00
Ce	NIST SRM 1633a	168.30
Cl	Cl-standard	
Co	NIST SRM 1633a	44.10
Cr	NIST SRM 1633a	193.00
Cs	NIST SRM 1633a	10.42
Cu	NIST SRM 1633a	120.
Eu	NIST SRM 1633a	3.58
Fe	NIST SRM 1633a	94000.00
F	F-standard	
Hf	NIST SRM 1633a	7.29
I	NIST SRM 1648	18
In	In-standard	
	NIST SRM 1648	.98
K	NIST SRM 1633a	18800.00
La	NIST SRM 1633a	79.10
Lu	NIST SRM 1633a	1.08
Mn	NIST SRM 1633a	188.
Mo	NIST SRM 1633a	29.00
Na	NIST SRM 1633a	1700.00
Nd	NIST SRM 1633a	75.70
Ni	NIST SRM 1633a	130.00
Rb	NIST SRM 1633a	1077.20
Sb	NIST SRM 1633a	6.15
Sc	NIST SRM 1633a	38.60
Se	NIST SRM 1633a	10.00
Sm	NIST SRM 1633a	16.83
Sr	NIST SRM 1633a	514.00
Ta	NIST SRM 1633a	1.93
Tb	NIST SRM 1633a	2.53
Th	NIST SRM 1633a	24.00
Ti	NIST SRM 1633a	8230.
U	NIST SRM 1633a	10.3
V	NIST SRM 1633a	294.
W	NIST SRM 1633a	5.70
Yb	NIST SRM 1633a	7.50
Zn	NIST SRM 1648	4760.
Zr	NIST SRM 1633a	240.00

* source: Gladney *et al.* (1987).

Analytical uncertainty, precison and accuracy of the method

The errors associated with the calculated concentrations are mostly due to difficulty in calculating areas of photopeaks mainly because of problems with peaks resolution due to high background or photopeak overlap. In case of the data reduction software such as TEABAGS, these errors can be partially overcome by selecting well resolved, interference free peaks and using peak fit algorithm. Recounting of the sample after suitable decay time also may free it from the interfering nuclide. Care is taken in the laboratory to shield the counted samples from the background radiation which may produce additional interferences. The other, important source of systematic errors is the non-reproducible sample-to-detector geometry. The difference in positioning affects strongly low activity samples (such as aerosol samples in the study) which are often position very close to detector or even on the detector itself.

The accuracy of the measurements was assessed by comparing the obtained values for quality assurance standards with the recommended values for the standard; it was found to be within 1-2 sigma from recommended values. The precision of measurements was evaluated by counting samples and standards in duplicates and triplicates, and then by calculating the value of standard deviation from the mean. The overall precision was found to be better than 10%.

A2. ION CHROMATOGRAPHY

Sulfur on all filters, as well as F on particulate (Teflon) filters were analyzed separately using ion chromatography. A portion of each filter (1/4 of 110 mm filter and 1/2 of 47 mm filter) was leached in 10 g of deionized water to which 1 g of 3 % H_2O_2 (Baker Analyzed) was added. Plastic vials containing sample in leaching solution were first placed in hot water bath for 30 to 40 min, then placed on the shaker for 24 hrs. Such treatment usually resulted in disintegration of fibers in treated filters. The solution was then filtered through 22 μm filters.

All analyses were performed at the New Mexico Bureau of Mines and Mineral Resources laboratory using a Dionex 4000i model with HPIC AS4A column, using carbonate/bicarbonate eluant and H_2SO_4 as suppressor. Usual run times varied from 6 to 9 minutes depending on the strength of eluant. When stronger eluant solution was used, the retention time of SO_4^{2-} was ~3 min, thus the total run time was decreased. The use of weaker eluant allowed for better separation of F and Cl peaks, and was used in analyses of particulate filters on which these two peaks can be observed. The retention times were ~1.3 min for F^-, ~1.8 min for Cl^-, and ~6 min for SO_4^{2-}. In the treated filter leachate, F^- and Cl^- peaks were usually obscured by a broad OH^- peak, and were not resolved.

To assure the similarity of matrix in samples and standards, a large quantity of treated filters was leached using the same proportion of filter-to-leaching solution (deionized water + 3 % H_2O_2). The leachate was then filtered and used as the matrix in standard preparation. All standards were prepared gravimetrically by dissolving a known amount of K_2SO_4, KCl, and KF reagent grade salt in matrix, and then by proportional dilution. In the analysis of particulate filters deionized water + H_2O_2 was used as the matrix for standard preparation. Quality assurance standards were prepared by pipetting a known amount of K_2SO_4, KCl, and KF water based solution on treated filters, which were then processed in the same manner as other unknowns.

B1. EREBUS FILTERS AND BLANKS DATA

Note:

Data in the appendix (Tables B1.1 - B1.3) is given in μg per 1/2 or 1/4 filter. As explained in text (Chapter 3), a half of a filter was used in the analysis of small filters (47 mm), and a quarter of a filter in the analysis of large (110mm) filters. For each sample, the size of a filter can be determined from Table 3.1. For blanks (Tables B1.4 - B1.6), the filter size is indicated in the table header.

Table B1.1. Erebus 1988 blank corrected filter data in μg per 1/2 or 1/4 filter. A-particle filter, B, C-treated filters. S and F on A-filters by ion chromatography, rest by INAA. Concentrations of elements marked with (*) from long irradiation.

	88-1A	1B	1C	88-1	88-2A	2-B	2-C	88-2	88-3A	3B	3C	3D	88-3
F	23.44	52	42	117.44	19.89	212		231.89	23.03	177			200.03
Na	18.08		5.88	23.95	17.88	5.88	4.88	28.63	29.38	1.79	2.68	2.29	36.13
Na*	17.78		6.31	24.09	18.34	6.83		25.17	30.50				30.50
avg Na	17.93		6.09	24.02	18.11	6.35	4.88	29.33	29.94	1.79	2.68	2.29	36.70
Al				0	18.95			18.95	2.95				2.95
S	4.63	311.7	280.7	597.03	3.83	636.7	56.2	696.73	8.24	462.7	138.5		609.44
Cl	18.6	161.68	172.68	352.96	24.6	582.68	57.675	664.955	45.6	551.68	36.675	2.675	636.63
K				0				0	42				42
K*	23.60			23.60	21.91			21.91	34.46				34.46
avg K	23.60			23.60	21.91			21.91	38.23				38.23
Ca	3			3				0					0
Ca*				0				0					0
avg Ca	3			3				0					0
Sc	0.0002		0.0003	0.0005	0.0006		0.0004	0.001	0.0002			0.0003	0.0005
Ti	0.5			0.5				0					0
V	0.01			0.01				0		0.1			0.1
Cr	0.027			0.027	0.07			0.07					0
Mn				0	0.17			0.17					0
Fe	1.9415			1.9415	12.725			12.725	3.1705				3.1705
Co	0.0033			0.0033				0					0
Ni				0				0					0
Cu				0				0					0
Zn	0.396			0.396	0.414			0.414	0.653				0.653
As	0.279	0.027	0.082	0.388	0.255	0.162	0.050	0.467	0.471	0.095	0.014	0.005	0.585
Se				0				0					0
Br		0.67	0.35	1.02		1.70	0.53	2.23		1.22	0.35		1.57
Br*		0.66	0.36	1.02		1.60	0.62	2.22	0.07	1.11	0.29		1.47
avg Br		0.67	0.35	1.02		1.65	0.58	2.23	0.07	1.17	0.32		1.55
Rb	0.138			0.138	0.132			0.132	0.231				0.231
Mo	0.0218			0.0218	0.0208			0.0208					0
Cd	0.094			0.094	0.09			0.09	0.173				0.173
In	0.037			0.037	0.029			0.029	0.055				0.055
Sb	0.0097		0.0061	0.0158	0.0077	0.0063	0.0082	0.0222	0.0119				0.0119
Cs	0.0051			0.0051	0.005			0.005	0.009				0.009
La				0	0.0056			0.0056	0.0032				0.0032
Ce				0	0.0092	0.0087	0.0014	0.0193					0
Nd				0				0					0
Sm				0	0.0007			0.0007	0.0006				0.0006
Eu				0				0					0
Tb				0				0					0
Yb				0				0					0
Lu				0				0					0
Hf				0				0					0
Ta				0				0					0
W				0	0.0145			0.0145					0
Au				0		0.0012	0.0009	0.0021		0.0007	0.0049	0.0007	0.0063
Th				0				0					0
U				0				0					0

Table B1.1 (cont.)

	88-4A	4B	4C	88-4	88-5A	5B	5C	88-5	88-6A	6B	6C	88-6
F	2.04	64	12	78.04	1.16	40	29	70.16	0.1	60		60.1
Na	6.98			6.98	4.28			4.28	3.98			3.98
Na*	7.44			7.44	4.54			4.54	4.59			4.59
avg Na	7.21			7.21	4.41			4.41	4.28			4.28
Al	2.95			2.95	4.95	5.75		10.7				0
S	2.35	85.6	60.8	148.75	1.13	53.8	42.6	97.53	0.75	93.3	46.1	140.15
Cl	11.6	154.7	24.68	190.98	9.4	69.675	71.675	150.75	7.6	128.68	6.675	142.955
K				0				0				0
K*	10.46			10.46	8.69			8.69				0
avg K	10.46			10.46	8.69			8.69				0
Ca				0	4			4	13			13
Ca*	3			3				0				0
avg Ca	3			3	4			4	13			13
Sc	0.0002			0.0002	0.0025			0.0025	0.0002			0.0002
Ti				0				0				0
V				0				0				0
Cr	0.071			0.071	0.066			0.066	0.054			0.054
Mn	0.015			0.015	0.025			0.025	0.02			0.02
Fe	1.1305			1.1305				0				0
Co				0				0				0
Ni				0				0				0
Cu				0				0				0
Zn	0.476			0.476	0.160	0.235		0.394	0.326			0.326
As	0.136			0.136	0.120	0.047	0.045	0.211	0.087	0.049	0.007	0.143
Se				0				0				0
Br	0.22			0.22	0.125			0.125	0.15			0.15
Br*	0.16			0.16	0.08	0.07	0.10	0.26	0.14	0.11	0.01	0.26
avg Br	0.19			0.19	0.10	0.07	0.10	0.28	0.14	0.11	0.01	0.26
Rb				0	0.037			0.037				0
Mo				0				0				0
Cd	0.035			0.035				0				0
In	0.014			0.014	0.0077		0.0021	0.0098	0.0076	0.0027	0.0006	0.0109
Sb	0.0025		0.013	0.0155	0.0016			0.0016	0.0016			0.0016
Cs				0	0.001			0.001	0.001			0.001
La				0				0				0
Ce				0				0				0
Nd				0				0				0
Sm				0				0				0
Eu				0				0				0
Tb				0				0				0
Yb				0				0				0
Lu				0				0				0
Hf				0				0				0
Ta				0				0				0
W				0				0				0
Au				0				0		0.0002	0.0005	0.0007
Th				0				0				0
U				0				0				0

Table B1.1. (cont.)

	88-7A	7B	7C	88-7	88-8A	8B	8C	88-8	88-9A	9B	9C	88-9
F	8.38	49		57.38			65	65	4.07	49	31	84.07
Na	6.48			6.48	1.08		4.98	6.05	6.68			6.68
Na*	5.57			5.57	1.21		4.82	6.03	6.44			6.44
avg Na	6.02			6.02	1.14		4.90	6.04	6.56			6.56
Al				0				0				0
S	4.765	91.6	31.8	128.165	0.38	30.3	165.7	196.38	2.76	75	53.3	131.06
Cl	12.6	119.68	5.075	137.355	2.9	6.675	154.68	164.255	12.6	105.68	68.675	186.955
K				0				0				0
K*	6.69			6.69			8.90	8.90	7.80			7.80
avg K	6.69			6.69			8.90	8.90	7.80			7.80
Ca	9			9				0				0
Ca*				0				0				0
avg Ca	9			9				0				0
Sc		0.0002		0.0002			0.0012	0.0012	0.0002			0.0002
Ti	0.5			0.5	0.5			0.5	0.5			0.5
V				0				0				0
Cr				0				0	0.035			0.035
Mn	0.01			0.01				0	0.02			0.02
Fe	0.4705			0.4705			1.3163	1.3163				0
Co	0.0043			0.0043			0.0002	0.0002				0
Ni				0				0				0
Cu				0				0				0
Zn	0.142			0.142				0.00	0.251	0.395		0.645
As	0.107	0.021	0.001	0.128	0.030	0.013	0.142	0.185	0.132	0.015	0.068	0.215
Se				0				0				0
Br	0.2			0.2				0	0.19		0.17	0.36
Br*	0.14	0.09		0.23	0.03	0.04	0.33	0.39	0.17	0.08	0.14	0.39
avg Br	0.17	0.09		0.26	0.03	0.04	0.33	0.39	0.18	0.08	0.16	0.42
Rb	0.034			0.034			0.058	0.058	0.052			0.052
Mo				0				0				0
Cd				0				0				0
In	0.014			0.014	0.0029	0.0021	0.013	0.018	0.014			0.014
Sb	0.0047			0.0047	0.0027			0.0027	0.0021		0.0045	0.0066
Cs	0.0015			0.0015			0.0016	0.0016	0.0022			0.0022
La				0				0				0
Ce				0				0				0
Nd				0				0				0
Sm				0				0				0
Eu				0				0				0
Tb				0				0				0
Yb				0				0				0
Lu				0				0				0
Hf				0				0				0
Ta				0				0				0
W				0				0				0
Au		0.0002		0.0002				0		0.0002	0.0041	0.0043
Th				0				0				0
U				0				0				0

Table B1.1. (cont.)

	88-11A	11B	11C	88-11	88-13A	13B	13C	88-13	88-15A	15B	15C	88-15
F	5.82	81		86.82	9.02	92		101.02	8.63	69	50	127.63
Na	11.98			11.98	13.78			13.78	11.38			11.38
Na*				0.00	12.87			12.87	10.64			10.64
avg Na	11.98			11.98	13.32			13.32	11.01			11.01
Al				0				0				0
S	1.03	210		211.03	1.64	210.7	37.9	250.24		141.7	120.7	262.4
Cl	14.6	137.68	5.675	157.955	21.6	232.68	6.675	260.955	18.6	207.68	155.68	381.96
K	16			16	15			15	20			20
K*	13.12			13.12				0				0
avg K	14.56			14.56	15			15	20			20
Ca				0				0				0
Ca*				0				0				0
avg Ca				0				0				0
Sc	0.0002			0.0002	0.0001			0.0001				0
Ti				0				0				0
V	0.02			0.02				0				0
Cr				0		0.004		0.004				0
Mn	0.07			0.07	0.06			0.06	0.04			0.04
Fe	0.9005	1.4953		2.3958	2.0885			2.0885	3.1195			3.1195
Co	0.0004			0.0004	0.0005			0.0005	0.0002			0.0002
Ni				0				0				0
Cu				0				0				0
Zn	0.286			0.286	0.292		0.118	0.409	0.363			0.363
As	0.165	0.011	0.008	0.184	0.144	0.039		0.183	0.108	0.041	0.034	0.183
Se	0.0059			0.0059				0				0
Br		0.31		0.31	0.12	0.42		0.54		0.6	0.15	0.75
Br*		0.32	0.04	0.36	0.08	0.45	0.01	0.53	0.02	0.40	0.09	0.50
avg Br		0.31	0.04	0.36	0.10	0.44	0.01	0.54	0.02	0.50	0.12	0.63
Rb	0.073			0.073	0.087			0.087	0.056			0.056
Mo	0.0116			0.0116	0.0128			0.0128	0.0128			0.0128
Cd	0.096			0.096	0.102			0.102	0.064	0.098		0.162
In	0.023			0.023	0.027			0.027	0.023			0.023
Sb	0.004			0.004	0.0047	0.0006	0.0014	0.0067	0.035	0.0007	0.0001	0.0358
Cs	0.0027			0.0027	0.0034			0.0034	0.0027			0.0027
La	0.0003			0.0003	0.0011			0.0011	0.0008			0.0008
Ce	0.0012			0.0012	0.0028			0.0028				0
Nd				0				0				0
Sm	0.0001			0.0001	0.0001			0.0001				0
Eu				0				0				0
Tb				0				0				0
Yb				0				0				0
Lu				0				0				0
Hf				0				0				0
Ta				0				0				0
W				0				0				0
Au				0				0				0
Th				0				0				0
U				0				0				0

Table B1.2. Erebus 1989 blank corrected filter data in μg per 1/2 or 1/4 filter. A-particle filter, B, C-treated filters. S and F on A-filters by ion chromatography, rest by INAA. Concentrations of elements marked with (*) from long irradiation.

	89-1A	1B	1C	89-1	89-2A	2B	2C	89-2	89-3A	3B	3C	89-3
F	14.98	48	8	70.98	44.68	140		184.68	14.34	70		84.34
Na	7.3		8.4	15.7	14.8			14.8	6.1			6.1
Na*	7.5		10.0	17.5	14.6			14.6	6.4			6.4
avg Na	7.4		9.2	16.6	14.7			14.7	6.2			6.2
Al				0				0				0
S	8.7	137.0	12.0	157.8	11.6	109.8	41.5	162.9	7.9	79.8	42.5	130.1
Cl	3.4	101.5	8.0	112.9	4.5	244.0	1.0	249.5	3.6	86.0	15.0	104.6
K				0				0				0
K*	7.03			7.03	16.4			16.4	7.0			7.0
avg K	7.03			7.03	16.4			16.4	7.0			7.0
Ca	18	14		32	5			5		13	9	22
Ca*	17.4			17.4	17.5			17.5	15.8			15.8
avg Ca	17.7	14		31.7	11.3			11.3	15.8	13	9	37.8
Sc	2.4e-04			2.4e-04				0	1.5e-04			1.5e-04
Ti	6			6				0	5			5
V				0				0				0
Cr	0.015			0.015	0.025	0.249	0.223	0.496	0.079			0.079
Mn	0.05			0.05	0.04			0.04	0.02			0.02
Fe	1.639			1.639	0.846	1.445		2.291	0.583	2.715	2.445	5.742
Co	0.002			0.002	0.001			0.001	0.001			0.001
Ni	0.093			0.093	0.031			0.031	0.049			0.049
Cu				0				0				0
Zn	0.341	0.704	0.303	1.347	0.493	0.255	0.079	0.826	0.255	3.192	1.451	4.897
As	0.100	0.015	0.007	0.121	0.167	0.062	0.005	0.235	0.047	0.048	0.006	0.101
Se			0.0048	0.0048				0			0.0078	0.0078
Br			0.17	0.17		0.27		0.27		0.14		0.14
Br*	0.152	0.096	0.129	0.376	0.064	0.354	0.029	0.447	0.105	0.160	0.075	0.340
avg Br	0.152	0.096	0.149	0.397	0.064	0.312	0.029	0.404	0.105	0.150	0.075	0.330
Rb	0.046			0.046	0.09			0.09	0.035			0.035
Mo	0.011			0.011				0				0
Cd				0	0.102			0.102	0.048			0.048
In	0.014			0.014	0.003			0.003	0.012			0.012
Sb	0.006	0.004	0.012	0.022	0.008			0.008	0.004	0.020	0.019	0.044
I	n.d.	n.d.	0.06	0.06	n.d.	n.d.	n.d.	0	n.d.	n.d.	n.d.	0
Cs	0.0021			0.0021	0.0038			0.0038	0.0017			0.0017
La	0.0026			0.0026	0.0005			0.0005	0.0003			0.0003
Ce	0.0038			0.0038	0.006			0.006	0.0018			0.0018
Nd				0				0				0
Sm	0.00036			0.00036	0.00021			0.00021				0
Eu				0	0.00016			0.00016				0
Tb				0				0				0
Yb				0				0				0
Lu				0				0				0
Hf				0				0				0
Ta				0	0.00014			0.00014				0
W				0				0				0
Au				0				0				0
Th				0				0				0
U				0				0				0

Table B1.2. (cont.)

	89-4A	4B	4C	89-4	89-5A	5B	5C	89-5	89-6A	6B	6C	89-6
F	9.24	210	34	253.24	42.08	290	10	342.08	19.7	330		349.7
Na	24.2			24.2	29.9			29.9	40.9			40.9
Na*	21.7			21.7	30.0			30.0	40.7			40.7
avg Na	23.0			23.0	29.9			29.9	40.8			40.8
Al	2.2			2.2				0	1.1			1.1
S	12.2	569.6	4.8	586.6	12.2	184.0	14.3	210.5	16.0	350.9	10.9	377.8
Cl	48.8	259.0		307.8	29.6	524.0	18.0	571.6	227.6	384.0	2.0	613.6
K				0	17			17				0
K*	27.7			27.7	36.2			36.2				0
avg K	27.7			27.7	26.6			26.6				0
Ca				0	22	11	7	40				0
Ca*				0				0				0
avg Ca				0	22	11	7	40				0
Sc	5.2e-04			5.2e-04				0	3.4e-04			3.4e-04
Ti				0	6			6				0
V				0				0	0.02			0.02
Cr				0				0.000	0.086			0.086
Mn	0.057			0.057		0.07		0.07				0
Fe	1.978	1.058		3.036	1.324	10.018		11.342	3.373	1.745		5.118
Co	0			0	0.001	0.002		0.004	0.001			0.001
Ni				0				0	0.092	0.023333		0.115333
Cu				0				0				0
Zn	1.133			1.133	0.737		2.221	2.958	1.167	2.477	0.474	4.117
As	0.190	0.053	0.009	0.2518	0.556	0.064	0.026	0.646	0.569	0.012	0.006	0.587
Se			0.0114	0.0114		0.0038		0.0038	0.0069			0.0069
Br	0.23	0.36		0.59	0.29	0.44		0.73				0
Br*	0.243	0.379	0.012	0.635	0.288	0.480	0.056	0.824	0.311	0.379	0.000	0.690
avg Br	0.237	0.370	0.012	0.619	0.289	0.460	0.056	0.805	0.311	0.379	0.000	0.690
Rb	0.16			0.16		0.012		0.012	0.253			0.253
Mo	0.028			0.028	0.174	0.0193		0.1933	0.043			0.043
Cd	0.162			0.162	0.2	0.119		0.319	0.234			0.234
In	0.054			0.054	0.065	0.0044	0.0022	0.0716	0.083			0.083
Sb	0.010			0.010	0.012	0.003		0.015	0.025			0.025
I	n.d.	n.d.	n.d.	0	n.d.	n.d.	n.d.	0	n.d.	n.d.	n.d.	0
Cs	0.0070			0.0070	0.0075			0.0075	0.0119			0.0119
La	0.0014			0.0014	0.0018			0.0018	0.0038			0.0038
Ce	0.0037			0.0037	0.0034			0.0034	0.0067			0.0067
Nd				0				0				0
Sm	0.00012			0.00012	0.00022			0.00022	0.00041			0.00041
Eu	0.00014			0.00014				0				0
Tb				0				0				0
Yb	0.00032			0.00032				0				0
Lu				0	0.00057			0.00057	0.00018			0.00018
Hf				0				0				0
Ta				0	0.00032			0.00032				0
W	0.0012			0.0012				0		0.0093	0.0031	0.012467
Au				0				0				0
Th	0.00025			0.00025				0				0
U				0				0				0

Table B1.2. (cont.)

	89-8A	8B	8C	89-8	89-9A	9B	9C	89-9	89-11A	11B	11C	89-11
F	2.32	350	21	373.32	5.63	120		125.63	16.2	140		156.2
Na	5.7			5.7	11.9			11.9	24.5			24.5
Na*	5.5			5.5	10.7			10.7	18.8			18.8
avg Na	5.6			5.6	11.3			11.3	21.7			21.7
Al				0				0				0
S	6.6	255.0	19.7	281.3	7.6	139.7	18.8	166.1	11.2	121.3	43.9	176.4
Cl	15.6	234.0	26.0	275.6	25.6	184.0	9.0	218.6	51.6	306.0	0.8	358.4
K				0				0				0
K*				0	13.4			13.4	23.8			23.8
avg K				0	13.4			13.4	23.8			23.8
Ca				0				0				0
Ca*				0				0	17.31	11.77		29.07
avg Ca				0				0	17.31	11.77		29.07
Sc	3.0e-04			3.0e-04				0				0
Ti				0				0				0
V				0	0.01			0.01	0.02			0.02
Cr	0.100			0.100	0.028			0.028	0.011	0.018	0.042	0.070
Mn	0.03			0.03	0.03			0.03	0.18			0.18
Fe	0.675	0.496	1.000	2.170	0.795			0.795	1.918	0.032		1.950
Co	0.001	0.000	0.001	0.002	0.001			0.001	0.003	0.000	0.001	0.004
Ni	0.026			0.026	0.058			0.058	0.141		0.002333	0.143333
Cu				0				0				0
Zn	0.373			0.373	0.407			0.407	0.496	1.596	1.149	3.240
As	0.1211	0.016		0.137	0.173	0.004		0.176	0.190	0.076	0.000	0.266
Se				0				0				0
Br	0.27			0.27				0				0
Br*	0.171	0.048	0.018	0.237	0.105	0.081		0.186	0.150	0.111		0.260
avg Br	0.221	0.048	0.018	0.287	0.105	0.081		0.186	0.150	0.111		0.260
Rb	0.036			0.036	0.089			0.089	0.115			0.115
Mo	0.012			0.012	0.019			0.019	0.021			0.021
Cd				0	0.092			0.092	0.11			0.11
In	0.013			0.013	0.028			0.028	0.037			0.037
Sb	0.003			0.003	0.005			0.005	0.007			0.007
I	n.d.	n.d.	n.d.	0	n.d.	n.d.	n.d.	0	n.d.	n.d.	n.d.	0
Cs	0.0016			0.0016	0.0036			0.0036	0.0052			0.0052
La	0.0036		0.0006	0.0041	0.0034			0.0034	0.0029			0.0029
Ce	0.0079			0.0079	0.0052			0.0052	0.0038			0.0038
Nd				0				0				0
Sm				0				0	0.00034			0.00034
Eu				0				0				0
Tb				0				0				0
Yb				0	0.00045			0.00045				0
Lu				0				0				0
Hf				0				0				0
Ta				0				0				0
W				0	0.0113			0.0113				0
Au				0				0				0
Th				0				0	0.00071			0.00071
U				0				0				

Table B1.2. (cont.)

	89-13A	13B	13C	89-13	89-15A	15B	15C	89-15	89-16A	16B	16C	89-16
F	4.9	93		97.9	3.74	63	21	87.74	5.79	92		97.79
Na	10.5			10.5	7.0			7.0	11.1			11.1
Na*	10.5			10.5	7.4			7.4	11.1			11.1
avg Na	10.5			10.5	7.2			7.2	11.1			11.1
Al	2.1		3.6	5.7		4.6		4.6	1.1	9.6	7.6	18.3
S	9.4	103.6	17.1	130.1	7.6	109.6	27.9	145.1	8.4	94.8	35.8	139.0
Cl	18.2	207.2	2.2	227.6	14.2	157.2	48.2	219.6	18.2	212.2	1.2	231.6
K	15			15				0				0
K*	13.3			13.3	9.7			9.7	14.1	2.1	1.7	17.9
avg K	14.1			14.1	9.7			9.7	14.1	2.1	1.7	17.9
Ca	7	16	12	35	10	2		12		6	9	15
Ca*				0				0		19.186		19.186
avg Ca	7	16	12	35	10	2		12		12.593	9	21.593
Sc				0	7.0e-04			7.0e-04	3.2e-04			3.2e-04
Ti			0.6	0.6	0.6			0.6	1.6			1.6
V				0				0				0
Cr		0.070		0.070	0.030			0.030				0.000
Mn	0.057		0.012	0.069	0.017	0.03		0.047	0.077		0.01	0.087
Fe				0.000	0.954			0.954	2.447			2.447
Co	0.001			0.001	0.001			0.001	0.001			0.001
Ni				0				0				0
Cu				0				0				0
Zn	0.281			0.281	0.240	5.150		5.390	0.617			0.617
As	0.132	0.080	0.001	0.213	0.139	0.051	0.023	0.212	0.138	0.054		0.193
Se				0				0			0.0099	0.0099
Br		0.33	0.1	0.43		0.39		0.39		0.36		0.36
Br*	0.070	0.315	0.004	0.389	0.038	0.285	0.036	0.358	0.043	0.366	0.012	0.421
avg Br	0.070	0.322	0.052	0.444	0.038	0.337	0.036	0.411	0.043	0.363	0.012	0.418
Rb	0.072			0.072	0.05			0.05	0.074			0.074
Mo	0.015			0.015	0.019			0.019	0.028		0.011	0.039
Cd			0.046	0.046	0.063			0.063	0.075		0.022	0.097
In	0.022			0.022	0.014			0.014	0.021			0.021
Sb	0.002			0.002	0.002			0.002	0.002		0.000	0.003
I	n.d.	n.d.	n.d.	0	n.d.	n.d.	n.d.	0	n.d.	n.d.	n.d.	0
Cs	0.0029			0.0029	0.0016			0.0016	0.0030			0.0030
La	0.0012			0.0012	0.0002			0.0002	0.0039			0.0039
Ce	0.0035			0.0035				0	0.0105			0.0105
Nd				0				0				0
Sm	0.00017			0.00017				0	0.00058			0.00058
Eu				0				0				0
Tb				0				0				0
Yb				0				0				0
Lu				0				0				0
Hf				0				0				0
Ta				0				0				0
W	0.0012			0.0012				0	0.001	0.0432	0.0009	0.0451
Au				0				0				0
Th				0				0	0.00075			0.00075
U												

Table B1.2. (cont.)

	89-17A	17B	17C	89-17	89-18A	18B	18C	89-18	89-20A	20B	20C	89-20
F	4.44	87		91.44	4.11	150		154.11	39.09	180		219.09
Na	2.9		2.5	5.4	7.5			7.5	35.9			35.9
Na*	2.3		2.2	4.5	7.5			7.5	32.5			32.5
avg Na	2.6		2.4	5.0	7.5			7.5	34.2			34.2
Al	1			1				0	1.1			1.1
S	5.6	108.8	50.1	164.5	10.1	218.2	36.8	265.1	18.2	332.9	14.7	365.8
Cl	1.6	173.0	11.0	185.6	70.6	148.0		218.6	97.6	221.0		318.6
K				0				0	37			37
K*	1.3			1.3	7.6			7.6	38.2	0.4		38.6
avg K	1.3			1.3	7.6			7.6	37.6	0.4		38.0
Ca		6		6	2			2	15		1	16
Ca*				0		4.199	2.077	6.276	48.587	40.055	21.325	109.967
avg Ca		6		6	2	4.199	2.077	8.276	31.7935	40.055	11.1625	83.011
Sc	1.1e-04			1.1e-04	1.2e-04	8.1e-04	5.1e-03	6.0e-03				0
Ti	6.5			6.5	6.2	1.2		7.4	7.6e+00			7.6e+00
V				0				0	0.01			0.01
Cr	0.052			0.052	0.083	0.004	0.009	0.095				0
Mn	0.05			0.05	0.04	0.01		0.05			0.01	0.01
Fe	0.847		1.037	1.884	1.445			1.445	2.351			2.351
Co	0.001			0.001	0.001			0.001	0.001			0.001
Ni	0.041			0.041				0	0.094			0.094
Cu				0				0				0
Zn	0.136	1.369	1.575	3.079	0.546			0.546	1.912	1.046	0.865	3.822
As	0.077	0.059	0.024	0.159	0.142	0.038	0.003	0.183	0.406	0.032	0.002	0.439
Se				0	0.012			0.012	0.017			0.017
Br		0.17		0.17	0.280			0.280	0.800		0.130	0.930
Br*	0.024	0.167	0.035	0.226	0.239	0.036		0.276	0.911	0.056	0.047	1.014
avg Br	0.024	0.169	0.035	0.228	0.260	0.036		0.296	0.855	0.056	0.089	1.000
Rb				0	0.05			0.05	0.214			0.214
Mo				0	0.015			0.015	0.044			0.044
Cd				0	0.059			0.059		0.05		0.05
In	0.0025	0.0026	0.0041	0.0092	0.0172			0.0172	0.089			0.089
Sb	0.030			0.030	0.005			0.005	0.011			0.011
I	n.d.	n.d.	n.d.	0	n.d.	n.d.	n.d.	0	n.d.	n.d.	n.d.	0
Cs	0.0007	0.0009	0.0011	0.0027	0.0020			0.0020	0.0092			0.0092
La	0.0114			0.0114	0.0026			0.0026	0.0024			0.0024
Ce	0.0167			0.0167	0.0058			0.0058	0.0045			0.0045
Nd				0				0				0
Sm	0.00029			0.00029	0.000287			0.000287	0.00023			0.00023
Eu				0				0				0
Tb				0				0				0
Yb				0	0.00036			0.00036				0
Lu				0				0				0
Hf	0.0013			0.0013				0				0
Ta				0				0				0
W				0				0	0.0073			0.0073
Au				0				0				0
Th	0.00134			0.00134	0.00082			0.00082	0.0014			0.0014
U												

Table B1.2. (cont.)

	89-21A	21B	21C	89-21	89-23A	23B	23C	89-23	89-24A	24B	24C	89-24
F	19.79	170		189.79	47.12	21	485	553.12	34.61	190	9	233.61
Na	9.6			9.6	56.9			56.9	18.9	0.4		19.3
Na*				0.0	59.4			59.4	20.0	1.5		21.5
avg Na	9.6			9.6	58.2			58.2	19.4	1.0		20.4
Al				0	6.1			6.1				
S	7.8	217.1	35.8	260.7	20.5	574.4	16.8	611.7	12.1	326.2		338.3
Cl	43.6	196.0	4.5	244.1	81.6	3.0	868.5	953.1	20.3	547.5	5.0	572.8
K				0	64			64				
K*				0	68.5			68.5	23.3			23.3
avg K				0	66.2			66.2	23.3			23.3
Ca	5			5		5	3	8	9	9		18
Ca*				0								
avg Ca	5			5		5	3	8	9	9		18
Sc	3.7e-03			3.7e-03	2.3e-04			2.3e-04	1.9e-04			1.9e-04
Ti	3.5e+00			3.5e+00					4			4
V				0								
Cr	0.019			0.019	0.038			0.038	0.021	1.553		1.574
Mn	0.03	0.02		0.05			0.02	0.02	0.08	0.01		0.09
Fe	0.422			0.422	4.812			4.812	2.178			2.178
Co	0.001			0.001	0.002	0.000	0.000	0.003	0.002	0.000	0.000	0.002
Ni	0.046			0.046	0.024			0.024	0.068	0.053		0.121
Cu				0		0.3		0.3				
Zn	0.448		0.219	0.667	1.604			1.604	0.527			0.527
As	0.235	0.005	0.002	0.243	0.875	0.0019	0.0257	0.9026	0.358	0.0543	0.0195	0.4318
Se		0.008	0.005	0.013		0.0028		0.0028		0.0058	0.0031	0.0089
Br	0.160			0.160	0.58	0.12		0.7	0.26			0.26
Br*	0.134	0.010	0.001	0.145	0.643	0.010	0.022	0.675	0.254	0.123	0.016	0.393
avg Br	0.147	0.010	0.001	0.158	0.611	0.065	0.022	0.699	0.257	0.123	0.016	0.396
Rb	0.059			0.059	0.457			0.457	0.148			0.148
Mo	0.018			0.018	0.078			0.078	0.027			0.027
Cd	0.078			0.078	0.36			0.36	0.13			0.13
In	0.023			0.023	0.11			0.11	0.055	0.0041	0.0023	0.0614
Sb	0.004			0.004	0.022			0.022	0.008		0.002	0.010
I	n.d.	n.d.	n.d.	0	n.d.	n.d.	n.d.		n.d.	n.d.	n.d.	
Cs	0.0031			0.0031	0.0185			0.0185	0.0062	0.0012	0.0007	0.0080
La	0.0054			0.0054	0.0057			0.0057	0.0025	0.0012	0.0001	0.0037
Ce	0.011			0.011	0.0135			0.0135	0.0049	0.0041	0.0024	0.0114
Nd				0								
Sm				0	0.00059			0.00059	0.0004	0.0002	0.0001	0.0007
Eu				0				0				
Tb				0								
Yb				0				0				
Lu				0						0.0001		0.0001
Hf				0								
Ta				0	0.00052			0.00052				
W				0	0.0043			0.0043				
Au				0							0.006248	0.006248
Th	0.00079			0.00079				0	0.0012	0.00079		0.00199
U				0				0		0.0024		0.0024

Table B1.2. (cont.)

	89-25A	25B	25C	89-25	89-26A	26B	26C	89-26
F	53.83	360	9	422.83	9.14	116	70	195.14
Na	44.9			44.9	12.3		7.2	19.5
Na*	43.0	0.1		43.0	12.9			12.9
avg Na	43.9	0.1		44.0	12.6		7.2	19.8
Al	1.1			1.1	0.5			0.5
S	18.1	336.8	0.0	354.9	9.5	65.9	0.0	75.4
Cl	59.6	988.0	2.0	1049.6	26.2	279.7	200.2	506.1
K	48			48				
K*	50.7			50.7	16.3			16.3
avg K	49.4			49.4	16.3			16.3
Ca	10		7	17		6		6
Ca*								
avg Ca	10		7	17		6		6
Sc	3.1e-04			3.1e-04	1.9e-05			1.9e-05
Ti			0.667	0.667	0.2			0.2
V	0.01			0.01				
Cr	0.038	0.518	0.133	0.688	0.046	0.035		0.081
Mn			0.013	0.013		0.06		0.06
Fe	5.815			5.815	1.165			1.165
Co	0.002	0.001		0.002	0.001	0.000		0.002
Ni	0.451	0.002		0.453	0.056	0.078		0.134
Cu								
Zn	1.428	0.635	0.008	2.070	1.323			1.323
As	0.611	0.0439	0.0023	0.6572	0.1217	0.0706	0.1006	0.2929
Se		0.0052	0.0066	0.0118		0.0035		0.0035
Br					0.24	0.25		0.49
Br*	0.154	0.250		0.405	0.248	0.156	0.170	0.573
avg Br	0.154	0.250		0.405	0.244	0.203	0.170	0.616
Rb	0.327			0.327	0.101		0.05	0.151
Mo	0.057			0.057	0.017	0.01	0.015	0.042
Cd	0.249			0.249	0.095			0.095
In	0.09			0.09	0.028		0.024	0.052
Sb	0.019			0.019	0.004			0.004
I	n.d.	n.d.	n.d.		n.d.	n.d.	n.d.	
Cs	0.0138	0.0005		0.0143	0.0037		0.0025	0.0063
La	0.0074	0.0011	0.0008	0.0092	0.0007	0.0006	0.0005	0.0017
Ce	0.0165	0.0017	0.0054	0.0236		0.0005		0.0005
Nd								
Sm	0.0010	0.0003	0.0002	0.0014	0.00008			0.00008
Eu								
Tb								
Yb	0.0009			0.0009				
Lu	0.00011			0.00011				
Hf								
Ta	0.00097		0.00053	0.0015				
W					0.0036	0.0024		0.006
Au					0.000147			0.000147
Th	0.002		0.00053	0.00253				
U		0.0023	0.0021	0.0044				

Table B1.3. Erebus 1991 blank corrected filter data in μg per 1/2 filter. A-particle filter, B, C-treated filters. S and F on A-filters by ion chromatography, rest by INAA. Concentrations of elements marked with (*) from long irradiation.

	91-1A	1B	1C	91-1	91-2A	2B	2C	91-2	91-3A	3B	3C	91-3
F	7.39	54.4		61.79	39.72	113.2		152.92	32.19	46.2		78.39
Na*	11.7	4.1	3.9	19.7	21.9	3.1	23.8	48.9	16.5	3.3	5.7	25.5
Na	8.8			8.8	20.1		20.1	40.2	19.2		6.1	25.3
avg Na	10.3	4.1	3.9	18.3	21.0	3.1	22.0	46.1	17.8	3.3	5.9	27.1
Mg	8.71	7.87	3.68	20.26		1.22	5.93	7.15		2.36	2.03	4.39
Al	2.30	1.93	0.94	5.17	2.32		1.92	4.24	6.79		1.74	8.53
S	1.64	118.38		120.03	8.95	363.96	38.67	411.57	7.75	184.17	46.02	237.94
Cl	8.59	172.62	0.04	181.25	16.71	358.39	15.90	390.99	7.03	201.79	10.38	219.20
K*	12.15			12.15	24.15		0.48	24.63	18.39		0.47	18.86
K				0	22.89			22.89	26.04			26.04
avg K	12.15	0	0	12.15	23.52	0	0.48	24.00	22.22	0	0.47	22.68
Ca		2.11		2.11			1.33	1.33			0.71	0.71
Sc	1.1e-04			1.1e-04	1.1e-04	2.0e-04	1.1e-04	4.1e-04	1.6e-04			1.6e-04
Ti	0.34			0.34			1.08	1.08				0.00
V	0.066		0.077	0.143			0.009	0.009	0.058		0.004	0.063
Cr	0.030	0.252	0.159	0.441			0.032	0.032				0.000
Mn	0.039	0.008	0.003	0.051	0.051	0.004	0.013	0.068	0.140	0.020	0.028	0.188
Fe	1.96	1.06	0.39	3.41	2.18	0.37	0.65	3.20	2.34			2.34
Co	1.38			1.38			0.00	0.00	0.00			0.00
Ni			0.07	0.07				0.00				0.00
Cu				0			1.0896	1.0896			1.0839	1.0839
Zn	0.178			0.178	0.381		0.127	0.508	0.216			0.216
As	0.136	0.005	0.008	0.150	0.263	0.060	0.016	0.339	0.181	0.025	0.013	0.219
Se		0.020		0.020		0.023	0.017	0.040				0.000
Br*	0.013	0.646	0.048	0.707	0.031	0.667	0.100	0.798	0.022	0.260	0.077	0.360
Br		0.667		0.667		0.668	0.033	0.701	0.028	0.220	0.056	0.304
avg Br	0.013	0.657	0.048	0.717	0.031	0.667	0.066	0.765	0.025	0.240	0.067	0.332
Rb				0.000	0.139			0.139				0.000
Cd	0.101			0.101	0.148			0.148	0.119			0.119
In	0.017		0.001	0.018	0.040			0.040	0.034			0.034
Sb	0.008			0.008	0.008		0.005	0.013	0.006	0.002		0.008
I		0.0224		0.0224			0.0272	0.0272			0.0058	0.0058
Cs	0.0030			0.0030	0.0080			0.0080	0.0048		0.0002	0.0050
La	0.0032			0.0032	0.0042			0.0042	0.0057			0.0057
Ce	0.0005			0.0005				0				0
Nd				0				0				0
Sm				0	0.0006			0.0006	0.0008			0.0008
Eu	0.0002			0.0002				0	0.0002			0.0002
Tb				0				0				0
Yb				0				0				0
Lu				0				0	0.0001			0.0001
Hf				0				0				0
Ta	0.0006			0.0006				0				0
W				0				0		0.0113	0.0038	0.0150
Au	0.0239	0.2367	0.0184	0.2791	0.0480			0.0480				0
Th				0				0				0
U				0				0				0

Table B1.3. (cont.)

	91-5A	5B	5C	91-5	91-6A	6B	6C	91-6	91-7A	7B	7C	91-7
F	39.33	155.9		195.23	4.53	13.3		17.83	41.59	94.5		136.09
Na*	47.7	5.5	2.4	55.5	6.7			6.7	30.1	2.7	3.5	36.2
Na	37.6	4.6		42.2	4.7			4.7	26.1			26.1
avg Na	42.6	5.0	2.4	50.0	5.7			5.7	28.1	2.7	3.5	34.3
Mg	1.58	6.13	5.77	13.48		1.12		1.12	6.16			6.16
Al	12.05			12.05	2.44	0.73	1.00	4.16	13.63			13.63
S	9.69	599.73	5.24	614.67	1.73	43.77		45.49	9.95	401.76	12.39	424.11
Cl	20.82	627.03	4.61	652.45	2.85	20.43	0.97	24.25	11.63	282.19	55.95	349.77
K*	49.87			49.87	3.26			3.26	15.05			15.05
K	37.25			37.25				0	25.98			25.98
avg K	43.56		0	43.56	3.26			3.26	20.51			20.51
Ca				0				0				0
Sc	4.8e-04			4.8e-04	3.1e-04			3.1e-04	4.5e-04			4.5e-04
Ti				0			1.13	1.13	1.46			1.46
V			0.004	0.004		0.003		0.003	0.077	0.068		0.145
Cr			0.029	0.029		0.042	0.090	0.132	0.031	0.112	0.068	0.211
Mn	0.291	0.023		0.315	0.058	0.007	0.010	0.075	0.273		0.000	0.273
Fe	8.65			8.65	2.19			2.19	7.15			7.15
Co				0.00				0.00				0.00
Ni				0.00				0.00				0.00
Cu				0				0			0.9918	0.991773
Zn	0.881			0.881	3.922		4.338	8.261	3.950	2.070		6.021
As	0.755	0.010	0.003	0.768	0.062	0.006		0.068	0.414	0.005	0.005	0.424
Se			0.013	0.013	0.015	0.007		0.022	0.007	0.011	0.002	0.021
Br*	0.321	0.850	0.063	1.234	0.017	0.019	0.001	0.037	0.050	0.259	0.053	0.362
Br	0.321	0.760	0.001	1.082	0.005	0.034		0.038	0.031	0.310	0.041	0.382
avg Br	0.321	0.805	0.032	1.158	0.011	0.026	0.001	0.038	0.041	0.285	0.047	0.372
Rb				0.000	0.039			0.039	0.180			0.180
Cd	0.286			0.286				0	0.180			0.180
In	0.068		0.000	0.068	0.007	0.001		0.008	0.043		0.001	0.045
Sb	0.019			0.019				0.000	0.007			0.007
I				0				0		0.0333		0.0333
Cs	0.0134			0.0134	0.0012			0.0012	0.0074			0.0074
La	0.0193	0.0002		0.0196	0.0100	0.0002		0.0102	0.0226			0.0226
Ce	0.0470			0.0470	0.0279			0.0279	0.0520			0.0520
Nd				0				0				0
Sm	0.0025			0.0025	0.0013			0.0013	0.0028			0.0028
Eu	0.0006			0.0006	0.0003			0.0003	0.0008			0.0008
Tb				0				0				0
Yb				0				0				0
Lu	0.0002			0.0002				0				0
Hf	0.0042			0.0042	0.0027			0.0027	0.0056			0.0056
Ta	0.0033			0.0033				0	0.0033			0.0033
W				0				0				0
Au	5.1720	0.0459		5.2179		0.0017		0.0017	0.0152			0.0152
Th	0.0035			0.0035	0.0026			0.00263	0.0041			0.0041
U	0.0014	0.0018		0.0032				0				0

Table B1.3. (cont.)

	91-8A	8B	8B-2	8C	91-8	91-9A	9B	9C	91-9	91-11A	11B	11C	91-11
F	44.01	10.9		0	54.91	41.34	0.4		41.74	7.99	5.113		13.103
Na*	29.6	1.4	3.4	2.8	34.7	31.3	2.0	2.0	35.2	4.3			4.3
Na	28.2	1.3		3.2	32.7	31.9	1.3	2.1	35.3	4.1			4.1
avg Na	28.9	1.3	3.4	3.0	34.2	31.6	1.7	2.0	35.2	4.2			4.2
Mg		3.04			3.04	5.93	1.99	8.51	16.43	1.22	1.25	4.03	6.5
Al	34.66	2.30			36.96	41.09	2.36	41.69	85.13	2.97	0.58	1.55	5.10
S	8.19	240.48			248.67	5.67	146.67	28.57	180.90	2.15	15.16	1.04	18.34
Cl	65.82	14.17		5.31	85.30	37.36	12.14	20.21	69.71		16.12	9.60	25.72
K*	28.86				28.86	31.68			31.68				0
K	22.92				22.92	25.51			25.51				0
avg K	25.89				25.89	28.60			28.60				0
Ca	2.22	2.44			4.67				0				0
Sc	1.1e-03				1.1e-03	1.1e-03			1.1e-03				0
Ti	1.28				1.28	2.76			2.76				0
V	0.002	0.017		0.005	0.025		0.003	0.060	0.063			0.067	0.067
Cr	0.009	0.034	0.171	0.051	0.163	0.018	0.099	0.134	0.251	0.103	0.211	0.140	0.454
Mn	0.711	0.053		0.054	0.818	0.797	0.021	0.004	0.822	0.078			0.078
Fe	17.33	0.23	0.51	1.39	19.10	19.58			19.58	1.79			1.79
Co	0			0	0	0			0				0
Ni	0	0.06	0.02	0.16	0.20				0				0
Cu		1.1908		0.7986	1.9894				0			1.0709	1.0709
Zn			0.474	0.117	0.590		0.364		0.364				0
As	0.305		0	0.004	0.309	0.236		0.024	0.260	0.039	0.010	0.005	0.054
Se	0		0		0				0.000	0.030	0.019		0.049
Br*	0.417		0.047	0.030	0.494	0.418	0.020	0.040	0.478	0.020	0.013	0.015	0.048
Br	0.410	0.049			0.459	0.424		0.057	0.480			0.036	0.036
avg Br	0.413	0.049	0.047	0.030	0.492	0.421	0.020	0.048	0.489	0.020	0.013	0.025	0.058
Rb	0.161		0.000		0.161	0.139			0.139				0
Cd			0		0	0.094			0.094	0.029			0.029
In	0.027		0		0.027	0.024	0	0.001	0.026	0.004	0		0.004
Sb	0.003		0.0046	0.003	0.011	0.004	0.013	0.001	0.017				0
I			0		0			0.0134	0.0134				0
Cs	0.0049		0		0.0049	0.0047			0.0047	0.0011			0.0011
La	0.0620		0.0006	0.0019	0.0645	0.0663			0.0663	0.0067			0.0067
Ce	0.1460				0.1460	0.1510			0.1510	0.0182			0.0182
Nd	0.0620				0.0620	0.0370			0.0370				0
Sm	0.0076				0.0076	0.0085			0.0085	0.0008			0.0008
Eu	0.0019				0.0019	0.0022			0.0022				0
Tb					0	0.0011			0.0011				0
Yb					0	0.0033			0.0033				0
Lu					0	0.0004			0.0004				0
Hf	0.0136				0.0136	0.0151			0.0151				0
Ta	0.0083				0.0083	0.0094			0.0094				0
W					0	0.0002			0.0002			0.1985	0.1985
Au	0.0482				0.0482		0.0035		0.0035	0.0142	0.0099		0.0241
Th	0.0125				0.0125	0.0137			0.0137	0.0048			0.00484
U					0				0	0.0000			0

Table B1.3. (cont.)

	91-21A	21B	21C	91-21	91-23A	23B	23C	23C-2	91-23
F	39.87	246		285.87	16.12	182.5		0	198.62
Na*	48.9	8.6	9.4	66.9	10.8	5.3	5.0	6.6	21.9
Na	41.1	4.9	4.1	50.0	9.7	4.6	2.6		16.8
avg Na	45.0	6.8	6.7	58.5	10.2	4.9	3.8	6.6	20.4
Mg	4.29	4.10	9.35	17.74	8.72	12.39	8.86		29.97
Al	7.42		1.50	8.92	7.85	1.42	1.54		10.81
S	16.55	637.56	141.14	795.25	5.10	183.86	3.89		192.85
Cl	16.76	622.10		638.86		426.99			426.99
K*				0					0
K	53.16			53.16					0
avg K	53.16			53.16					0
Ca				0	5.76			0	5.76
Sc	3.2e-04			3.2e-04	2.2e-04	2.7e-04	2.4e-04		7.3e-04
Ti				0				0	0
V	0.069	0.082	0.006	0.157	0.060	0.028	0.015		0.103
Cr	0.049	0.076	0.234	0.359	0.039		0.156	0.097	0.166
Mn	0.278	0.160	0.100	0.538	0.264	0.157	0.123		0.543
Fe	6.88	1.03	1.45	9.36	4.89	2.26			7.15
Co				0					0
Ni				0					0
Cu			0.6119	0.612			1.0413		1.041
Zn	6.061	4.123	3.219	13.402	5.319	4.794		3.825	13.938
As	0.409	0.147	0.008	0.564	0.112	0.156	0.009	0.010	0.277
Se	0.014		0.006	0.021		0.018		0.004	0.022
Br*	0.188	1.215	0.580	1.982	0.050	0.901	0.180	0.217	1.149
Br	0.140	1.164	0.500	1.804	0.030	0.965	0.158		1.153
avg Br	0.164	1.189	0.540	1.893	0.040	0.933	0.169	0.217	1.166
Rb	0.291			0.291	0.079			0	0.079
Cd	0.347			0.347	0.072			0	0.072
In	0.081			0.081	0.015	0.007	0.001		0.024
Sb	0.016		0.003	0.019	0.004	0.010	0.101		0.115
I				0		0.0342	0.0225		0.0567
Cs	0.0128			0.0128	0.0030				0.0030
La	0.0130			0.0130	0.0205			0.0006	0.0211
Ce	0.0284			0.0284	0.0473	0.0051			0.0524
Nd				0					0
Sm	0.0015			0.0015	0.0021				0.0021
Eu				0	0.0005				0.0005
Tb				0	0.0006				0.0006
Yb	0.0040			0.0040	0.0014				0.0014
Lu				0					0
Hf	0.0022			0.0022	0.0036				0.0036
Ta	0.0015			0.0015	0.0020				0.0020
W		0.0121	0.0055	0.0176	0.0006	0.0023	0.0012	0.0029	0.0049
Au	0.0372		0.1357	0.1729	0.0026	0.9681			0.9707
Th	0.0151			0.01507	0.0047	0.0041	0.0043		0.01321
U				0	0.0015				0.00154

Table B1.4. Erebus 1988 blank filters data in μg per 1/2 (small, 47 mm) or 1/4 (large, 110mm) filter.

	88-12A large	88-12B	88-12C	88-14A small	88-14B	88-14C
F		0	0		0	0
F(ic)	14.73			10.61		
Na	1.49	5	5	1.16	2.9	3.6
Na*			4.303	0.819		
Al	9.3	10.4	9.1	10.8	10.5	11
S(ic)	2.9	5.29		3.96	5.3	
Cl	3.2	17	16	3.6	8.1	8.2
K						
K*			1.186			
Ca	48	51	54	48	51	47
Ca*	16.688					
Sc*	8.93e-04	1.32e-03	1.24e-03	1.01e-03		
Ti	6	5	5	5	3.6	5
V	0.16					
Cr*	0.08	0.0825	0.082	0.206		
Mn	0.14	0.15	0.15	0.12	0.13	0.13
Fe*	4.552	6.208	6.389	4.925		
Co*	0.00295	0.0034	0.00367	0.00328		
Ni*						
Cu						
Zn*	0.161	0.439	0.425	0.214		
As*	0.0017	0.0107	0.0058			
Se*			0.011			
Br						
Br*	0.0666	0.1032	0.0672	0.0871		
Rb*						
Mo*	0.0065	0.0084				
Cd*						
In						
Sb*	0.00167	0.0032	0.00389	0.00105		
I						
Cs*		0.00055	0.0005	0.00038		
La*	0.00424	0.00464	0.00619	0.00433		
Ce*	0.0095	0.0095	0.012			
Nd*						
Sm*	0.000735	0.000791	0.00113	0.00084		
Eu*	0.00019	0.00019	0.00019	0.0002		
Tb*				0.00014		
Yb*	0.00039	0.00022		0.00022		
Lu*		0.000044				
Hf*						
Ta*	0.00023			0.00023		
W*	0.0016	0.005	0.0055			
Au*	0.000058	0.000037	0.000062	0.000048		
Th*	0.00068	0.00055		0.00068		
U*	0.0013	0.0014		0.0014		

Table B1.5. Erebus 1989 blank filters data in μg per 1/2 or 1/4 filter. Z-Zeflor; F-Fluoropore; s-47mm; b-110 mm filters; A-particle, L-treated filters

	BL-3 A-s(F)	BL-8 A-b(Z)	BL-9 A-b(F)	BL-4 L-s	BL-5 L-b	BL-6 L-b	BL-7 L-b	Avg L-b
F	n.a.	n.a.	n.a.	0	0	0	0	0
F (IC)	10	10	10					
Na	1.2	3.8	1.1	5.2	5.8	6	5.6	5.8
Na*	0.698	3.069	0.645	3.85	4.736	4.64	4.222	4.688
Al	8.9	9.8	9.9	12.4	10	12	11.9	11.3
S (IC)	0	0	0	0	0	0	0	0
Cl	1.8	4.2	2.4	8.8	17	17	14	16
K								0
K*			0.939	21.52	0.977	1.272	1.348	1.1245
Ca	45	55	41	41	50	50	53	51
Ca*	16.716	0	0	21.854	14.532	19.32	20.64	16.926
Sc*	0.0012	0.0013	0.0010	0.0020	0.0012	0.0016	0.0013	0.0014
Ti	4.4	3.1		5.4	6.1	5.7	4.2	5.3
V	0.035		0.16					0
Cr*	0.059	0.138	0.126	0.084	0.136	0.142	0.086	0.139
Mn	0.123	0.143	0.12	0.13	0.13	0.15	0.14	0.14
Fe*	5.621	6.846	5.136	7.174	6.375	7.567	7.011	6.971
Co*	0.0032	0.00371	0.00251	0.00356	0.00341	0.00401	0.00394	0.00371
Ni*					0.061	0.151	0.051	0.106
Cu					2.9	3.1	2.7	2.9
Zn*	0.299	0.287	0.148	28.184	2.886	0.909	0.535	1.8975
As*	0.0012	0.0042	0	0.0054	0.0124	0.0063	0.0041	0.00935
Se*					0.0072			0.0072
Br								0
Br*	0.0208	0.0232	0.0145	0.0553	0.0829	0.0822	0	0.08255
Rb*								
Mo*					0.019		0.0084	0.019
Cd*								
In								0
Sb*	0.0035	0.0099	0.00031	0.00446	0.0136	0.0131	0.00531	0.01335
I				0.08				0
Cs*	0.0004							
La*	0.0043	0.00458	0.00363	0.00662	0.00451	0.00613	0.00411	0.00532
Ce*	0.0105	0.0113	0.0085	0.0157	0.01	0.0092	0.0087	0.0096
Nd*	0	0	0	0	0	0	0	0
Sm*	0.0009	0.00094	0.00076	0.00132	0.00085	0.00089	0.00074	0.00087
Eu*	0.0002	0	0	0.0003	0.00021	0.00016	0.00019	0.000185
Tb*	0	0	0	0	0	0	0	0
Yb*	0	0	0	0.0005	0.00055	0	0	0.000275
Lu*	0	0	0	0	0	0	0	0
Hf*	0	0	0	0	0	0	0	0
Ta*	0	0	0	0	0	0	0	0
W*	0.0014	0.0033	0	0.0028	0.0047	0.008	0.0046	0.00635
Au*	7e-05	0.000062	0.000055	0.000066	0.000092	0.000127	0.000088	0.00011
Th*	0.0006	0.00071	0	0.00101	0	0	0.00058	0
U*	0	0	0	0	0	0	0	0

Table B1.6. Erebus 1991 blank filters data in μg per 1/2 filter. (A-1, L-1) first set of blanks (used to blank-correct samples 6, 7, 8, 9, 11, 21, 23); (A-2, L-2) second set of blanks (used for samples 1-5, 8-11, 23, 24); A-particle filter, L-treated filter.

	A-1	L-1	A-2	L-2	91-4A	4B	4C	91-13A	13B	13C
F					n.a.	3.400	0			
F (IC)	12.1									
Na					0.62	8.00	6.99		8.42	8.11
Na*	0.83	2.52	3.39	7.50						
Mg					28.13	25.44	30.28		26.33	33.48
Al					1.30	2.91	1.89		4.88	4.21
S (IC)	2.42	27.06								
Cl					43.05	46.99	50.53		49.95	52.99
K					0	0	0			
K*				1.575						
Ca					0	4.146	3.582		4.068	2.435
Sc*	0.0002	0.0004	0.0001	0.0003						
Ti					0.766	0.000	0.000			
V					0.097	0.094	0.103		0.096	0.108
Cr*	0.048	0.070	1.342	1.378						
Mn					0.034	0.051	0.057		0.084	0.054
Fe*	4.2735	4.4836	0.887	1.791						
Co*	0.002	0.003	0.001	0.002						
Ni*				0.085						
Cu					0	0	0			1.224
Zn*	8.70	8.04	0.23	0.50						
As*	0.001	0.009		0.008						
Se*		0.00671								
Br					0.062	0.099	0.091		0.123	0.086
Br*	0.051	0.066	0.028	0.037						
Rb*										
Cd*										
In					0	0	0			
Sb*	0.006	0.008	0.004	0.008						
I					0	0	0			
Cs*				5.0e-04						
La*	2.4e-03	5.1e-03	4.7e-04	1.2e-03						
Ce*		0.011		0.012						
Nd*										
Sm*	1.8e-04	2.8e-04		1.8e-04						
Eu*		2.3e-04								
Tb*										
Yb*										
Lu*										
Hf*		0.001								
Ta*	1.5e-04	4.3e-04								
W*	0.002		0.001	0.003						
Au*	0.013	0.048	0.028	0.060						
Th*		0.006								
U*										

B2. RESULTS OF T-TEST FOR F, S, CL DATA COLLECTED IN YEARS 1986, 1988, 1989, 1991

T-test was performed on F, S, Cl data to determine whether the mean normalized concentrations were statistically different between 2 groups of data. As shown in Figure 5.8, mean values from 1986 and 1989 form one cluster of values, data from 1988 and 1991 another. The concentration of each element was normalized by dividing by the sum of concentrations of all three elements, and thus obtained values were used in calculations. Each cluster contains 23 data points. The mean and variance for each cluster are given in each case.

The t-test was performed 3 times, separate for each element. In each case we test the hypothesis that the means for the two clusters are the same, and calculate the probability of that event. First, values of the random variable t are calculated and then compared with the critical value $t_{critical}$. $T_{critical}$ depends on the choice of the level of significance α (here = 0.05%) and the number of degrees of freedom df which depends on the number of data points (in this example df=23+23-2=44). $T_{critical}$ is usually taken from tables, here it was calculated by the statistical package in Quattro Pro. If t is $>t_{critical}$ or $t< -t_{critical}$, the hypothesis that the means of the two clusters are the same can be rejected and it means that the two groups of data are statistically different. Table B2.1 shows the results of calculations. The results indicate that means calculated for F and S are statistically different between the two groups of data, whereas means calculated for Cl are statistically the same (Miller and Freund, 1987).

Table B2.1. Results of t-test analysis for two samples (clusters) assuming unequal variance.

	Cluster 1 86 and 89 data	Cluster 2 88 and 91 data
Calculations using F data	F-1	F-2
Mean	0.24	0.17
Std	0.06	0.03
Variance	0.004	0.001
Observations	23	23
Pooled Variance	0.002466	
df	44	
t	5.08	
P(T<=t) one-tail	0.000007	
t Critical one-tail	1.69	
P(T<=t) two-tail	0.000013	
t Critical two-tail	2.03	
Calculations using S data	S-1	S-2
Mean	0.32	0.42
Std	0.12	0.10
Variance	0.015	0.010
Observations	23	23
Pooled Variance	0.012175	
df	44	
t	-3.24	
P(T<=t) one-tail	0.001177	
t Critical one-tail	1.68	
P(T<=t) two-tail	0.002355	
t Critical two-tail	2.02	
Calculations using CI data	CI-1	CI-2
Mean	0.44	0.40
Std	0.11	0.08
Variance	0.012	0.006
Observations	23	23
Pooled Variance	0.009207	
df	44	
t	1.09	
P(T<=t) one-tail	0.140337	
t Critical one-tail	1.68	
P(T<=t) two-tail	0.280675	
t Critical two-tail	2.02	

This dissertation is accepted on behalf of the faculty of the Institute by the following committee:

Adviser

Date

I release this document to New Mexico Institute of Mining and Technology.

Students Signature Date